STATE OF CALIFORNIA • DEPARTMENT OF TRANSPORTATION
TECHNICAL REPORT DOCUMENTATION PAGE
TR0003 (REV 10/98)

1. REPORT NUMBER	2. GOVERNMENT ASSOCIATION NUMBER	3. RECIPIENT'S CATALOG NUMBER
CA10-1098		

4. TITLE AND SUBTITLE	5. REPORT DATE
STABILITY OF BRIDGE COLUMN REBAR CAGES DURING CONSTRUCTION	11/30/2010
	6. PERFORMING ORGANIZATION CODE

7. AUTHOR	8. PERFORMING ORGANIZATION REPORT NO.
J. Camilo Builes-Mejia, Ahmad M. Itani, and Hassan Sedarat	UNR/CCEER-10-07

9. PERFORMING ORGANIZATION NAME AND ADDRESS	10. WORK UNIT NUMBER
Department of Civil and Environmental Engineering University of Nevada, Reno, Nevada 89557-0208 Fax: A. Itani: (775) 784-1362, e-mail: itani@unr.edu	
	11. CONTRACT OR GRANT NUMBER
	59A0648

12. SPONSORING AGENCY AND ADDRESS	13. TYPE OF REPORT AND PERIOD COVERED
State of California, Business, Transportation and Housing Agency Department of Transportation, Engineering Service Center P.O. Box 942874, Sacramento, California 94274-0001	Final
	14. SPONSORING AGENCY CODE

15. SUPPLEMENTARY NOTES

16. ABSTRACT

The lateral behavior and stability of bridge column rebar cages were investigated to reduce the potential of failure and collapse during construction. Rebar cages are temporary structures made of longitudinal and transverse reinforcing bars that are connected by tie wire connections. Recent collapses during construction exposed the vulnerabilities of these temporary structures to accidental loads that may occur at this stage. Therefore, experimental and analytical investigations were conducted to understand the lateral behavior of bridge column rebar cages. Experimental work was performed on individual components of rebar cages, such as tie wire connections and reinforcing bars, under various types of loading. Two fullscale bridge column rebar cages were subjected to incremental loading to determine the lateral behavior, identify failure modes, and calibrate the analytical models. Using the results from the experimental study, nonlinear finite element analyses were developed to determine the effect of critical parameters on the lateral behavior of column rebar cages. The investigated parameters were: tie wire connections, internal braces, column diameter, longitudinal and transverse reinforcement ratios, and column height. The results of these analyses showed that the internal braces have a significant effect on the lateral behavior and failure mode of bridge column rebar cages. Guidelines for determining the lateral stiffness and improving the bridge column rebar cage stability are proposed.

17. KEY WORDS	18. DISTRIBUTION STATEMENT
Rebar cages, tie wires connections, internal braces,	No restriction.

19. SECURITY CLASSIFICATION (of this report)	20. NUMBER OF PAGES	21. COST OF REPORT CHARGED
Unclassified	256	

Reproduction of completed page authorized.

**Stability of Bridge Column Rebar Cages
during Construction**

J. Camilo Builes-Mejia
Ahmad M. Itani
Hassan Sedarat

_____

Center for Civil Engineering Earthquake Research
Department of Civil Engineering/258
University of Nevada
Reno, NV 89557

November 2010

DISCLAIMER STATEMENT

This document is disseminated in the interest of information exchange. The contents of this report reflect the views of the authors who are responsible for the facts and accuracy of the data presented herein. The contents do not necessarily reflect the official views or policies of the State of California or the Federal Highway Administration. This publication does not constitute a standard, specification or regulation. This report does not constitute an endorsement by the Department of any product described herein.

For individuals with sensory disabilities, this document is available in Braille, large print, audiocassette, or compact disk. To obtain a copy of this document in one of these alternate formats, please contact: the Division of Research and Innovation, MS-83, California Department of Transportation, P.O. Box 942873, Sacramento, CA 94273-0001.

Disclaimer

Any opinions, findings, and conclusions or recommendations expressed in this publication are those of the authors and do not necessarily reflect the views of University of Nevada, Reno; Center for Civil Engineering Earthquake Research; Department of Civil and Environmental Engineering; or their sponsors. This report does not constitute a standard, specification or regulation.

Abstract

The lateral behavior and stability of bridge column rebar cages were investigated to reduce the potential of failure and collapse during construction. Rebar cages are temporary structures made of longitudinal and transverse reinforcing bars that are connected by tie wire connections. Recent collapses during construction exposed the vulnerabilities of these temporary structures to accidental loads that may occur at this stage. Therefore, experimental and analytical investigations were conducted to understand the lateral behavior of bridge column rebar cages. Experimental work was performed on individual components of rebar cages, such as tie wire connections and reinforcing bars, under various types of loading. Two full-scale bridge column rebar cages were subjected to incremental loading to determine the lateral behavior, identify failure modes, and calibrate the analytical models. Using the results from the experimental study, nonlinear finite element analyses were developed to determine the effect of critical parameters on the lateral behavior of column rebar cages. The investigated parameters were: tie wire connections, internal braces, column diameter, longitudinal and transverse reinforcement ratios, and column height. The results of these analyses showed that the internal braces have a significant effect on the lateral behavior and failure mode of bridge column rebar cages. Guidelines for determining the lateral stiffness and improving the bridge column rebar cage stability are proposed.

Acknowledgements

Disclaimer

Any opinions, findings, and conclusions or recommendations expressed in this publication are those of the authors and do not necessarily reflect the views of University of Nevada, Reno; Center for Civil Engineering Earthquake Research; Department of Civil and Environmental Engineering; or their sponsors. This report does not constitute a standard, specification or regulation.

Table of Contents

List of Tables

List of Figures

xiv

Chapter 1
Introduction

1.1 Background

Rebar cages are the skeleton of Reinforced Concrete bridge columns. These cages are formed by tying the longitudinal and the transverse reinforcement bars together by tie wire connections. Seismic research on reinforced concrete bridge columns revealed that longitudinal bars cannot be spliced in the location of plastic hinge zones (Caltrans, 2004). Therefore, bridge column rebar cages are constructed in steel fabrication shops and shipped to the construction site as one. Depending on the length of the cage, the diameter of the cage, and the experience of the fabricator, internal braces **may** be placed inside the cage. Then, the bridge column rebar cage is attached to the bottom mat of the footing and guyed with at least four guy cables. When placing the steel column forms, at least two of the guy cables are removed from the column rebar cage. Most of the instability instances have occurred at this phase of construction due to accidental loads and loss of the lateral stiffness of bridge column rebar cages. The instability of column rebar cages is a rare incidence. However, it is associated with life safety, injury, litigation, schedule delay, and cost. It has been reported that in the last 15 years around 56 cage collapses occurred in California.

Analytical and experimental investigations were conducted to determine the lateral behavior of bridge column rebar cages. The experimental work was conducted on individual components of rebar cages as well as two full-scale column rebar cages. Based on the experimental results, nonlinear finite element analyses were conducted on different computational models to determine the effect of various parameters on the lateral behavior of bridge column rebar cages. Parameters included: tie wire connections, internal braces, column diameter, longitudinal and transversal reinforcement ratios, and column height. Based on the analytical results, guidelines for determining the lateral stiffness of bridge column rebar cages were proposed.

1.2 Literature Review

Little information was found in the literature that deals with stability of rebar cage columns and Cast-In-Drilled-Hole (CIDH) cages. The latter is used as a foundation for different kinds of structures such as highway bridges, towers, buildings, etc. Contractors for this type of foundation have reported difficulties in fabricating and placing the rebar cages in the drilled holes. The difficulties occur due to the flattening of the cage that occurs while it is lying horizontal before it is placed in the drilled hole. Gupta studied the design of longitudinal and transverse reinforcing bars of CIDH rebar cages to overcome this problem (Gupta S. R. D. et al 1993). Recommendations for the selection of transverse bar spacing and size, and longitudinal bar size are discussed. The authors concluded that stresses can be high in the circular hoops of CIDH rebar cages during construction, especially for hoops with diameters larger than 48 inches. Design curves and tables are provided as design aids to obtain an optimal weight of the rebar cage that reduces the stresses in the hoops.

An analytical analysis on the pick-up of CIDH rebar cages was developed by Condon-Johnson & Associates, Inc in a submittal prepared for the CIDH Rebar Cages at Bent No. 3 and Bent No. 4 of the S67-W52/Magnolia Avenue UC (Condon-Johnson & Associates, Inc, 2008). The length of the CIDH rebar cage was around 61 ft. A 20-foot long frame was analyzed; the frame weighed 13,300 pounds and included a welded frame made of two interior hoops. Four cross braces were located at each interior hoop, and eight diagonal braces located between adjacent interior hoops. The welded frame was assumed to be tied to the longitudinal reinforcing bars, and the tie wire connections were assumed to be made of four wraps of No. 15 gauge tie wire. The yield strength of each wrap was estimated to be equal to 244 lb, assuming that the yield strength of both wire legs can be developed. The shear strength was assumed to be 40% of the tensile strength. Based on the analysis results, it was recommended to increase the number of tie wire connections on the picking bars, i.e. bars from where the rebar cage is lifted.

Caltrans Standard Specifications Section 52: "Reinforcement" under 1.07 "Placing" requires the contractor to submit a temporary support system plan to the engineer for approval (Caltrans, 2006). Usually, column rebar cages are guyed in at least four locations; but depending on the height, multiple levels of guy cables could be used. Donatas proposed a new support system for guyed structures that are used as permanent structures such as transmission towers (Donatas J. et al, 2007). The typical system of straight guy cables was improved by using guy cables composed of primary and secondary cables. The additional secondary cables increase the number of intermediate elastic supports and reduce the effective buckling lengths of the guyed structure. Also, the authors showed that the combined guy cables reduce the bending moments and horizontal displacements in the structure under lateral loading.

Longitudinal and internal brace reinforcing bars in column rebar cages are subjected to a combination of forces and moments, such as axial, shear forces, bending, and torsion moments. Studies have been conducted on the interaction between bending moment, axial force, transverse force and torsion. A numerical investigation was developed by Imegwu on prismatic beams loaded by terminal bending and torsion moments (Imegwu E. O., 1960). Acting together, these two moments cause full plastic flow. An interaction curve was recommended with non-dimensional coordinates that compared well with previous experimental investigations. The results showed that the interaction curve seems to be practically independent of the shape of the cross-section of the beam. Wei showed that an envelope of the interaction hypersurface for the plastic yielding of beams due to the combined influence of bending, tension, shear and torsion could be obtained by solving a variational problem (Wei Q. S., 1995). The lower bounds of the interaction yield curves bending moment-torsion and axial tension-torsion were obtained for beams with rectangular cross-section. The investigation proved that the widely interaction equation presented below is statically admissible because it lies within the lower bound of the envelope.

$$\left(\frac{M}{M_p}\right)^2 + \left(\frac{T}{T_p}\right)^2 \left(\frac{T_p}{T_e}\right)^2 = 1$$

where M_p, T_p are the plastic bending moment and plastic twisting moment, respectively. T_e is the plastic twisting moment without warping.

1.3 Collapse Information

It has been reported by the major steel fabricators in California, Harris steel, Pacific Coast Steel, and Fontana steel that around 56 rebar cage collapsed in the last 15 years at bridge construction sites in the State of California. Normally, the collapse of bridge column rebar cages is associated with a significant cost, delay in schedule, and unfortunately, injuries or deaths. However, the legal consequences of such collapses have limited the access to the engineering details and the sequence of progressive collapse of these column rebar cages. With Caltrans consent, it was possible to obtain information about several collapses of bridge column rebar cages for this investigation.

Milpitas Bent 6

A bridge column rebar cage at the Highway 237/880 Project in Milpitas, California fell over after several guy cables were removed in November, 1999. The contractor reported some findings and descriptions about the collapse (Caltrans, 2003):

- *The right column rebar cage at Bent #6 was supported by a total of eight guy cables before the steel column form was placed.*

- *The column was approximately 48 feet tall from the top of the footing to the top of the cage.*

- *Four guy cables were located at quarter points around the cross section of the column cage halfway up the column. The other four guy cables were located at quarter points around the cross section near the top of the cage.*

- *Six of the eight guy cables were removed to allow for the placement of one-half of the steel column form. The only two guy cables remaining were located at the top of the cage on the north/northwest corner and the south/southeast corner of the cage and were secured to a concrete block dead-man.*

- *The crane operator was directed to lift and fly the first half of the steel column form into place on the west side of the column cage. As the form was swung into place, it made contact with the column cage. The contact was not abrupt nor was it severe. Upon contact with the steel column form, the column cage began to fall slowly toward the south/south east corner of the footing where it came to rest shortly thereafter.*

Figure 1.1 shows the bridge column rebar cage after collapse. Based on the report presented by the contractor about the collapse of the bridge column rebar cage in Milpitas, CA, it could be concluded that the removal of six of the eight guy cables followed by the slight contact of the column form at the top caused the rebar cage collapse.

Bent 7 Carquinez Bridge

Two bridge column rebar cages collapsed at Bent 7 of the Carquinez Bridge in California in April, 2002. Figure 1.2 shows both column rebar cages after the collapse. Both columns were interlocking and fixed at the base. Figure 1.3 shows that the collapse of both column rebar cages occurred before the concrete footing was poured. The deformed shapes after collapse showed a combination of bending and torsion of the column rebar cages as shown in Fig. 1.4. Usually, damage to the longitudinal bars raises concerns about the future cyclic performance of the column, and requires replacement of the cage. The presence of internal braces could not be confirmed, and it was not possible to see from the pictures obtained that are shown in Fig. 1.5.

Sweetwater River Connection

A bridge column rebar cage at pier 3 of the Sweetwater River Connection collapsed in November, 2006. Little information about this collapse was obtained other than the cross section of the bridge column rebar cage was rectangular. Figure 1.6 shows the bridge column rebar cage after collapse.

SFOBB West Approach

A bridge column rebar cage at bent 23 of the San Francisco-Oakland Bay Bridge West Approach collapsed in November, 2009. The height and diameter of the column rebar cage were equal to 38 ft and 54-in, respectively. The column rebar cage was made of 36 bundled #11 longitudinal reinforcing bars and bundled #8 hoops spaced at 5-in. Thus, the longitudinal and transverse reinforcement ratios were equal to 2.45% and 2.33%, respectively. Figure 1.7 shows the plans for bents 22 to 27. The bridge column rebar cage was supported by four guy cables located at one fourth of the height from the top of the cage as shown in Fig. 1.8. Notice that internal braces were not used in this column rebar cage. It was not possible to obtain information about the cause of the collapse. Figure 1.9 shows the collapsed bridge column rebar cage.

From the information collected on bridge column rebar cage collapses, it could be concluded that:

1. Most collapses involve bridge column rebar cages with fixed base.
2. Collapses occur due to accidental loading and loss of lateral stiffness in bridge column rebar cages after the removal of the temporary support system.
3. Collapses occur in the absence of any kind of internal braces in the column rebar cages.

1.4 Objective and Scope

The main objective of this study was to develop analytical tools and specifications to predict and control the properties of tied bridge column rebar cages to reduce the potential of failure and collapse.

To achieve this objective, analytical and experimental investigations were conducted to understand the lateral behavior of bridge column rebar cages. The experimental work was divided into two phases. The first experimental phase was conducted on components of bridge column

rebar cages, tie wire connections, and reinforcing bars to determine their behavior under various types of loading. The second experimental phase was conducted on two full-scale bridge column rebar cages under incremental loading to better understand the lateral behavior, identify failure modes, and provide data to calibrate the analytical investigation. Based on these experiments, a calibrated three-dimensional finite element model was developed and utilized to investigate the lateral behavior of bridge column rebar cages with various parameters such as the type of tie wire connections, internal braces, column diameter, longitudinal reinforcement ratio, transversal reinforcement ratio, and column height.

1.5 Report Summary

This report presents the results of experimental and analytical investigations of the lateral behavior of bridge column rebar cages. The assembly and construction practices of bridge column rebar cages are discussed in Chapter 2. The results of the experimental investigation on individual components of column rebar cages and on two full-scale bridge column rebar cages are presented in Chapter 3. Chapter 4 covers the calibration of a finite element model based on the results from the experimental investigation. The results of parametric analysis and the effect of critical parameters on the lateral behavior of column rebar cages are also discussed in this chapter. Finally, in Chapter 5 guidelines for improved rebar cage stability are proposed and concluding remarks based on the experimental and analytical investigations are listed.

Chapter 2
Bridge Rebar Cage Assembly, Construction Practices and Pretest Analysis

2.1 Introduction

This chapter discusses the construction specifications for bridge column rebar cages established by Caltrans, the components of column rebar cages, the assembly and construction practices. This chapter also presents the pretest analysis results of bridge column rebar cages. The finite element software ADINA (ADINA R & D, Inc., 2010) was used to create the computational models and perform the nonlinear analyses of column rebar cages under lateral loading. The kinematics and the type of analysis are described in this chapter. The elements used to model the longitudinal and transverse reinforcing bars along with the braces and tie wire connections of the column rebar cages are also presented in this chapter. The analytical investigation showed that the connection flexibility between the longitudinal and transverse reinforcement and the behavior of braces havr critical effect on the lateral stiffness and strength of column rebar cages. Without realistic models of connection flexibility (translation in x, y, and z directions and rotation about x, y, and z axes), the behavior of column rebar cages under lateral loading cannot be assessed. Upper and lower bounds were utilized in the computational model for the connection flexibility to determine the overall lateral behavior and to aid in the selection of the test specimens.

2.2 Caltrans Standard Specifications and Column Rebar Cages

Few guidelines exist on the assembly of bridge column rebar cages. The general requirements are presented by Caltrans Standard Specifications (2006) in Section 52: "Reinforcement" under 1.07 "Placing". "*Reinforcement shall be accurately placed as shown on the plans and shall be firmly and securely held in position by wiring at intersections and splices.*" No specifications exist for the type or strength of tie wires; the type and number of tie wire connections and the presence of internal braces. These decisions are left to the steel fabricator discretion which indeed vary from one fabricator to another.

The stability and lateral support provisions for column rebar cages are presented also in Section 52-1.07 Placing: "*Whenever a portion of an assemblage of bar reinforcing steel that is not encased in concrete exceeds 20 feet in height, the Contractor shall submit to the Engineer for approval, in accordance with the provisions in Section 5-1.02, "Plans and Working Drawings," working drawings and design calculations for the temporary support system to be used. The working drawings and design calculations shall be signed by an engineer who is registered as a Civil Engineer in the State of California. The temporary support system shall be designed to resist all expected loads and shall be adequate to prevent collapse or overturning of the assemblage.*" This shows that temporary support system needs to be designed to provide adequate bracing to the column rebar cage to prevent any lateral instability. Finally, the specifications regulate the procedure for the removal of the temporary support system: "*If the installation of*

forms or other work requires revisions to or temporary release of any portion of the temporary support system, the working drawings shall show the support system to be used during each phase of construction."

An amendment in the new Standard Specifications in 2010 presents information on column rebar cages with diameters of at least 4 ft and larger. Minimum tying requirement and the need for internal bracing are also presented. The three main requirements are:

1. *At least 4 vertical bars of each cage shall be tied at all reinforcement intersections with double wires.*
2. *At least 25% of remaining reinforcement intersections in each cage shall be tied with single wires. Tied intersections shall be staggered from adjacent ties.*
3. *Bracing shall be provided to avoid collapse of the cage during assembly, transportation and installation.*

It is note here that these three new requirements are coupled with current investigation that showed the importance of internal braces and the type and number of tie wire connections. Pacific Coast Steel pioneered this amendment based on discussion with the authors of this report.

2.3 Bridge Column Rebar Cage Assembly

Bridge column rebar cages in zones with high seismicity are normally assembled in steel fabricator shops. Reinforcing bars are tied at intersections in order to maintain their position during work. It is known that tying does not add strength to the finished reinforced concrete structure, but it plays a significant role in the stability of a rebar cage during construction. This sometimes simple connection, allows the cage becomes a stable structure, which can be transported, lifted, placed and held during construction before pouring of concrete. The components used in the assembly of column rebar cages are: reinforcing bars and tie wires connections. The reinforcing bars form the longitudinal and transverse reinforcement that are normally #11 and #8 bars, respectively. Internal braces when used are normally #8 bars.

Bridge column rebar cages are assembly in steel fabrication shops. Two steel W-shape sections with properly spaced drilled holes at the flanges are used to support the hoops. All the hoops are placed into the holes, spaced out as indicated on the placing drawings as shown in Fig. 2.1. Then four longitudinal bars that form the shape of a square and normally identified as "pick-up" bars are tied to each hoop. Figure 2.2 shows these bars in a assembled column rebar cage. It is to note here that these bars are responsible for holding the weight of the cage during the pick-up process, hence their name. The remaining longitudinal bars are added and tied to the template hoops, which are spaced around 8 to 10 ft intervals along the length of the cage. Figure 2.3 shows the markings made on a template-hoop during the assembly of a column rebar cage. The region between the template hoops is identified as the field-zone and the longitudinal bars are tied to staggered hoops in this zone. Figure 2.4 shows a rebar cage with the locations of pick-up bars, template hoops, field zone along the height of the cage.

2.3.1 Tie Wires

Tie wires in column rebar cages are made of black soft-annealed steel wires that have minimum ultimate strength of 40 ksi. Different gauges are available in the market, ranging from No. 16½ to No. 14. The most common gauge used in the State of California is No. 15, although occasionally No. 16 gauge wire is used by some fabricators. The practice of carrying tie wire varies somewhat in different regions across the country. Tie wires are usually available in 3 to 4 pound coils. The coils are readily placed in a tie wire holder or reel specially designed for this purpose. The reel is suspended from the iron worker belt for accessibility and use (CRSI, 2005). The diameter and cross sectional area of No. 16½ through No. 14 gauge wire are tabulated in Table 2.1. Figure 2.5 shows coils of No. 15 tie wires.

2.3.2 Tie Wire Connections

Different types and methods for tying reinforcing bars can be found in construction practices. The Concrete Reinforcing Steel Institute defines five types of tie wire connections as the most common: snap (single and double snap), wrap-and-snap, saddle (single and double U), wrap-and-saddle, and figure-eight (CRSI, 2005). Several steel fabricators and iron workers were interviewed throughout this investigation to identify the most common types of tie wire connections used in bridge column rebar cages. Single-snap, double-snap, single-U, double-U, column-tie, wrap-and-saddle and strong-tie connections were found to be the most common among the fabricators and iron workers in California.

Each type of tie wire connection has its own particular way of connecting the reinforcing bars. However, the tying procedure is the same for all of them. The intersection between reinforcing bars is wrapped differently depending on the type of tie wire connection. No matter which wrapping style is used for the connection, the two ends of the wire come together on the top and are twisted together and "heeled" with a pair of pliers until they are tightly fit against the reinforcing bars. Special care must be taken as the ends are twisted and heeled because excess of twisting and "heeling" may break the wire. Experienced iron workers produce "tight-fit" connections while inexperienced ones produce "loose" connections.

Single-snap

The single-snap connection is a very simple and fast-made tie wire connection. The intersection of the reinforcing bars is wrapped once around in a diagonal manner. Figure 2.6 shows a photo of this type of connection.

Double-snap

The single-snap tie wire connection can be made stronger by doubling the wire and producing a double-snap connection. Figure 2.7 shows a photo of this type of connection.

Single-U

The single-U connection is a more complicated connection than the double-snap; therefore, the single-U takes more time to make, but it will create a stronger connection. The

wires pass halfway around one of the bars on each side of the crossing bars. The ends of the wire are then brought squarely around the crossing bar, then up and around the first bar where the ends are twisted and healed. Figure 2.8 shows a photo of this type of connection.

Double-U

The single-U tie wire connection is made stronger by doubling the wire thus creating a double-U connection. Figure 2.9 shows a photo of this type of connection.

Wrap-and-Saddle

The wrap-and-saddle tie wire connection is similar to Double-U except that an extra wrap is added to the first bar. Figure 2.10 shows a photo of this type of connection.

Figure-Eight

The intersection of the reinforcing bars is wrapped two times around in a diagonal manner, forming an X-shape with the wires in the figure-eight connection. Figure 2.11 shows a photo of this type of connection.

Column-Tie

The column-tie connection mixes the single-U and single-snap tie wire connections. It is made similarly to the single-U except one of the ends is wrapped around in a diagonal manner and then both ends are twisted and healed. Figure 2.12 shows a photo of this type of connection.

Strong-tie

The strong-tie is made similarly to the double-U except more than three wraps are used. The number of wraps depends on the iron worker. It is made in particular intersections of reinforcing bars that will be presented in following sections. Figure 2.13 shows a photo of this type of connection. It is to note that there are no special guidelines or procedures for this tie wire connection. It is normally used during the first stages of the process of tying the cage.

Wrap-and-snap

The wrap-and-snap connection is made by wrapping the wire around one of the bars and then making a diagonal wrap around the intersecting bar. The connection is completed in the same manner as a snap-tie. This type of tie wire connection is not used in the assembly of column rebar cages.

2.3.3   Distribution of Tie Wire Connections in Column Rebar Cages

The patterns and distribution of tie wire connections in bridge column rebar cages vary among fabricators and state Departments of Transportation. According to CRSI Placing Reinforcing Bars: "*The proper tying of reinforcing bars is essential in order to maintain their position during work done by other trades and during concrete placement. It is not necessary to*

tie reinforcing bars at every intersection". Tying adds nothing to the strength of the finished structure. The pick-up bars are tied to the transverse reinforcement at every intersection with double-snap, or quadruple snap tie wire connections. The intersections between template hoops and longitudinal bars are tied with either double-U, wrap-and-saddle, column-tie, or strong-tie. In the field-zone the intersections between longitudinal and transverse reinforcement bars are usually tied with single-snap or double-snap tie wire connections. Figure 2.14 shows the field-zone of a column rebar cage and the single-snap tie wire connections that were used. The percentage of intersections between longitudinal and transverse reinforcing bars that are tied up in the field-zone varies between 25% and 30% and are staggered from each other. Different States have various requirements for the percentage and the type of connections in the field-zone. Caltrans Standard Specifications Section 52-1.07 "Placing" says: "*Reinforcement shall be firmly and securely held in position by wiring at intersections*" Some fabricators tie 20% to 30% of the field zone. Nevada Standard Specifications Section 505.03.04; Placing and Fastening of the Reinforcing Steel specification along with Arizona Standard Specifications Section 605-3; Construction Requirements of the Steel Reinforcement Specification states: "*Where reinforcement spacing is less than 12-in each direction alternate intersections may be tied.*" While the Nevada DOT Standard Specification Section 509.03.11 Reinforcing Steel for drilled shaft foundations does require "Double tie, with double wires" However it specifically says "every other intersecting vertical and spiral or hoop member of the reinforcing cage in each direction." Arizona DOT Standard Specification Section 609-2.02 Reinforcing Steel references Section 605. Double wire is not specified.

2.3.4   Internal Braces

According to CRSI Placing Reinforcing Bars: "*For large square or rectangular column cages, it may be necessary to provide diagonal reinforcing bar braces or wire bracing to stiffen the bars and to prevent the column cage from collapsing as it is lifted off the ground to a vertical position and set into place*". Depending on the length, diameter of the cage and the experience of the fabricator, internal braces **may** be placed inside the cage. These internal braces vary in detail and location from one fabricator to another. Two braces are commonly used in California, X-braces and Square braces. The X-braces are normally made of 4 #8 bars, bent in a Z-shape and welded to two inner rings at the ends of the bars. The braces are tied to the longitudinal bars and spaced at 10 ft intervals along the length of the rebar cages. The X-braces bars have a point in common in the center of the brace where they are welded to each other. Figure 2.15 shows a detail of an X-brace.

The Square brace is made of 8 #8 bars that are also bent in a Z-shape, welded to two inner rings at the ends of the bars, and tied to the longitudinal bars at 10 ft intervals. The square braces bars have three points in common with adjacent bars; two of the points are close to the ends and one in the center of the brace where they are welded to each other. Figure 2.16 shows a detail of square brace. The square brace is preferred by many contractors since it allows the concrete to be poured in through the "tremi-tube" without the interruption of the X-brace.

2.4 Construction Practices of Bridge Column Rebar Cages

After the column rebar cage is assembled in the shop, it is delivered to the construction site. Caltrans Standard Specifications (Caltrans, 2006) Section 52-1.07 requires the contractor to submit a temporary support system plan, commonly called "Guy Wire Plan", to the engineer for

approval. A properly designed system with a proper installation sequence will ensure the stability of the column rebar cage. Depending on the type of the base of the column, the sequence and installation procedure varies.

2.4.1 Pinned Base Columns

A field trip was made to the construction site of a bridge close to Livingston, California. The bridge has two spans with three columns bent. The columns are pinned at the base. Figure 2.17 shows one of the column rebar cage with two X-braces ready to be installed inside the column forms. The contractor used a crane to erect the column forms first. While the crane was holding the column forms, the temporary support system was installed. Figure 2.18 shows the column forms with the temporary support. Thereafter, the same crane was used to lift the column rebar cage as shown in Fig. 2.19. Figure 2.20 shows the rebar cage being placed inside the column forms. For this type of column, the rebar cage is always held by the crane during the installation procedure. Therefore, collapse for the column rebar cage is very small. This construction practice should be encouraged at construction sites for pinned columns.

2.4.2 Fixed Base Columns

There are two procedures for the installation of column rebar cages with a fixed base: one using two cranes and the other using one crane. In the two crane procedure, the contractor uses one of the cranes to support the column rebar cage while the guy cable system is temporarily removed. The second crane is used to install the column forms, and then the guy cable system is reinstalled. Similar to the procedure for a column with pinned base, the rebar cage is always being held by the crane and no potential of collapse is presented.

The construction of a bridge column with fixed base was visited during this investigation. The construction site was located close to Lincoln, California. It is a two span bridge with single column bent. Only one crane was used for the installation of the column rebar cage. Figure 2.21 shows the column rebar cage with two internal X-braces ready to be erected. After the erection, the rebar cage was swung into the footing location as shown in Fig. 2.22. While the crane was holding the cage, the iron workers attached the bottom of the cage to the bottom mat of the footing as shown in Fig. 2.23. The rebar cage was guyed at four locations according to the guy cable plan, as shown in Fig. 2.24. Depending on the height of the column rebar cage, multiple levels of guy cables could be used, as shown in Fig. 2.25. The common practice is that for height larger than 40 ft two levels of four guy cables have to be used. The guy cables were attached to anchor points and the slack of the cables was removed as shown in Fig. 2.26. If the rebar cage shows no indications of instability, the crane is released and the column rebar cages stands by itself with the help of the guy cables as shown in Fig. 2.27. Thereafter, the concrete of the footing is poured and the column forms are installed. However, the guy cable locations usually conflict with the column forms and at least two guy cables must be temporarily removed. It is important to note here that most of the instability incidences occur at this phase of construction. Once the column forms are securely guyed using the two guy cables that were previously removed, the other two guy cables are removed from the rebar cage and the second piece of the column form is attached to the first piece and guyed using the guy cables that were removed the second time. When the column forms are installed, the rebar cage is laterally braced by the column forms.

2.4.3 Guy cables

A survey on the guy cables used in California among several contractors. The results of the survey show that contractors typically use 6x19 Independent Wire Rope Core (IWRC) and the diameter could vary from 3/8 to 5/8 inch. The cross sectional properties, the nominal breaking strength and the weight per foot of these types of cables are summarized in Table 2.2.

2.5 Rebar Cage Computational Models

The general purpose finite element analysis software ADINA (ADINA R & D, Inc., 2010) was used to study the behavior of bridge column rebar cages. ADINA offers both eigenvalue buckling analysis and nonlinear analysis.

2.5.1 Modeling of Reinforcing Bars

The longitudinal and the internal braces bars were modeled with the ADINA Elastic-Plastic Multilinear Moment-Curvature beam element. This element allows for the behavior of members to be described in the form of bending moment-curvature relationships and torsional moment-angular twist relationships with the presence of axial forces. The geometric and material nonlinearities are incorporated in the model with plasticity based on the von-Mises-yield condition. The flexural behavior of the element is defined by two bending moment-curvature relationships, one for each principal plane of inertia. Multilinear functions are used to express the bending moment in terms of curvature and the torsional moment in terms of twist angle per unit length. The moment-curvature relationships were obtained using a section analysis program based on material properties. The transverse bars were modeled with the ADINA linear beam element. This element is a 2-node Hermitian beam element with a constant cross-section and 6 degrees of freedom at each node.

The cross sectional properties of the longitudinal, transverse and internal brace elements are summarized in Table 2.3. These bars are the most commonly used in the assembly and construction of column rebar cages in the State of California.

Axial Behavior of Internal Braces

Analytical analyses on a #8 half length brace bar were performed to determine the behavior under axial loading. The length of the brace bar modeled was equal to 5'-2.4"; thus, the slenderness ratio (*L/r*) was equal to 250. Therefore, the stability of these bars is dominated by elastic buckling. Models with different boundary conditions were analyzed: both ends pinned (pinned-pinned), one end fixed and the other end pinned (fixed-pinned) and both ends fixed (fixed-fixed) as shown in Fig. 2.28. Figure 2.29 compares the axial force-axial displacement curves obtained from the analyses. The buckling loads for the three cases analyzed pinned-pinned, fixed-pinned and fixed-fixed were equal to 3,586 lb, 7,338 lb and 14,340 lb, respectively. The deformed shapes of the three cases are shown in Fig. 2.28. Since the slenderness ratio is high, 250; the buckling loads obtained from the analytical models are similar to the buckling loads calculated using the classical Euler buckling load equation:

$$P_{cr} = \frac{\pi^2 EI}{(kL)^2}$$

Using the adequate value of k based on the boundary conditions: 1 (pinned-pinned), 0.7 (fixed-pinned), and 0.5 (fixed-fixed) as shown in Fig. 2.28. The buckling loads for the three cases are 3,610 lb, 7,601 lb and 14,899 lb, respectively. Therefore, it could be concluded that the analytical model captures the elastic buckling of the brace bars.

The boundary conditions of the bracing bars are complex and cannot be idealized as pinned or fixed. Figure 2.30 shows a close-up of the connection between the end of one brace bar to the longitudinal bar. The end of the brace bar is welded to the inner ring, and the latter is tied to the longitudinal bar. An idealization of the boundary conditions of the X-brace bars is shown in Fig. 2.31. The top end boundary condition was idealized as restricted in the translational degree of freedom and semi-rigid in the rotational degree of freedom. This represents the brace bar to the longitudinal bar connection. The bottom end boundary condition was idealized as fixed in the rotational degree of freedom and semi-rigid in the translational degree of freedom, which represents the connection at the common point of the brace bars. Analytical analyses were performed to determine the effect of the top rotational spring stiffness (k_θ) and bottom translational spring stiffness (k_Δ) on the buckling load of the bar. The results of the analysis are shown in Fig. 2.32. The buckling load of the #8 bar increases with the stiffness of the lateral spring and the stiffness of the rotational spring. However, the results are limited by upper and lower bounds. For large values of the rotational and translational spring stiffnesses, the buckling load of the #8 bar approaches to 14,899 lb which is the buckling load of a bar with both ends fixed (fixed-fixed). For small values of the rotational and translational spring stiffnesses, the buckling load of the #8 bar approaches to 897 lb which is the buckling load of a bar with one end pinned and the other end fixed in the rotation degree of freedom but free in the translation degree of freedom.

The same analysis discussed above was done for a Square brace bar. An idealization of the boundary conditions of the Square brace bar is shown in Fig. 2.33. The top and bottom boundary conditions are the same as the X-brace bar. An intermediate lateral support was added, which represents the connection at the common point with the adjacent bar brace. The results of the analysis are shown in Fig. 2.34. The buckling load of the #8 bar increases with the stiffness of the lateral springs and the stiffness of the rotational spring.

The buckling loads of the bars for both X-brace and Square brace depend on the boundary conditions. The top boundary condition is provided by the connection between the brace bar to the longitudinal bar. Therefore, the rotational stiffness (k_θ) depends on the weld between the brace bar and the inner hoop, and on the tying between the inner hoop and the longitudinal bars. The bottom and intermediate boundary condition (k_Δ) are provided by the connection between the brace bars which are welded to each other in the common points.

2.5.2   Computational Model of Tie Wire Connection

In the computational model the tie wire connections between the longitudinal and transverse reinforcing bars were modeled with nonlinear translational trusses and nonlinear rotational springs as shown in Fig. 2.35. At the intersection between the vertical and horizontal

elements (longitudinal and transverse bars), two nodes were defined with the same coordinates. One node belongs to the vertical elements and the other belongs to the horizontal elements. The link between these two nodes, representing the connection between vertical and horizontal elements (tie wire connection), was divided into six degrees of freedom, three translational (Δx, Δy, and Δz) and three rotational (θx, θy, and θz). At each intersection three orthogonal directions were defined, normal, tangential and vertical. In each direction, a node was defined 1 ft away from the intersection point of the elements. To simulate the semi-rigid behavior of the tie wire connections in the six degrees of freedom, three truss elements and three spring elements were added between the node of the vertical elements and the three 1-ft spaced orthogonal nodes. Each orthogonal node was connected to the horizontal element node with rigid links. Figure 2.36 shows the discretization of the translational trusses in the normal, tangential and vertical directions, and Fig. 2.37 shows the discretization of the rotational springs in the normal, tangential and vertical directions.

A study of a local model of tie wire connection was performed. The structure consisted of two vertical beam elements and one horizontal truss element as shown in Fig. 2.38. The force of a truss element under various analysis options were investigated: 1) all members subjected to large displacement theory, 2) all members subjected to small displacement theory, and 3) beam elements subjected to large displacement theory and truss elements subjected to small displacement theory. Figure 2.39 shows the results of the analysis of the three cases. The three cases show different results as displacement gets large. As expected, Case 2 showed linear behavior because all elements were subjected to small displacement theory. The truss member force for Case 1 showed nonlinear behavior and after 4.8-in of top displacement a softening behavior was seen. However, the reaction at support B for this case consisted of components in X-direction and Z-direction. The resultant force for these reaction components was the same as the truss force. The truss member force variation for Case 3 showed hardening behavior and only X-direction reaction component. The direction of the truss member force is horizontal through all loading steps; however the deformed shape is significantly deviate from the horizontal line.

2.5.3 Model of Guy Cables

The guy cables were modeled using the ADINA 2-node truss element. To be able to capture only the tensile force behavior of a cable, an elastic material model with only tensile stresses was defined for these elements. In the computational model, the diameter used for the guy cable was 7/16-in as shown in Table 2.2. Manufactures of this type of wire report a typical value for the elastic modulus equal to 14,500 ksi.

2.5.4 Load Application and Analysis Procedure

The instability incidences in bridge column rebar cages have occurred when two guy cables from the temporary support system were removed and the bridge column rebar cage is left being supported by the other two guy cables. The lateral behavior of bridge column rebar cages under this circumstance was investigated using nonlinear pushover analysis. Furthermore, thinking in future experimental investigation is a simple mode of load application that can be implemented in a full-scale test. Displacement control was applied at two nodes 90 degrees apart and located at two thirds of the total height above the base. The angle between the horizontal plane and the guy cables was named alpha (α) as shown in Fig. 2.40. Equal incremental displacement was applied along both directions of the two guy cables.

Nonlinear push-over analysis was used to determine the stiffness and strength of bridge column rebar cages. The solution to the static equilibrium equations in each iteration is obtained using Full Newton procedure with line search. The Automatic-Time-Stepping (ATS) method was used to obtain a converge solution. This method automatically subdivides the load step increment to help reach convergence. The tolerances were based on both energy and force balances and were selected to make sure that the solution follows a physical path. The convergence criteria are used in each subdivision of load step. Large displacements were used in the analytical analysis which accounts for geometric nonlinearity.

2.6 Preliminary Pretest Analysis Results

Nonlinear analytical analyses were performed to determine the effect of the connection between the longitudinal and transverse bars on the overall response of bridge column rebar cages. A rebar cage for a column diameter of 4 ft (44 in diameter of rebar cage) and height equal to 34 ft was selected. The longitudinal reinforcement and the transverse reinforcement were equal to 2%, resulting in 24 #11 longitudinal bars and #8 hoops spaced at 3.5-in. A tie wire connection was defined for every intersection between longitudinal and transverse bars; this represents the maximum tying a bridge column rebar cage can have. Analytical analyses were conducted on seven column rebar cage models. The results were summarized in the form of resultant cable displacement-resultant cable force relations. The flexibility of the connection was changed in the models; each degree of freedom (Δx, Δy, Δz, θx, θy, and θz,) in the connections between longitudinal and transverse bars was released. Figure 2.41 compares the response obtained from the analytical analyses. The resultant curves show that the behavior of column rebar cages is affected by the connection at the intersections between longitudinal and transverse bars. The release of the θy, and θz did not affect the behavior of rebar cage models. Instead the release of Δx, Δy, Δz, and θx have a significant effect on the lateral response of column rebar cages. A close up of the response curves for the releases of the normal, tangential, and vertical translational (Δx, Δy, and Δz) and normal rotational (θx) degrees of freedom is shown in Fig. 2.42. The lateral response of column rebar cages is significantly affected by the flexibility of the connection between longitudinal and transverse bars in Δz. The release of this degree of freedom produces an instable behavior of the column rebar cage model because the hoops and the longitudinal bars were not connected and large displacements in the hoops along the vertical direction were obtained. Therefore, a realistic model of the connection between longitudinal and transverse bars is required to determine accurately the behavior of bridge column rebar cages under lateral loading.

Analytical analyses were conducted to determine the effect of internal braces in the behavior of bridge column rebar cages. The properties and dimensions of the column rebar cage models were the same as the presented above. The connections between longitudinal and transverse bars were modeled as pinned. The analyses performed were in a rebar cage model without internal braces, with X-braces and with Square braces. The height of the braces was 9'-7.5" and they were spaced 10'-6" apart as shown in Fig. 2.43. The braces were rigidly connected to the corresponding longitudinal bars. Figure 2.44 compares the results obtained from the analytical analyses conducted on the three models. The resultant curves show that the behavior of column rebar cages is affected by the use of internal braces. However, the increase on the stiffness is not significant, 10% when X-braces were used and 14% when Square braces were used. This could be attributed to the model of the connection between longitudinal and transverse bars. Although, they were modeled pinned, the flexibility of the connections is still too high

which generates a rigid behavior of the column rebar cage, even without braces. Figures 2.45 and 2.46 show the axial force of the brace bars for both rebar cages, with X-braces and Square braces. Buckling of the brace bars was not observed. Linear behavior for all the brace bars was seen through all loading steps.

Chapter 3
Experimental Investigation

3.1 Introduction

This chapter discusses the experimental investigations that were conducted to evaluate the lateral behavior of bridge column rebar cages. The experimental program was divided into two parts:

1. Establish the behavior of column rebar cage components under various types of loading
2. Determine the behavior of full scale column rebar cages under lateral loads.

3.2 Components of Bridge Column Rebar Cages

The components of column rebar cages are: tie wire connections and reinforcing bars. The longitudinal and transverse bars in column rebar cages are tied together with tie wires at certain intersections creating a stable temporary structure, that can be transported, lifted, placed, and supported before the concrete is poured. Therefore, the response of these components under various types of loading is essential for understanding the behavior of column rebar cages under lateral loading.

3.2.1 Tie Wires

Tie wires in column rebar cages are made of black soft-annealed steel wires with a minimum ultimate strength of 40 ksi. Different gauges are available in the market, from No. 16½ to No. 14. The most common gauge used in the State of California is No. 15; although occasionally No. 16 gauge wire is used by some fabricators. Fig. 2.5 shows coils of No. 15 tie wires. The diameters and areas of No. 16½ to No. 14 gauge wire are tabulated in Table 2.1.

3.2.1.1 Stress-strain Response of Tie Wires

In bridge construction, tie wires are only used to hold the reinforcing bars in place before the concrete is poured; therefore their strength have not been of concern after the concrete is poured. However, in this study the tie wires are essential to the stability of bridge column rebar cages. Tie wire connections consist of wraps of wire around the bars that are being connected. When these bars are moved away from each other, then the tie wires are subjected to various forces. Therefore, the mechanical properties of tie wires influence the response and strength of tie wire connections.

Pacific Coast Steel, a steel contractor based in Fairfield, CA, conducted tests to determine the ultimate strength of different gauges of tie wires. Three different gauges were tested, No. 16½, 16 and 15. The ultimate strength values obtained from the tests are presented in Table 3.1.

The average ultimate strengths for these gauges were equal to 47.5 ksi, 48.1 ksi, and 49.1 ksi respectively.

Little information is known about the stress-strain response of tie wires. A series of tensile tests were conducted according to ASTM-370 procedure to determine the stress-strain response of No. 15 tie wire. The tensile tests were carried out on a MTS loading frame with displacement control. Two threaded rods were used to attach the tie wire samples to the loading frame. An inclined hole with a diameter slightly greater than the wire was drilled in the center of the cross section to one side of each rod. The ends of the tie wire were threaded through the drilled holes and wrapped around the rods providing adequate clamping. The samples had a total length around 25-in and a final straight length between rods of 9.0-in. The deformation was measured with an Epsilon axial extensometer with 8-in gauge length that allowed the capture of the full stress-strain curve to failure. The load was measured with a 5,000-lb axial load cell located in between the grip and the threaded rod. Figure 3.1 shows a photo of the tie wire, threaded rods, load frame, load cell, and extensometer. The stress-strain curves obtained from the tensile tests are shown in Fig. 3.2, and the ultimate strength for each coupon is tabulated in Table 3.1. Figure 3.3 shows a fracture within the gauge length of the tie wire coupon. The average ultimate strength obtained from the conducted tests was equal to 47.3 ksi. Therefore, the average tensile strength of No. 15 gauge tie wire is equal to 194 lb.

3.2.2   Nonlinear Behavior of Tie Wire Connections

As explained in Section 2.5.2, the tie wire connection was modeled with nonlinear translational trusses and nonlinear rotational springs at the intersection between longitudinal and transverse bars. A series of experiments were carried out to determine the force-deformation responses of six different tie wire connections. The connections tested were: single snap, double-snap, single-U, double-U, column-tie and wrap-and-saddle. Figure 3.4 shows close-up photos and details of these connections. These six types of connections represent the most used tie wire connections in column rebar cages. The tie wire connections were for #11 and #8 bar because these are the most commonly used rebar sizes in California for longitudinal and transversal reinforcement, respectively.

The effect of workmanship on the tie wire connection deformation response was also investigated. A total of 152 specimens equally divided into two groups were tested, with each group having 4 specimens per type of tie wire connection. The first group of tie wire connection utilized an experienced iron worker while the second group utilized an inexperienced one to determine the effect of workmanship on the overall deformation response.

3.2.2.1 Translational Springs

3.2.2.1.1   Test Fixture

A fixture was designed and constructed to represent the intersection between reinforcing bars of column rebar cages. The fixture was made of two C-shaped steel frames with the reinforcing bars welded to them. The normal translational (Δx) direction of the tie wire connection was tested by connecting the bars welded to the C-shaped frames perpendicular to each other. This test fixture configuration simulated a hoop being pulled out-of-plane of the longitudinal bar, as shown in Fig. 3.5.

A separate fixture was used to test the tangential (Δy) and vertical (Δz) translational directions of tie wire connections. The C-shaped frame with the #11 bar was attached to the bottom grip of the loading frame. A vertical #8 bar attached to the top grip was connected perpendicularly to the #11 bar welded to the C-shaped frame. The Δy and Δz directions of the tie wire connections were tested by applying an upward displacement to the #8 bar. Some tie wire connections are symmetric in these two directions depending on how the wrapping is made. For example, the wrap-and-saddle connection may have the extra wrap around the hoop or around the longitudinal bar. For this reason, Δy and Δz directions were differentiated to determine the effect of the unsymmetrical wrapping. Figure 3.6 shows the test fixture configuration for the tangential and vertical directions.

An MTS loading frame with displacement control was used to apply the load in these tests. The load was measured with a 5,000-lb axial load cell placed in between the fixture and the top grip. The deformation data was obtained from the displacement transducer of the loading frame. The displacement was applied at a rate of 0.010-in per second and the data acquisition system sampling rate was equal to 4 Hz.

3.2.2.1.2   Tests Results

The test specimens were identified with the initial letters of the tie wire connection type, the direction tested, and the number of the specimen. If the specimen was made by an experienced iron worker "I" was set before the specimen name and if an inexperienced worker was utilized "II" was set before the specimen name. For example: I-CT-X-3 identifies the third specimen of a column-tie connection along Δx direction utilizing an experience iron worker. Figure 2.33 shows the discretization of the translational trusses in Δx, Δy and Δz directions. Figure 2.34 shows the discretization of the rotational springs in θx, θy and θz directions. The Δy and Δz responses of single-snap, double-snap, single-U, double-U and column-tie are the same due to the symmetry of their wraps. The Δy direction response corresponds to the wrap-and-saddle connection made with the extra wrap around the #8 bar. The Δz direction response corresponds to the wrap-and-saddle connection made with the extra wrap around the #11 bar. Table 3.2 presents the identification used in the experimental work.

Normal Translational Direction (Δx) of Tie Wire Connections made by Experienced Iron worker

The force-deformation responses for the single-snap and double-snap tie wire connections are shown in Fig. 3.7. The response curves for the I-2ST-X-2 and I-2ST-X-4 present very different relationships. Discrepancy in the responses could be attributed to a lack of tightening for specimen I-2ST-X-2 which allowed large deformation before failure and an excessive heeling for specimen I-2ST-X-4 that could have broken the tie wires before testing, ultimately causing failure at small deformations. However, the response curves for specimens I-2ST-X-1 and I-2ST-X-3 were similar in shape. The response curves obtained from the four single-snap tie wire connections specimens presented minimal differences.

Figure 3.8 shows the force-deformation responses for the single-U and double-U tie wire connections. The response curves for the single-U tie wire connections show good agreement in stiffness and maximum force. The stiffness in the response of specimen I-2U-X-4 was higher than the stiffnesses obtained from the other three specimens. This could be attributed to a lack of

tightening in specimen I-2U-X-4. The maximum load in the response of specimen I-2U-X-3 was lower than the obtained from the other specimens.

The force-deformation responses for the column-tie and wrap-and-saddle tie wire connections are shown in Fig. 3.9. Specimen I-CT-X-2 reached its maximum load at a smaller deformation than the other three specimens. This could be attributed to an excessive heeling similar to specimen I-2ST-X-4. However, the response curves for specimens I-CT-X-1, I-CT-X-3 and I-CT-X-4 presented minimal differences. The response curves for specimens with wrap-and-saddle tie wire connections were similar for deformation up to 0.20-in.

In general, the trend in the responses obtained in the normal direction (Δx) for the tie wire connections made by the experienced iron worker were similar and presented no large discrepancies. Most failures occurred at a deformation of less than 0.40-in. Figure 3.10 shows the fracture of single snap tie wire connection after being tested in the Δx direction.

Table 3.3 shows a comparison of the average maximum strength of the specimens made by the experienced iron worker in the normal direction (Δx) and the strength calculated by multiplying the number of wires that intersect a plane drawn between the connected bars with the ultimate strength of the wire. The experimental maximum strength obtained for each connection is less than the calculated strength based on the number of tie wires. The difference in strength is less than 18% for the single-U, double-U, column-tie and wrap-and-saddle connections. The single-snap and double-snap have a larger difference because the whole strength of the wire is not utilized due to the inclination of the wires with respect to the load line application. However, it could be concluded that the strength of the tie wires influences the strength of the tie wire connection in the Δx direction.

Tangential (Δy) and Vertical (Δz) Directions of Tie Wire Connections made by Experienced Iron worker

The force-deformation response curves in Δy and Δz directions for single-snap, double-snap, single-U, double-U and column-tie connections are shown from Fig. 3.11 to 3.13. Large deformations up to 1.60-in were seen before failure. The force-deformation response curves show sudden changes in strength and stiffness; and differences in the response curves for specimens of the same type of tie wire connection were seen. Figure 3.15 shows a fracture of a single-U tie wire connection. The discrepancies could be attributed to different tightening and heeling in the specimens. Figure 3.14 shows the force-deformation response curves for wrap-and-saddle tie wire connection. The response curves for both directions were similar in shape to the curves presented earlier. The maximum force was higher in the tangential direction, i.e. the extra wrap was made around the hoop.

The jumps in the force-deformation curves could be attributed to the grooves of the reinforcing bars. While the wires are in contact with a groove, deformation is restricted while force continues to increase. When the wires are in between grooves, a relatively low amount of force is needed to further the deformation. The same fixture was used in each experiment; two grooves were always encountered in the top bar as shown in Fig. 3.6; which explains why the response curves presented two peaks. The initial stiffness of the specimen was low because the wraps of the connection were always placed between bar grooves. Approximately 0.4-in of

displacement was required before encountering the first reinforcing bar groove, explaining the sudden increase in force that occurs around 0.4-in. of deformation. This issue cannot be controlled in the fabrication of column rebar cages because the spacing of the hoops is given in the design of the bridge columns. Therefore, the behavior of the tie wire connections in Δy and Δz directions could be different for each connection of a column rebar cage regardless of the type of connection. Because of this uncontrollable factor and the belief that deformations larger than 1-in. are not physically possible, the force-deformation curves for the vertical and tangential directions of tie wire connections were conservatively constructed in the analytical model without any sudden change in force until 1-in of deformation had occurred.

Based on the experimental results, the weakest tie wire connection is the single-snap. Doubling the wire, i.e. a double-snap connection, increased the translational strength by only 50%. A greater effect is presented in the single-U tie wire connection when the wire is doubled; the strength in the translational directions is increased almost two times. The strongest connections in the translational directions are the double-U and the wrap-and-saddle tie wire connections.

Normal Translational Direction (Δx) of Tie Wire Connections made by Inexperienced Iron worker

The force-deformation responses for the single-snap and double-snap tie wire connections are shown in Fig. 3.16. There is good agreement in the stiffness and maximum force in the responses between specimens for single-snap and double-snap tie wire connection. This could be attributed to homogenous tightening and heeling of each specimen. The experimental data of the fourth specimen with a double-snap tie wire connection could not be obtained due to an error in the data acquisition system.

Figure 3.17 shows the force-deformation responses for single-U and double-U tie wire connections. The response curves of the specimens with single-U tie wire connection were very similar in shape. The stiffnesses of specimens II-2U-X-1 and II-2U-X-3 were greater than the stiffnesses of specimens II-2U-X-2 and II-2U-X-4. Also, the failure of specimens II-2U-X-1 and II-2U-X-3 occurred at smaller deformations. The greater stiffnesses and premature failures could be attributed to an excessive heeling in the specimens.

The force-deformation responses for the column-tie and wrap-and-saddle tie wire connections are shown in Fig. 3.18. The trend in the responses obtained for the specimens with column-tie and wrap-and-saddle connections were similar in shape and presented no large discrepancies which could be attributed to equal tightening and heeling.

Tangential (Δy) and Vertical (Δz) Directions of Tie Wire Connections made by Inexperienced Iron worker

Figures 3.19 to 3.21 show the force-deformation responses for single-snap, double-snap, single-U, double-U and column-tie connections. The force-deformation response curves show sudden changes in force and stiffness similar to the responses of the connections made by the experienced iron worker. Similar trends in the force-deformation curves were obtained for each of specimens. This could also be attributed to similar tightening and heeling for each specimen.

The force-deformation for the wrap-and-saddle connection are shown in Fig. 3.22. The response curves in the vertical direction (extra wrap made around the longitudinal bar) did not present the two sudden increases in the stiffness that are present in the response curves in the tangential direction. Discrepancies in the responses could be attributed to a lack of tightening in the wrapping. Similar to the specimens made by the experienced iron worker, the forces are higher when the extra wrap is made around the hoop.

Workmanship effect on the response of Tie Wire connections in Δx, Δy and Δz

The average maximum strengths and stiffness in Δx, Δy and Δz directions obtained from the experiments conducted in tie wire connections made by the experienced iron worker and inexperienced worker are tabulated in Table 3.4 and 3.5, respectively. The average normal (Δx) response of tie wire connections made by experienced iron worker and inexperienced worker are summarized in Figs. 3.23 and 3.24. Based on these results, workmanship has a significant effect in the Δx strength of tie wire connections; the experienced iron worker produces stronger connections in comparison to the inexperienced worker. This is attributed to lack of tightening and heeling in the wrapping. The lack of tightening is also seen in the maximum deformations that occurred before the failure of the tie wire connections. The specimens made by the experienced iron worker had maximum deformations up to 0.40-in in comparison to the 0.60-in deformations obtained by the specimens made by the inexperienced worker.

Figures 3.25 and 3.26 show the average Δy, and Δz response of tie wire connections made by experienced iron worker and inexperienced worker. Although the effect of the workmanship is not as significant in the Δy, and Δz directions; the workmanship does affect the strength of the connections. The specimens made by the experienced iron worker withstood larger forces than those made by the inexperienced worker. However, the tendencies of the responses are similar. They include sudden changes in the strength and stiffness at the same deformations which could be attributed to the grooves of the reinforcing bars.

The effect of workmanship was mainly seen in the strength of tie wire connections. The connections made by the experienced iron worker were stronger than the connections made by the inexperienced one. This is attributed to a better tightening and heeling of the connection produced by the experienced worker. The workmanship does not have an effect on the overall behavior of tie wire connections. However, the responses obtained for the connections made by the iron worker show discrepancies in stiffness and maximum strength of specimens from the same type of connection; affirming the variability of tie wire connections behavior regardless of the worker skills.

Table 3.6 shows the recommended strength of tie wire connections that can be used in the pick-up of a column rebar cage. The strength was calculated based on the average of the experimental results of tie wire connections made by experienced and inexperienced iron worker. The recommended strength is the 90% of the calculated average.

3.2.2.2 Rotational Springs

3.2.2.2.1   Test Fixture

None of the tie wire connections tested provides rotational restraint around the vertical and tangential (θy and θz) directions. Therefore, only experiments corresponding to the normal rotational direction (θx) were conducted. The same fixture used earlier was utilized to determine the torque-rotation relationship of tie wire connections. The fixture was made of two C-shaped steel frames with the reinforcing bars welded to them. The normal rotational direction (θx) of the tie wire connection was tested by connecting the bars welded to the C-shaped frames perpendicular to each other. This tests fixture configuration simulates both bars, hoop and longitudinal bar, being rotated in-plane, as shown in Fig. 3.27. A Tinius Olsen torsion machine was used to apply the load at a constant rotational velocity in these tests. The applied rotation rate was 3 degrees per minute and the sampling rate was equal to 4 Hz. Figure 3.28 shows the fixtures, the torsion cell and the accelerometers. The torsion moment was measured with a 24,000 lb-in torsion cell placed between the right fixture and the right machine grip. The in-plane rotation between the two bars was measured with two accelerometers attached to each C-shaped steel frame.

3.2.2.2.2   Tests Results

The test specimens are identified with the initial letters of the tie wire connection type, the letter R for rotation and the number of the specimen. If the specimen was made by an experienced iron worker "I" was set before the specimen name and if an inexperienced worker was utilized "II" was set before the specimen name. For example: I-WS-R-3 identifies the third specimen made by an experienced iron worker for a wrap-and-saddle connection being tested in θx. Table 3.2 presents the identification used in the experimental work.

Normal Rotational Direction (θx) of Tie Wire Connections made by Experienced Iron worker

The responses for the single-snap and double-snap tie wire connections are shown in Fig. 3.29. A lower stiffness and a greater ultimate rotation were obtained for specimen I-ST-R-2 than for the other three specimens with single-snap connection. This could be attributed to a lesser tightening in the specimen. The response curves for specimens with double-snap tie wire connection were similar for rotation less than 30 degrees. For larger rotations, discrepancies were presented which could be attributed to different heeling in the construction of the specimens.

Figure 3.30 shows the responses for single-U and double-U tie wire connections. The tendencies in the responses of the specimens for both types of connections were similar and no large discrepancies were presented

The responses of the column-tie and wrap-and-saddle tie wire connections are shown in Fig. 3.31. Specimens with wrap-and-saddle connections showed similar response curves. Specimens I-CT-R-1, I-CT-R-2 and I-CT-R-4 exhibited differences in stiffness but similar ultimate torque values. Specimen I-CT-R-3 failed at a small rotation, which could be attributed to an excessive heeling.

All of the experiments conducted on the specimens made by the experienced iron worker produced a general trend in the torque-rotation responses; the stiffness increased when the rotation was between 30 and 40 degrees. As the rotation was close to 30 degrees, the wires in the tie wire connection began to be subjected to tensile forces. Therefore, the change in the stiffness could be attributed to the engaging of the wires in direct tension. Rotations of up to 70 degrees were recorded before failure in the specimens. Figure 3.32 shows the fracture of single-snap tie connection.

The maximum strength for each type of tie wire connection in the normal rotational direction (θx) is tabulated in Table 3.4. The weakest tie wire connection is the single-snap. Unlike the translational directions, doubling the wire in the single-snap connection, creating a double-snap, increases the strength by at least two times. The same effect was observed when the single-U connection was compared with the double-U connection; doubling the wire results in doubling the normal rotational strength. The connections with the largest rotational strengths are double-U and wrap-and-saddle connections.

Normal Rotational Direction (θx) of Tie Wire Connections made by Inexperienced worker

The responses for the single-snap and double-snap tie wire connections are shown in Fig. 3.33. The rotational stiffnesses and ultimate torques for specimens II-ST-R-2 and II-ST-R-4 were lower than those for specimens II-ST-R-1 and II-ST-R-3. These discrepancies could be attributed to a lack of tightening and heeling. The trends observed in the responses for specimens with double-snap tie connection were very different, which could be due to non-homogeneous tightening and heeling in the wrapping.

Figure 3.34 shows the responses for single-U and double-U tie wire connections. The overall behavior in the responses of the specimens for both types of connections were similar. The reason for this was probably that these two types of connections were easy to make, resulting in a similar tightening and heeling of the specimens.

The responses of column-tie and wrap-and-saddle tie wire connections are shown in Fig. 3.35. Specimen II-CT-R-4 presented a greater rotational stiffness and ultimate torque than specimens II-CT-R-1, II-CT-R-2 and II-CT-R-3. However, failure in this specimen occurred at a lower rotation. This could be attributed to an excessive heeling in the specimen. The rotational stiffness and ultimate torque for specimen II-WS-R-4 were greater than those for specimens II-WS-R-1, II-WS-R-2 and II-WS-R-3. However, the trend in the responses for the four specimens was similar and the change in the stiffness at rotations of approximately 30 degrees was not presented. The reason for this was probably an inadequate tightening of the specimens.

Workmanship effect on the response of Tie Wire connections in θx

The average maximum strength and average stiffness in the normal rotational direction (θx) of tie wire connections are summarized in Table 3.4 and 3.5, respectively. Figures 3.36 and 3.37 show the average θx response of tie wire connections made by experienced iron worker and inexperienced worker. The responses of the tie wire connections made by the inexperienced worker were not as consistent as the responses obtained from specimens made by the experienced iron worker. Similar to the effect of the workmanship in the translational directions, the rotational

strengths of the tie wire connections made by the experienced iron worker were greater compared to the connections made by the inexperienced worker. This could be attributed to lack of tightening in the wrapping and that the inexperienced worker was not able to "heel" the wire as well as the experienced iron worker during the wrapping.

Table 3.7 shows the recommended rotational strength of tie wire connections. Similar to the tangential translational direction, the recommended rotational strength was calculated taking the 90% of the average between the strength of tie wire connections made by experienced and inexperienced iron worker.

3.2.3 Reinforcing Bars

As presented in Section 2.5.1, the longitudinal bars and internal braces were modeled with the ADINA nonlinear moment-curvature beam element. The behavior of this element is described in the form of relationships between bending moment and curvature and torsional moment and angle of twist. These relationships are calculated based on the stress-strain and torsional moment-twist curves of reinforcing bars. Tension tests and torsion tests were conducted on #6 reinforcing bars to obtain these curves.

3.2.3.1 Tension Tests

To obtain the stress-strain curve of a reinforcing bar, two coupon tests of A709 #6 rebar were conducted based on ASTM-370 procedure. The length of the samples was 20-in and the clear length between grips was equal to 10-in. Figure 3.38 shows the test-set up for one of the #6 coupons. Figure 3.39 shows the stress-strain curves obtained from the tension tests. Based on coupon tests of #6 rebar, the average yield strength was equal to 68 ksi and the average ultimate strength was equal to 112 ksi.

3.2.3.2 Torsion Tests

Three 12-in #6 steel reinforcing coupons were tested to determine the torsional moment-twist response of reinforcing bars. The Tinius Olsen torsion machine, a 24,000 lb-in torsion cell, and two accelerometers were used to determine the moment-twist response of reinforcing bars. Each bar was welded using Complete Joint Penetration (CJP) to a steel plate with 5-in diameter and ¾-in thickness. The twist of the bar was measured with two accelerometers; one was attached to the left fixed grip of the torsion machine and the other to the 5-in steel plate. Figure 3.40 shows test set-up for torsion of a rebar. Therefore, the length of the bar between the grips is equal to 9-in.

The torsional moment-twist responses obtained from the tests are shown in Fig. 3.41. The torsional response could be described as linear behavior for small twist angles (less than 20 degrees) and plastic behavior thereafter. Failure in specimens 1 and 2 was occurred at twists of nearly 525 degrees. Specimen 3 reached twists of 745 degrees before failure. Figure 3.42 shows the fracture of the rebar at the end of the experiment. The specimens failure occurred in the vicinity of the weld of the bar with the circular steel plate. The discrepancy in the response of the specimen 3 could be attributed to the quality of the weld. Based on the test results, the yield and ultimate torsional moment for #6 rebar was equal to 3,750 lb-in and 7,680 lb-in.

3.3 Full-Scale Column Rebar Cage Experiments

Two full-scale static push-over tests were conducted to provide insights into the behavior of bridge column rebar cages, identify failure modes, and provide data to calibrate the computational models that can be used for further investigation. The loads were applied to the specimens at a very low loading rate in the direction of the guy cables until failure. Strains and displacements were measured during the tests.

Frequency analyses were conducted on a model of a column rebar cage to determine the principals mode shapes. The rebar cage model had 12 longitudinal #11 bars and hoops spaced at 7.0 in. The height was equal to 12 ft and the diameter equal to 3'- 8". All the intersections between longitudinal bars and hoops were tied with wrap-and-saddle tie wire connections. Figures 3.43 and 3.44 show the two principals mode shapes obtained from the analytical analyses. Notice that both modes are cantilever flexural modes, the deformed shapes show single curvature, with displacements in the X and Y directions. Similar shapes are obtained when the column rebar cage is pulled from two guy cables located in the X and Y axis. Therefore, the loading that was adopted in the full-scale experiments could be considerable the most adverse for bridge column rebar cages.

Based on information that was obtained during this investigation, the collapsed bridge column rebar cages were normally for fixed base column with minimum height-to-diameter ratio of 8, longitudinal reinforcement ratio (ρ) 1% to 2% and lateral reinforcement ration (ρ_s), 1% to 2%. Also, that the collapses occurred when part of the temporarily support system was removed. Therefore, two bridge column rebar cages were selected that represent the dimensions of the known collapsed cages and the application of the lateral load was performed representing the removal of two of the four guy cables in the temporarily support system. Two types of internal braces were selected, X-braces and square braces. The specimens were constructed at Pacific Coast Steel in Fairfield, CA. This fabricator produces many of California rebar cages. The fabricator was directed to fabricate rebar cages similar to the ones fabricated to the State of California.

3.3.1 Test Specimens

Two full-scale test specimens were selected for the experimental investigation. The height of both specimens was equal to 34 ft. Rebar cages for column diameter of 4 ft were selected, thus the height-to-diameter ratio of both experiments specimens were equal to 8.5. Assuming a 2-in clear cover, the outside diameter of the specimens was equal to 3'- 8". The longitudinal (ρ) and transverse (ρ_s) reinforcement ratios of Specimen I were 1% and 1%, respectively. Thus, 12 #11 bars and #8 hoops spaced at 7.0 in were chosen for Specimen I. For Specimen II, the longitudinal (ρ) and transverse (ρ_s) reinforcement ratios were 2% and 2%, respectively. Thus, 24 #11 bars and #8 hoops spaced at 3.5 in were chosen for Specimen II. The weights of Specimen I and II were equal to 4,100 lb and 8,200 lb, respectively. Table 3.8 summarizes the properties of these specimens and Figs. 3.45 and 3.46 show the geometry, the distribution of the template hoops, inner rings and braces of Specimen I and II respectively. The braces used in Specimen I were X-braces which were made of 4 #8 rebar. The height of the braces was equal to 9'- 4" and they were spaced at 10'- 6". The braces used in Specimen II were square braces made of 8 #8 rebar, with a height of 9'- 8" and spaced at 10'- 6". Figures 3.47 and 3.48 show the X-braces used in Specimen I and the square braces used in Specimen II,

respectively. The end of the brace bars were welded to the inner rings and the latter were tied to the longitudinal bars.

Five types of tie wire connections were used in the construction of the specimens: double-snap, quadruple-snap, wrap-and-saddle, column-tie and strong-tie; Fig. 3.49 shows details of each of them. These types of tie wire connections were presented in Section 2.3.2. The quadruple-snap tie wire connection is a double-snap using double wire.

A mapping of all the connections between the longitudinal bars and hoops was made for each specimen. A summary of the tie connection mapping for Specimen I is tabulated in Table 3.9. A total of 72.2% of the intersections between longitudinal bars and hoops were tied up; meanwhile 27.8% did not have any tie wire connection. The most used tie wire connection in the assembly of this specimen was the quadruple-snap which was used at 41% of the intersections. Strong tie wire connections as wrap-and-saddle, column-tie and strong-tie were used only in 10% of the intersections. Table 3.10 summarizes the type of tie wire connections used in the pick-up bars of Specimen I. The most used tie wire connections at the pick-up bars were double-snap and quadruple-snap. A summary of the tie wire connections in the template hoops of Specimen I is shown in Table 3.11. The most used tie wire connections at the template hoops were wrap-and-saddle and strong-tie.

A summary of the tie connection mapping for Specimen II is tabulated in Table 3.12. A total of 48% of the intersections between longitudinal bars and hoops were tied up; meanwhile 52% did not have any tie wire connection. The percentage of tied intersections is lower in comparison to Specimen I. The most used tie wire connection in the assembly of Specimen II was the double-snap which was used at 32.6% of the intersections. In the assembly of Specimen II an even smaller percentage of strong ties was used, only 5.6% of the intersections were tied with strong tie wire connections. Table 3.13 summarizes the type of tie wire connections used in the pick-up bars of Specimen II. The most used tie wire connection at the pick-up bars was double-snap. A summary of the tie wire connections in the template hoops of Specimen II is shown in Table 3.14. Similar to Specimen I, the most used tie wire connections at the template hoops were wrap-and-saddle and strong-tie. Figures 3.50 and 3.51 show each specimen standing without any temporary support before testing

3.3.2 Material Properties

Coupon tests of tie wire were conducted to determine the stress-strain response. The experimental stress-strain response was then compared to reference values already obtained. Figure 3.52 shows the stress-strain curves for the different coupons. The average ultimate strength obtained from the test conducted was equal to 45.3 ksi. This value is close to the value of 47.3 ksi obtained in Section 3.2.1.1 and greater than the value reported by fabricators as the minimum.

Tension tests were performed on coupons obtained from the reinforcing bars of Specimen II. Two #8 coupons were cut from the internal braces, and three #11 coupons were cut from one longitudinal bar. The stress-strain curves from the coupon tests are presented in Fig. 3.53. Based on tests of #8 coupon the yield strength was equal to 72.8 ksi, the yield strain to 0.0022 and the ultimate strength to 98.1 ksi. The results of the #11 coupon tests showed that the yield strength

was equal to 71.1 ksi, the yield strain to 0.0023 and the ultimate strength to 98.0 ksi. The Material Testing Report (MTR) for the rebars is shown in Appendix I.

3.3.3 Test Set-Up and Loading System

The reaction wall outside the Structures Laboratory at the University of Nevada, Reno was used for these experiments. A steel bracket was used to attach the base of the rebar cage to the reaction wall as shown in Fig. 3.54. The steel bracket was composed of a 8x6 feet vertical plate with a thickness equal to 1-in, a 8x6 ft horizontal 1-in thick plate and four 1-in thick stiffeners. Twelve dywidag bars prestressed to 120 kips were used to attached the bracket to the reaction wall. To represent a fixed connection at the bottom of the rebar cage, the longitudinal bars were CJP welded to a 1.5-in steel plate which was bolted with 16 A325 bolts to the horizontal plate of the fixture and attached to the reaction wall as shown in Fig. 3.55.

The displacement was applied to the column rebar cage with two 12-kip hydraulic winches located to the east and to the south of the rebar cage. Figure 3.56 shows the direction of the cardinal points based on the location of the rebar cage. Both winches were connected to the rebar cage at a height of 23-ft from the bottom. The shackle used to connect the cable to the rebar cage was big enough to embrace the longitudinal bar and the hoop as it is in the field. The shackle used to connect the cable in Specimen I is shown in Fig. 3.57. The displacement and the velocity were controlled in the hydraulic winches using a MTS FlexTest IIm controller. The load in both cables was measured with two 20-kip tension load cells located between the shackle and the cable. The displacement of the cables was measured with two displacement transducers. These transducers were attached between the winch and the point at which the cables were connected to the rebar cage; Fig. 3.58 shows the winch and the displacement transducer box located to the east of the rebar cage. The data acquisition system was a custom built module with LabView software incorporated. The sampling rate for both experiments was 8-Hz. Figure 3.59 shows the test-set up for Specimen I and Fig. 3.60 shows the set-up for Specimen II.

3.3.4 Instrumentation

Instruments were placed throughout the specimens to measure displacements, strains, and forces. As discussed in Section 3.3.3, two inline 20-kip tension load cells and two displacement transducers were used to measure the load and displacements in the cables.

The location of the strain gauges for Specimen I and II are shown in Figs. 3.61 and 3.62, respectively. A total of 48 strain gauges were used in Specimen I, and 80 strain gauges were used for Specimen II. Two sets of strain gauges were attached to each longitudinal bar, one at the bottom of the specimen and the other above the end of the bottom internal brace. The bottom internal brace of each specimen was also instrumented. Strain gauges were attached along the length of each bar to capture the strain on the onset of buckling. The strain gauges had a gauge length of 0.20-in since it was the maximum length that could be placed between the grooves of the reinforcing bars.

Displacement transducers were installed at nearly equal intervals along the height of each specimen. Figures 3.63 and 3.64 show the location of the transducers for each specimen. To obtain the three components of the displacement for each point, three transducers were placed at

each point, and each of them was attached to a fixed reference point. The reference points were located to the south, east and south-east of the specimen. Figure 3.65 shows the southern fixed point, and the displacement transducer boxes attached to it.

3.3.5 Experimental Results and Observations

3.3.5.1 Specimen I

The force-displacement responses of the cables are shown in Fig. 3.66. The initial response of the specimen could be considered linear up to 28-in of cable displacement in both directions. At this point, a small drop in the force was occurred followed by an increase in strength until 30-in of cable displacement was recorded. The maximum lateral force was reached at this point. Thereafter, sudden changes in strength and stiffness occurred until total collapse of the specimen. The collapse of the specimen was visibly progressive; no sudden collapse was observed. Figure 3.67 shows the collapsed rebar cage.

The three components of displacement were calculated by taking the results obtained from the displacement transducers attached to the specimen and making geometrical triangulations. The reference axes X and Y are located in the direction of the cardinal lines of the compass, South and East, respectively. Figure 3.68 shows the resultant displacement in the XY plane of each point along the height of the specimen in relation to cable displacement. For small values of cable displacement almost no drift occurred between the points where the braces were located, i.e. bottom brace located between points 0 and 2 and top brace located between points 4 and 6. The drift was larger in the zone between points 2 and 4 where there was no brace. This indicates the braces stiffen the zone where they are located. However, for values of cable displacement larger than 30 in, the drift between points 0 and 2 was increased. This is attributed to loss in lateral stiffness of the brace due to the buckling of the brace bars.

Figures 3.69 and 3.70 show the deformed shape observed from different points of view. Figure 3.71 shows a sequence of deformed shapes taken during testing from the east winch. The deformed shape profile presented in the photos is similar to the one obtained from the displacement transducers.

Figures 3.72 and 3.73 show two different types of tie connections after collapse. The first is a completely ruptured quadruple-snap tie wire connection, and the second is a strong-tie that remained intact, keeping the hoop normal to the longitudinal bar.

Figures 3.74 to 3.81 show the strain recorded in the longitudinal and bottom brace bars. At 28-in of cable displacement a small drop in the force was occurred which coincided with a large increase in strain at the middle of the north bar of the bottom brace (strain gauge is identified as SG29) as shown in Fig. 3.80. The strain values were greater than 2,200 micro strains which was the yielding strain determined for the brace bars in Section 3.3.2; thus the bar was yielding at this point. At 30-in of cable displacement a drop in the force considerably larger than the earlier drop occurred. This drop in force was attributed to the buckling of the north bar of the bottom brace based on the large strains that were recorded for this bar. Figure 3.82 shows one of the bars from the brace after the rebar cage collapsed. The large deformations and buckling of bars were concentrated in the bottom brace, the top one did not present any sign of buckling or

large deformations as shown in Fig. 3.83. The common point of the bottom braces, where each bar was welded to each other, was preserved after collapse as shown in Fig. 3.84.

After the drop in force and buckling of the north bar of the bottom brace, there was an increase in the force capacity of the rebar cage until 36-in of cable displacement was recorded where another drop took place. This drop in force could be attributed to the buckling of the east bar in the bottom brace based on the large strains that were recorded for the strain gauge SG32, as shown in Fig. 3.80. The increase of capacity at 30-in of cable displacement was due to the change in the load path after the buckling of the north bar in the bottom brace. The strain in the middle of the east bar (SG32) increased considerably after the buckling of the north bar (SG29). This indicates that the load of the north bar was transmitted to the east bar. The increase in strains was almost at the same rate as the north bar until 36-in of cable displacement. It can be concluded that the bar buckled based on the drop in the force of the cables and the large strains recorded.

Figure 3.74 shows the strains recorded at the bottom of the specimen. Negative values of strain represent tensile strains and positive values represent compression strains. It can be concluded that half of the longitudinal bars are subjected to compression and the other half to tension. The neutral axis was parallel to a line running in the North-East direction.

The strains obtained at the bottom of the specimen and the top of the bottom brace for the longitudinal bars are plotted in Figs. 3.74 and 3.75, respectively. These two plots show how the internal brace changes the load path inside the rebar cage. For cable displacement values less than 30-in, the deformations in the longitudinal bars were concentrated at the top of the bottom brace. Some of the bars even reached strains up to their yielding point. The deformations in the bottom of the rebar cage for this range of cable displacement were small (less than 1000 micro strains). It is to note that the bottom brace carried the load and transferred it directly to the support of the rebar cage. After 30-in of cable displacement, the bars of the bottom brace started to buckle and the braces lost its ability to withstand any load. The strains at the top of the bottom brace decreased and the strains at the bottom of the cage increased gradually. This indicates that the load was transferred from the bottom brace to the longitudinal bars. For values of cable displacement greater than 35-in some of the longitudinal bars reached their yielding strain, affirming the transfer of the load to the longitudinal bars. Figure 3.85 shows a close up of the bottom of the rebar cage after collapse; loss of tie wires and displacement of hoops were observed.

The strains recorded at the first level of the bottom brace, at height equal to 11-in, are shown in Fig. 3.76. Strain values less than the yield strain were recorded. There is no indication of large deformation in the bars of the bottom brace at this point. The strains recorded at the second and third level of the bottom brace are shown in Figs. 3.77 and 3.78. Strains less than the yield strain were also recorded at these locations. It can be concluded that the bars below the common point of the bottom brace did not undergo large deformations. Furthermore, the weld used in the common point of the bars in the bottom brace could be taken as a rigid connection that restrained the deformation of the brace bars.

Figure 3.77 shows an increase in strains at the middle length of the south bar in the bottom brace (SG19). This bar is the same as north bar that first buckled at 30-in of cable displacement in all respects except that the location of the strain gauge is below the common

point of the bars. The increase of strain at SG19 could be attributed to the initiation of the buckling at the north bar and the sudden decrease in strain was due the loss of strength produced by the absolute buckling of the north bar.

The strains recorded at the fourth level of the bottom brace, just above the common point of the brace bars, are shown in Fig. 3.79. Strains recorded in SG28 were greater than the yield strain for values of cable displacement larger than 30-in. A decrease in strain was presented at 36-in of cable displacement which confirms the buckling of the west bar of the bottom brace.

Figure 3.81 shows the strains recorded at the sixth level of the bottom brace. This location of strain gauges was close to the top end of the brace. Small strains were recorded, which could be attributed to the closeness of the strain gauges to the connection between the brace bars and longitudinal bars. It could be concluded that the tie wires used to connect the brace bars with the longitudinal bars were rigid enough to restrain the deformation of the bars.

3.3.5.2 Specimen II

The force-displacement responses in the direction of both cables are shown in Fig. 3.86. The initial lateral response of the rebar cage is linear until 24-in of cable displacement where the first drop in the force was observed. Unlike the first specimen, the drop is not large and the force kept increasing showing variable stiffness until 50-in of cable displacement. At this point a sudden change in strength and stiffness was exhibited, and sudden changes in strength and stiffness occurred until the collapse of the specimen. The collapse of the specimen was progressive; no sudden collapse was observed. Figure 3.87 shows the collapsed rebar cage.

The resultant displacement of each point in the XY-plane along the height of the specimen in relation to cable displacement is shown in Fig. 3.88. For this specimen only five points were plotted because no data was obtained from the displacement transducer at the top point due to instrument failure. The behavior is similar to Specimen I; for small values of cable displacement almost no drift was obtained between the points where the bottom brace was located, points 0 and 2. The drift was significantly greater between points 2 and 4 where there was no brace. As the cable displacement increased, the drift between the points 0 and 2 increased, which could be attributed to the buckling of the bars in the bottom brace. Figure 3.89 shows a sequence of deformed shapes during the testing taken from the northern side of the specimen. The shape in the deformed profile presented in the photos is similar to the one obtained from the displacement transducers.

Unlike the first specimen, some connections between the bars in the brace at common points failed toward the end of the experiment as shown in Fig. 3.90. Large deformations were observed at the top brace as shown in Fig. 3.91.

Figures 3.92 to 3.99 show the strain recorded in the longitudinal and bottom brace bars. The behavior of the strain response for the longitudinal bars at the bottom of the rebar cage and at the top of the bottom brace is similar to the response of Specimen I, as shown in Fig. 3.92 to 3.95. After 24-in of cable displacement, when the first drop of force in the cables was shown, the strains of the longitudinal bars at the bottom of the rebar cage increased gradually, and the strains of the longitudinal bars at the top of the bottom brace decreased. This same behavior was

observed in the Specimen I and it was concluded that the load was transferred from the braces to the longitudinal bars due to the buckling of the brace bars. The lack of big drops in the force and large strains in the brace bars could be attributed to the larger number of bars that the Square brace has. This allowed a better distribution of the force through the cage. Also, the bars of the square brace have more common points between each other than the bars of the X-brace, which made their buckling more gradual and not as sudden as the buckling presented in Specimen I. Figure 3.100 shows a close up of the bottom of the rebar cage after collapse.

Figures 3.92 and 3.93 shows the strains recorded at the bottom of the specimen. It can be concluded that half of the longitudinal bars are subjected to compression and the other half to tension. The neutral axis was parallel to a line running in the North-East direction. However, unlike Specimen I, the direction of the neutral axis was slightly changed due to the change in sign of SG4 and SG16 which occurred at a value of cable displacement around 40-in.

The strains obtained from the instrumentation of the first level of the brace do not show any indication of large strains as shown in Fig. 3.96. Strains less than the yield strain were recorded. Figures 3.97 and 3.98 show the strains recorded at the second and third level of the bottom brace. These locations were below and above the common point of the 8 brace bars, respectively. Strains greater than the yield strain were experienced by SG38 and SG46.

The strains recorded at the fourth level of bottom brace are shown in Fig. 3.99. Strains slightly greater than the yield strain were obtained at this location. A drop in the strain for SG53, SG56, and SG55 was presented around 24-in of cable displacement. This could be an indication of loss in the strength. A possible buckling of these bars may have occurred causing the first drop in the force-displacement response of the cables.

At 51-in of cable displacement, a large drop in force occurred. This drop could be attributed to the buckling of a bar brace or a failure of one of the connections between the bar braces. This was concluded from observations after the collapse of the specimen because the data recorded from the strain gauges in the bar braces did not show any indication of this phenomenon. After this drop, the force increased at sporadic increments with subsequent drops until the progressive collapse was reached.

Chapter 4
Calibration of Computational Model and Parametric Studies

4.1 Introduction

This chapter discusses the calibration of the analytical model based on the results obtained from the full-scale column rebar cage experiments and the results of the parametric analysis. The analysis results showed that the internal braces and their boundary conditions play a critical role in the overall lateral behavior and response of bridge column rebar cages. Using the calibrated computational model, analyses were conducted to identify the effect of different aspects on the lateral behavior of bridge column rebar cages. The parameters used in this study were: tie wire gauge, type and number of tie wire connections, longitudinal and transverse reinforcement, presence and type of braces, location of pick-up bars and height of braces.

4.2 Material Properties and Modeling

The longitudinal and internal brace bars were modeled with the ADINA Elastic-plastic Moment-Curvature beam element with multilinear plasticity as presented in Section 2.5.

4.2.1 Stress-Strain Curves

The stress-strain curve of steel used in the computational model was obtained from the coupon tests performed on #8 and #11 bars as presented in Section 3.3.2. Based on these tests, the yield strength and ultimate strength of #8 rebar were equal to 72.8 ksi and 98.1 ksi, respectively. The results of the #11 coupon tests showed that the yield strength and ultimate strength were equal to 71.1 ksi and 98.0 ksi, respectively. Figure 4.1 shows the stress-strain curves for both #8 and #11 reinforcing bar.

4.2.2 Flexural Moment-Axial Force-Curvature Curves

The moment-curvature relations (M-P-ϕ) for #8 and #11 reinforcing bars were obtained using the section analysis program XTRACT (TRC, 2006) for a series of axial loads. Figures 4.2 and 4.3 show the results of the section analyses.

4.2.3 Torsional Moment-Axial Force-Twist Curves

A nonlinear three-dimensional finite element model of a #6 reinforcing bar under torsion was developed as shown in Fig. 4.4. The model matched the experimental conditions, the bar diameter was equal to 0.75-in and the free length was equal to 9.25-in. The finite element model was calibrated based on the torsion test conducted and discussed in Section 3.2.3.2. Figure 4.5 shows the comparison of the experimental and analytical results. Using the calibrated computational model, torsional moment-axial force-twist (T-P-θ) curves were determined for a #11 reinforcing bar. Figures 4.6 and 4.7 show the torsional moment-twist curves for tension and compression axial loads, respectively.

4.2.4   Tie Wire Connection Behavior

The tie wire connections were modeled with nonlinear translational and rotational springs as shown in Section 2.5.2. Section 3.2.2 discussed series of experiments that were carried out to determine the force-deformation responses of six different tie wire connections made by an experienced iron worker. The tested connections were: single snap, double-snap, single-U, double-U, column-tie, and wrap-and-saddle. From the results of these experiments, nonlinear relationships for the translational (Δx, Δy and Δz) and rotational (θx) springs were defined for the six types of connection. Figure 4.8 shows the idealized force-deformation curves for the spring (Δx) for all the connections. Figure 4.9 shows the idealized force-deformation curves for the translational spring (Δy and Δz) for all the connections. The force-deformation relationship of the tie wire connections was assumed to be symmetrical in these two directions. The force-deformation curve for Δy and Δz of wrap-and-saddle tie wire connection illustrates the relationship that occurs when an extra wrap is made around the hoop. This is based on construction practices for this type of tie wire connection. Figure 4.10 shows the torque-rotation curves for the rotational spring (θx) for all the connection.

The force-deformation curves defined for a 4-snap tie wire connection were calculated based on a double-snap. The response of a 4-snap was idealized as two times the response obtained from a double-snap tie wire connection.

The behavior of a strong-tie connection was idealized as a rigid connection in the three translational degrees of freedom as well as in the normal rotational degree of freedom.

4.3 Analytical Model Calibration

Analytical models for the full-scale experimental specimens were created using the ADINA finite element program. The geometry, the number of longitudinal bars, the hoop spacing, the location of internal braces, and the distribution of tie wire connections were defined based on the experimental specimen properties, as shown in Table 3.8 and Figs. 3.45 and 3.46. Figures 4.11 and 4.12 show the analytical models for both specimens. The properties, load application and the analysis method of the computational model were discussed in Section 2.5.

The calibration of the analytical model was accomplished by performing sensitivity analyses for the connections between longitudinal bars and brace bars. Figure 2.30 shows a close-up of the connection between the end of one brace bar to the longitudinal bar. The end of the brace bars is welded to the inner ring and tied to the longitudinal bar. The experimental and analytical results were compared in the form of resultant cable forces vs. resultant cable displacements.

4.3.1   Brace Boundary Conditions

Two analytical models were defined to determine the upper and lower bounds of the sensitivity analyses on the end brace boundary condition. A model with rigid connections between longitudinal and brace bars was defined as the upper bound, and a model with pinned connections was defined as the lower bound. The analytical and experimental results are compared in Figs. 4.13 and 4.14. The force-displacement curves of the model with rigid

connections showed a greater stiffness and strength in comparison to the experimental curves. The force-displacement curve of the rigid connection model for Specimen I showed a linear response until the maximum force of about 4,000 lb was reached. A similar trend is present in the experimental results. The curve representing the model with rigid connections for Specimen II showed an initial linear response, followed by a gradual loss of stiffness until the maximum force of about 7,000 lb was reached. Again a similar trend is present in the experimental results. The responses of the models with pinned connections underestimate the stiffness of the specimens, and no ultimate strength was evident. Therefore, the flexibility of the connection between longitudinal bars and brace bars should be defined as semi-rigid connections.

As a first estimate, the behavior of the connection between longitudinal bars and brace bars was defined as linear. The translational and rotational stiffnesses were defined based on the stiffnesses of a column-tie tie wire connection. The stiffness of the normal translational spring (Δx) was equal to 16,000 lb/in, the stiffnesses of the tangential (Δy) and vertical (Δz) springs were equal to 875 lb/in, and the stiffness of the rotational spring (θx) was equal to 172 lb-in/rad. The results from the analyses of the models assuming a linear column-tie connection and the experimental results are also compared in Figs. 4.13 and 4.14. The initial stiffnesses of the experimental and analytical models were similar for resultant cable displacements of less than 10-in. For larger resultant displacements, the stiffnesses of the specimens were underestimated, and no noticeable ultimate strength was obtained for either of the analytical models.

4.3.2   Sensitivity Analysis on End Brace Boundary Condition

Analyses were performed to study the effect of each degree of freedom of the longitudinal bar to brace bar connection on the overall response of column rebar cages. The boundary condition of each degree of freedom for the bracing elements was made rigid to determine the effect in the overall behavior of column rebar cages. The results obtained from the analytical analyses of Specimen I and II are shown in Figs. 4.15 and 4.16. It is clear that the vertical translation (Δz) degree of freedom has a greater effect on the lateral response of column rebar cages than the other boundary conditions. Therefore, the calibration process was based on sensitivity analyses for this translational degree of freedom.

4.3.3   Vertical Translational Linear Spring at Brace Boundary

Sensitivity analyses were performed to determine the effect of the vertical translational (Δy) spring stiffness on the lateral behavior of column rebar cages. The sensitivity analyses were performed on the connection between longitudinal reinforcing bars and brace bars. Three vertical translational stiffnesses were defined based on the initial stiffness of a column-tie tie wire connection. The values were equal to 4,375 lb/in, 8,750 lb/in, and 87,500 lb/in, which correspond to 5, 10, and 100 times the initial translational vertical stiffness of a column-tie tie wire connection. Figures 4.17 and 4.18 compare the experimental results and the results obtained from the analytical models. The initial lateral stiffness of column rebar cages increases with the stiffness of the vertical translational springs at the bracing elements. An increase in the stiffness of the vertical translational springs generates a greater contribution of the braces in the overall lateral response. The stiffnesses of the curves representing 10 times the initial stiffness of a column-tie (8,750 lb/in) and 100 times the initial stiffness of a column-tie (87,500 lb/in) were greater than the stiffnesses of the experimental curves. However, the stiffness of the curve representing 5 times the initial stiffness of a column-tie (4,375 lb/in) for Specimen I was similar

to the stiffness of the experimental curve for resultant cable displacements up to 22-in. An ultimate strength was obtained from the response curves of the analytical models which, based on the analytical results, is not sensitive to the translational vertical stiffness of the connection between longitudinal and brace bars. However, the analytical models underestimate the ultimate strengths of the specimens obtained from the experiments.

The results of the sensitivity analyses for the vertical translational linear springs showed that the best correlation to experimental results was obtained with a vertical spring stiffness of 4,375 lb/in.

4.3.4 Vertical Translational Nonlinear Springs at Brace Boundary

The force-deformation relationship (Curve-1) for the vertical translational spring was defined as bilinear and shown in Fig. 4.19. The initial stiffness is the same as a column-tie connection, 875 lb/in. The second stiffness was defined as equal to 4,375 lb/in, five times the initial stiffness. The analytical and experimental responses are shown in Fig. 4.20 and 4.21. A better agreement was obtained between the experimental and analytical curves using this bilinear definition. A slight change in the model response stiffness was seen at 7-in of resultant cable displacement for Specimen I and at 12-in of resultant cable displacement for Specimen II. This could be attributed to the vertical translational bilinear spring (Δx) at the bracing elements boundary condition. The correlation between the analytical model and the experimental results was highly improved while the strength was underestimated.

A force-deformation relationship (Curve-2) for the vertical translational degree of freedom was defined as shown in Fig. 4.19. The second stiffness of the translational spring (Δz) was doubled to increase the strength of the computational model.

4.3.5 Analytical Model Calibration of Bridge Column Rebar Cages

The calibration of the analytical model was achieved by performing sensitivity analyses on the longitudinal bar to brace bar connection. The analyses showed that this connection should be defined as semi-rigid and the critical degree of freedom was the vertical translational (Δz). The behavior of this spring was defined as linear based on the stiffness of a column-tie connection. The results of these analyses showed a good correlation with the initial stiffness of the experimental curve, but the strength was greatly underestimated. Thus, a bilinear behavior (Curve-1) was defined for the same spring improving the correlation with the experimental results, but the strength was still underestimated. The calibration of the computational models with X-braces and Square braces were achieved defining the behavior of the vertical translational (Δz) spring in the longitudinal bar to brace bar connection as Curve-2 shown in Fig. 4.19. The following two sections discuss the results of the analytical analyses for both experimental specimens.

4.3.5.1 Calibrated Analytical Model of Specimen I

The analytical model results and the experimental results for Specimen I are compared in Fig. 4.22. The results show a good correlation between the response of the analytical model and the experimental curve for resultant cable displacements less than 50-in. The initial linear

36

response shown by the experimental curve was captured by the computational model. The analytical model also matched the maximum resultant cable force obtained from the test; the difference in maximum force was less than 2%. Following the first drop in the force, the experimental response curve showed an increase in the force up to 3,200 lb which was also captured by the computational model with a difference less than 6.5%.

Figure 4.23 shows the axial force-resultant cable displacement curves for the north bar (Brace A) and west bar (Brace B) of the bottom brace from the analytical model. The maximum axial force of "Brace A" was obtained at 40-in followed by a loss of strength. The buckling load of this bar was equal to 4,976 lb based on the analytical results. Figure 4.24 shows the deformed shape of the bottom brace at 40-in of resultant cable displacement obtained from the computational model. The maximum force of "Brace B" was obtained at 48-in followed by a loss of strength. The buckling load of this bar was equal to 4,620 kips. The lower buckling load of "Brace B" could be attributed to the boundary conditions. After buckling had occurred in "Brace A", the common point of the brace bars had consequently experienced deformations that affected the behavior of the "Bar B". It could be concluded that the analytical model captured the buckling of both brace bars. The buckling loads of both braces are in between the upper and lower bounds discussed in Section 2.5.1 and shown in Fig. 2.32.

Figure 4.25 compares the measured displacement with the computational model displacements of one of the longitudinal bars in the XY plane. Ratios of experimental results over the analytical model results are tabulated in Table 4.1. The profile of the deformed shape was captured by the analytical model. In general, the computational model overestimated the displacements by an average of 6%. Good agreement was obtained between the measured displacements and the analytical model for resultant cable displacements of 30.0-in and 43.4-in. The displacements obtained from the computational model at Point 2, located at the top of the bottom brace, were overestimated by an average of 30%.

Figure 4.26 shows the location of the fractured tie wire connections up to 40-in of resultant cable displacement obtained from the computational model of Specimen I. The fracture of the tie wire connections initiated at 34-in of resultant cable displacement. A total of eleven (11) tie wire connections were fractured, about 2% of the total of tie wire connections used in Specimen I. Two of them were located at the template hoops and one of them was located at the pick-up bars. The rest of them, eight, were located at the field zone.

In general, a good overall correlation was seen between the experimental and analytical results for resultant cable displacements less than 50-inch. This range of displacement covers the linear behavior and the ultimate strength of the bridge column rebar cage which is the scope of this investigation.

4.3.5.2 Calibrated Analytical Model of Specimen II

Figure 4.27 shows the comparison between the experimental results and the computational model results for Specimen II. There was reasonably good agreement between the analytical model and the experimental test curves for resultant cable displacement less than 33-in. After this displacement, the experimental curve was slightly lower than the analytical, and the changes in the stiffness were not captured by the analytical model. The maximum force obtained

from the test was equal to 7,180 lb. The computational model maximum force was slightly higher than the experimental, 7,300 lb; a difference of less than 5%. A drop in cable force at 72-in of resultant cable displacement was shown by the experimental response curve. This drop was attributed to the buckling of the bottom brace based on the data obtained from the instrumentation of the specimen. The drop in stiffness was captured by the analytical model at 74-in of resultant cable displacement, a difference of less than 3% when compared to the experimental response curve. The experimental curve showed an increase in force after the drop at 72-in of resultant cable displacement, which was not captured by the analytical model.

The axial force-resultant cable displacement curves obtained from the analytical model for four bars of the bottom brace are shown in Fig. 4.28. The curves show a loss of strength at about 33-in of result cable displacement for all of the bars. This is coincident with the change in stiffness in the resultant cable force-resultant cable displacement curve response. The loss of strength in the bars was gradual. This could be attributed to the number of brace bars, which allowed a better distribution of stiffness at that location. The axial force in "Brace 1" increased until 66-in of resultant cable displacement which coincided with the maximum force at the cables. This increase could be attributed to a redistribution of the force inside the bottom brace bars. The stiffness of the column rebar cage was reduced because a lower number of bottom brace bars were engaged. The column rebar cage reached its maximum load when "Brace 1" reached its maximum load too.

For resultant cable displacements between 33-in and 72-in, the computational model overestimated the force. The drastic changes in stiffness shown by the experimental curve were not captured by the analytical model; instead, the change in stiffness shown by the analytical curve was gradual until the maximum load was reached. Redistribution of the load inside the bottom brace bars occurred within this range of displacement, which could be the reason for the changes in the stiffness.

The measured and the computational model displacements of one of the longitudinal bars in the XY plane are compared in Fig. 4.29. It is to note here that for this specimen only 5 points along the length of the rebar cage were measured. However, the analytical result for this point is showed. Ratios of the experiment results over the analytical model results are tabulated in Table 4.2. The profile of the deformed shape was captured by the analytical model. For resultant cable displacements less than-16 in, the displacements were overestimated by an average of 28%. For resultant cable displacements larger than 29-in, the displacements were underestimated by an average of 22%. The agreement between computational and experimental results of Specimen II was not as good as the one obtained for Specimen I. However, it could be considered a good agreement for the elastic range and ultimate strength.

Figures 4.30 and 4.31 show the location of the fractured tie wire connections up to 70-in of resultant cable displacement obtained from the computational model of Specimen II. The fracture of the tie wire connections initiated at 55-in of resultant cable displacement. A total of forty two (42) tie wire connections were fractured, about 1.5% of the total of tie wire connections used in Specimen II. Only two of them were located at the template hoops and the rest of them were located at the field zone.

In general, there was a good overall correlation between the experimental and the analytical results for resultant cable displacements less than 72-inch. This range of displacement covers the linear behavior and the ultimate strength of the bridge column rebar cage which is the scope of this investigation.

Based on the results obtained from the analysis, it could be concluded that the correlation level in both computational models is good in relation to the overall response, elastic and inelastic stiffness, and ultimate strength. It is to note here that both calibrated models were obtained with equal force-deformation relationship for the vertical translational spring at the bracing elements boundary conditions. Therefore, the computational models can be used to predict the lateral behavior of bridge column rebar cages with X-braces and Square braces.

4.4 Influence of Critical Parameters on the Overall Behavior of Bridge Column Rebar Cages

A series of analytical models were investigated to identify the effect of critical aspects in the behavior of bridge column rebar cages. The below parameters were investigated:

- Tie wire gauge
- Type and number of tie wire connections
- Longitudinal and transverse reinforcement ratios
- Presence and type of internal braces
- Location of pick-up bars to internal braces
- Height of braces

The dimensions, and longitudinal and transverse reinforcement ratios of the computational models were the same as the experimental specimens. The minimum tying consists of only tie wire connections along the length of pick-up bars and at template hoops representing the lower bound. The maximum tying consists of tie wire connections at every intersection between longitudinal and transverse bars representing the upper bound.

4.4.1   Effect of Tie Wire Gauge

Analytical studies were conducted to determine the effect of the tie wire gauge on the lateral response. No. 15 gauge tie wire connections and No. 16 gauge tie wire connections were used in models of column rebar cages without braces. The dimensions of both tie wires gauges are presented in Table 2.1, the diameters of No. 15 and No. 16 gauge tie wires are equal to 0.072 in and 0.062 in, respectively. Therefore, the geometric length scaling factor is equal to 0.861. Based on this factor, the force-deformation relations and the torque-rotation relations for tie wire connections made of No. 15 gauge were scaled to obtain the relations for tie wire connections made of No. 16 gauge. The force scaling factor was calculated by raising the geometric length scaling factor to the second power, and the moment scaling factor was calculated by raising the geometric length scaling factor to the third power. The force was scaled by 0.742, the deformation by 0.861, and the torque by 0.639. Figure 4.32 compares the results obtained from the analyses of Specimen I without braces and minimum tying with No. 15 gauge and No. 16 gauge wrap-and-saddle tie wire connections. The force-displacement curves show that the response of bridge column rebar cages is affected by the tie wire gauge of the tie wire

connections. The use of No. 16 gauge tie wires in the tie wire connections reduced the lateral stiffness of the bridge column rebar cages by 40%. The use of a smaller tie wire gauge produces connections with lower strength, which reduces the stiffness and strength of bridge column rebar cages.

4.4.2   Effect of Tying

4.4.2.1 *Tie Wire Connections at Template hoops*

Based on the mapping of tie wire connections for the test specimens discussed in Section 3.3.1, the most common types of tie wire connections used at template hoops were wrap-and-saddle and strong-tie. In Specimen I, around 50% of the tie wire connections at the template hoops were wrap-and-saddle and 22% were strong-tie. The remaining 28% was a combination of quadruple-snap and column-tie connections, as shown in Table 3.11. In Specimen II, the distribution of tie wire connections at template hoops was 68% wrap-and-saddle, 16% strong-tie, and 16% other tie wire connections (double-snap, quadruple-snap, and column-tie), as shown in Table 3.14. Computational models of column rebar cages without braces and consisting of wrap-and-saddle and strong-tie tie wire connections at template hoops were analyzed. The results of these analyses are compared with the results of rebar cage models without braces and with experimental tying in Figs. 4.33 and 4.34. It is clear that the use of strong-tie tie wire connections at the template hoops increases the stiffness and strength of bridge column rebar cages. The increase is most evident in Specimen II because there are more intersections between longitudinal bars and template hoops due to the larger longitudinal reinforcement ratio. The increase in the stiffness and strength of bridge column rebar cages due to the use of strong-tie tie wire connections at the template hoops could be attributed to the large stiffness assigned to this type of connection in the computational model. The use of strong-tie connections increases the framing action between longitudinal and transverse reinforcement bars which, in turn, increases the stiffness and strength of column rebar cages. The curves in Fig. 4.30 show that the stiffness of the model with experiment tying is larger than the stiffness of the model with wrap-and-saddle tie wire connections at the template hoops. The use of strong-tie in 22% of the connections of template hoops increased the stiffness by almost 3.2 times. A similar observation can be made in Fig. 4.31; the use of strong-tie in 16% of the connections of template hoops increased the stiffness by almost 8 times.

Based on the results presented above, it could be concluded that the lateral stiffness of bridge column rebar cages is increased by the percentage of strong-ties at template hoops.

Welded Template Hoops

Analytical studies were conducted to determine the effect of welding the template hoops to the longitudinal bars. In the computational model, the connections template hoops to longitudinal bars were modeled rigid in all the degree of freedoms (Δx, Δy, Δz, θx, θy, and θz). Figures 4.35 and 4.36 show the results for Specimen I and II without braces and experimental tying condition, and template hoops welded to the longitudinal bars, respectively. It is evident that welding the template hoops to the longitudinal bars increases the lateral stiffness and strength of bridge column rebar cages. The strength of Specimen I with template hoops welded to longitudinal bars is almost seven times the strength of the cage with experimental tying. The strength of Specimen II increased nearly nine times with the welded template hoops. Similar

conclusions can be made for the stiffness, for both specimens the increase was almost ten times. Therefore, welding the template hoops to the longitudinal bars has a significantly effect on the behavior of bridge column rebar cages without braces.

4.4.2.2 Tie Wire Connections at Pick-up bars

Based on the mapping of tie wire connections for the test specimens, most of the tie wire connections used at pick-up bars were double-snap and quadruple-snap. In Specimen I, 24% of the connections at pick-up bars were double-snap and 66% were quadruple-snap. In Specimen II, the distribution of tie wire connections at pick-up bars was 86% double-snap and 6% quadruple-snap. Computational models of column rebar cages without braces and with double-snap and quadruple-snap tie wire connections at pick-up bars were analyzed. Figures 4.37 and 4.38 show the comparison of the results of these analyses with the results of rebar cage models without braces and with experimental tying. The stiffness and strength of bridge column rebar cages are increased by the strength of the tie wire connections used at the pick-up bars. Similar trends are apparent when comparing the response curves of the analyzed models with slightly greater stiffness and strength of models with quadruple-snap tie wire connections at pick-up bars. The response curve for experimental tying is located between the upper bound (quadruple-snap tie wire connections at pick-up bars) and lower bound (double-snap tie wire connections at pick-up bars) due to the combination of both types of connections at the pick-up bars.

The increase in the stiffness produced by the use of quadruple-snap at pick-up bars was around 6% for Specimen I and 4% for Specimen II. Therefore, it can be concluded that the lateral response of bridge column rebar cages is slightly affected by the type of tie wire connection used at pick-up bars.

4.4.2.3 Number of Tie Wire Connections

The number of tie wire connections was varied between minimum tying and maximum tying. The responses of Specimen I without braces for minimum and maximum tying conditions using wrap-and-saddle connections are shown in Fig. 4.39. The curves show how the number of tie wire connections affects the stiffness of bridge column rebar cages. The lateral stiffness of Specimen I without braces and with maximum tying is nearly 2.5 times greater than with minimum tying. Therefore, it can be concluded that the stiffness of bridge column rebar cages increases with the number of tie wire connections.

4.4.2.4 Type of Tie Wire Connection

The effect of the type of tie wire connection on the lateral response of bridge column rebar cages was also investigated. Models of column rebar cages without braces and with minimum tying condition using double-snap, column-tie, and wrap-and-saddle tie wire connections were analyzed. Figure 4.40 compares the response curves of the analyzed models and the effect of the type of tie wire connection on the stiffness of bridge column rebar cages. The lowest stiffness was obtained from the model with double-snap tie wire connections which is the connection with the lowest strength among the three connections. The use of column-tie connections increased the stiffness almost two times. The stiffness was increased almost 2.8 times by using wrap-and-saddle, which is the tie wire connection with the highest strength among the

three connections. Therefore, it can be concluded that the stiffness of bridge column rebar cages increases with the strength of tie wire connections.

4.4.3 Effect of Transverse and Longitudinal Reinforcement Ratios

Computational models of column rebar cages without braces and with minimum tying using wrap-and-saddle connections and longitudinal and transverse reinforcement ratios between 1% and 2% were analyzed. Figure 4.41 shows the results of models with transverse reinforcement ratios of 1% and 2%. Increasing the transverse reinforcement ratio reduced the stiffness of the column rebar cages. The stiffness was reduced almost 12%. Although increasing the transverse reinforcement ratio increases the number of tie wire connections at pick-up bars, the total weight of the reinforcement is also increased. Therefore, the reduction in stiffness could be attributed to the increase in weight produced by the greater number of hoops in the column rebar cage. The results of models with longitudinal reinforcement ratios of 1% and 2% are compared in Fig. 4.42. The increase of the longitudinal reinforcement ratio nearly doubled the stiffness.

Based on the results of the analyses presented previously, it could be concluded that the lateral stiffness of bridge column rebar cages is slightly affected by the transverse reinforcement ratio in comparison to the effect of the longitudinal reinforcement ratio. Therefore, the effect of the lateral reinforcement ratio on the stiffness of column rebar cages can be neglected. Furthermore, it can be concluded that the stiffness of bridge column rebar cages increases with the longitudinal reinforcement ratio.

4.4.4 Effect of Presence and Type of Internal Braces

Analytical analyses were conducted to determine the effect of the presence and type of internal braces on the lateral stiffness and strength of bridge column rebar cages. The two calibrated computational models were used. These models have the same geometrical properties and tying as the experimental specimens without braces. The response curves of the models for Specimen I with X-braces, Square braces, and without braces are compared in Fig. 4.43. The response curves of the models for Specimen II are compared in Fig. 4.44. It is evident that the use of braces increased the lateral stiffness and strength of the column rebar cages. The strength of Specimen I using X-braces is almost three times the strength of the cage without braces. The strength of Specimen II without braces was nearly doubled when X-braces were used. The use of Square braces had a greater effect on the strength of both specimens without braces. The strength was increased almost 4.8 times for Specimen I and 3.6 times for Specimen II. Adding X-braces to Specimen I and Specimen II increased the lateral stiffness by 2.5 and 1.8 times, respectively. The use of Square braces generated a greater increase of the lateral stiffness for both specimens without braces; almost 3.2 times for Specimen I and 2.3 times for Specimen II.

Based on the results from the models with and without braces, it could be concluded that the stiffness and strength of bridge column rebar cages is significantly increased by the presence of internal braces. Furthermore, the increase in the lateral stiffness and strength produced by the use of Square braces is greater than X-braces.

4.4.5 Effect of the Location of Pick-Up Bars

Analytical analyses were conducted to determine the effect of the location of pick-up bars on the lateral stiffness and strength of bridge column rebar cages. Two locations were defined: 1) pick-up bars not coincident with internal braces and 2) pick-up bars coincident with internal braces. Figure 4.45 illustrates the locations of the pick-up bars for the two types of internal braces. The comparisons of the responses of column rebar cages with minimum tying using wrap-and-saddle with different locations of the pick-up bars are presented in Figs. 4.46 and 4.47. The curves show how the location of pick-up bars affects the behavior of bridge column rebar cages. When the pick-up bars were located coincident with the internal braces the strength of column rebar cages with X-braces was increased 1.41 times. A similar effect was presented for column rebar cages with Square braces; the increase in strength was around 1.43 times. Therefore, it could be concluded that locating the pick-up bars coincident with the internal braces increases the strength of column rebar cages, due to the enhancement of the boundary condition of the braces.

4.4.6 Effect of Height and Inclination of Internal Braces

Parametric studies were conducted to determine the effect of the height of internal braces on the elastic lateral stiffness of bridge column rebar cages. The height of the computational models was 34 ft, the longitudinal and transverse reinforcement ratios were 2%, and the type of brace studied was the Square brace. The height of the brace was varied from 4-ft to 12-ft, and the diameter of the rebar cages was varied from 4-ft to 8-ft. The results of the parametric analyses are presented in Fig. 4.48. It is clear that the elastic lateral stiffness of bridge column rebar cages increases with the inclination angle (β) of the internal braces. However, the elastic lateral stiffness of bridge column rebar cages is sensitive to the height-diameter ratio of bridge column rebar cages. For the same value of inclination angle (β), the elastic lateral stiffness of bridge column rebar cages is larger for small height-diameter ratios. When considering a constant height-diameter ratio, the stiffness increases with the inclination ratio. Therefore, it can be concluded that the lateral stiffness of bridge column rebar cages increases as the height-diameter ratio decreases and the stiffness becomes greater with the inclination angle.

4.5 Frequency Analysis of Calibrated Computational Models

Frequency analyses were conducted on the calibrated computational models to determine the mode shapes and periods of the test specimens. Figures 4.49 and 4.50 show the three principal mode shapes obtained from the analytical analyses for each specimen. It can be observed that the profile of the deformed shape shows a double curvature. It is also evident that modes 1 and 2 are not symmetrical for either of the specimens. The lack of symmetry on the mode shapes is attributed to the unsymmetrical tying of the specimens along the height of the column rebar cages. Mode 3 for both specimens is a torsional mode. The periods of Specimen I were equal to 2.03, 1.83 and 1.61 seconds for the first, second and third mode, respectively. The first, second and third periods for Specimen II were equal to 2.13, 1.90 and 1.33 seconds, respectively.

The principal mode shapes and periods of computational models for the specimens without braces were also determined. The first three principal mode shapes of Specimen I and II without braces are shown in Fig. 4.51 and 4.52, respectively. The first and second periods for Specimen I without braces were equal to 3.26 sec and 2.66 sec, respectively. The periods of Specimen II without braces were equal to 2.03 sec and 1.83 sec for the first and second modes.

The modes are cantilever flexural with displacements in the X and Y directions. However, the profile of the deformed shape is single curvature unlike the column rebar cages with braces which were double curvature. Therefore, the internal braces change the profile of the mode shapes of bridge column rebar cages. Furthermore, the periods were increased when the internal braces were removed, confirming the significant role of internal braces in the lateral stiffness of bridge column rebar cages.

4.6 Static Analysis of Bridge Column Rebar Cages under Accidental loading

Analytical analyses were conducted to determine the response of the test specimens under accidental lateral loading. The rebar cages were modeled without any lateral support system, i.e. without guy cables. The accidental lateral loading was defined as an incremental distributed load at the top of the column rebar cage as shown in Fig. 4.53. The load was only applied to half of the cross section and only to the top 4 ft of the column. This type of loading represents contact by a crane block to which the bridge column rebar cage could be subjected. Figure 4.54 shows the lateral response of Specimen II under accidental lateral loading. The maximum lateral load obtained from the push-over analytical analysis was equal to 7,100 lb. Similar trends were observed when comparing the response of Specimen I in Fig. 4.54 and the analytical curve in Fig. 4.27. Elastic lateral behavior was seen until about 55-in of lateral displacement and 6,600 lb of lateral force. Thus, the elastic lateral stiffness of Specimen II under accidental loading is equal to 120 lb/in. Figure 4.55 shows the deformed shape of Specimen I under accidental lateral loading. The profile of the deformed shape is double curvature. The zone where the braces are located is more rigid, thus less displacement was obtained; unlike the zone between braces, where the displacement was greater.

Other type of accidental lateral loading was defined similar to the presented above to determine the effect of an unsymmetrical loading. The new load was only applied to a quarter of the cross section and only to the top 4 ft of the cage a shown in Fig. 4.56. The response of the rebar cage under unsymmetrical loading was the same as under symmetrical lateral loading.

4.7 Static Analysis of Bridge Column Rebar Cages under Torsion

A computational model of Specimen II under torsion was analyzed to determine the torsional response of a rebar cage. The load was defined at the top of the cage as shown in Fig. 4.57. The response of the cage was obtained in the form of base torque vs. top twist and Fig. 4.58 shows the results of the analysis. The deformed shape of the longitudinal bars of the cage and a top-view of the deformed shape are shown in Fig. 4.57. The computational model exhibited a linear behavior until the maximum torque was reached. The analysis was interrupted due to a fail in the connection between the longitudinal bar and hoop where the load was applied. The maximum torque was around 28,800 lb-in at 0.95 rad (54 degrees) of twist, therefore it could be concluded that the rotational stiffness of Specimen II without braces is around 30,315 lb-in.

4.8 Dynamic Analysis of Bridge Column Rebar Cages under Accidental loading

Analytical analyses were conducted to determine the response of the test specimens under a rectangular pulse force at the top of the cage. Newmark method was used in the time integration of the governing dynamic equations. The special Newmark's case, constant average acceleration scheme was used; thus the parameters β and γ were equal to 0.5 and 0.25, respectively. Most of

the damping in bridge column rebar cages is from the deformation of the tie wire connections. The damping was assumed be equal to 5% based on Rayleigh damping. It is to note that the first and second period of Specimen I were equal to 2.03 and 1.83 seconds as discussed in Section 4.5. Assuming the same damping for both modes, the coefficients of Rayleigh damping matrix are defined by (Chopra, 2007):

$$a_0 = \xi \frac{2\omega_1 \omega_2}{\omega_1 + \omega_2} \qquad\qquad a_1 = \xi \frac{2}{\omega_1 + \omega_2}$$

Using the first and second periods of Specimen I, and a damping ratio equal to 0.05 the coefficients of the Rayleigh damping matrix, a_0 and a_1 are equal to 0.1627 sec^{-1} and 0.0153 sec.

The loading was defined as a distributed load at the top of the column rebar cage similar as the accidental loading described in Section 4.6. The dynamic analysis of a single degree of freedom system under a rectangular pulse force can be divided into two phases: forced vibration phase and free vibration phase (Chopra, 2007). During the first phase, the system is subjected to a step force. After the force ends, the second phase starts and the structure experiences free vibration. The analysis of a single degree of freedom system (Chopra, 2007) shows that the response history of the structure varies significantly by changing the duration of the pulse (t_d). The time history of the lateral displacement for different values of ratio of the pulse duration to the natural period of Specimen I is shown in Figs. 4.59 and 4.60. Similar to the response of a single degree of freedom system, the response of Specimen I varies by changing the duration of the pulse (t_d). During the application of the force, the bridge rebar cage oscillates about the static displacement with decay of motion due to damping at approximately its own natural period. After the end of the pulse, the rebar cage oscillates freely about the initial position with decay of motion. The decay could be attributed to the damping of the system and to an increase in the perpendicular displacement (Displacement-Y) due to a combination of modes as shown in Figs. 4.59 and 4.60.

The number of peaks during the forced vibration phase depends on the duration of the pulse (t_d); it increases with the duration of the pulse. The overall maximum lateral displacement of the rebar cage over the static displacement is plotted against the ratio of the pulse duration to the natural period in Fig. 4.61. This type of plot is called shock spectrum, and it can be used to find the maximum lateral displacement of the bridge column rebar cage as a function of the natural period. For ratios of the pulse duration to the natural period larger than 0.50, the overall maximum is less than 1.75 times the static displacement. For ratios less than 0.25, the overall maximum varies approximately linearly with the ratio of the pulse duration to the natural period. The maximum value of the shock spectrum is at a ratio equal to 0.50, where the maximum dynamic displacement is equal to 1.71 times the static displacement. The maximum value of the dynamic magnification factor in a single degree of freedom without damping is two. The lower value for the rebar cage is attributed to the defined damping. Therefore, it can be conservatively concluded that the maximum lateral displacement of a bridge column rebar cage under a pulse force is less than 1.75 the static displacement no matter the duration of the pulse.

The accidental contact of a crane block over a bridge column rebar cage could be described as sudden. The accidental contact could be idealized as an impulse force at the top with duration less or equal to 1 second. Based on the dynamic analysis presented above, the maximum

45

displacement on a bridge column rebar cage produce by a sudden contact of a crane hook block is 1.75 times the displacement produce by a static contact.

4.9 Parametric Analysis

Parametric analyses were conducted on bridge column rebar cages with square braces to determine the effect of critical dimensions on the lateral elastic stiffness. The investigated parameters are:

- Height: 30 ft, 40 ft, 50 ft, 60 ft, 70 ft, and 80 ft
- Column diameter: 4 ft, 6 ft and 8 ft
- Longitudinal reinforcement ratio (ρ): 1.0%, 1.5%, 2.0% and 2.5%
- Braces: #8 and #11

A typical layout of the rebar cage models with the braces and template hoops, tying, and parameters investigated, is shown in Fig. 4.62. Figure 4.63 and 4.64 show the height of the rebar cage models with the spacing between braces and template hoops. The loading used in the study was the accidental static lateral loading defined in Section 4.6. All of computational models were in the minimum tying condition and wrap-and-saddle tie wire connections were used. Based on the study of critical parameters presented in Section 4.4, the pick-up bars were selected coincident with the location of the braces. The results from the parametric analysis with brace bars #8 and #11 are shown in Appendix II. Figures from 4.65 to 4.68 show the elastic stiffness obtained from the parametric analysis. The elastic stiffness of bridge column rebar cages greatly decreases with the height-diameter ratio. Furthermore, the relationship between these two variables (elastic stiffness - height-diameter ratio) could be fitted as a linear regression using a power function as shown from Figs. 4.65 to 4.68. The approach used to fit the linear regression models was the ordinary least squares. The values of the coefficient of determination (R^2) for the model curves were larger than 0.97, which shows the goodness of fit of the model curves. The power functions are plotted in Figs. 4.69 and 4.70 for #8 and #11 brace reinforcing bars, respectively. When these figures are compared, it can be concluded that the elastic stiffness of bridge column rebar cage increases with the size of the brace bars. It can be also observed that the elastic stiffness of bridge column rebar cages increases with the longitudinal reinforcement ratio (ρ). However, the differences between the curves of ρ (1%, 1.5%, 2% and 2.5%) decrease with the height-diameter ratio (H/D) of the rebar cages. Furthermore, for values of *H/D* larger than 19 the elastic stiffness tends to about 27 lb/in no matter the size of the brace reinforcing bars.

Based on the information obtained during this investigation, most of the collapsed bridge column rebar cages had a minimum height-diameter ratio (H/D) of 8.0 and longitudinal reinforcement ratio, ρ, between 1% and 2%. The elastic stiffness of a bridge column rebar cage with #8 brace reinforcing bars, H/D equal to 8, and ρ equal to 1%, is equal to 91.8 lb/in. Doubling the longitudinal reinforcement ratio increases the lateral stiffness about 43%. The same rebar cage with #11 brace reinforcing bars, has an elastic stiffness equal to 97.7 lb/in with ρ equal to 1%, and 157.7 lb/in with ρ equal to 2%. For the latter case, the stiffness increases about 61%. For this column rebar cage, the increase in the stiffness by the use of #11 brace reinforcing bars is equal to 6% with ρ equal to 1%, and 20% with ρ equal to 2%. It is evident the #11 brace reinforcing bars is better for the lateral stability of bridge column rebar cages, particularly for a large longitudinal reinforcement ratio.

The exponents of the trend line curves for rebar cage models with #8 brace reinforcing bars were equal to -1.68, -1.59, -1.59, and -1.63 corresponding to longitudinal reinforcement ratios of 1.0%, 1.5%, 2.0%, and 2.5% as shown in Figs. 4.65 and 4.66. The average of these exponents is equal to -1.62. The proximity of these values indicates that the elastic stiffness could be approximately taken as an inverse function of the height-diameter ratio to the power of 1.62. Furthermore, the constant of the trend line curves increases with the longitudinal reinforcement ratio as shown in Fig. 4.71. The relationship between the constants and ρ could be fitted as a linear regression, with a coefficient of determination (R^2) equal to 0.93. Therefore, the elastic stiffness of bridge column rebar cages with #8 brace reinforcing bars ($K_{\#8-brace}$) in lb/in can be approximately defined by the following equations:

$$K_{\#8-brace} = \frac{G_{\#8-brace}}{\left(\dfrac{H}{D}\right)^{1.62}} \qquad (4.1)$$

where $G_{\#8\text{-brace}}$ is:
$$G_{\#8-brace} = 85000\rho + 2031 \qquad (4.2)$$

Taking the properties of Specimen II, height (H) equal to 34 ft, diameter (D) equal to 4 ft and the longitudinal reinforcement ratio (ρ) equal to 0.02, the constant $G_{\#8}$ is equal to 3,731 using Equation 4.2. Consequently, the elastic stiffness of Specimen II using Equation 4.1 is equal to 116 lb/in. The lateral analysis under static accidental loading for Specimen II discussed in Section 4.6 showed that the elastic stiffness was equal to 120 lb/in. Therefore, the stiffness calculated with Equation 4.1 is within the 97% of the stiffness based on the analytical analysis.

The same observations can be made for rebar cage models with #11 brace reinforcing bars. For this case, the exponents of the trend line curves are equal to -1.82, -1.77, -1.74, and -1.79 for longitudinal reinforcement ratios of 1.0%, 1.5%, 2.0%, and 2.5%, respectively, as shown in Figs. 4.67 and 4.68. The average of the exponents is equal to -1.78. The elastic stiffness could be approximately taken as an inverse function of the height-diameter ratio to the power of 1.78. The relationship between the constant of the curves and the longitudinal reinforcement ratio is shown in Fig. 4.72. The coefficient of determination (R^2) of the model curve was equal to 0.98 Therefore, the elastic stiffness of bridge column rebar cages with #11 brace reinforcing bars ($K_{\#11-brace}$) in lb/in can be approximately defined by the following equations:

$$K_{\#11-brace} = \frac{G_{\#11-brace}}{\left(\dfrac{H}{D}\right)^{1.78}} \qquad (4.3)$$

where $G_{\#11\text{-brace}}$ is:
$$G_{\#11-brace} = 188113\rho + 2412 \qquad (4.4)$$

These equations allows an easy, effective, and fast way to calculate the lateral elastic stiffness of bridge column rebar cages knowing the height-diameter ratio (H/D) and longitudinal

reinforcement ratio (ρ). To be able to use Equations 4.1 to 4.4, the bridge column rebar cage shall have Square braces with height equal to 10 ft, minimum tying using wrap-and-saddle, pick-up bars coincident with braces, and template hoop spaced at 7 ft.

Figures 4.73 and 4.74 shows the results of the parametric analysis for bridge column rebar cages with #8 and #11 brace bars. The elastic stiffness was plotted against the ratio height to longitudinal reinforcement ratio (H/ρ). It can be observed that it is not possible to obtain a tendency as in Figs. 4.65 to 4.68. However, it can be concluded that the elastic stiffness decreases with the ratio height to longitudinal reinforcement ratio (H/ρ). The increase in the elastic stiffness produced by changing the size of the brace bars can also be observed when Figs. 4.73 and 4.74 are compared.

The drift limit from each computational model in the parametric analysis was obtained. The drift limit was defined as the ratio of the lateral displacement before collapse to the height of the bridge column rebar cage. A total of 72 values were obtained for each size of brace bars, #8 and #11. The average and standard deviation for the drift limits of bridge column rebar cages with #8 brace bars were equal to 8.5% and 3.5%, respectively. The same parameters for bridge column rebar cages with #11 brace bars were equal to 10.9% and 3.9%, respectively. A conservative drift limit is calculated subtracting the standard deviation from the average drift limit; hence the drift limits under incremental loading of bridge column rebar cages with #8 and #11 brace bars are equal to 5% and 7%, respectively. The dynamic response of bridge column rebar cages under a pulse force is 1.75 times the static response under the same force. Therefore, the static drift limit should be divided by 1.75 to obtain a dynamic stability reference limit. Consequently, it is proposed in this investigation a reference drift limit for bridge column rebar cages with #8 and #11 brace bars equal to 3% and 4%, respectively. These drift limits take to account the stability under a sudden accidental load such as the contact of a crane block.

4.10   Reinforced Concrete Section Analysis

Section analysis using XTRACT (TRC, 2006) were performed to determine the effect of Square braces in the final ultimate strength of R/C bridge columns. The material properties were defined base on Caltrans Seismic Design Criteria (Caltrans, 2004). A concrete compressive strength equal to 4 ksi was defined and the Mander's stress-strain model for confined concrete was used. The diameter of the bridge column was equal to 4-ft and the longitudinal and transverse reinforcement ratios were equal to 2% and 2%, respectively. The properties of the rebar cage are the same as Specimen II. Five sections along the height of the column were analyzed as shown in Fig. 4.75. The results of the sectional analysis are shown in Fig. 4.76. The plastic moment of the R/C bridge column increases nearly 12% due to the internal Square brace at Section-2. This section is the upper bound because the eccentricity of the brace bars in the other sections is lower. At Section-5, where the brace bars have the lower eccentricity, the increase on the plastic moment is around 10%.

Chapter 5
Summary and Proposed Guidelines for Improved Rebar Cage Stability

5.1 Summary

This report presents the results of experimental and analytical investigations of the lateral behavior and stability of bridge column rebar cages. The main objective of this research was to develop analytical tools and specifications to predict and control the properties of tied bridge column rebar cages and reduce the potential of failure and collapse. To achieve this objective, experimental investigations were conducted on individual components of rebar cages and on two full-scale bridge column rebar cages. Using the results from the experimental studies, nonlinear finite element analyses were conducted on computational models to determine the effect of several parameters on the lateral behavior of bridge column rebar cages.

Experimental work was conducted on tie wire connections and reinforcing bars as individual components of bridge column rebar cages. The stress-strain response of No. 15 gauge tie wires were determined through coupon tests. A series of experiments were conducted to determine the nonlinear translational (Δx, Δy, and Δz) and rotational (θx) responses of the most commonly used tie wire connections under various type of loading for. The connections tested were: single-snap, double-snap, single-U, double-U, column-tie, and wrap-and-saddle. Tension and torsion tests were also carried out on different sizes of reinforcing bars to obtain the response relationships under these types of loading.

Two full-scale bridge column rebar cages were subjected to incremental loading which provided information of the lateral behavior, and failure modes, and also provided data to calibrate the computational models.

Analytical investigations were performed on a calibrated-three dimensional finite element model. The results of these analyses were used to investigate the effect of several critical parameters on the lateral behavior of bridge column rebar cages. The parameters included: tie wire connections, internal braces, column diameter, longitudinal and transverse reinforcement ratios, and column height. Based on nonlinear static and dynamic analyses, guidelines for determining the lateral stiffness and drift limit of bridge column rebar cages were proposed.

5.2 Proposed Guidelines for Improved Rebar Cage Stability

The stability of bridge rebar cages depends on the lateral stiffness provided by the guy cables and the inherent lateral stiffness of the rebar cage. Construction practices using only one crane for the erection of rebar cages has the most significant influence on the rebar cage stability for fixed base columns. When placing the steel column forms, at least two of the guy cables are released from the rebar cage. At that instance, the stability of the column rebar cage depends on its inherent stiffness, and any accidental load could easily result in the collapse of the cage. The proposed guidelines are based on experimental and analytical investigations that will enhance the lateral stiffness of the rebar cage. Any rebar cage instability based on these guidelines will be

gradual since it involves buckling of the internal braces and yielding of the longitudinal "pick-up" bars.

Based on the experimental observations, analytical results, and conclusions made in this study, the following is proposed to be added to the Caltrans Standard Specifications in Section 52: "Reinforcement" under 1.07 "Placing":

For bridge column rebar cages with diameters of 4 ft and larger:
1. *Tie wire connections shall use No. 15 gauge tie wires, soft annealed black steel with a minimum F_u = 40 ksi.*
2. *At least four vertical bars forming a square shall be tied at every intersection with at least double tie wire connections. The strength of these connections shall be adequate for cage pick-up.*
3. *At a maximum of 8 (eight) feet increments, template hoops shall be tied at every intersection with at least wrap-and-saddle tie wire connections.*
4. *At a maximum of alternating 10 (ten) feet increments, internal braces with square configurations, minimum #8 reinforcing bars, and with interlocking hoops at the ends shall be provided and connected to the longitudinal bars by at least wrap-and-saddle tie wire connections. This bracing shall be adequate for cage lift and transportation.*
5. *At least 20% of the remaining reinforcement intersections shall be tied with single tie wire connections. The connections shall be staggered from adjacent connections.*

5.3 Concluding Remarks

Based on the experimental and analytical investigations of this study the following concluding remarks may be derived.

Tie Wire Connections

- Tie wire connections made by an experienced iron worker are about 18% stronger than connections made by an inexperienced worker. The stiffness of tie wire connections made by an experienced iron worker is about 196% larger than the stiffness of connections made by an inexperienced worker. This is attributed to a better tightening and "heeling" of the connection made by an experienced iron worker producing a "tight-fit" connection.

- The experimental results of single-snap and double-snap, and single-U and double-U tie wire connections showed that doubling the wire nearly doubled the strength of tie wire connections. The double-U and the wrap-and-saddle tie wire connections have the highest connection strength among all the tested connections.

Bridge Column Rebar Cages

- Internal braces have a significant effect on the lateral behavior and failure mode of bridge column rebar cages. The stiffness and strength of bridge column rebar cages are considerably increased by the presence of internal braces. The use of X-braces almost doubled the stiffness and strength of bridge column rebar cages. The use of Square braces increased the stiffness and strength by about 2.8 and 4.2 times, respectively.

- The tie wires gauge affects the stiffness and strength of bridge column rebar cages. The use of No. 16 gauge produced connections with lower strength and reduced the stiffness of bridge column rebar cages by 40%.

- The tying at the template hoops is critical for the lateral behavior of bridge column rebar cages. If the template hoops are welded to the longitudinal bars the lateral stiffness and strength of column rebar cages are increased up to ten times.

- The transverse reinforcement ratio (ρ_s) has a small effect on the lateral behavior of bridge column rebar cages. Increasing the longitudinal reinforcement ratio (ρ) increases the stiffness and strength of column rebar cages. Doubling the longitudinal reinforcement ratio almost doubles the stiffness of bridge column rebar cages.

- The number of tie wire connections in the field zone does not have significant effect on the lateral stiffness and strength of bridge column rebar cages with internal braces.

- Placing the pick-up bars coincident with the internal braces increases the strength of bridge column rebar cages, regardless of the type of internal brace.

- The elastic stiffness of bridge column rebar cages greatly decreases with increasing the height-diameter ratio. Based on the parametric analyses conducted in this study, two equations are proposed to calculate the elastic stiffness of bridge column rebar cages.

$$K_{\#8-brace} = \frac{85000\rho + 2031}{\left(\frac{H}{D}\right)^{1.62}} \qquad K_{\#11-brace} = \frac{188113\rho + 2412}{\left(\frac{H}{D}\right)^{1.78}}$$

$K_{\#8\text{-brace}}$ = elastic stiffness of bridge column rebar cages with #8 brace bars, (lb/in)
$K_{\#11\text{-brace}}$ = elastic stiffness of bridge column rebar cages with #11 brace bars, (lb/in)
ρ = longitudinal reinforcement ratio
H = height of the column, (ft)
D = diameter of the column, (ft)

- The elastic stiffness of bridge column rebar cages increases with the size of the reinforcing bars used within the brace. The average failure drift of rebar cages with #11 brace bars is almost 1.3 times the average failure drift of rebar cages with #8 brace bars.

- The dynamic response of bridge column rebar cages under a step pulse force varies by changing the duration of the pulse. However, the maximum dynamic response is less than 1.75 times the static response and occurs about 0.5 times the period of the bridge column rebar cage.

- The drift limits for bridge column rebar cages with #8 and #11 brace bars are equal to 2.9% and 4.0%, respectively.

- The Square braces increase the final ultimate strength of R/C bridge column rebar cages around 10%.

5.4 Future Research Work

An accidental contact could produce the collapse of a rebar cage during the fraction of time that it is standing by itself or laterally supported by guy cables. However, if the rebar cage has been constructed under the guidelines proposed in this investigation, the collapse will be gradual. Regardless of this, contractors should take all care to avoid this to happen. Sometimes, the collapse of a rebar cage is inevitable; therefore the engineer needs to decide what to do with the collapsed cage. The options are to replace the complete rebar cage or repaired the damaged reinforcing bars. Therefore, it is suggested for future work to perform analytical and experimental investigations to study the behavior of R/C columns with repaired reinforcing bars after the failure of the rebar cage. The repair of the reinforcing bars could be made either by heat straightening, bar splices or other techniques that are normally used in these situations. The future investigation could evaluate which of the options, replace or repair the rebar cage, is the most economical and adequate.

References

ADINA R&D, Inc., 2010. ADINA 8.6.4, Watertown, MA

Caltrans, 2003. *Reviewing Guy Cable Plans*. California Department of Transportation, Sacramento, CA.

Caltrans, 2004. *Caltrans Seismic Design Criteria, Version 1.3*. California Department of Transportation, Sacramento, CA.

Caltrans, 2006. *Standard Specifications*. California Department of Transportation, Sacramento, CA.

Condon-Johnson & Associates, Inc, 2008. *Reinforcement Submittal – CIDH Rebar Cage*. San Diego, CA

Chopra, A. K. 2007. *Dynamics of Structures (3rd Edition)*. Prentice Hall.

CRSI, Concrete Reinforcing Steel Institute, 2005. *Placing Reinforcing Bars (8th Edition)*. CRSI, Schaumburg, IL.

Donatas J., Zenonas K. and Algirdas J., 2007. *Static Behavior Analysis of Masts with Combined Guys*. Journal of Civil Engineering and Management, Vol. XIII, No. 3, pp. 177 - 182

Gupta S. R. D., Seshu M. R. A., and Murty K. S. M., 1993. *Design of Tie Bars for Large Drilled Pier Foundations*. ACI Structural Journal, V. 90, No. 3, pp. 231 - 241

Imegwu E. O., 1960. *Plastic Flexure and Torsion*. Journal of the Mechanics and Physics of Solids, Vol. 8, pp. 141- 146

TRC, 2006. XTRACT v. 3.0.8, Rancho Cordova, CA

Wei Q. S., 1995. *Interaction Yield Hypersurfaces for the Plastic Behavior of Beams-II. Combining Bending, Tension, Shear and Torsion*. International Journal of Mechanical Sciences, Vol. 37, No. 3, pp. 239 – 247

Tables

Table 2.1: Diameter and Area of Tie Wires

Gauge No.	Diameter (in)	Area (in^2)
16 ½	0.058	0.0026
16	0.062	0.0030
15	0.072	0.0041
14	0.08	0.0050

Table 2.2: Properties of Guy Cables

Cable Diameter (in)	Area (in^2)	Breaking Strength (kips)	Weight (lb/ft)
3/8	0.110	13.1	0.26
7/16	0.150	17.8	0.35
1/2	0.196	23	0.46
5/8	0.307	35.8	0.72

Table 2.3: Cross Section Properties of Elements

Element	Type	Nominal Diameter (in)	Area (in)
Longitudinal	#11	1.41	1.56
Transverse	#8	1.00	0.790
Internal Braces Bars	#8	1.00	0.790

Table 3.1: Tie Wire Ultimate Strength

Test	Tie Wire Ultimate Strength (ksi)			
	Pacific Coast Steel			UNR
	No. 16 1/2	No. 16	No. 15	No. 15
1	47.3	49.5	49.5	48.2
2	47.4	48.1	49.4	46.4
3	47.8	47.4	49.2	47.3
4	47.4	47.1	49.1	47.2
5	47.4	48.6	48.6	-
Average =	**47.5**	**48.1**	**49.1**	**47.3**

Table 3.2: Nomenclature of Tie Wire Connections Specimens

Item	Name
Single-Snap	ST
Double-Snap	2ST
Single-U	U
Double-U	2U
Column-Tie	CT
Wrap-and-Saddle	WS
Normal Translational Direction	X
Tangential Translational Direction	Y
Vertical Translational Direction	Z
Normal Rotational Direction	R
Specimen	1,2,3,4

Table 3.3: Normal (Δx) Strength Compared with Number of Wires in the Connection

Connection	Normal (Δx) Strength (lb)		Number of wires
	Iron Worker	Number Wires x Yield Strength	
Single-Snap	305	385	2
Double-Snap	465	770	4
Single-U	681	770	4
Double-U	1310	1540	8
Column-Tie	1101	1155	6
Wrap-and-Saddle	1393	1540	8

Table 3.4: Average Maximum Strength of Tie Wire Connections in Δx, Δy, Δz, and θx

Connection Type	Tie Wire Connections Strength					
	Experienced Iron Worker			Inexperienced Iron Worker		
	Δx (lb)	Δy (lb)	θx (lb-in)	Δx (lb)	Δy (lb)	θx (lb-in)
Single Snap	305	269	223	281	186	198
Double Snap	465	506	469	403	313	510
Single-U	681	469	479	541	544	448
Double-U	1310	1034	912	1025	721	845
Column Tie	1101	810	518	972	608	513
Wrap-and Saddle	1393	1139	865	1235	999	692

Table 3.5: Average Stiffness of Tie Wire Connections in Δx, Δy, Δz, and θx

Tie Wire Connection Stiffness						
Connection Type	Experienced Iron Worker			Inexperienced Iron Worker		
	Δx (lb/in)	Δy (lb/in)	θx (lb-in/degree)	Δx (lb/in)	Δy (lb/in)	θx (lb-in/degree)
Single Snap	11870	1203	6.9	8227	223	1.1
Double Snap	17527	600	10.4	10344	338	1.7
Single-U	27009	1245	5.6	11084	755	1.3
Double-U	34097	1875	5.7	14781	932	1.8
Column Tie	27818	1584	3.2	12004	318	1.1
Wrap-and Saddle	30635	2476	5.7	19887	1468	9.1

Table 3.6: Recommended Strength of Tie Wire Connections for Rebar Cage pick-up

Tangential Connection Δy Strength (lb)		
Connection Type	Average Experienced and Inexperienced	Recommended (90%)
Single Snap	228	205
Double Snap	410	369
Single-U	507	456
Double-U	878	790
Column Tie	709	638
Wrap-and Saddle	1069	962

Table 3.7: Recommended Rotational Strength of Tie Wire Connections

Rotational Connection θx Strength (lb-in)		
Connection Type	Average Experienced and Inexperienced	Recommended (90%)
Single Snap	211	189
Double Snap	490	441
Single-U	464	417
Double-U	879	791
Column Tie	516	464
Wrap-and Saddle	779	701

Table 3.8: Test Specimens Properties

Specimen	Height (ft)	Diameter (ft)	Longitudinal Reinforcement	Transversal Reinforcement	Type of Braces
I	34	3.67	1%	1%	2 X-braces
			12 #11	#8@7.0 in	
II	34	3.67	1%	1%	2 Square-braces
			12 #11	#8@7.0 in	

Table 3.9: Mapping of Tie Wire connections in Specimen I

TIE CONNECTION	Number	%
No tie wire connection	197	27.8%
4-snap tie	290	41.0%
2-snap tie	150	21.2%
Wrap-and-saddle	42	5.9%
Column-tie	14	2.0%
Strong-tie	15	2.1%
Total =	708	

Table 3.10: Tie Wire Connections in Pick-up bars in Specimen I

Pick-Up Bar	Tie Wire Connection				
	2-Snap	4-Snap	Colum-Tie	Wrap-&-Saddle	Strong-Tie
2	20.3%	69.5%	3.4%	6.8%	0.0%
6	25.4%	62.7%	5.1%	5.1%	1.7%
8	25.4%	66.1%	0.0%	6.8%	1.7%
12	25.4%	66.1%	0.0%	6.8%	1.7%

Table 3.11: Tie Wire Connections in Template hoops in Specimen I

Template Hoop	Tie Wire Connection				
	2-Snap	4-Snap	Colum-Tie	Wrap-&-Saddle	Strong-Tie
A	0.0%	33.3%	33.3%	0.0%	33.3%
B	0.0%	0.0%	41.7%	0.0%	58.3%
C	0.0%	8.3%	8.3%	83.3%	0.0%
D	0.0%	0.0%	0.0%	100.0%	0.0%
E	0.0%	0.0%	16.7%	66.7%	16.7%

Table 3.12: Mapping of Tie Wire connections in Specimen II

TIE CONNECTION	Number	%
No tie wire connection	1464	52.1%
4-snap-tie	269	9.6%
2-snap-tie	919	32.7%
Wrap-and-saddle	114	4.1%
Column-tie	14	0.5%
Strong-tie	28	1.0%
Total =	2808	

Table 3.13: Tie Wire Connections in Pick-up bars in Specimen II

Pick-Up Bar	Tie Wire Connection				
	2-Snap	**4-Snap**	**Colum-Tie**	**Wrap-&-Saddle**	**Strong-Tie**
2	89.7%	4.3%	0.0%	5.1%	0.9%
6	93.2%	0.9%	0.0%	6.0%	0.0%
8	76.9%	6.8%	0.0%	5.1%	0.9%
12	83.8%	13.7%	0.0%	2.6%	0.0%

Table 3.14: Tie Wire Connections in Template hoops in Specimen II

Template Ring	Tie Wire Connection				
	2-Snap	**4-Snap**	**Colum-Tie**	**Wrap-&-Saddle**	**Strong-Tie**
A	0.0%	16.7%	12.5%	50.0%	20.8%
B	0.0%	4.2%	25.0%	50.0%	20.8%
C	4.2%	0.0%	0.0%	83.3%	12.5%
D	4.2%	0.0%	0.0%	83.3%	12.5%
E	16.7%	0.0%	0.0%	70.8%	12.5%

Table 4.1: Experimental over Analytical Displacement Ratios for Specimen I

Point	Resultant Cable Displacement (in)					Average
	8.28	**15.4**	**29.66**	**43.44**	**57.71**	
0	0.00	0.00	0.00	0.00	0.00	**0.00**
1	1.31	1.19	0.80	0.88	0.68	**0.97**
2	1.78	1.60	1.04	1.11	0.94	**1.29**
3	1.04	1.00	0.89	0.89	0.78	**0.92**
4	1.15	1.07	1.00	0.98	0.90	**1.02**
5	1.18	1.09	1.01	1.00	0.97	**1.05**
6	1.29	1.15	1.04	1.05	1.11	**1.13**
1.06	**1.29**	**1.18**	**0.96**	**0.98**	**0.90**	Average

Table 4.2: Experimental over Analytical Displacement Ratios for Specimen II

Point	Resultant Cable Displacement (in)					Average
	14.3	**28.2**	**42.3**	**56.6**	**72.4**	
0	0.00	0.00	0.00	0.00	0.00	**0.00**
1	2.09	1.63	0.68	0.56	0.51	**1.10**
2	1.39	1.18	0.74	0.65	0.58	**0.91**
3	1.24	1.08	0.90	0.85	0.78	**0.97**
4	1.15	1.01	0.93	0.89	0.85	**0.97**
5	1.10	0.94	0.92	0.90	0.89	**0.95**
0.98	**1.39**	**1.17**	**0.83**	**0.77**	**0.72**	Average

Figures

Figure 1.1: Collapse of Bridge Column Rebar Cage in Milpitas, CA

Figure 1.2: Collapse of Bridge Column Rebar Cages in Bent 7 of Carquinez Bridge

Figure 1.3: Close-up of the footing for both Columns in Bent 7 of Carquinez Bridge

Figure 1.4: Bending and torsion suffered by Column Rebar Cages after collapse in Bent 7 of Carquinez Bridge

Figure 1.5: No presence of Internal Braces in Bridge Column Rebar Cage in Bent 7 of Carquinez Bridge

Figure 1.6: Bridge Column Rebar Cage after Collapse in Sweetwater River Connection

Figure 1.7: SFOBB West Approach Plans

Figure 1.8: Column Rebar Cage supported by four Guy cables in bent 23 of SFOBB West Approach
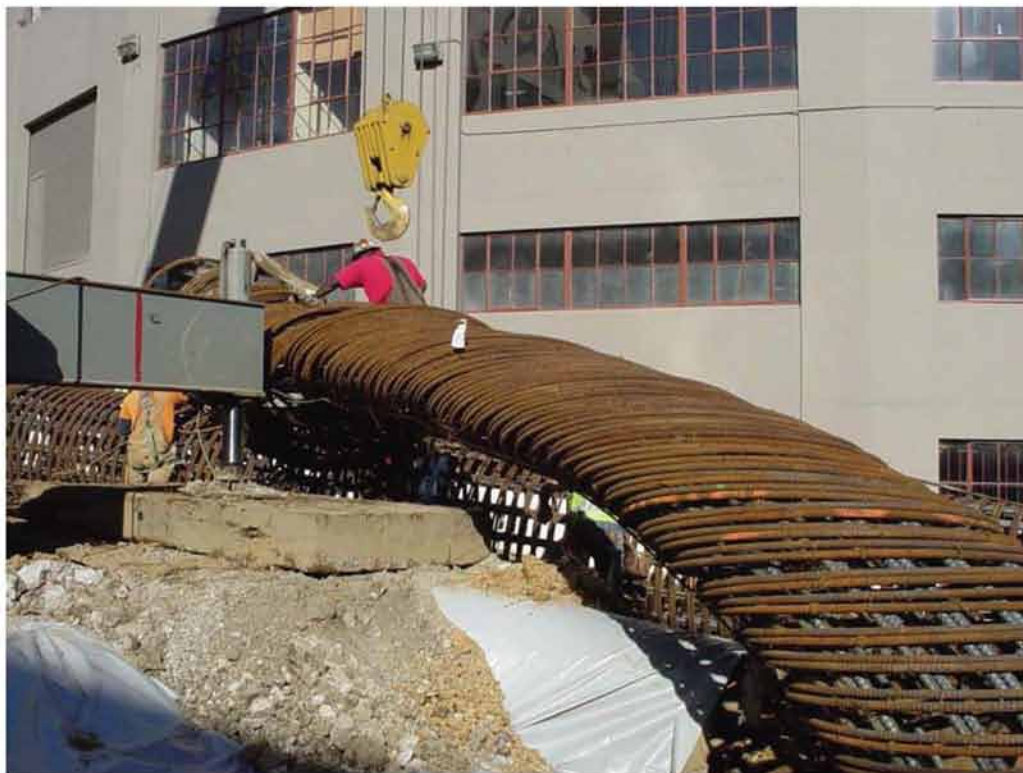
Figure 1.9: Bridge Column Rebar Cage Collapsed in bent 23 of SFOBB West Approach

Figure 1.10: Bridge Column Rebar Cage being held by a Crane

Figure 2.1: Placing of Hoops for the Assembly of a Rebar Cage

Figure 2.2: Pick-up Bars in a Column Rebar Cage

Figure 2.3: Template-hoops in a Column Rebar Cage
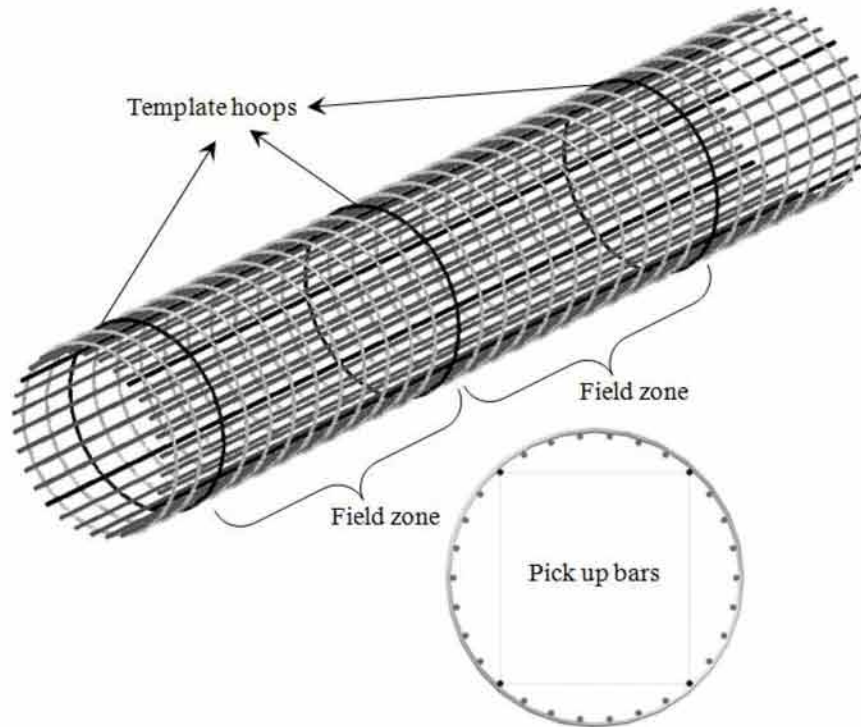
Figure 2.4: Pick-up bars, Template-hoops and Field-zone in Column Rebar Cages

Figure 2.5: No. 15 gauge Tie Wire Coils

Figure 2.6: Single-Snap Tie Wire Connection
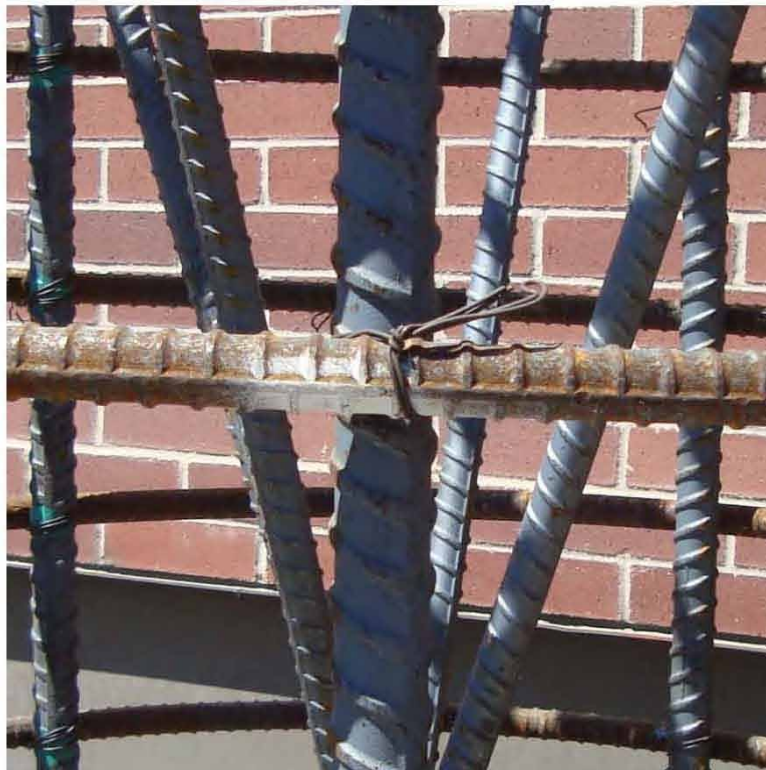
Figure 2.7: Double-Snap Tie Wire Connection

Figure 2.8: Single-U Tie Wire Connection

Figure 2.9: Double-U Tie Wire Connection

Figure 2.10: Wrap-and-Saddle Tie Wire Connection
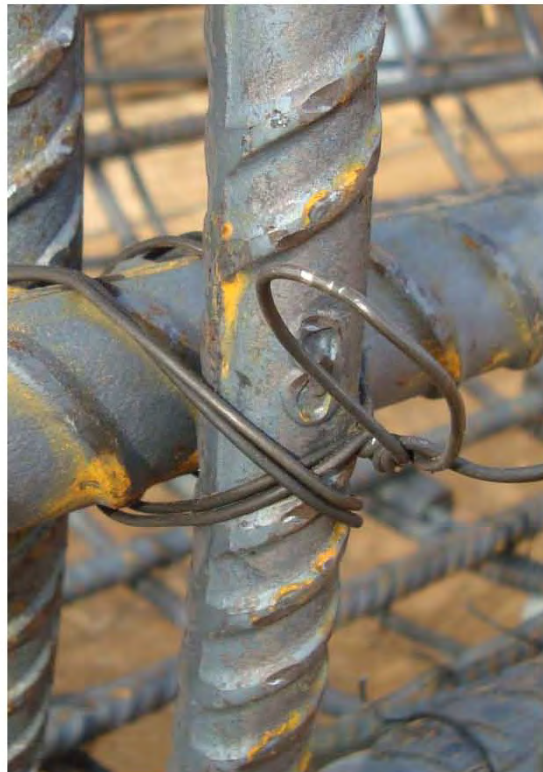
Figure 2.11: Figure-Eight Tie Wire Connection

Figure 2.12: Column-Tie Connection

Figure 2.13: Strong-Tie Connection

Figure 2.14: Field-zone in a Column Rebar Cage

Figure 2.15: Detail of Internal X-brace

Figure 2.16: Detail of Internal Square Brace

Figure 2.17: Rebar Cage with two X-braces ready to be lifted

Figure 2.18: Column Forms with Temporary Support installed

Figure 2.19: Column Rebar Cage being lifted by the Crane with the help of a Forklift

Figure 2.20: Column Rebar Cage being set inside the Column Forms

Figure 2.21: Rebar Cage with two X-braces ready to be lifted

Figure 2.22: Rebar Cage being swung into the location of the footing

Figure 2.23: Column Rebar Cage being Attached to the Bottom Mat of the Footing

Figure 2.24: Column Rebar Cage being guyed at four locations

Figure 2.25: Column Rebar Cage with Two Levels of Four Guy cables

Figure 2.26: Remove of slack in guy cables

Figure 2.27: Column Rebar Cage with four guy cables
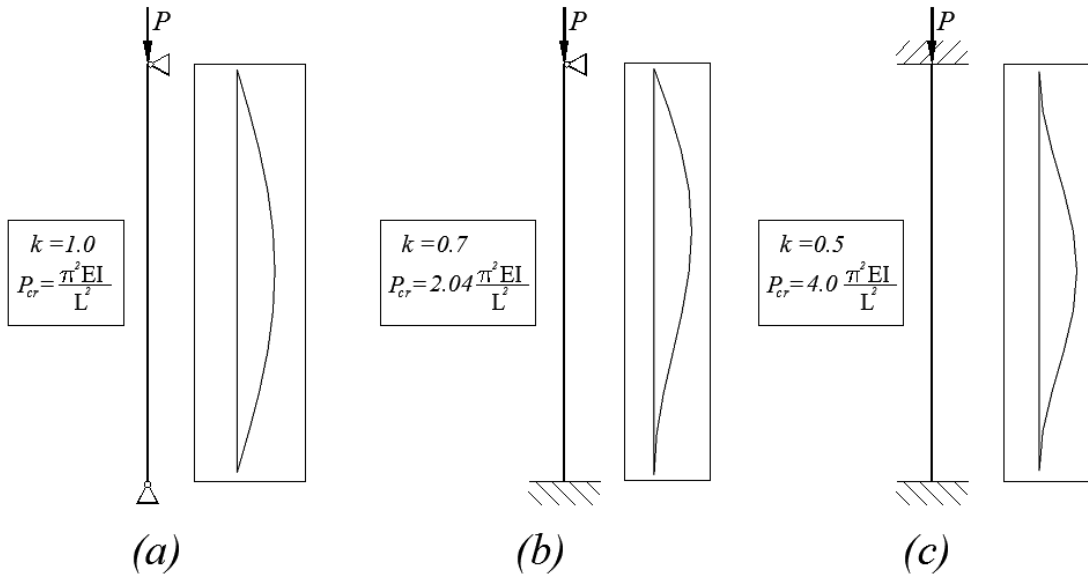
Figure 2.28: #8 Bar Boundary Conditions and Deformed Shapes: (a) Pinned-pinned, (b) Fixed-pinned and (c) Fixed-fixed
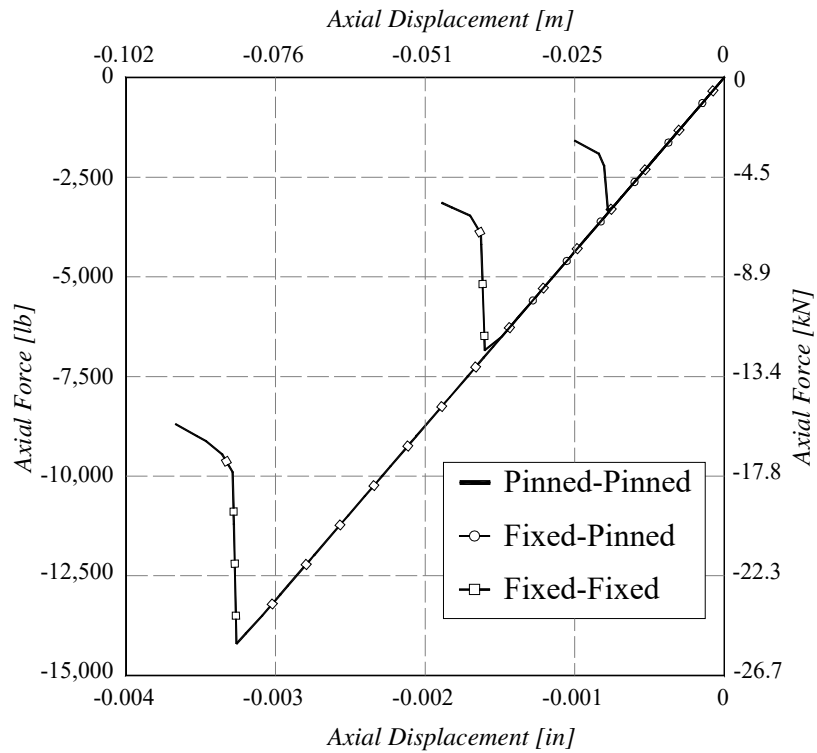
Figure 2.29: Axial force-Axial Displacement Response for a half length Brace Bar with different Boundary Conditions
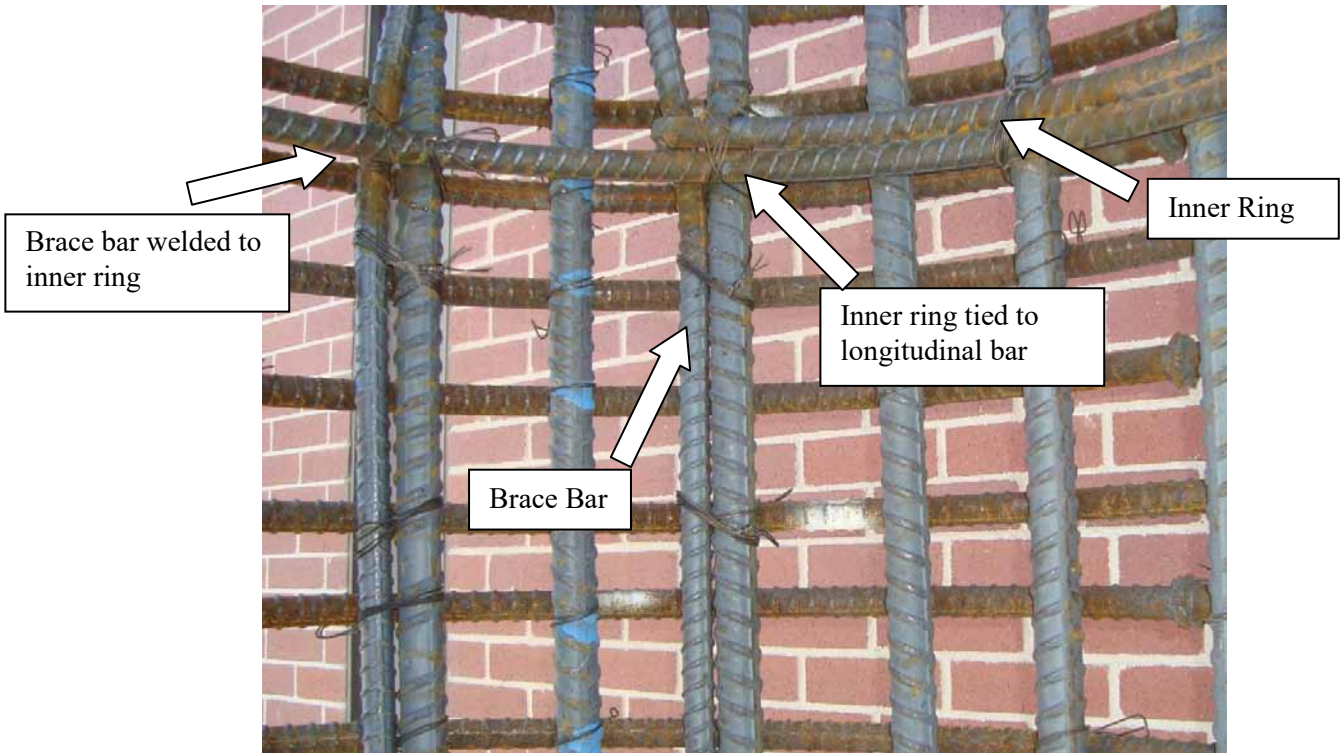
Figure 2.30: Close-up of the Connection Between the end of Braces to the Longitudinal Bar
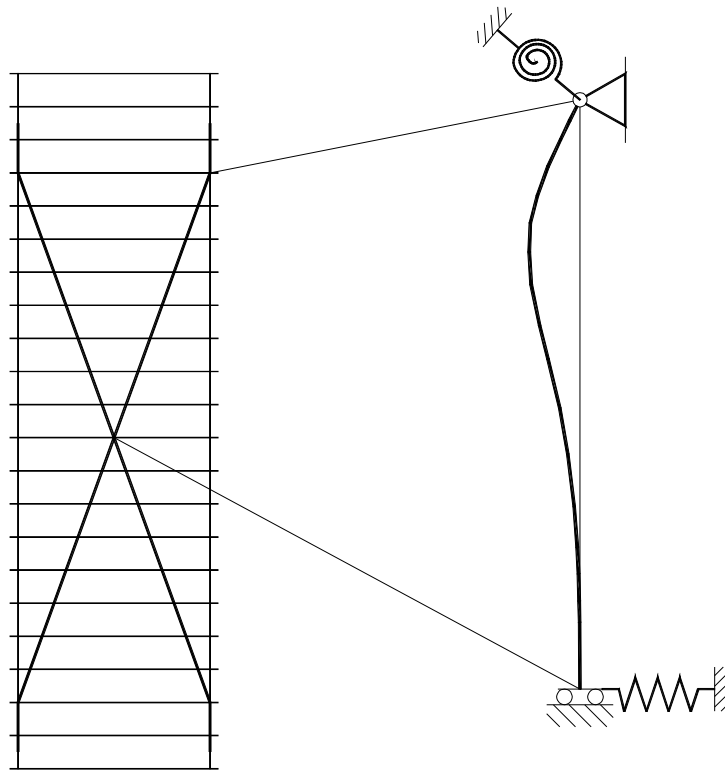
Figure 2.31: Idealization of the Boundary Conditions of the X-brace Bar
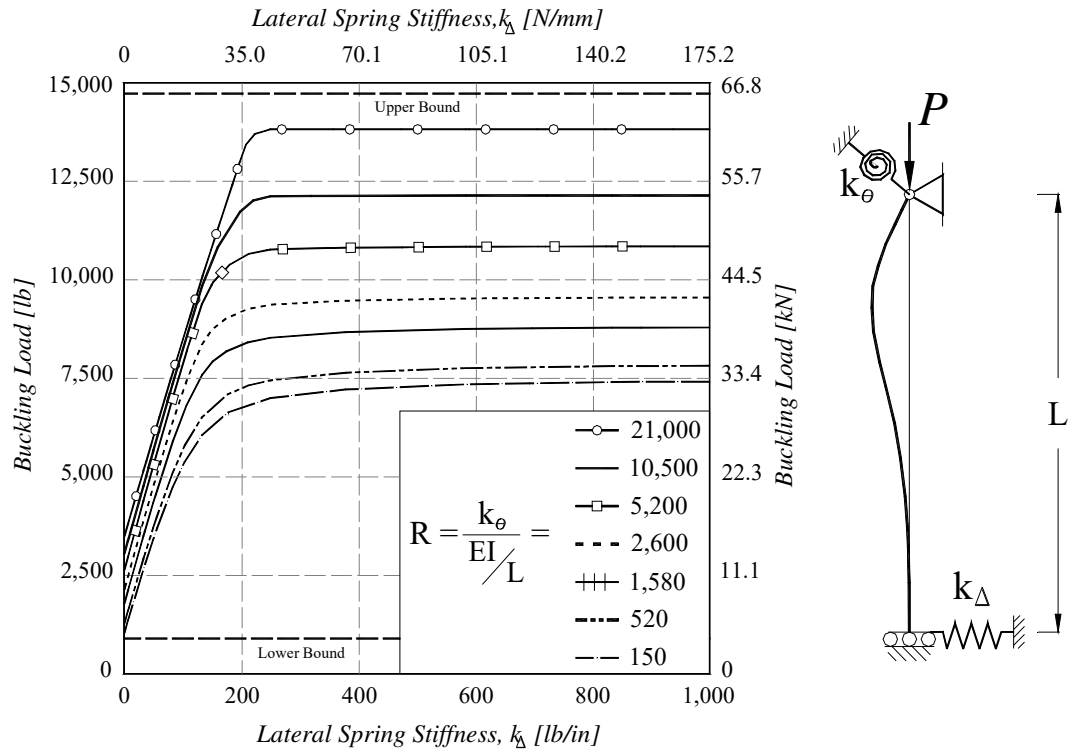
Figure 2.32: Buckling load of #8 X-brace Bar varying the Boundary Conditions
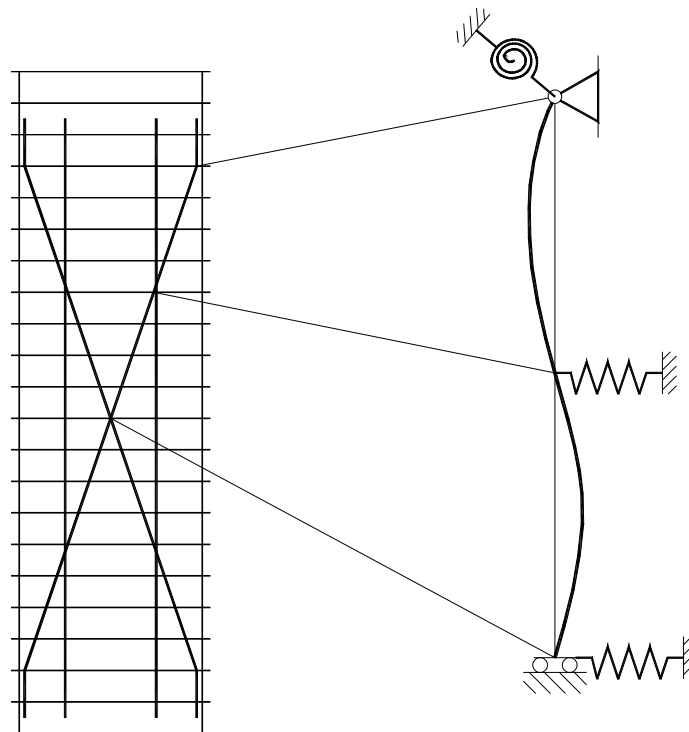
Figure 2.33: Idealization of the Boundary Conditions of the Square brace Bar
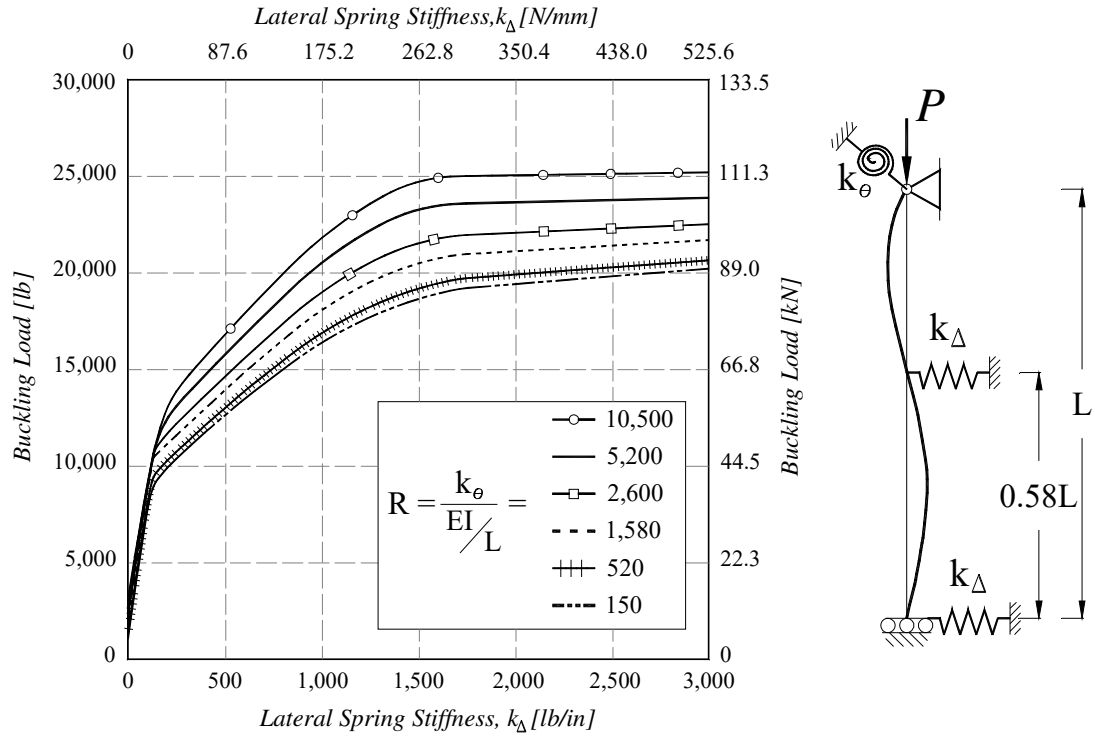
Figure 2.34: Buckling load of #8 Square-brace Bar varying the Boundary Conditions
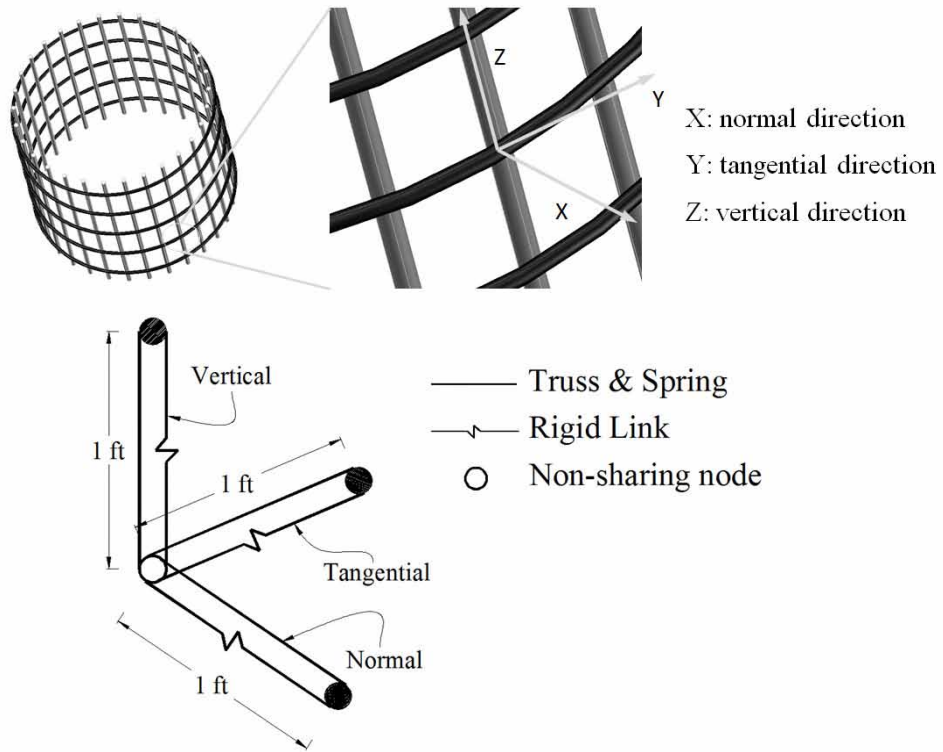
Figure 2.35: Tie Wire Connection Analytical Model
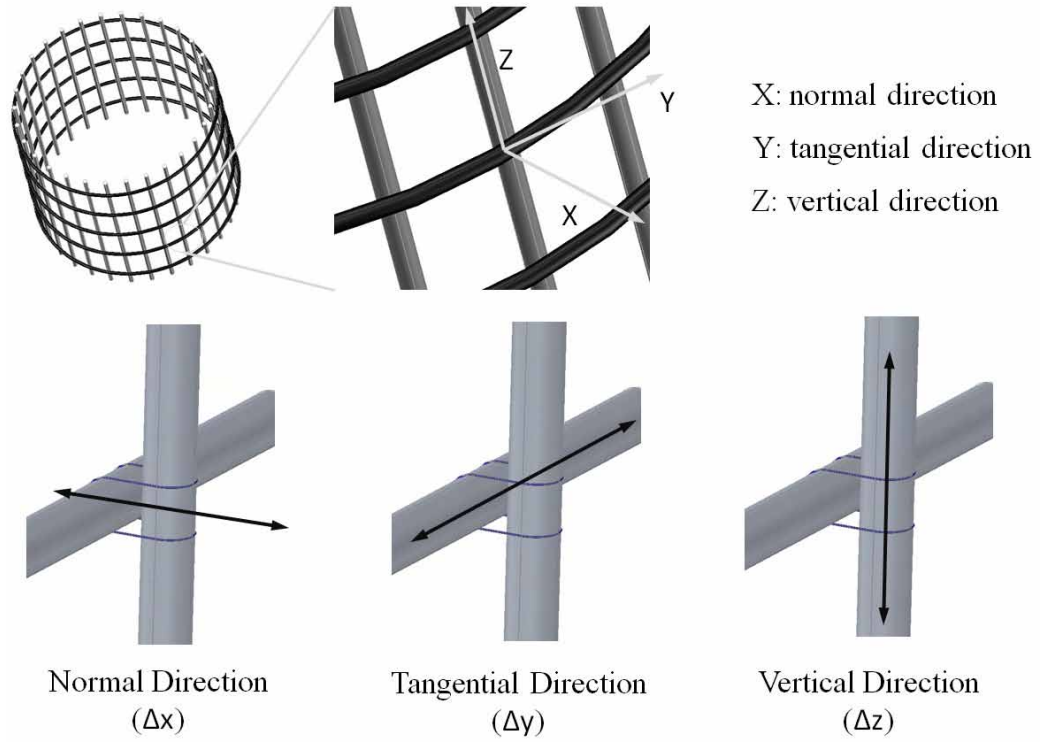
Figure 2.36: Translational Truss Directions of Tie Wire Connections
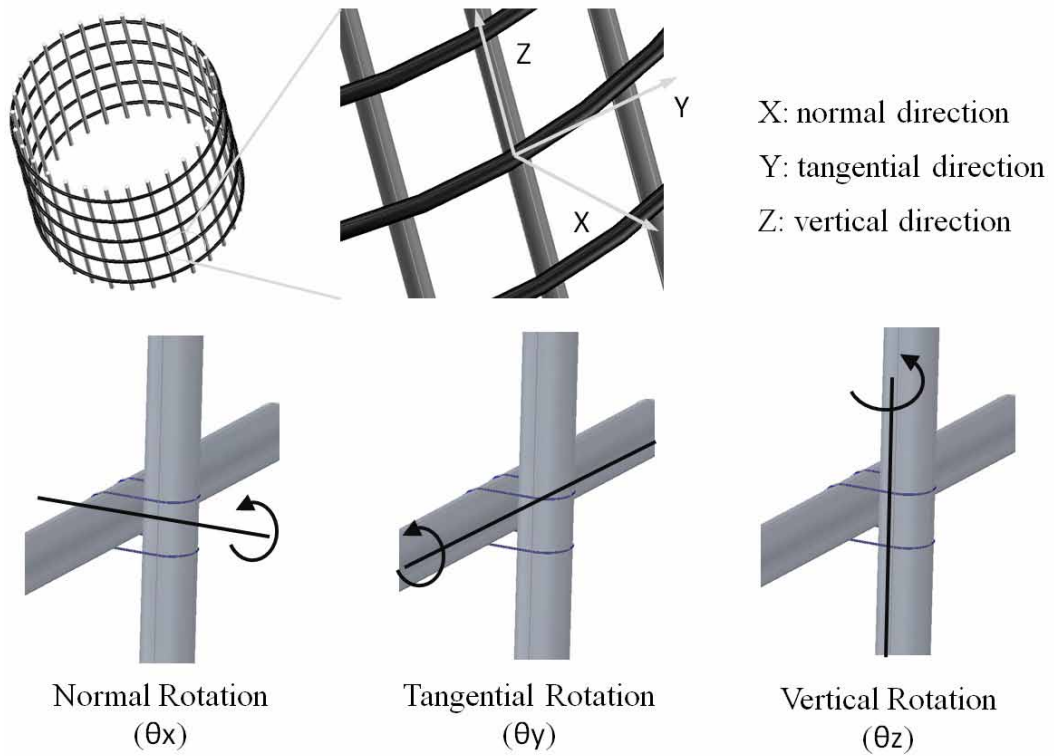
Figure 2.37: Rotational Spring Directions of Tie Wire Connections

Applied load in x-direction

D(0,0,4)

Truss elements

B(2,0,0)

Beam elements

A(0,0,0)

Fixed restraints

z

C(0,0,-4)

x
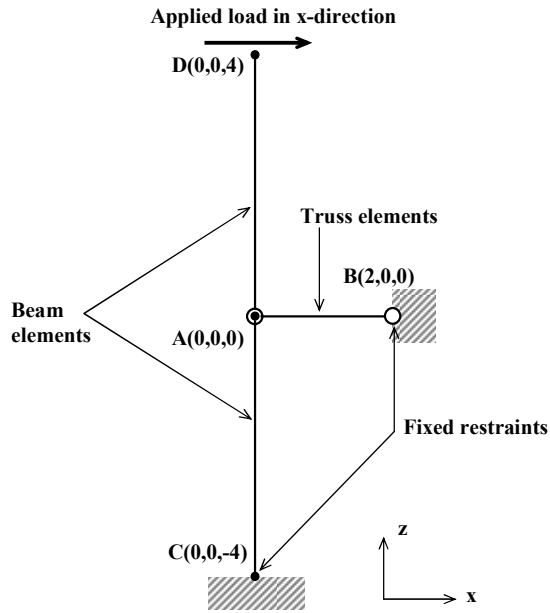
A,B,C,D = coordinates in the undeformed shape

Member AB = truss element

Members CA and AD = beam elements

Figure 2.38: Local Model of Tie Wire connection

Applied Displacement in x-direction at the top [mm]

Truss Force [kips]

Truss Force [kN]

— Case 1 (Large)
-○- Case 2 (Small)
-□- Case 3 (Large + Small)

Applied Displacement in x-direction at the top [in]
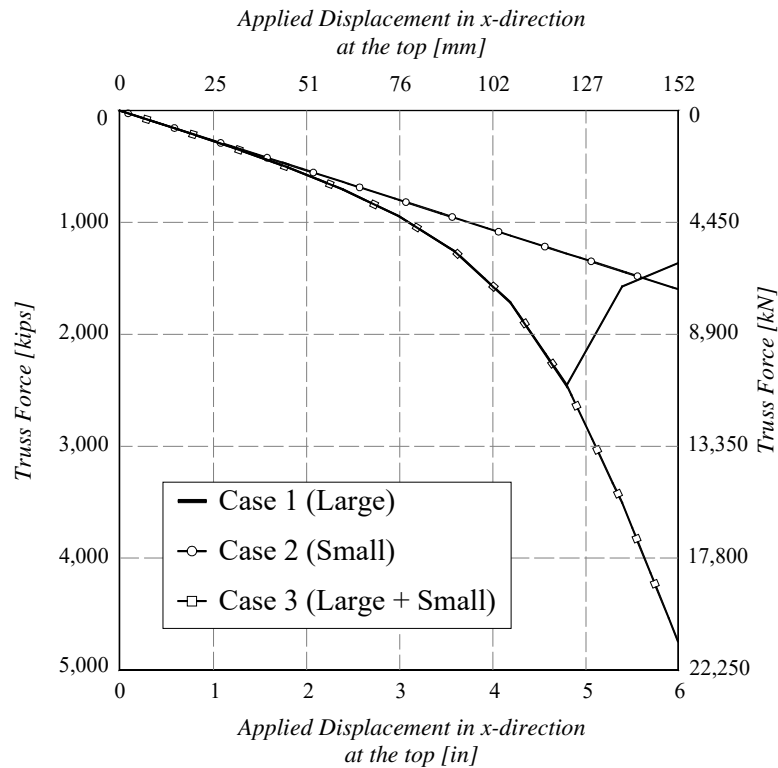
Figure 2.39: Analysis results of Local Model of Tie Wire Connection
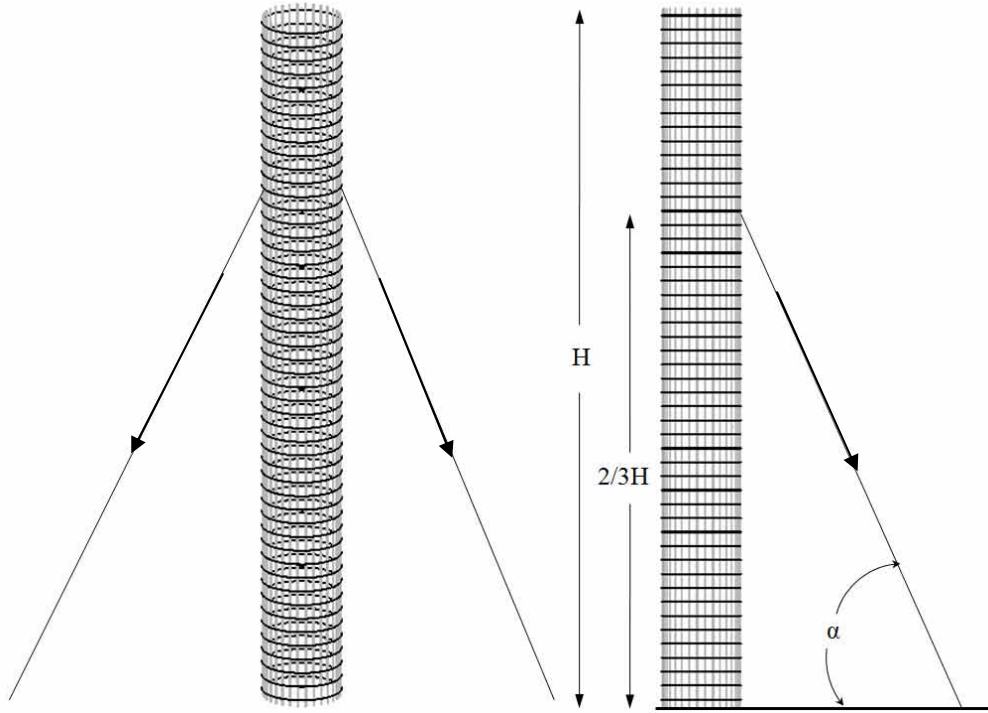
Figure 2.40: Location of Guy cables in Computational Model
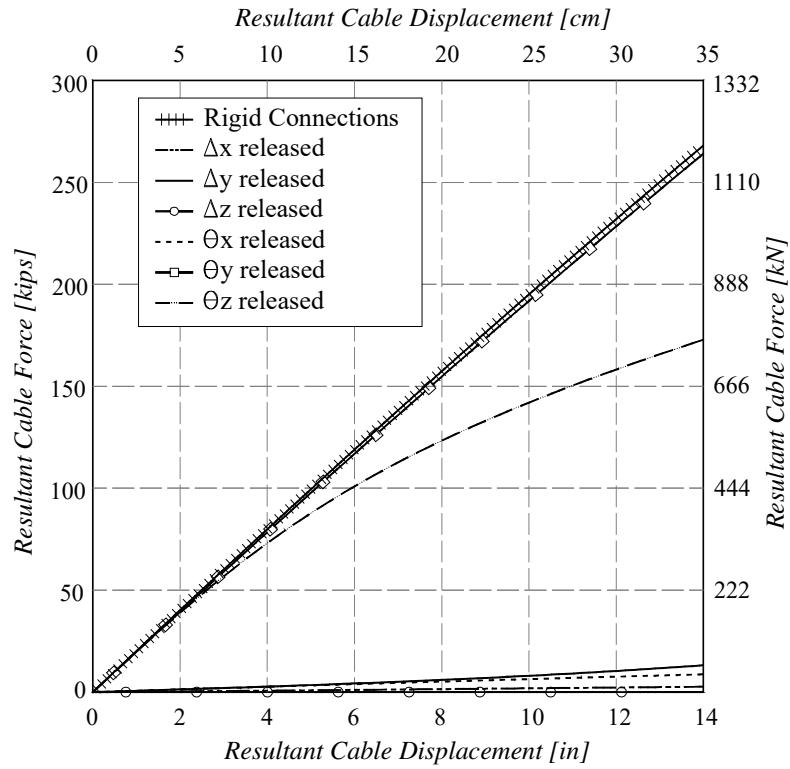
Figure 2.41: Sensitivity Analysis for the Connection between Longitudinal and Transverse Bars
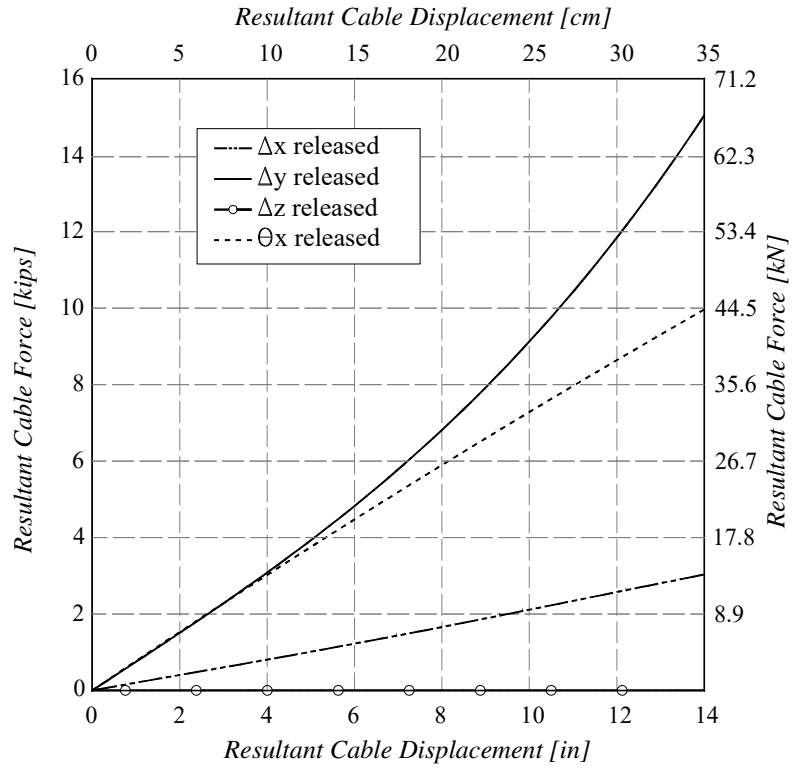
Figure 2.42: Close-up of the Models Response with Release of Δx, Δy, Δz, and θx
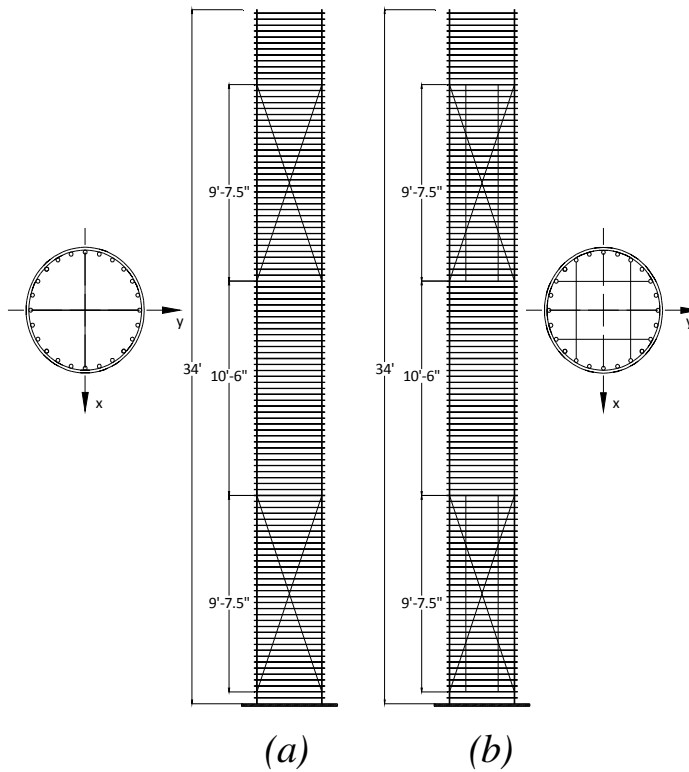
Figure 2.43: Types of Braces: (a) Rebar Cage with X-braces (b) Rebar Cage with Square Braces
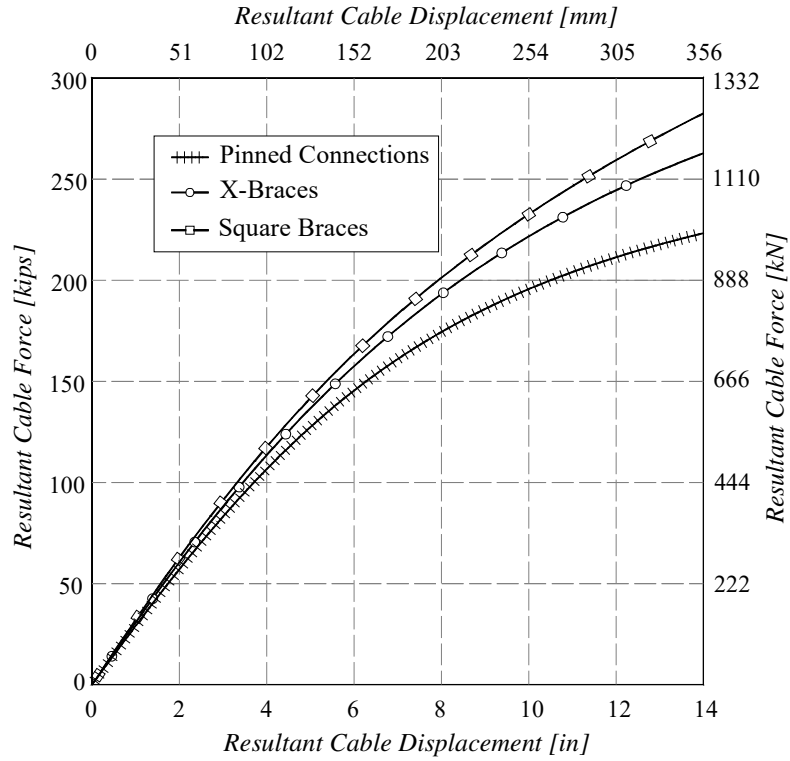
Figure 2.44: Comparison of the Response of Column Rebar Cage models with and without Braces
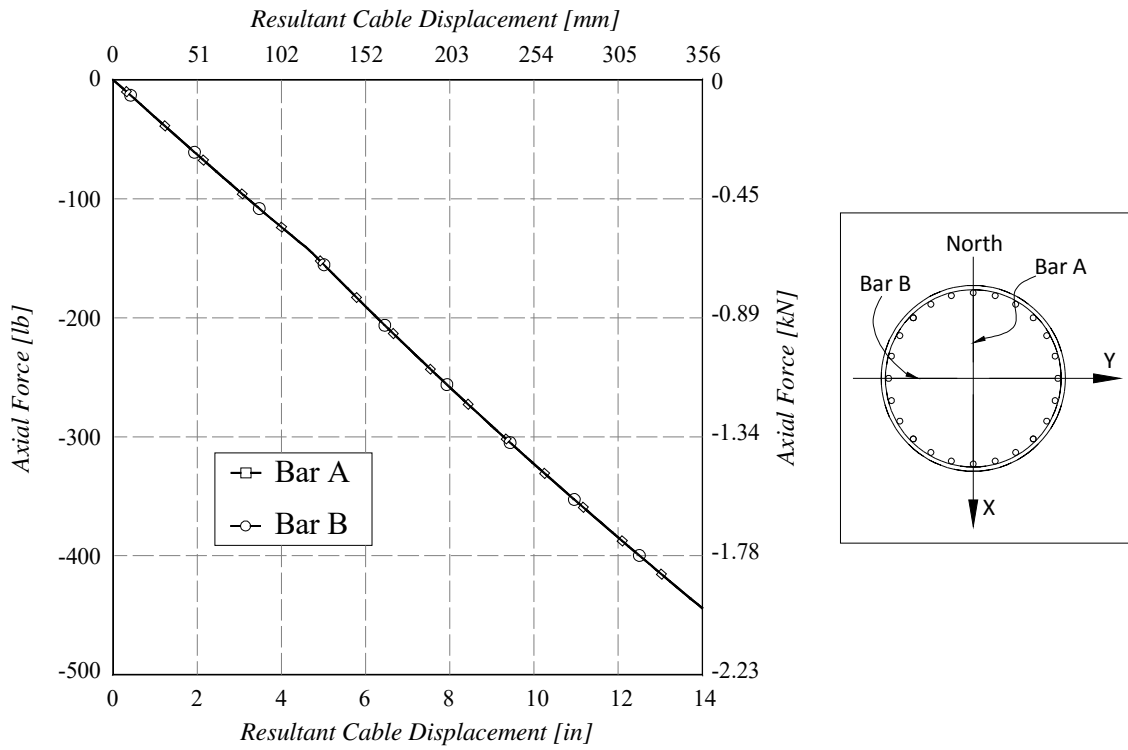
Figure 2.45: Axial force in bars of the Bottom Brace in Column Rebar Cage with X-braces

90
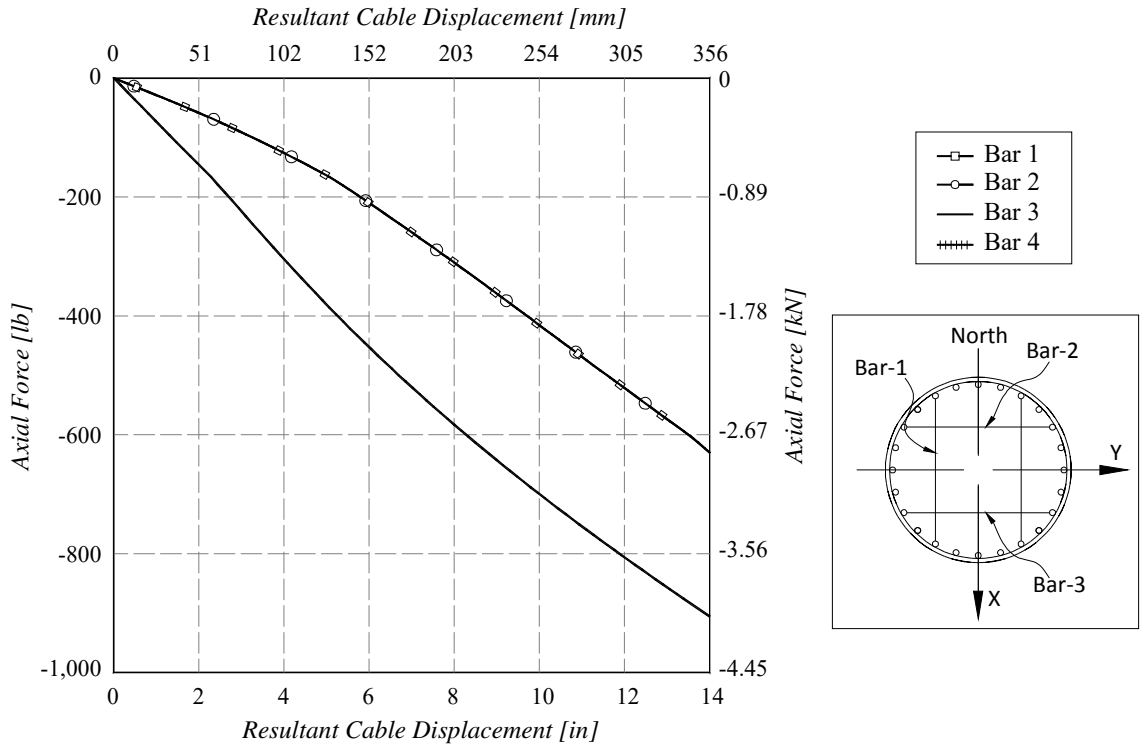
Figure 2.46: Axial force in bars of the Bottom Brace in Column Rebar Cage with Square braces
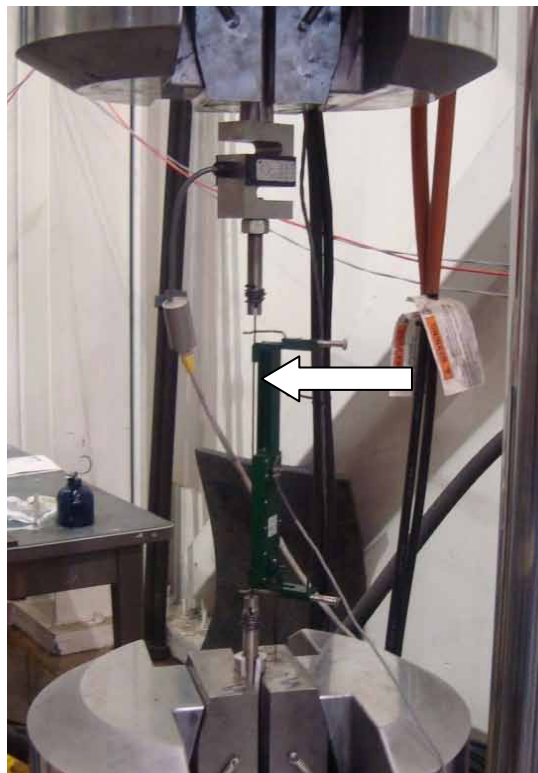
Figure 3.1: Tie Wires Coupon Test Set-Up
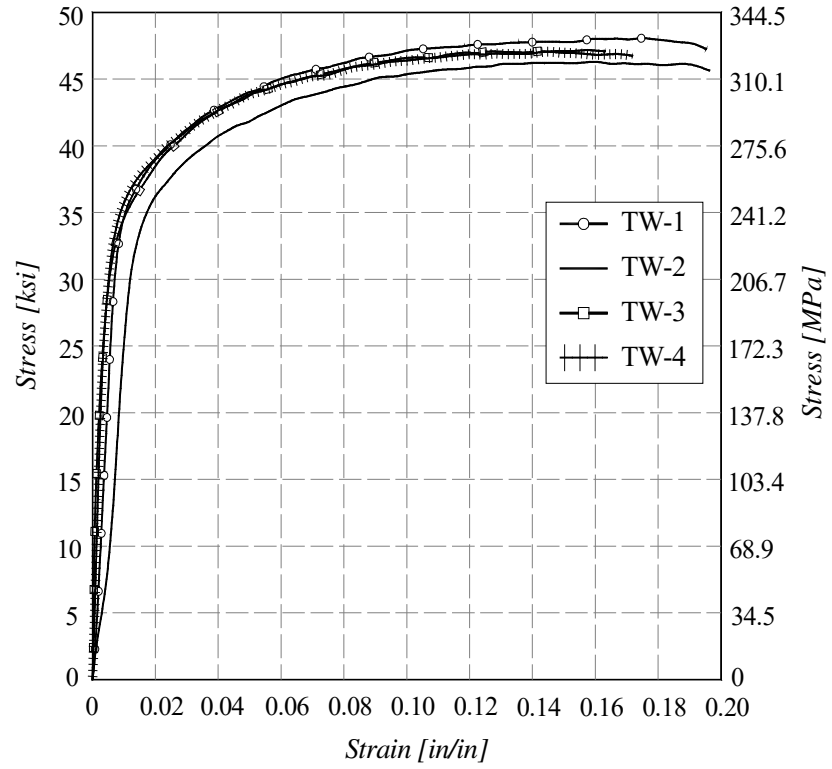
Figure 3.2: Stress-Strain Response of Tie Wires
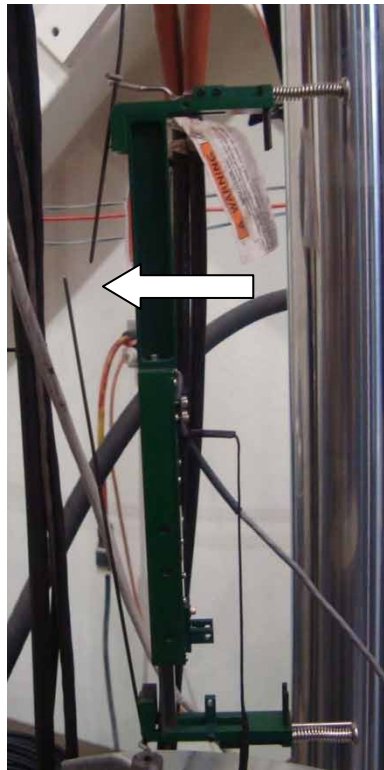
Figure 3.3: Failure of Tie Wire Coupon
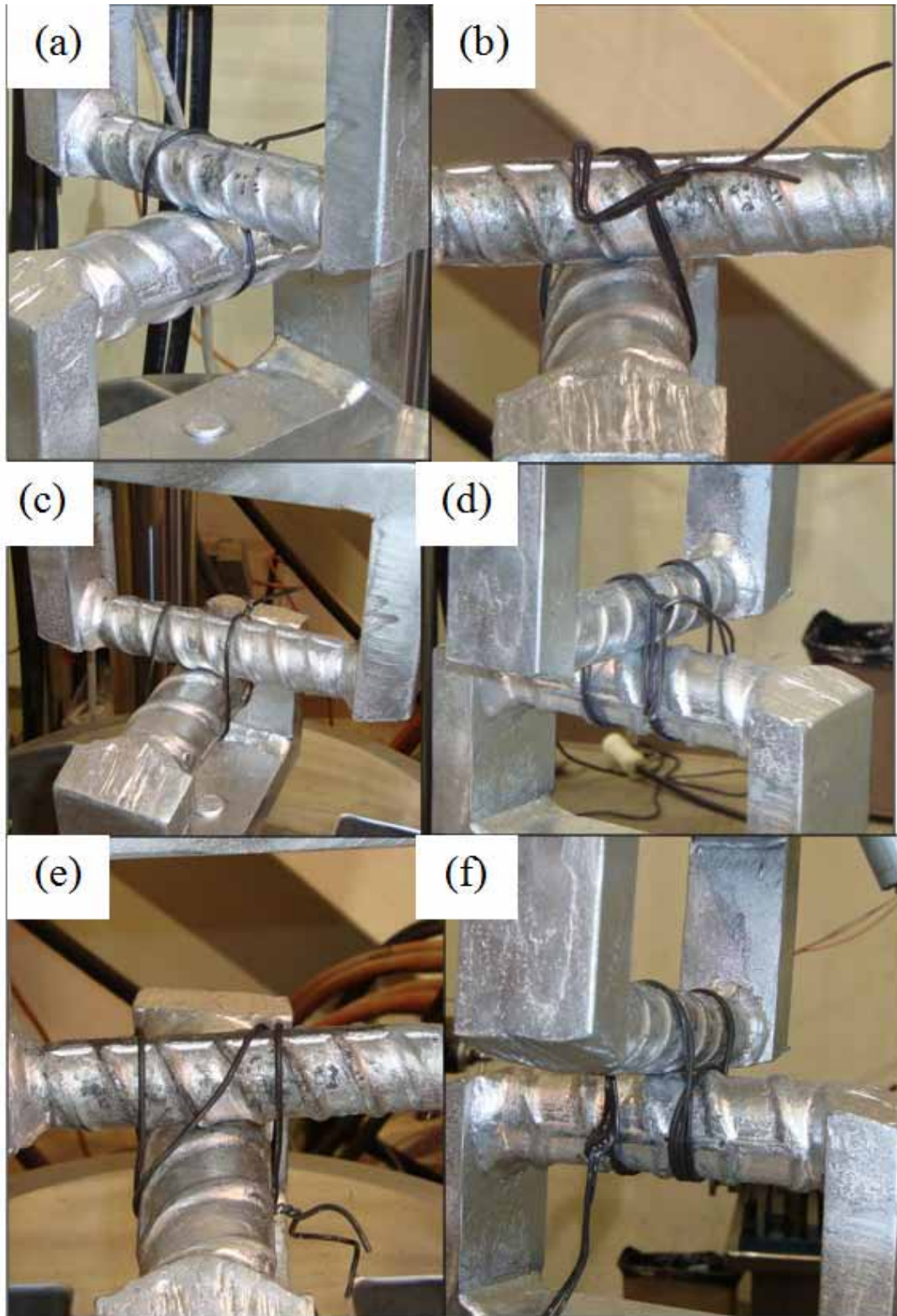
Figure 3.4: Tie Wire Connections: a) Single-Snap b) Double-Snap c) Single-U d) Double-U e) Column-tie f) Wrapn-and-Saddle
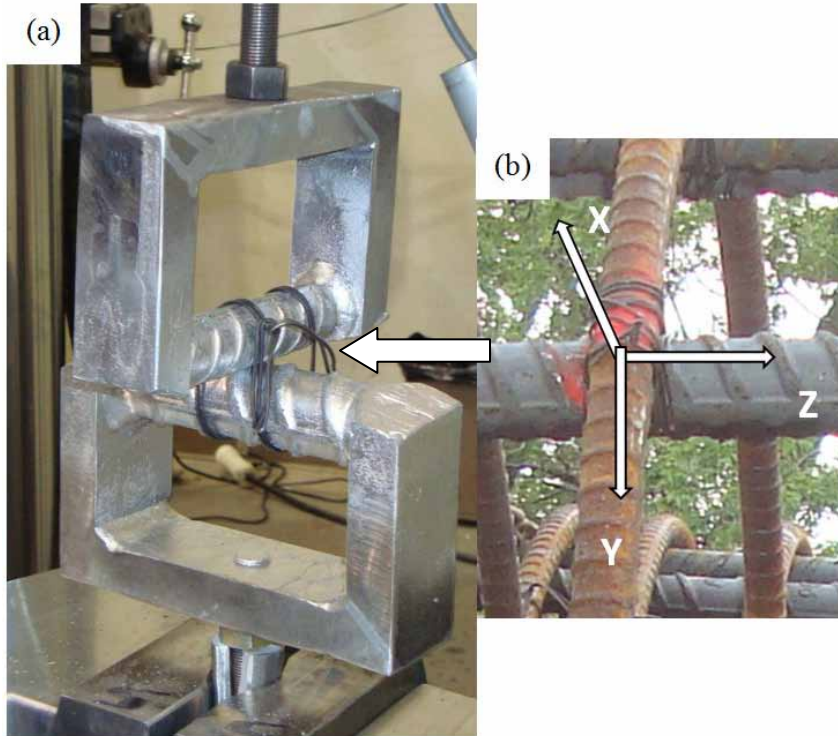
Figure 3.5: (a) Normal Translation (Δx) Test Fixture (b) Translational Directions in a Tie Wire Connection
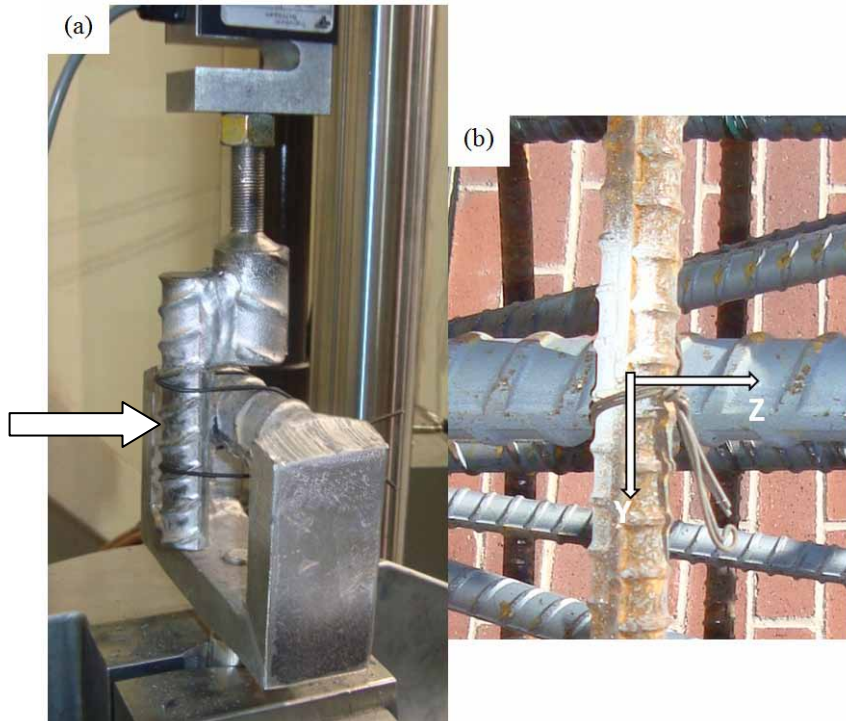
Figure 3.6: (a) Tangential (Δy) and Vertical Direction (Δz) Test Fixture (b) Translational Directions in a Tie Wire Connection
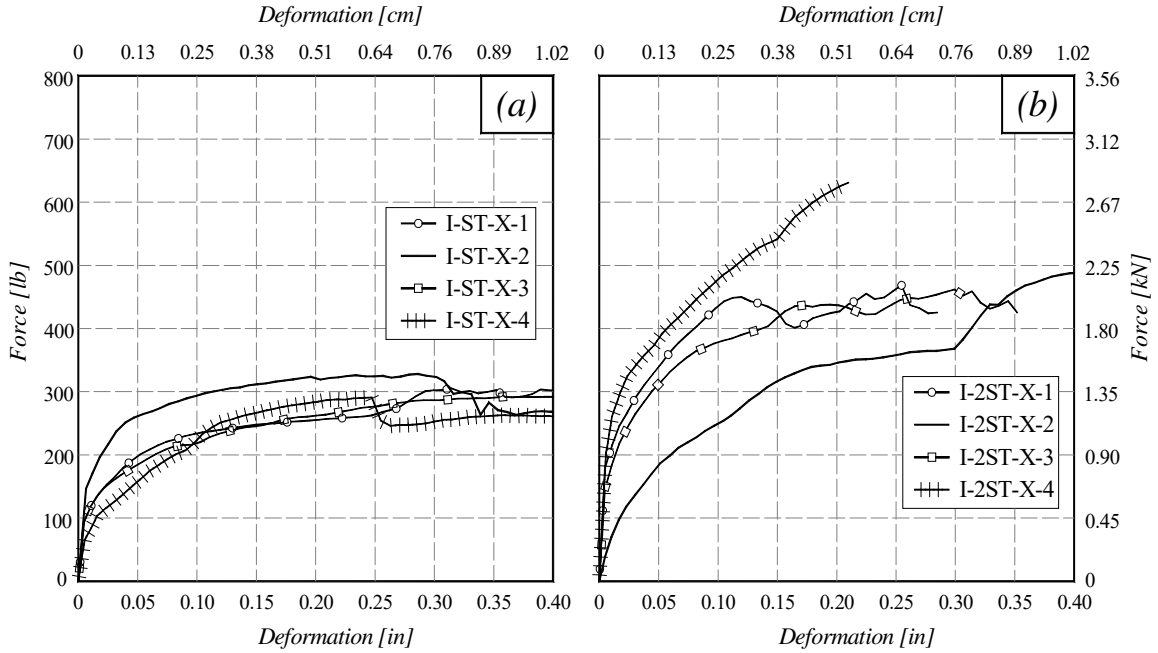
Figure 3.7: Normal Translation (Δx) Response of Tie Wire Connections made by Experienced Iron Worker: a) Single-Snap b) Double-Snap
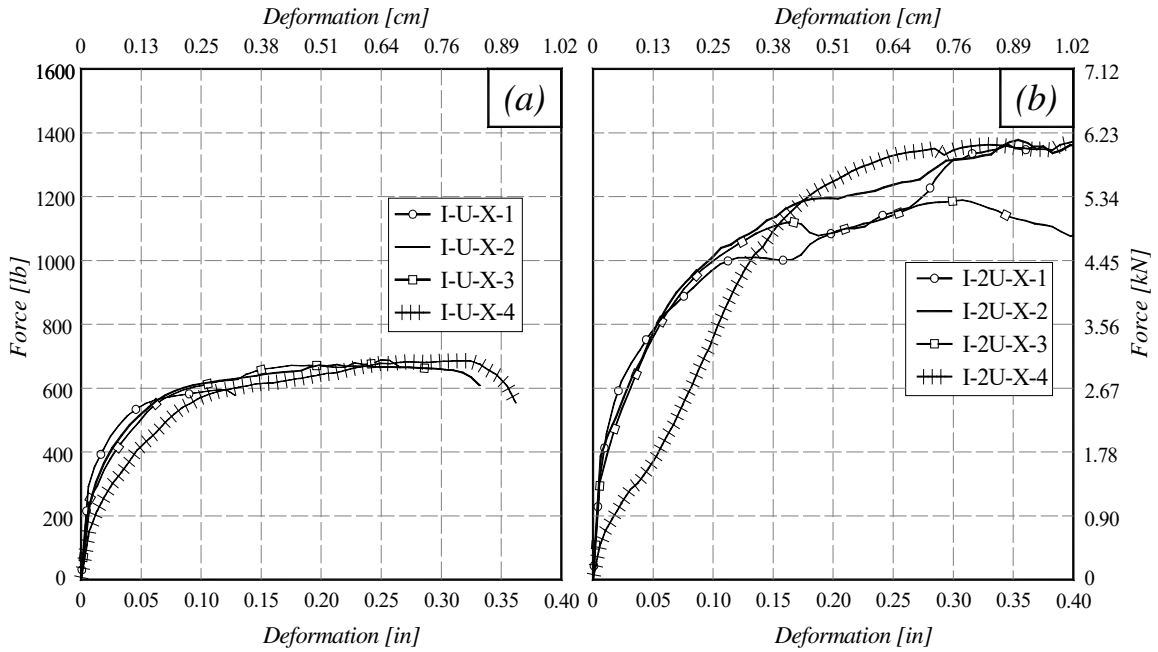
Figure 3.8: Normal Translation (Δx) Response of Tie Wire Connections made by Experienced Iron Worker: a) Single-U b) Double-U
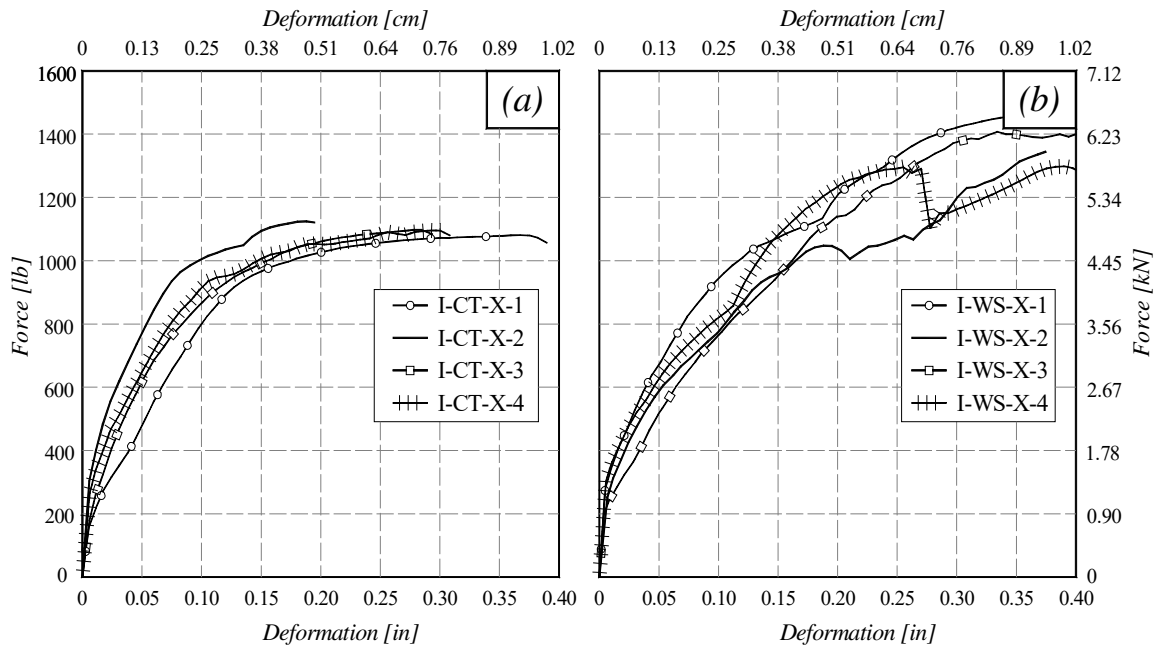
Figure 3.9: Normal Translation (Δx) Response of Tie Wire Connections made by Experienced Iron Worker: a) Column-Tie b) Wrap-and-Saddle
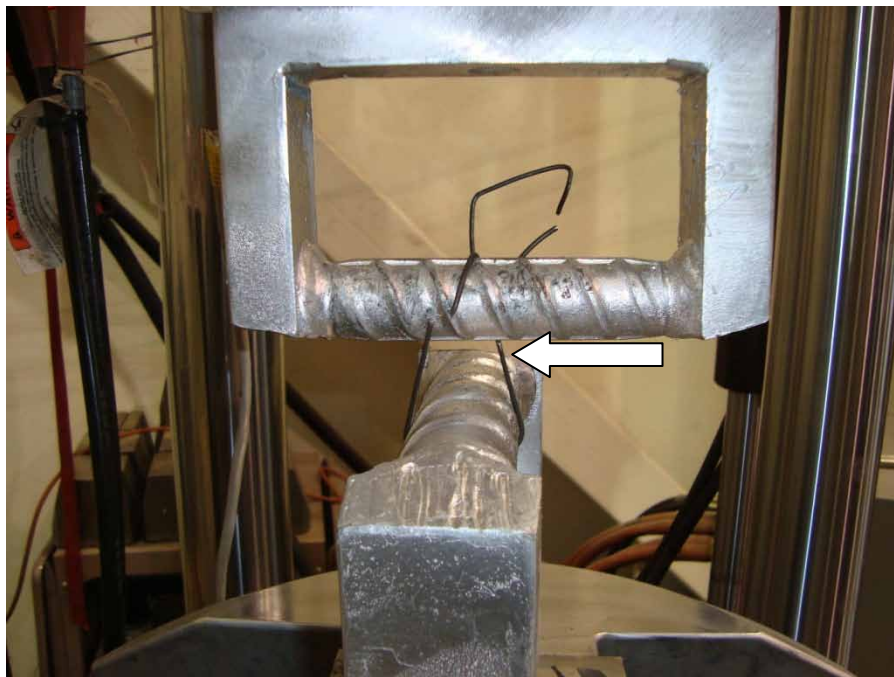
Figure 3.10: Fracture of Single Snap Tie Wire Connection
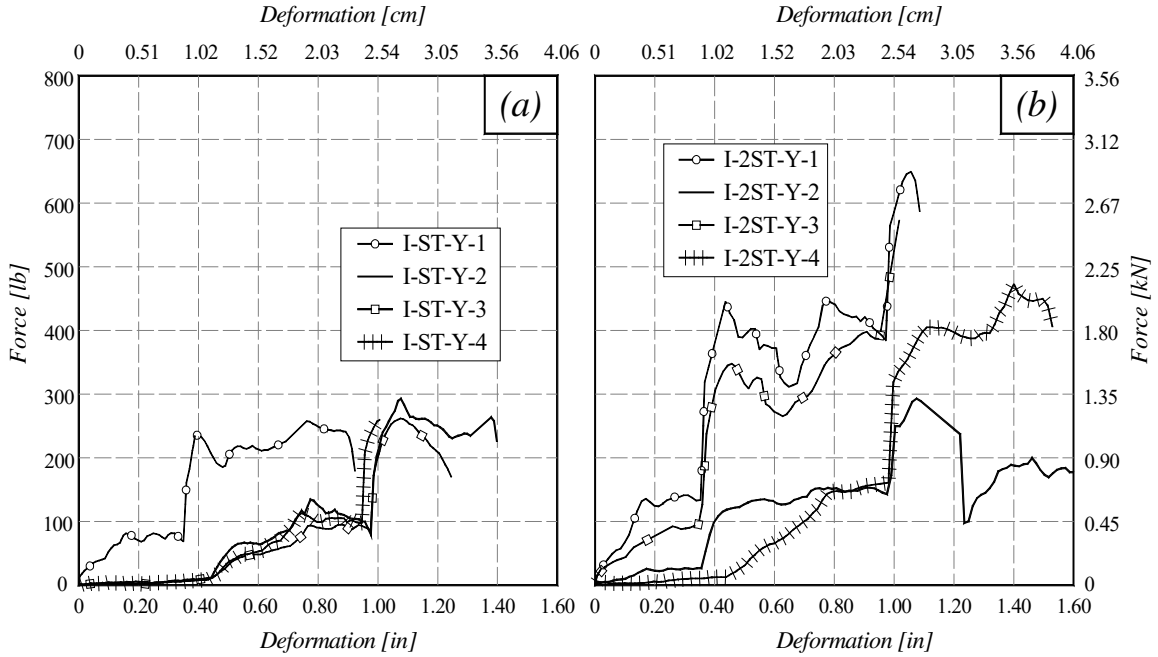
Figure 3.11: Tangential (Δy) and Vertical (Δz) Translation Response of Tie Wire Connections made by Experienced Iron Worker: a) Single-Snap b) Double-Snap
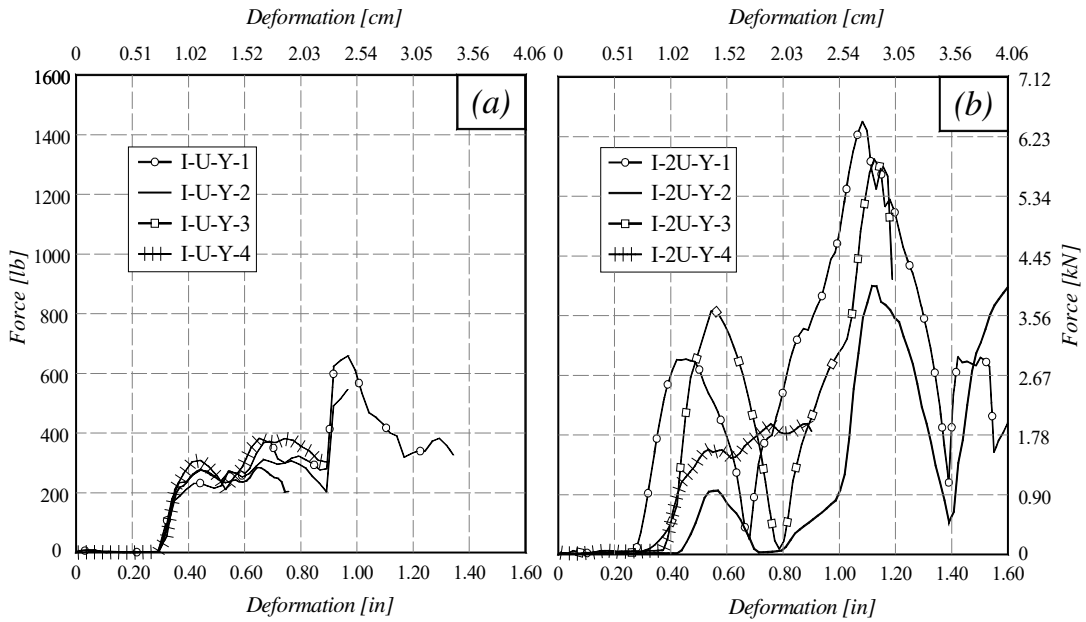
Figure 3.12: Tangential (Δy) and Vertical (Δz) Translation Response of Tie Wire Connections made by Experienced Iron Worker: a) Single-U b) Double-U

97
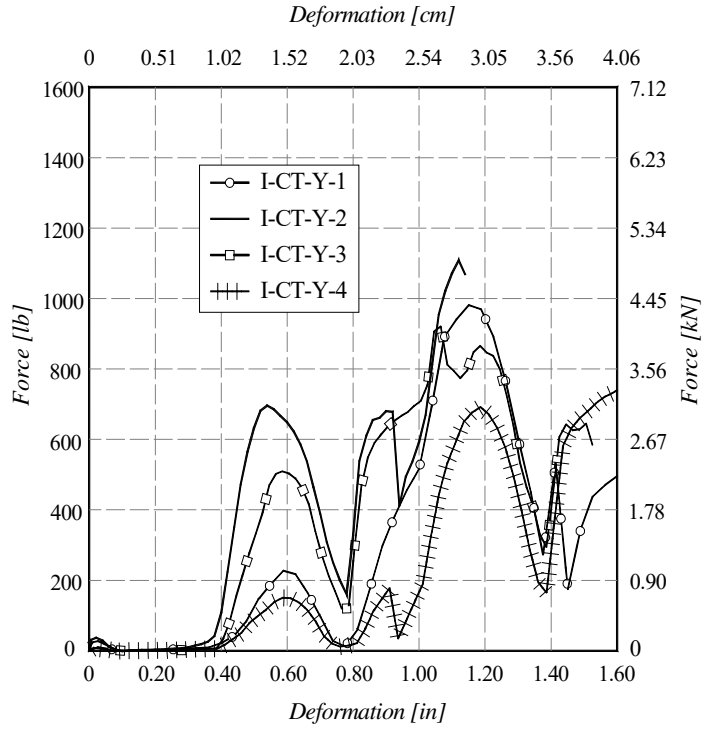
Figure 3.13: Tangential (Δy) and Vertical (Δz) Translation Response of Column-Tie Tie Wire Connections made by Experienced Iron Worker
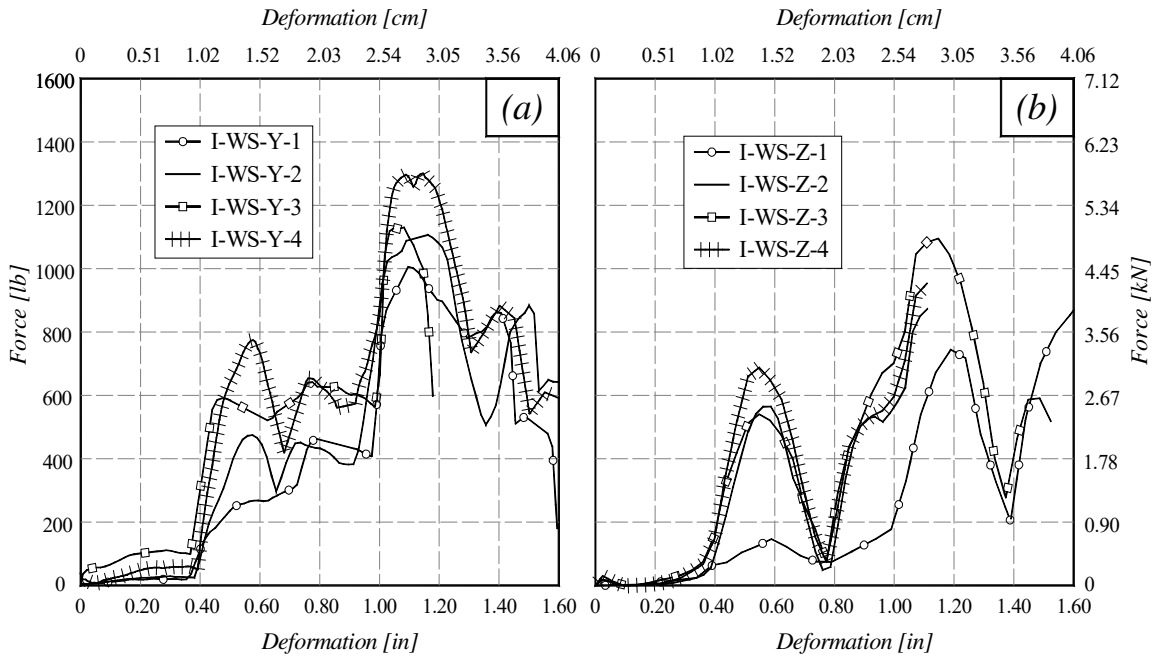
Figure 3.14: Response of Wrap-and-Saddle Tie Wire Connections made by Experienced Iron Worker: a) Tangential Direction (Δy) b) Vertical Direction (Δz)

Figure 3.15: Fracture of Single-U Tie Wire Connection
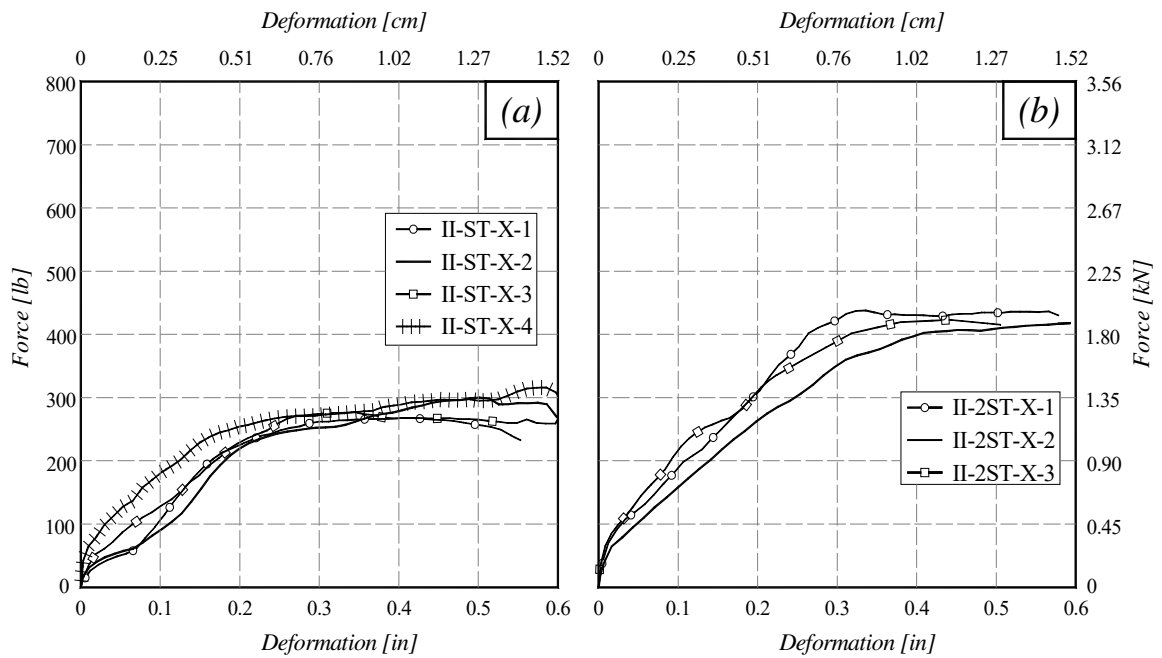
Figure 3.16: Normal Translation (Δx) Response of Tie Wire Connections made by Inexperienced Worker: a) Single-Snap b) Double-Snap
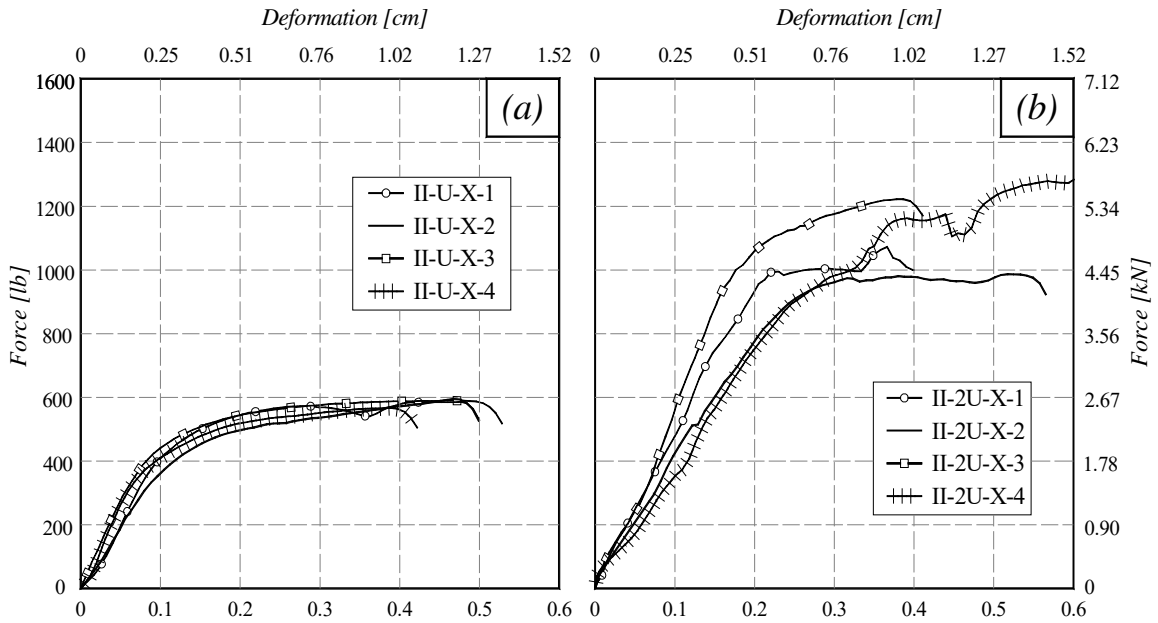
Figure 3.17: Normal Translation (Δx) Response of Tie Wire Connections made by Inexperienced Worker: a) Single-U b) Double-U
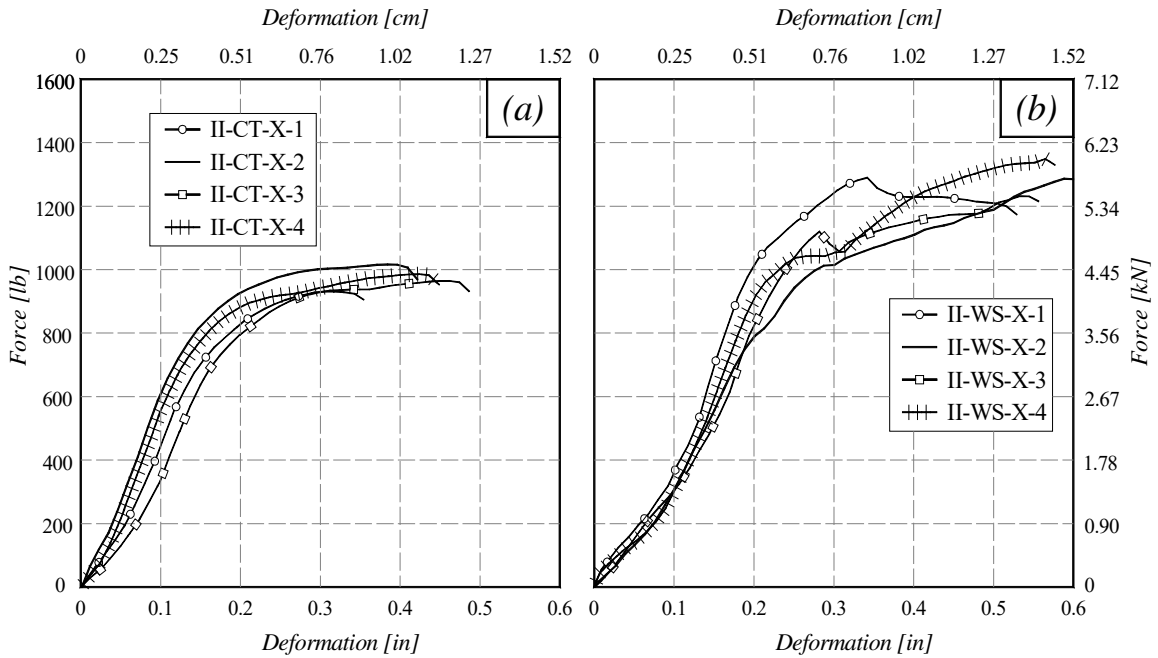
Figure 3.18: Normal Translation (Δx) Response of Tie Wire Connections made by Inexperienced Worker: a) Column-Tie b) Wrap-and-Saddle
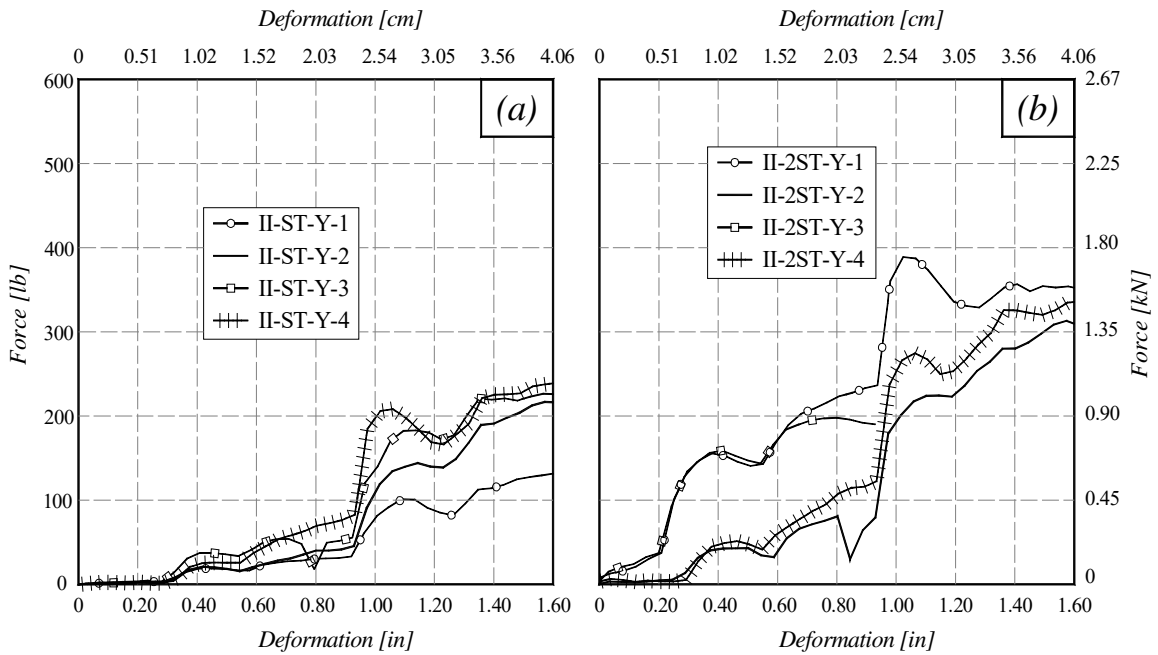
Figure 3.19: Tangential (Δy) and Vertical (Δz) Translation Response of Tie Wire Connections made by Inexperienced Worker: a) Single-Snap b) Double-Snap
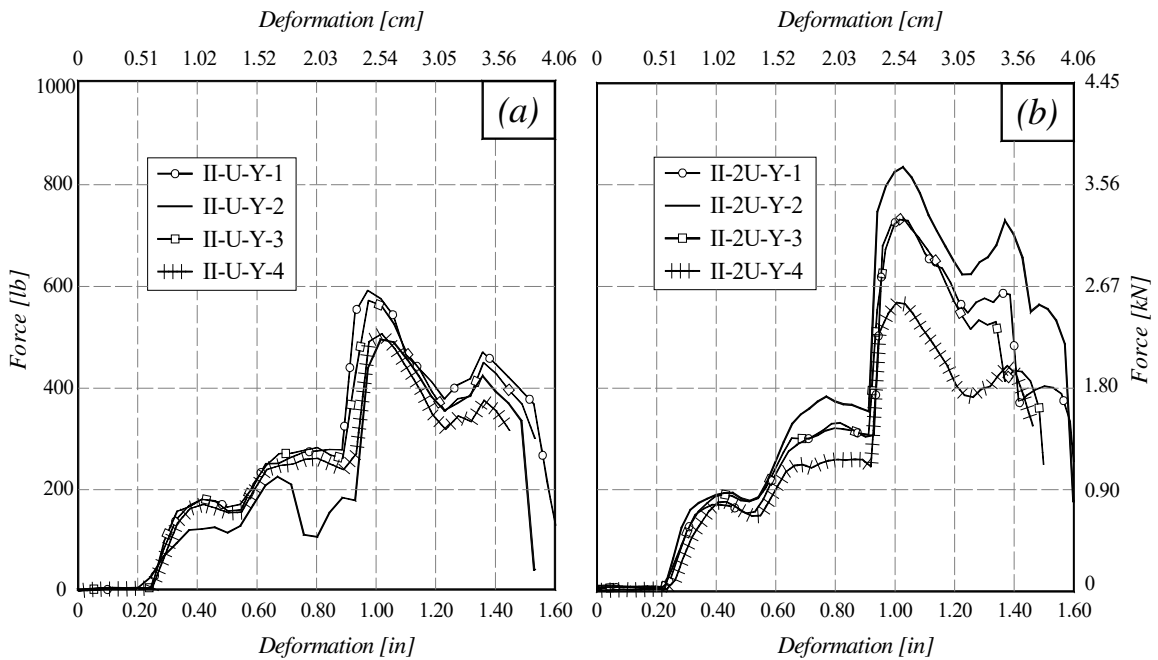
Figure 3.20: Tangential (Δy) and Vertical (Δz) Translation Response of Tie Wire Connections made by Inexperienced Worker: a) Single-U b) Double-U
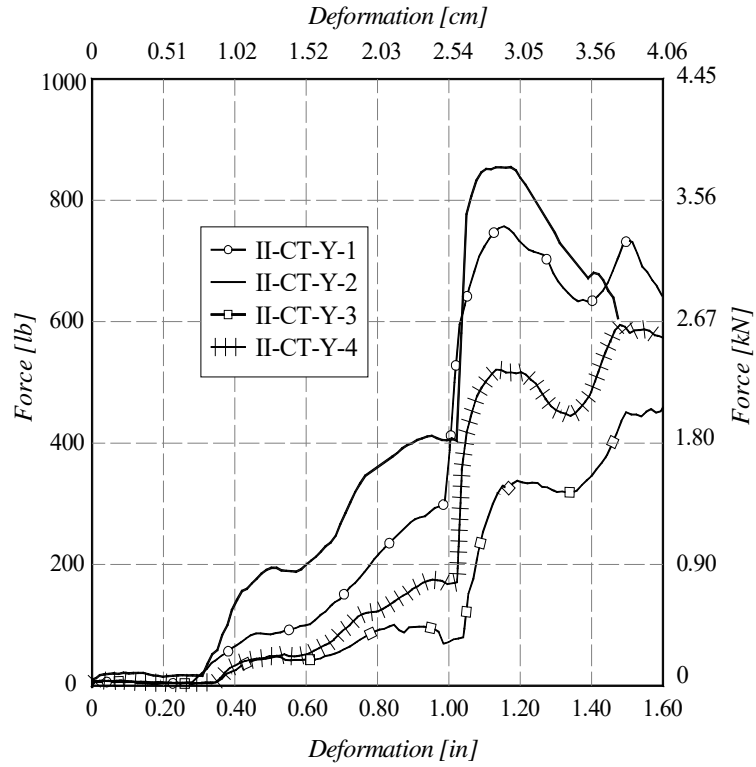
Figure 3.21: Tangential (Δy) and Vertical (Δz) Translation Response of Column-Tie Tie Wire Connections made by Inexperienced Worker
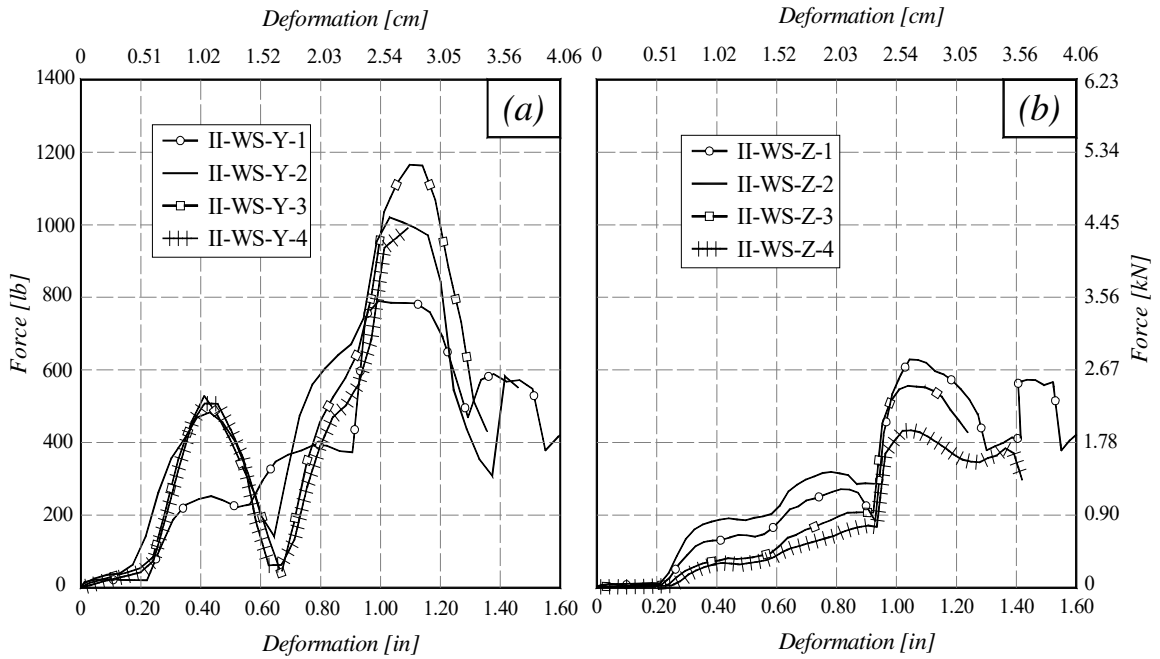
Figure 3.22: Response of Wrap-and-Saddle Tie Wire Connections made by Inexperienced Worker: a) Tangential Direction (Δy) b) Vertical Direction (Δz)
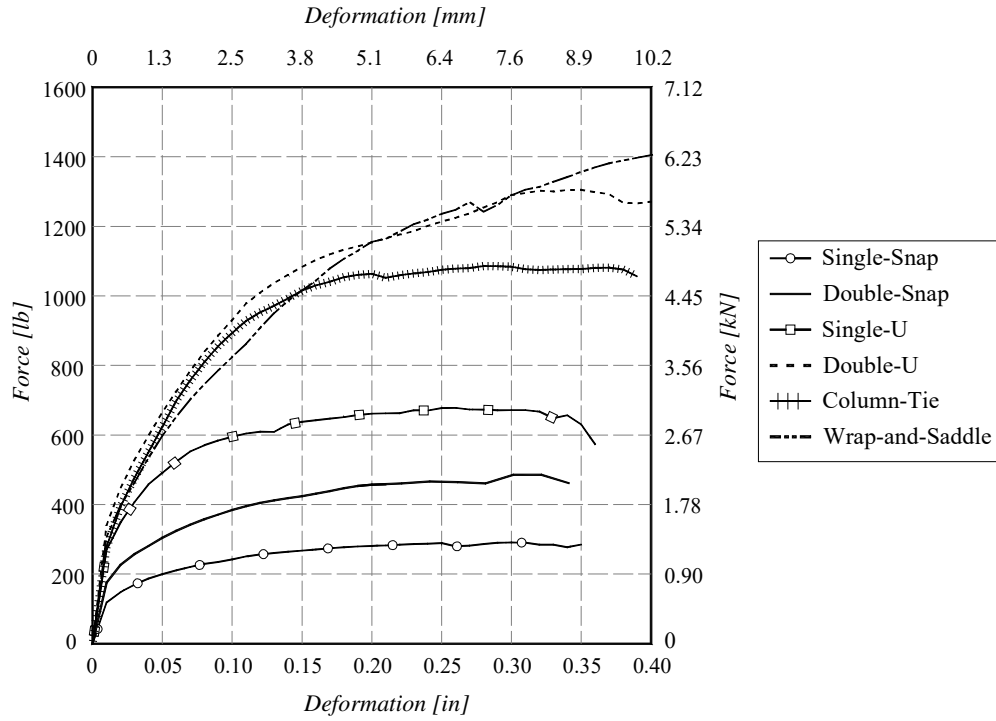
Figure 3.23: Average Normal Translation (Δx) response of Tie Wire Connections made by Experienced Iron worker
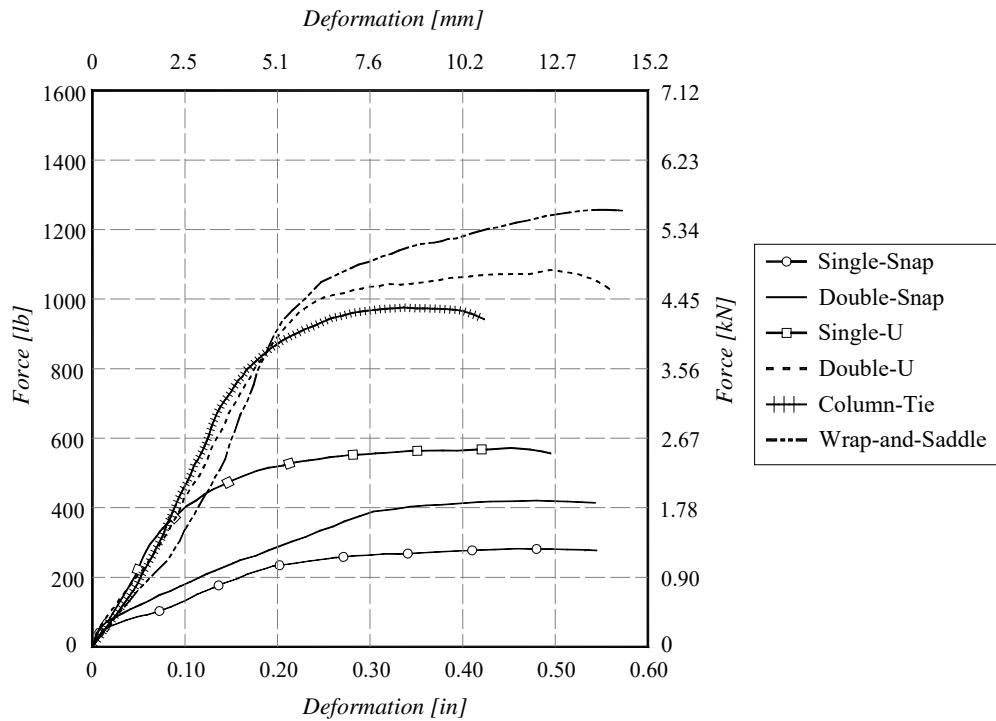
Figure 3.24: Average Normal Translation (Δx) response of Tie Wire Connections made by Inexperienced Worker

103
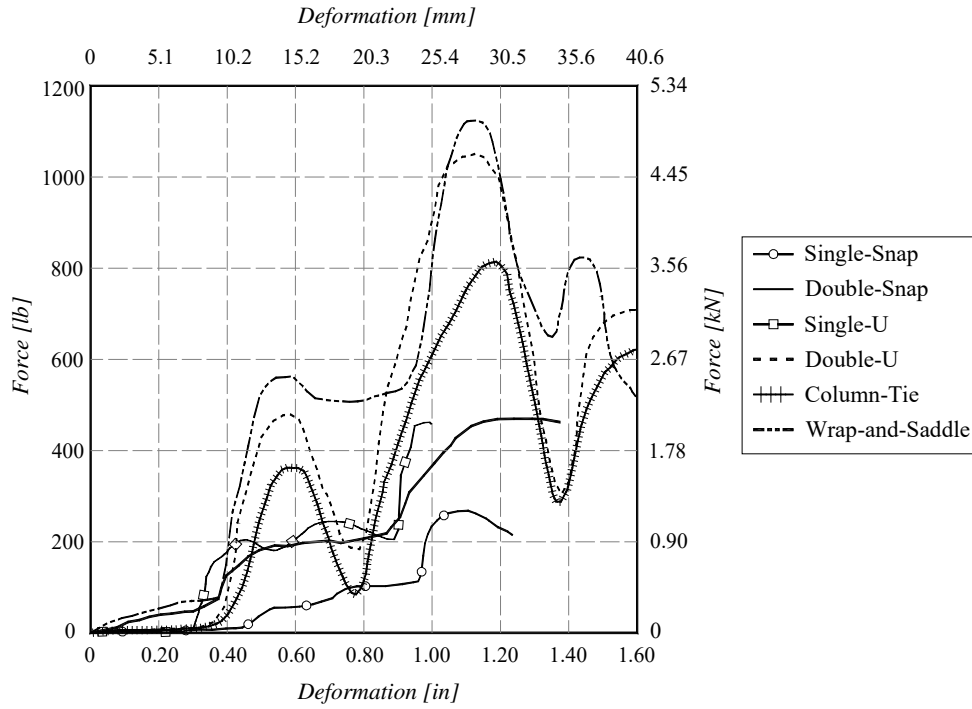
Figure 3.25: Average Tangential (Δy) and Vertical (Δz) Translation response of Tie Wire Connections made by Experienced Iron worker
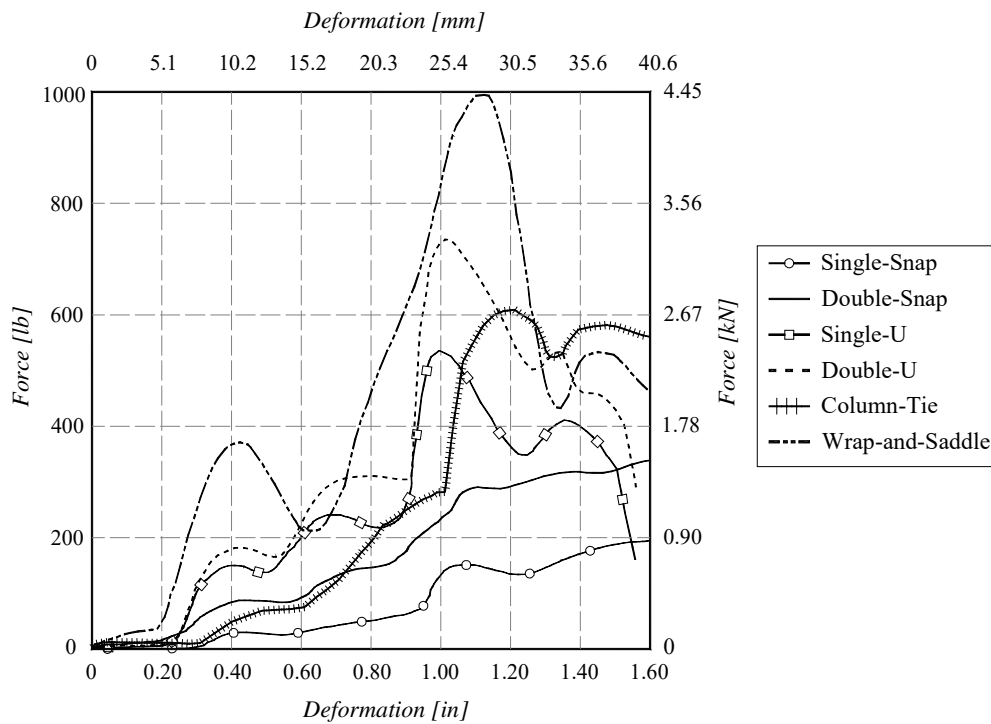
Figure 3.26: Average Tangential (Δy) and Vertical (Δz) Translation response of Tie Wire Connections made by Inexperienced Worker

Figure 3.27: Normal Rotation Fixture Test
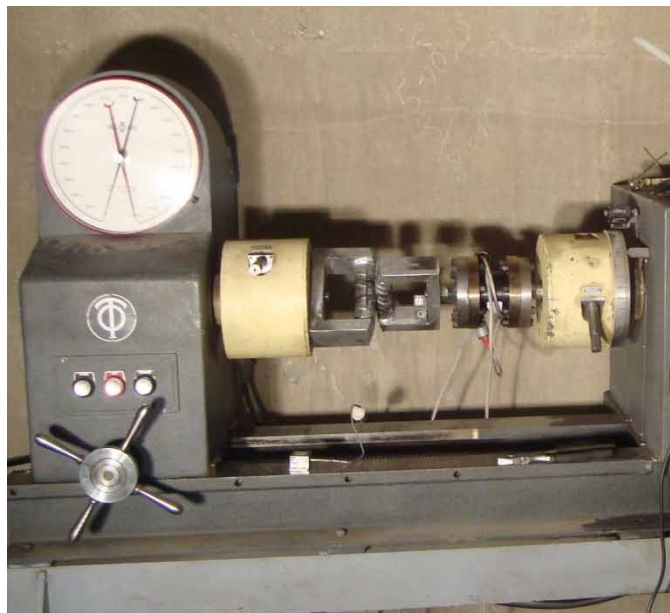
Figure 3.28: Normal Rotation Test Set-Up for Tie Wire Connection
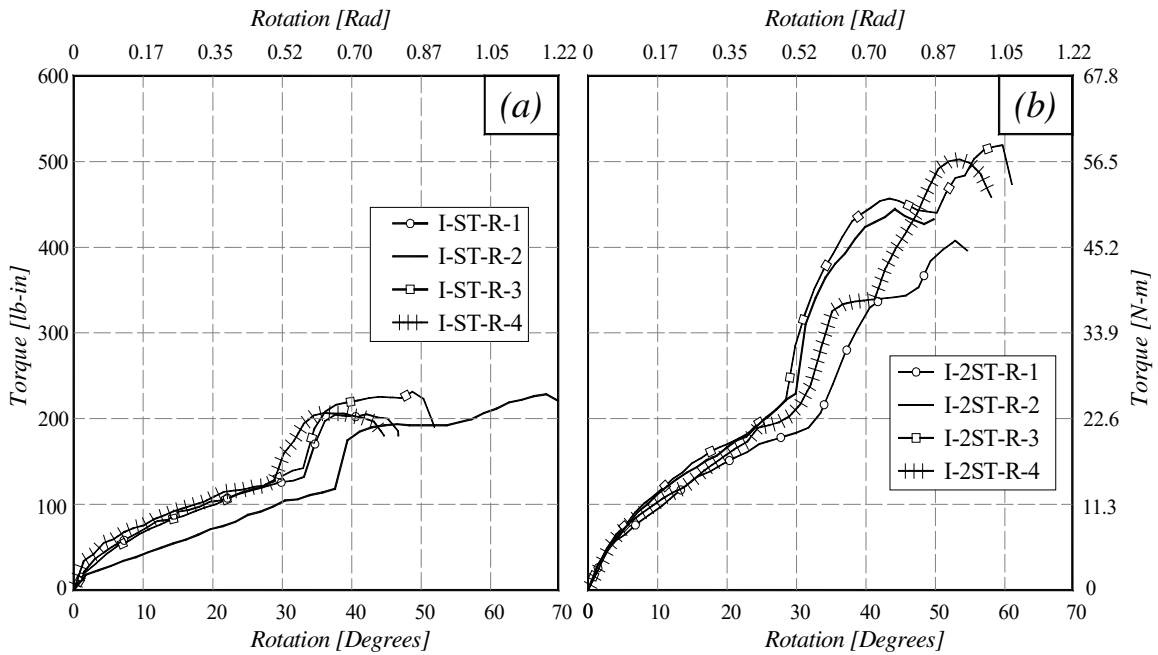
Figure 3.29: Normal Rotational (θx) Response of Tie Wire Connections made by Experienced Iron Worker: a) Single-Snap b) Double-Snap
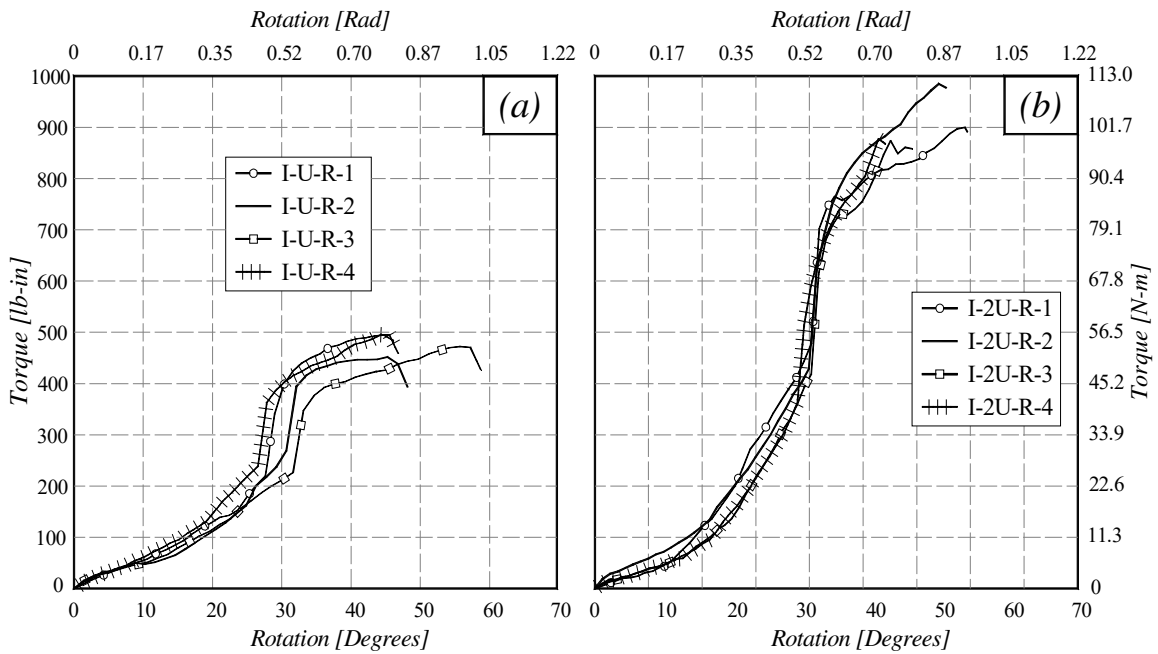
Figure 3.30: Normal Rotational Response (θx) of Tie Wire Connections made by Experienced Iron Worker: a) Single-U b) Double-U
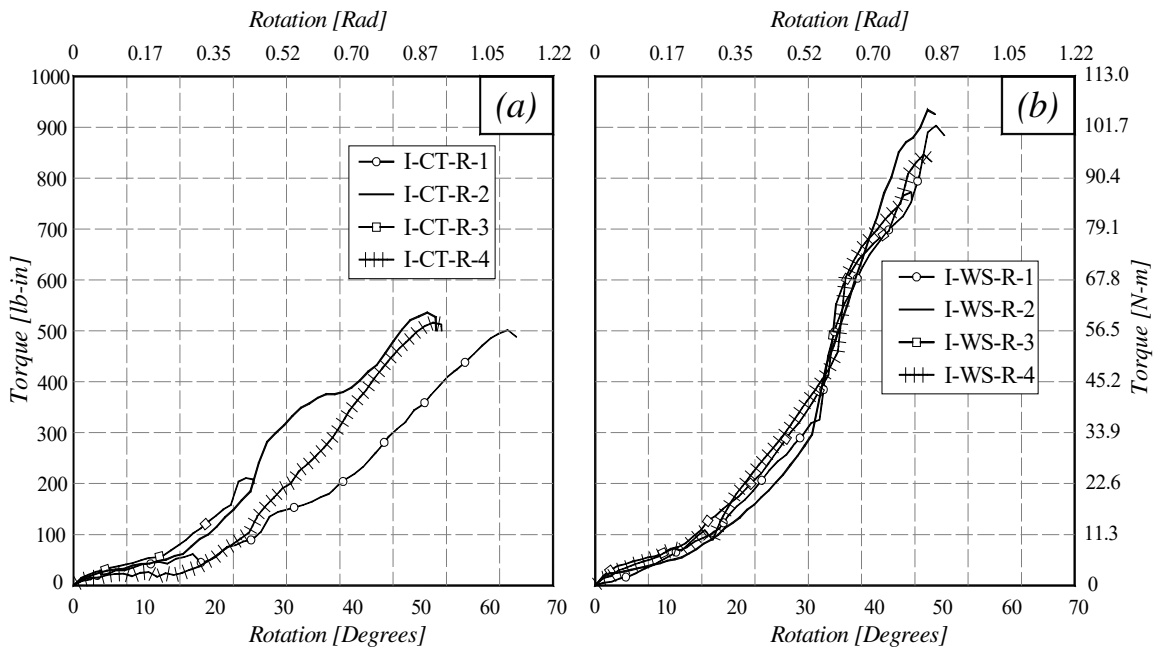
Figure 3.31: Normal Rotational Response (θx) of Tie Wire Connections made by Experienced Iron Worker: a) Column-Tie b) Wrap-and-Saddle
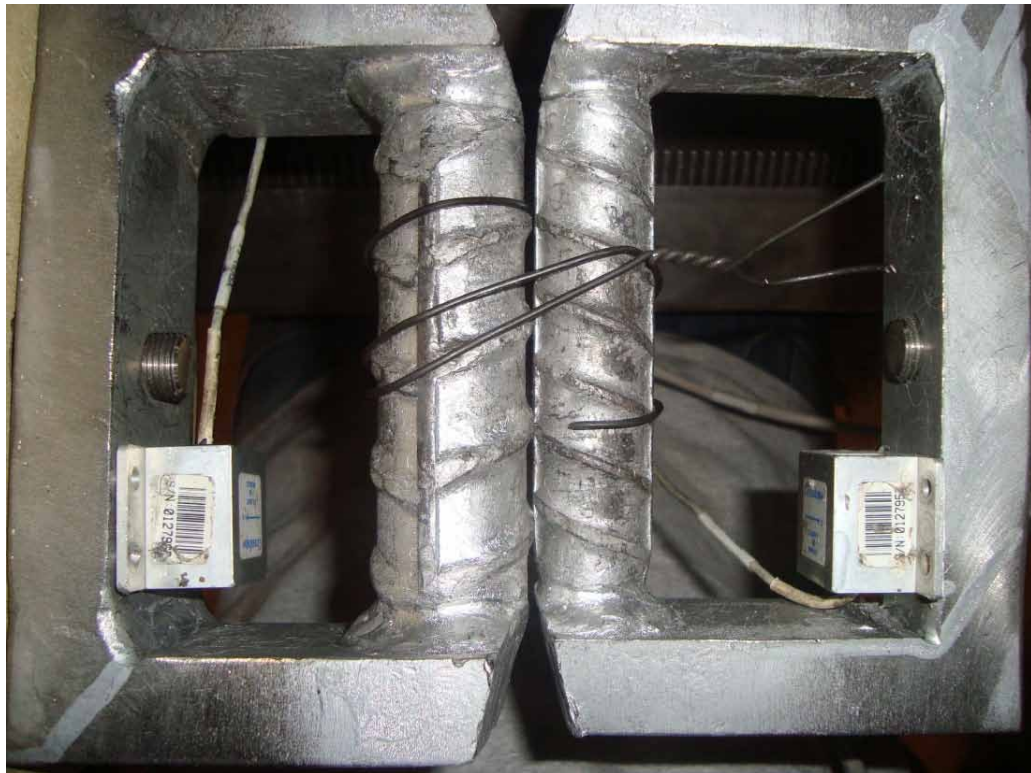
Figure 3.32: Fracture of Single-Snap Tie under Rotation

107
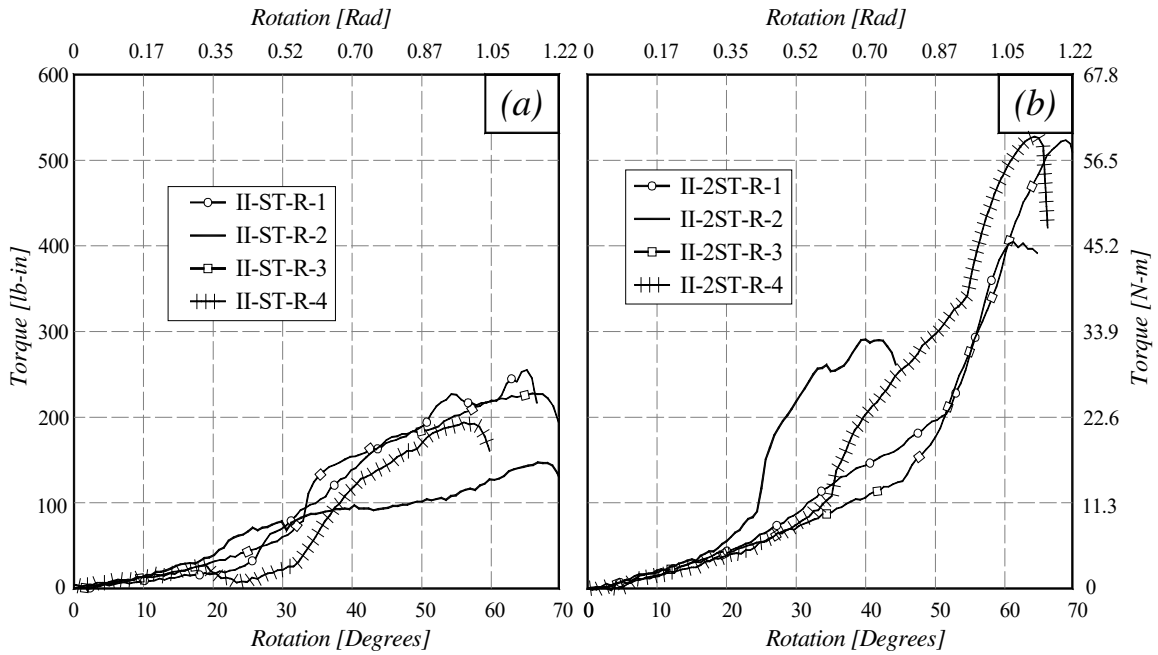
Figure 3.33: Normal Rotational Response (θx) of Tie Wire Connections made by Inexperienced Worker: a) Single-Snap b) Double-Snap
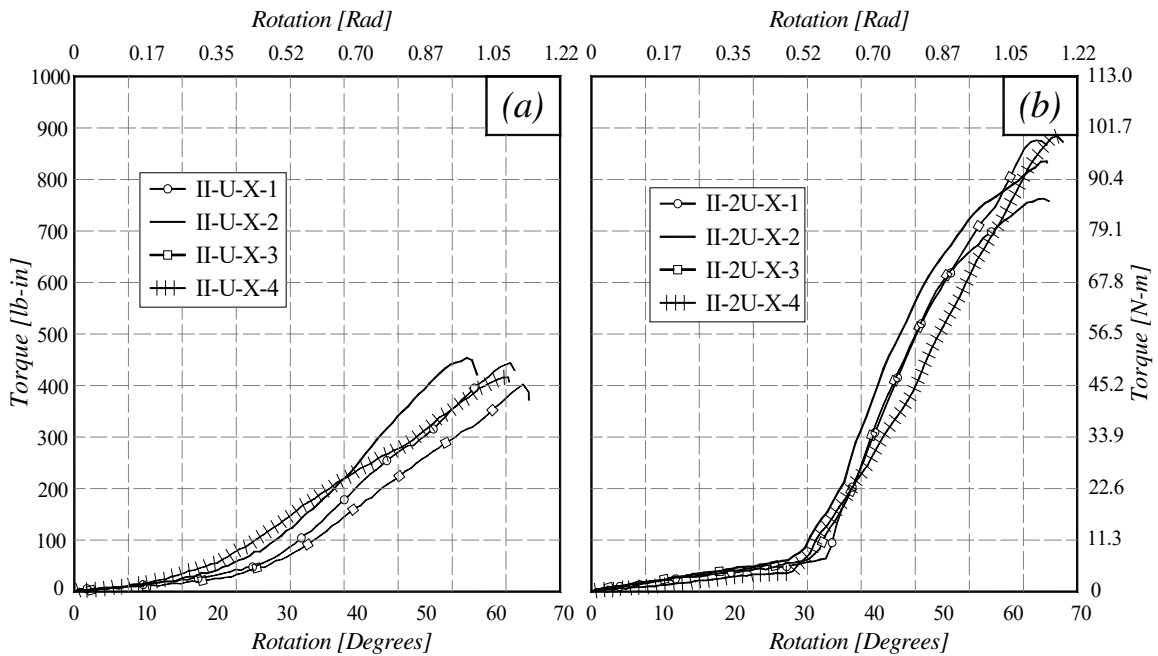
Figure 3.34: Normal Rotational Response (θx) of Tie Wire Connections made by Inexperienced Worker: a) Single-U b) Double-U
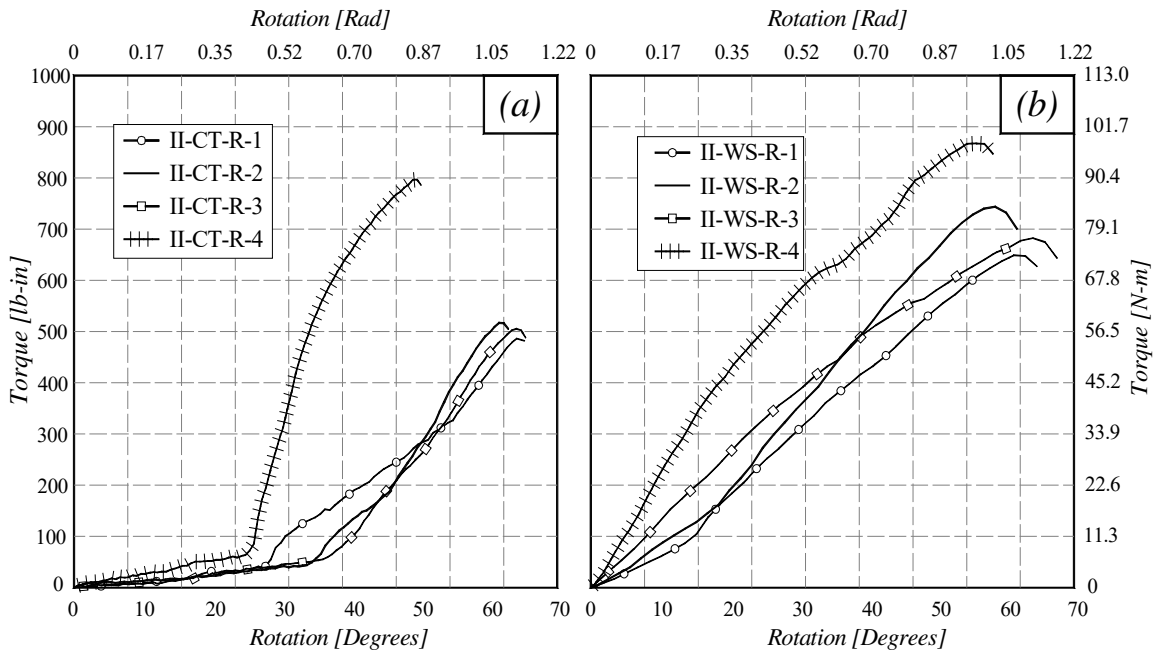
Figure 3.35: Normal Rotational Response (θx) of Tie Wire Connections made by Inexperienced Worker: a) Column-Tie b) Wrap-and-Saddle
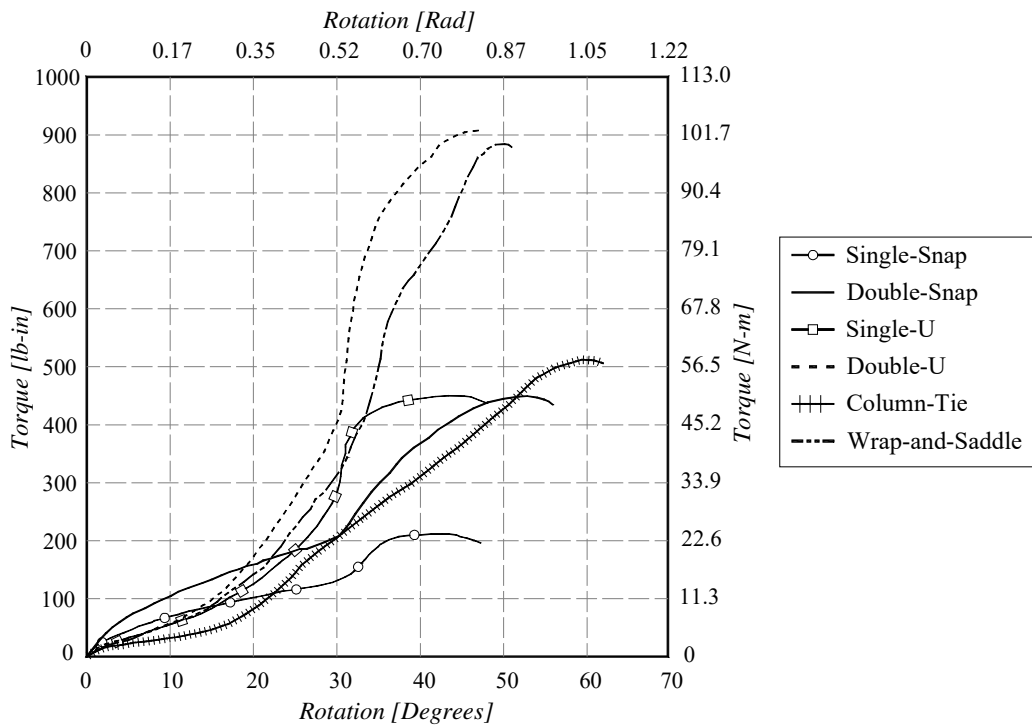
Figure 3.36: Average Rotational Response (θx) of Tie Wire Connections made by Experienced Iron worker

109
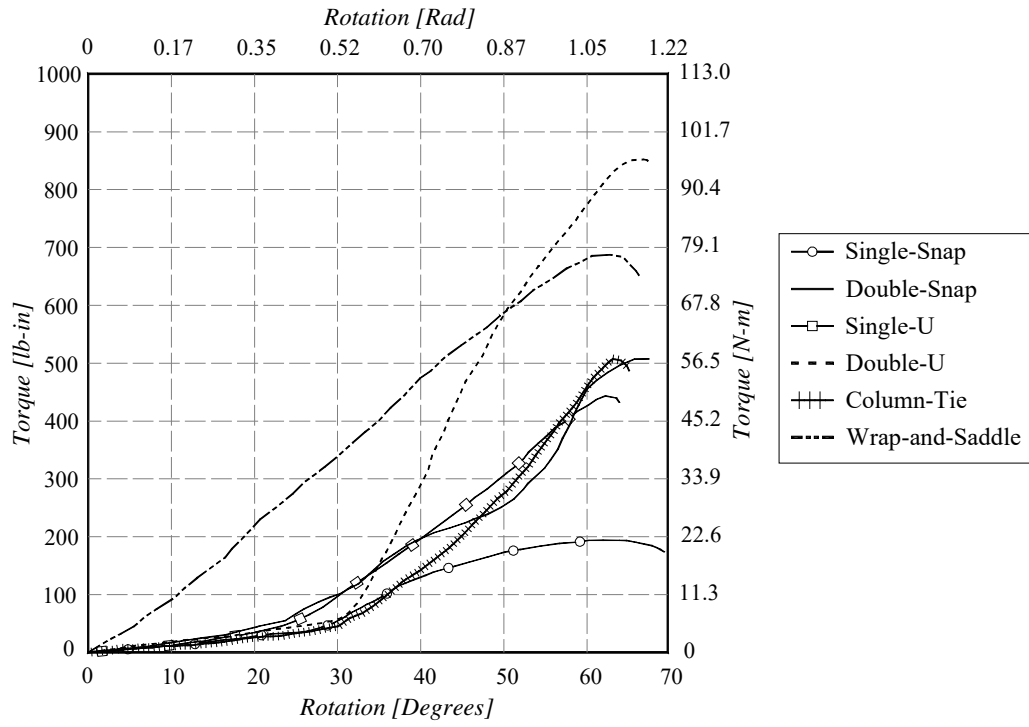
Figure 3.37: Average Rotational Response (θx) of Tie Wire Connections made by Inexperienced Worker
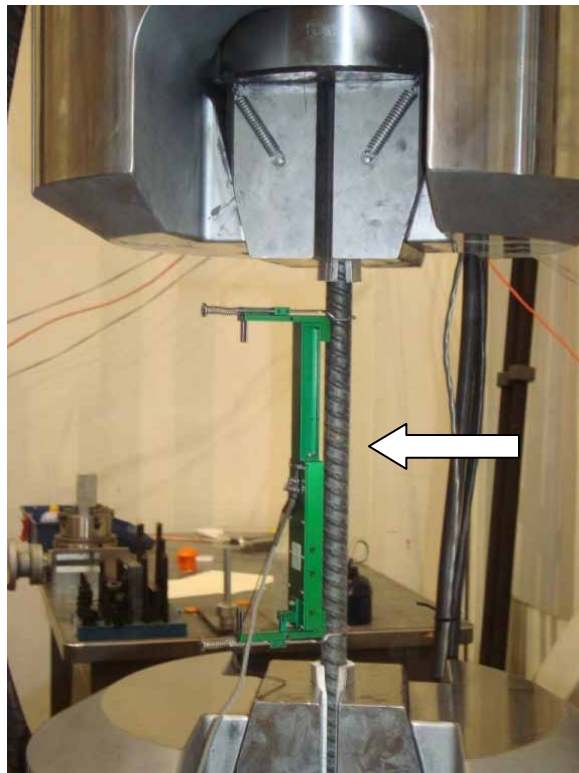
Figure 3.38: Coupon Test of Rebar
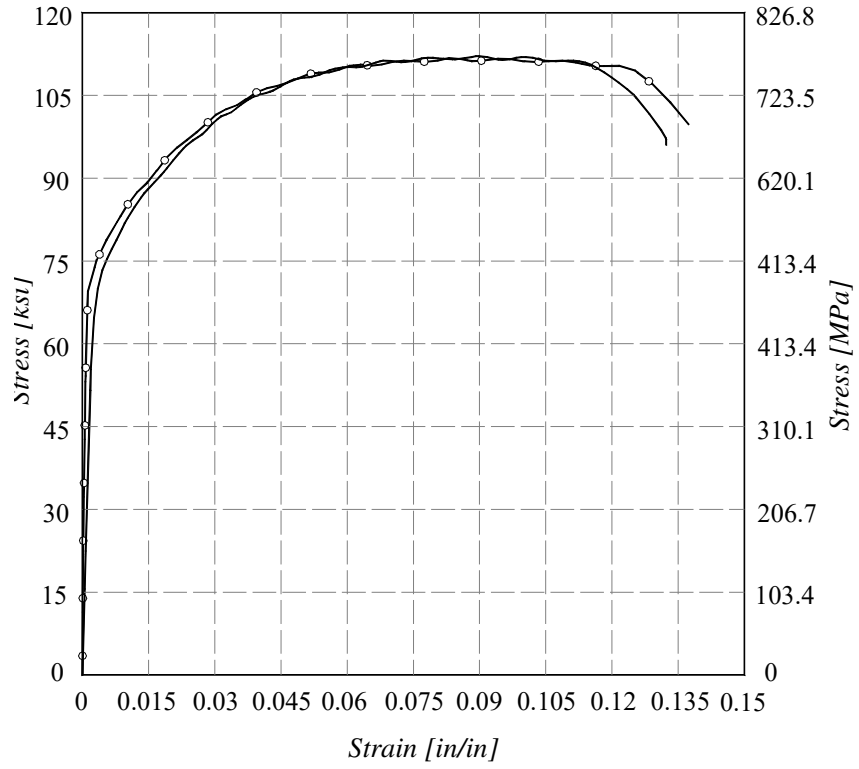
Figure 3.39: Stress-Strain curves for #6 Reinforcing Bars
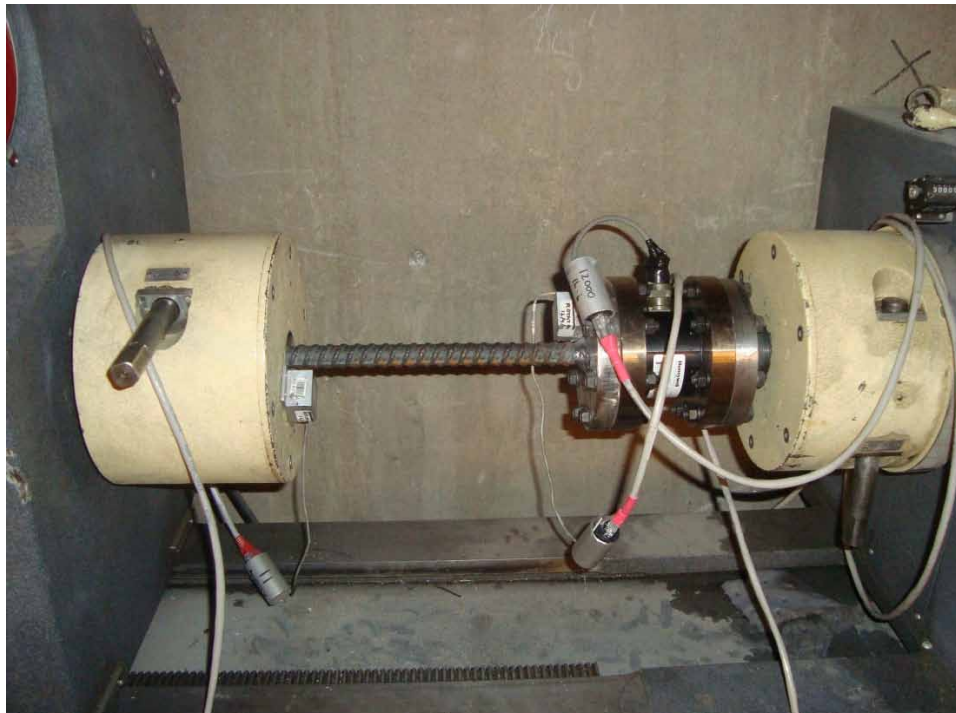
Figure 3.40: Test Set-up for Torsion of a rebar
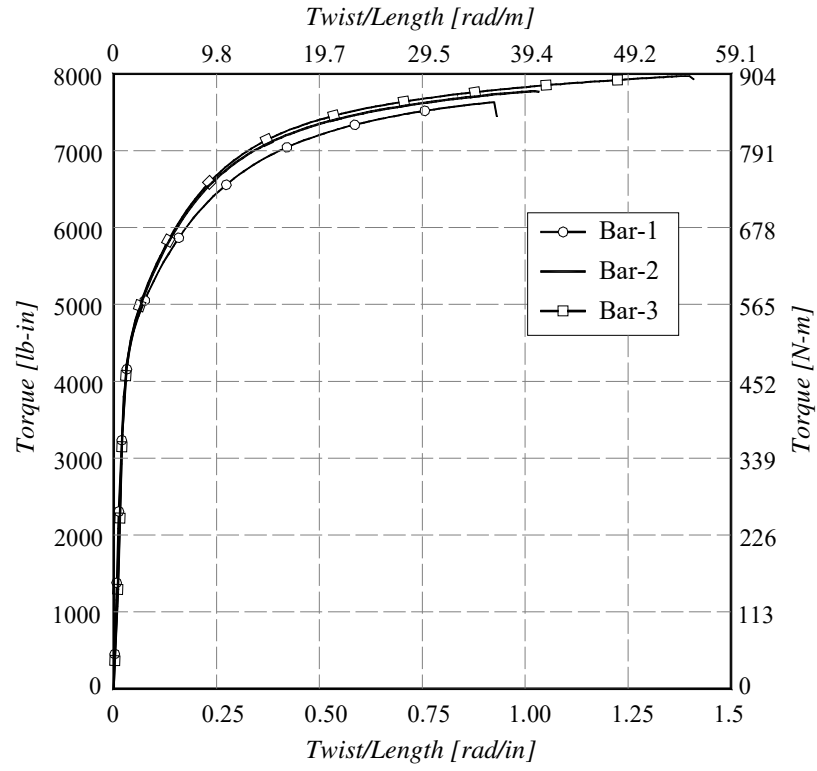
Figure 3.41: Torsional moment-twist Responses of Reinforcing Bars

Figure 3.42: Fracture of #6 Bar under Torsional Loading
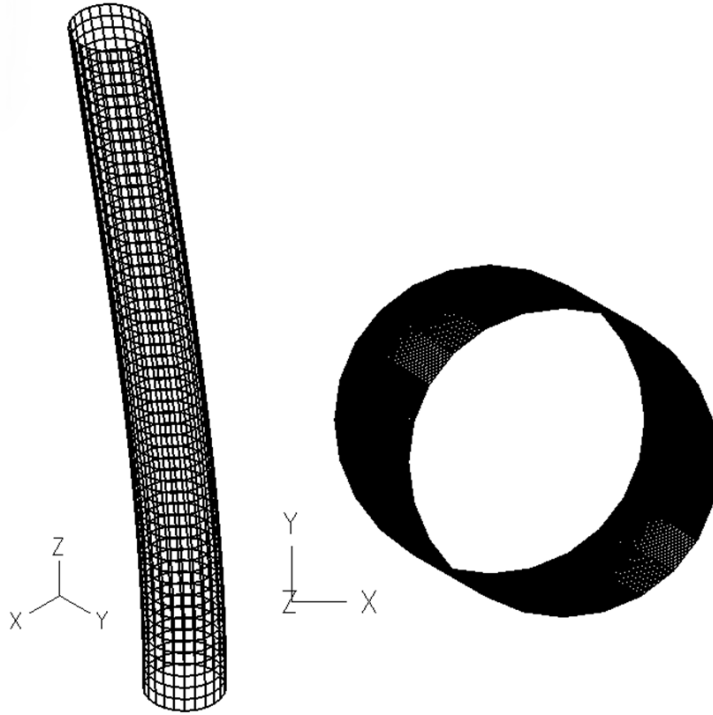
Figure 3.43: First Mode of Column Rebar Cage Model, (Left) 3D View, and (Right) Top View
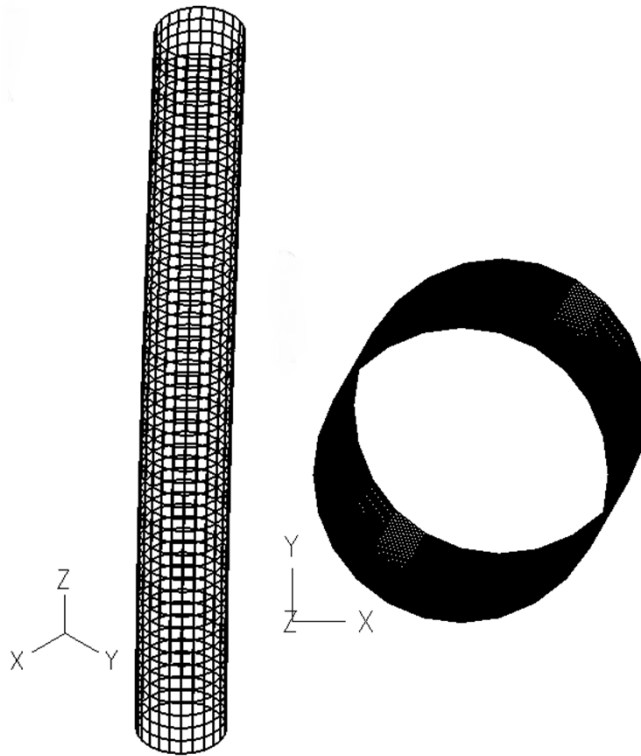
Figure 3.44: Second Mode of Column Rebar Cage Model, (Left) 3D View, and (Right) Top View
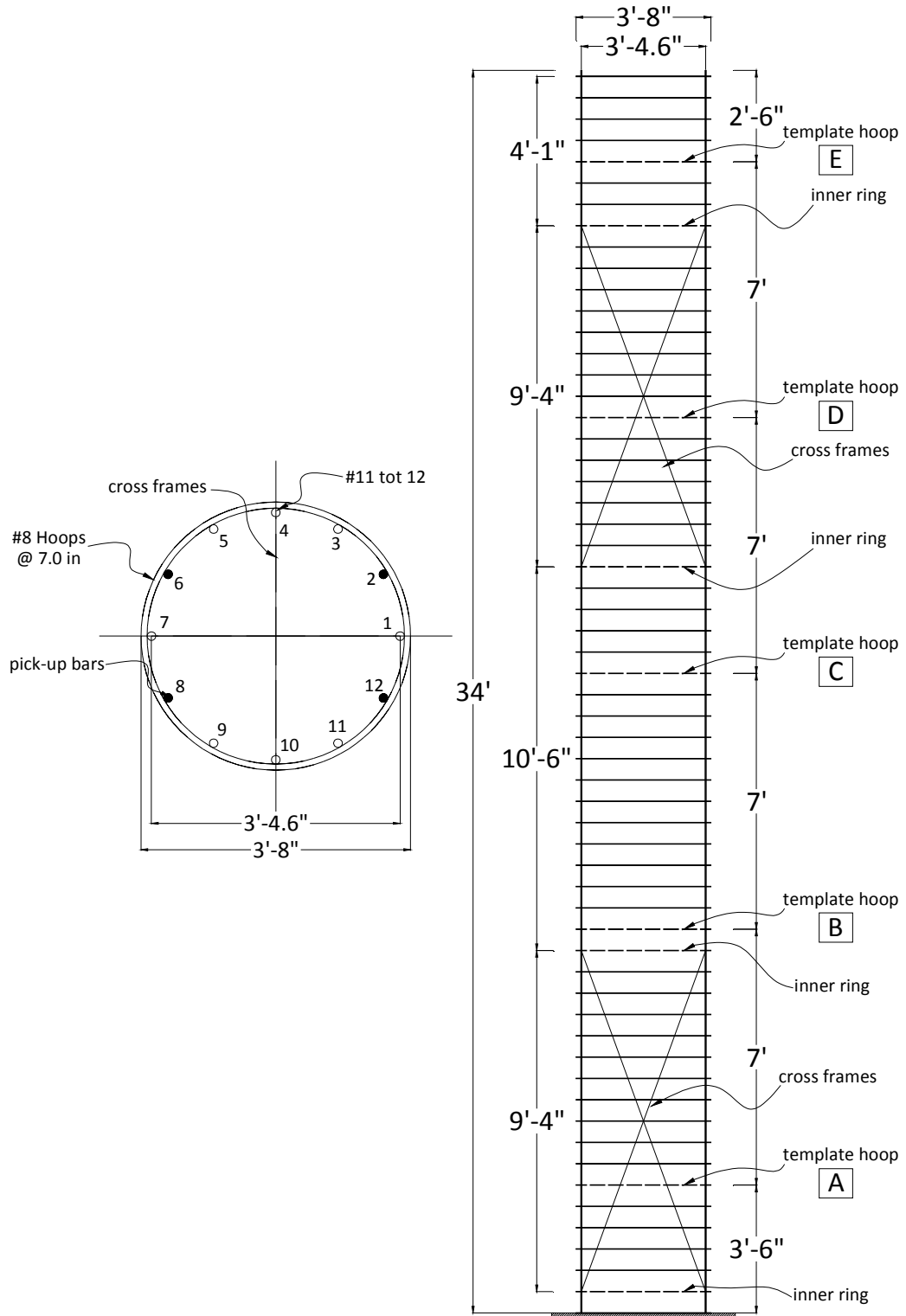
Figure 3.45: Specimen I Dimension and Details
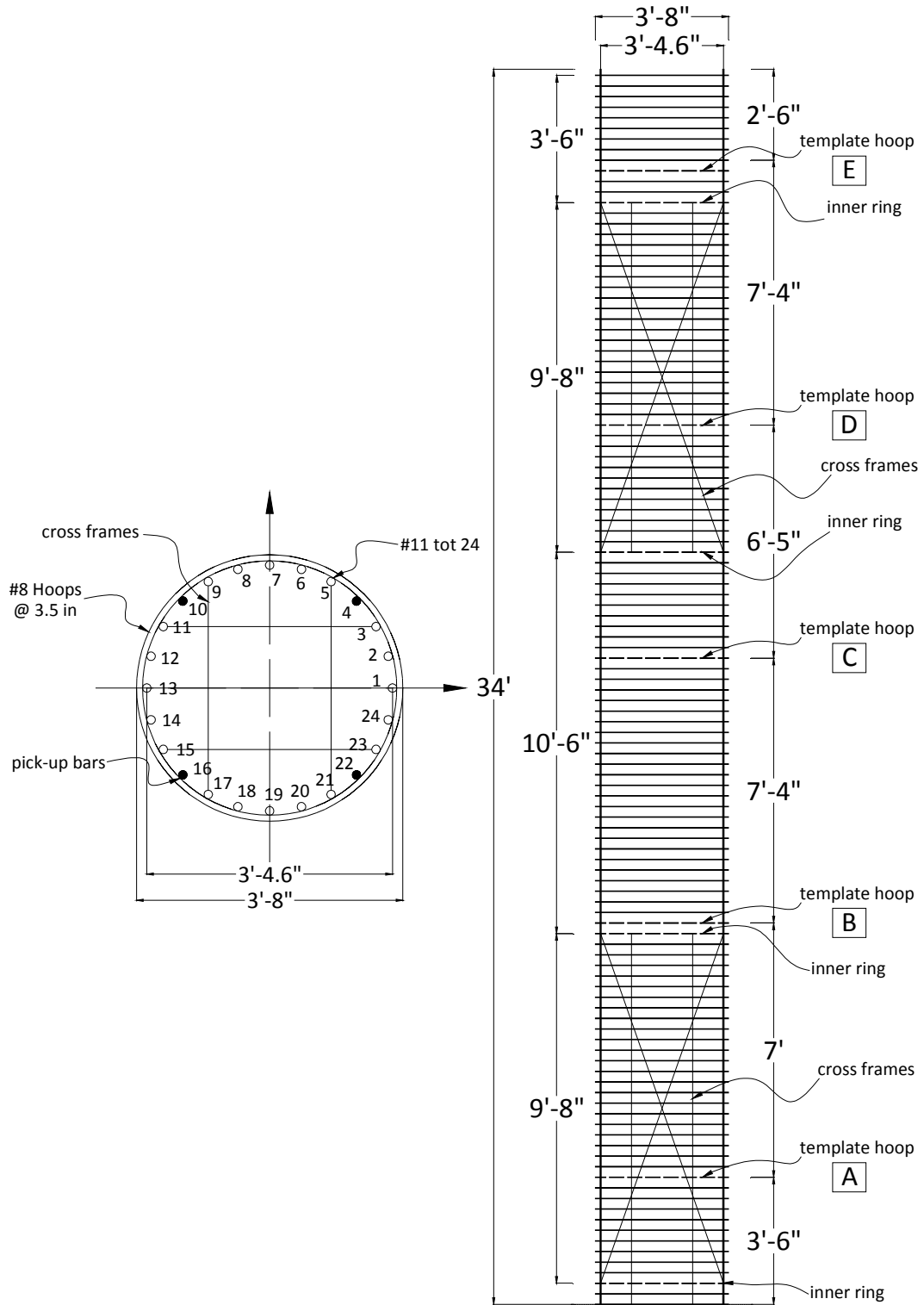
Figure 3.46: Specimen II Dimension and Details

Figure 3.47: X-braces of Specimen I

Figure 3.48: Square-braces of Specimen II
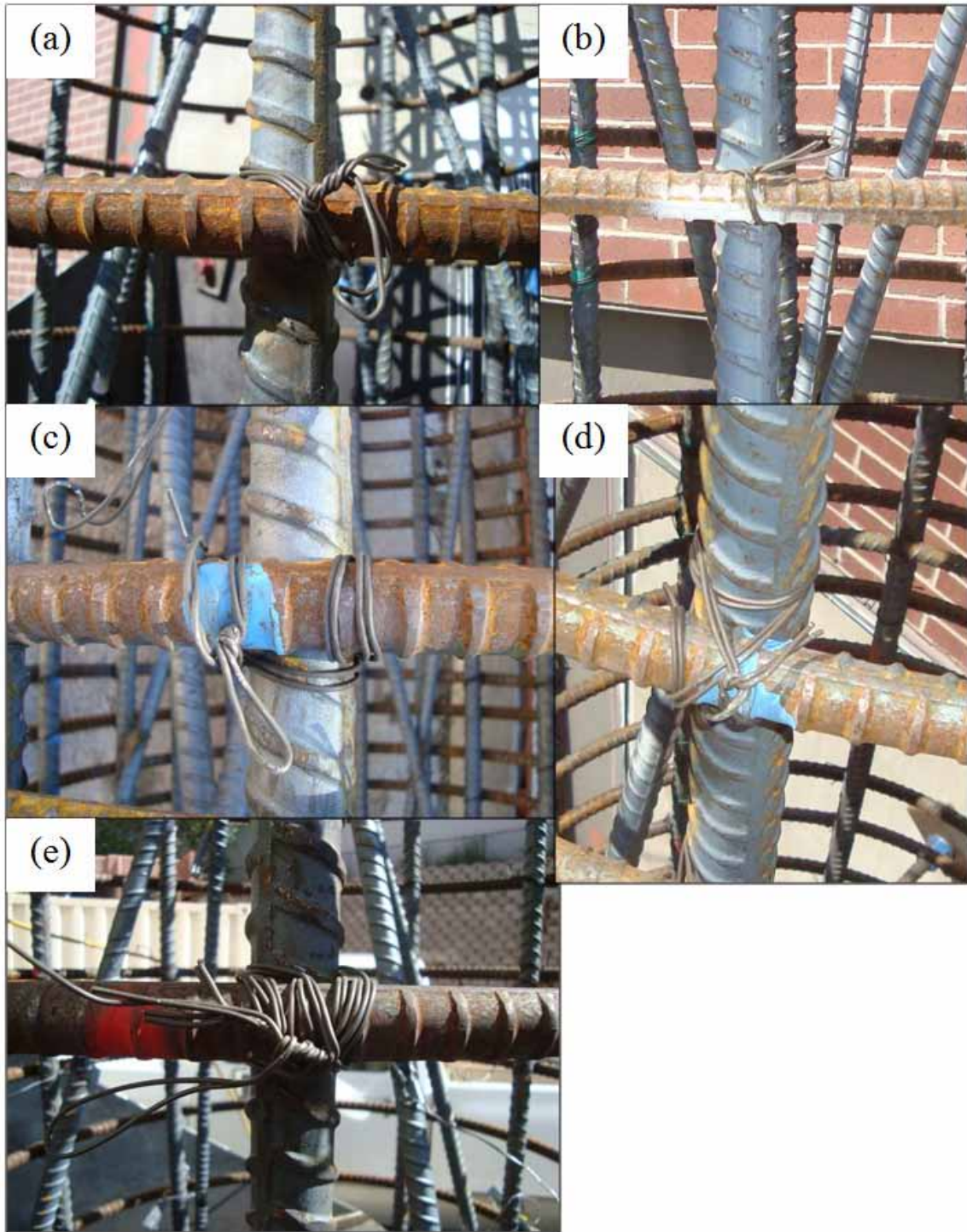
Figure 3.49: Tie Wire Connections used in the Specimens: a) Quadruple-Single-Snap b) Double-Snap c) Wrap-and-Saddle d) Column-Tie e) Strong-Tie

Figure 3.50: Specimen I standing without any Temporary Support

Figure 3.51: Specimen II standing without any Temporary Support
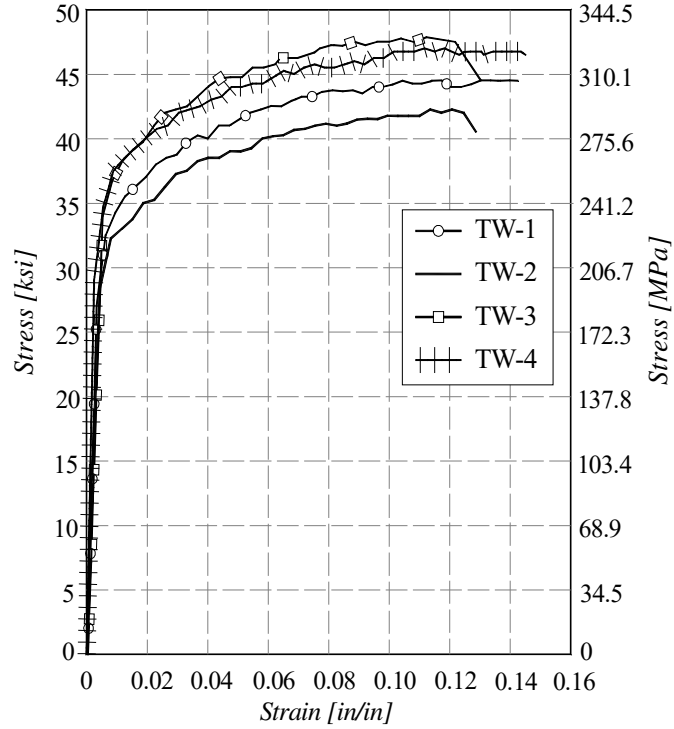
Figure 3.52: Tension Test of Tie Wire Used in the Specimens
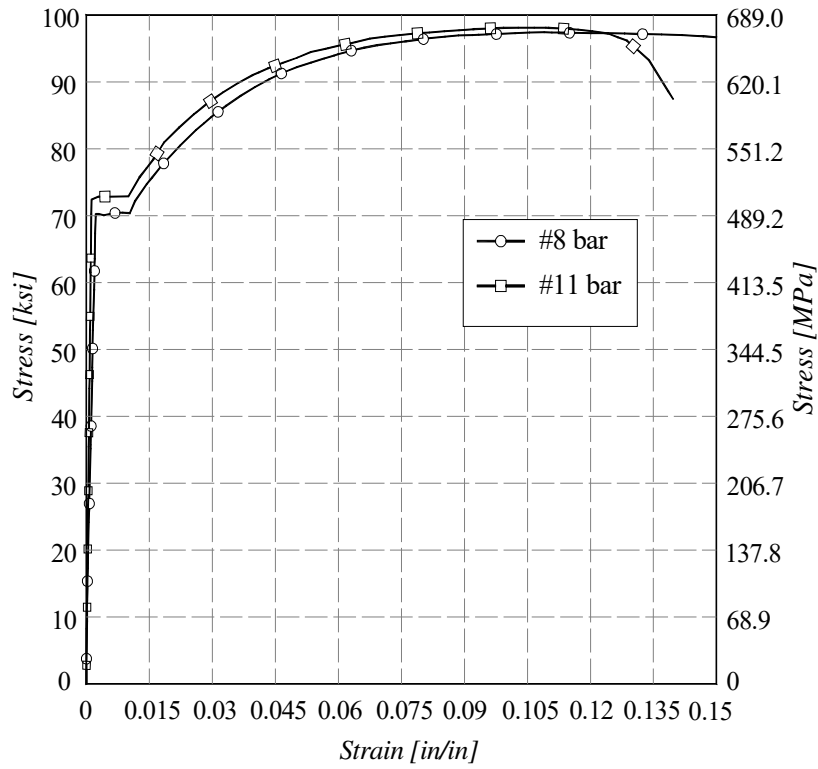
Figure 3.53: Coupon Test from Reinforcing Bars of Specimen II

119

Figure 3.54: Details of Steel Bracket Attachment
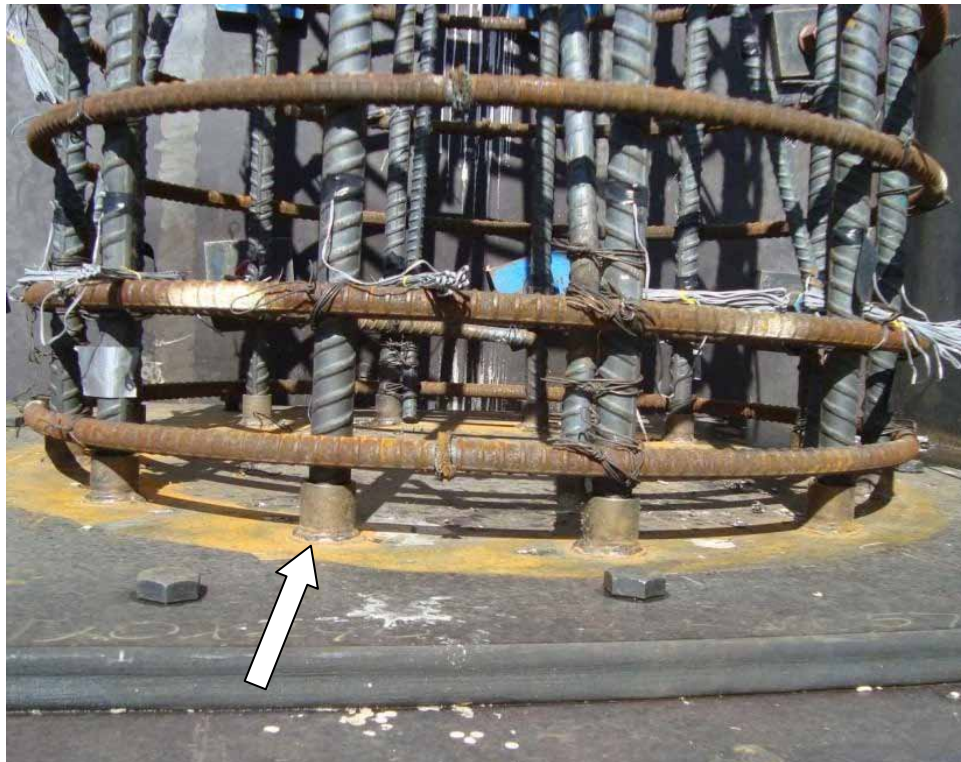
Figure 3.55: Base of the Rebar Cage with the Longitudinal Bars Welded to the Base Plate
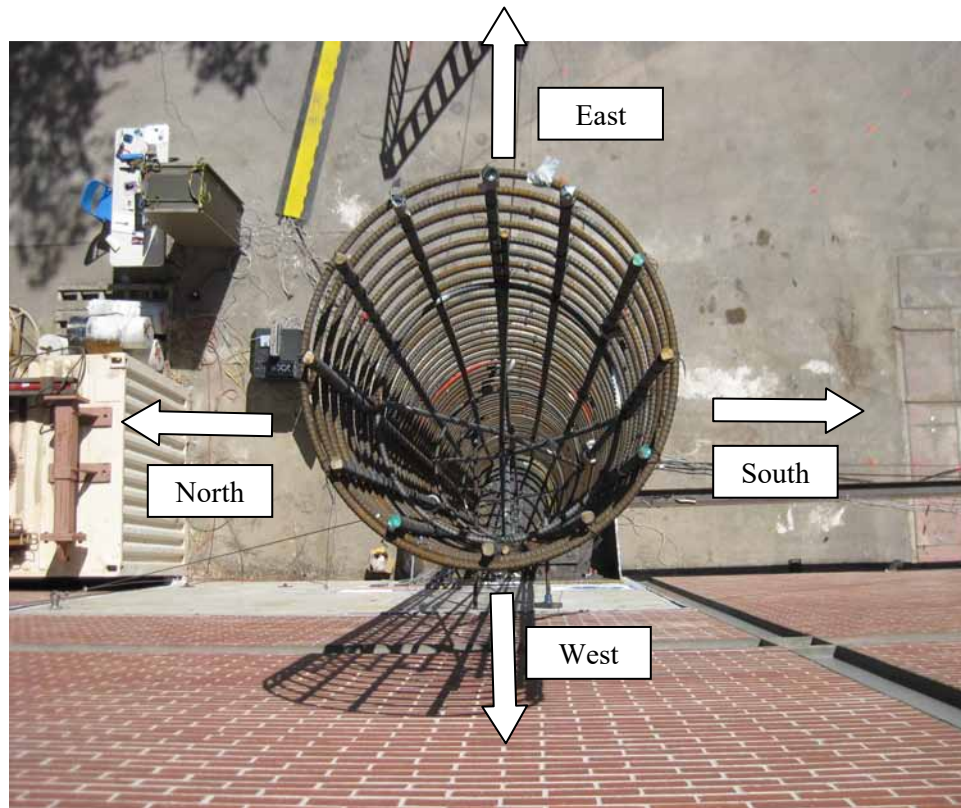
Figure 3.56: Direction of Cardinal Points
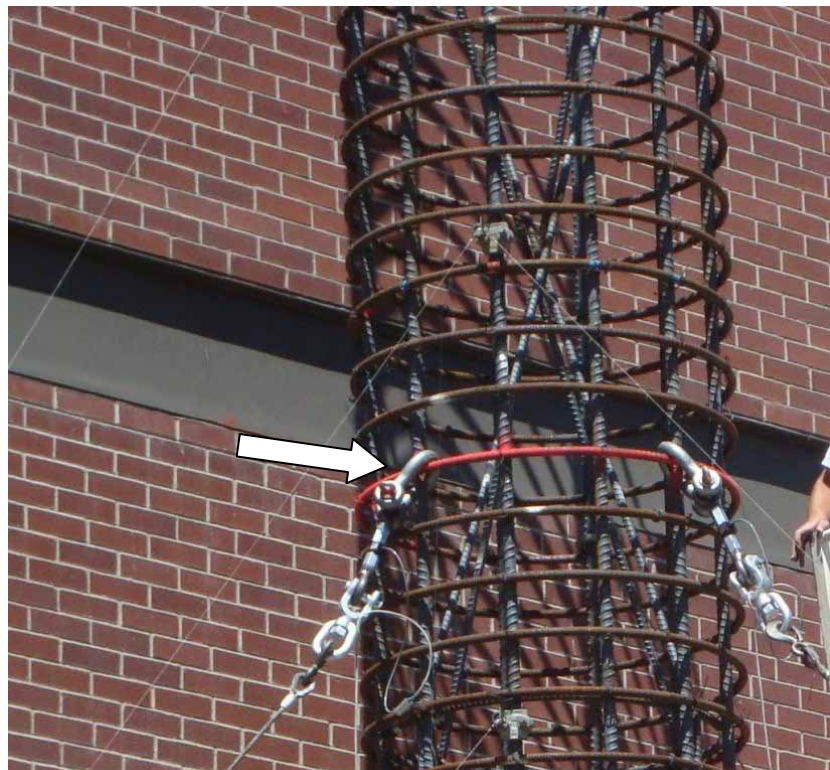
Figure 3.57: Attaching of the cables at the Rebar Cage

Figure 3.58: Winch and Displacement Transducer box located to the west of the Rebar Cage
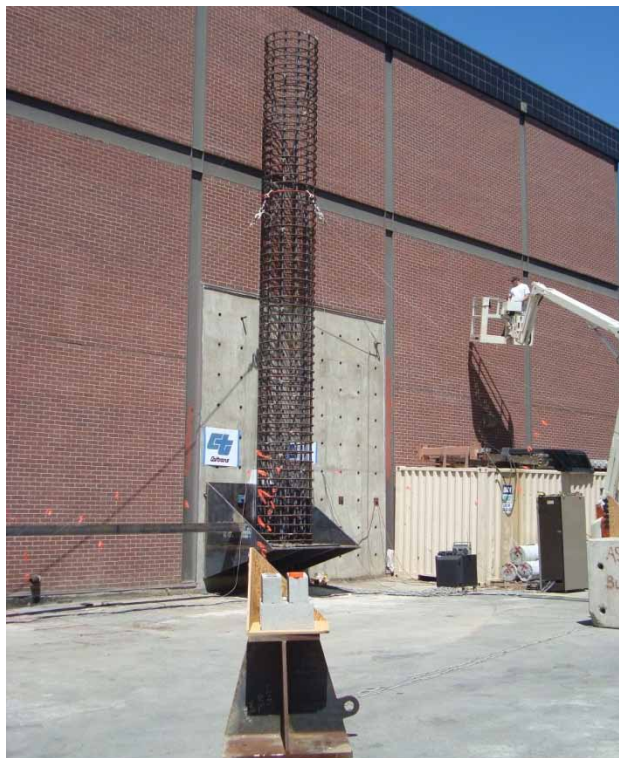
Figure 3.59: Specimen I Test Set-Up

Figure 3.60: Specimen II Test Set-Up
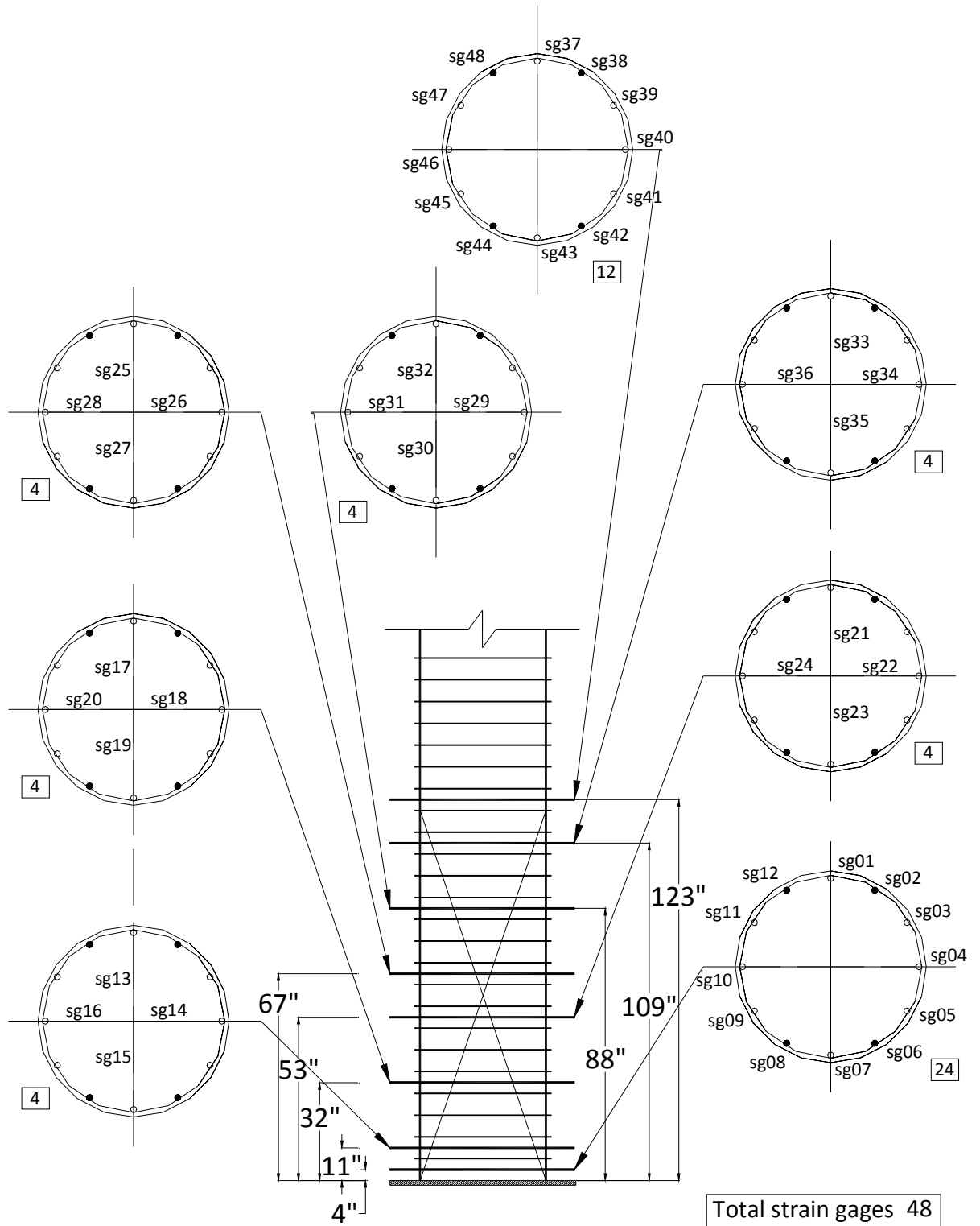
Figure 3.61: Strain Gages Location for Specimen I
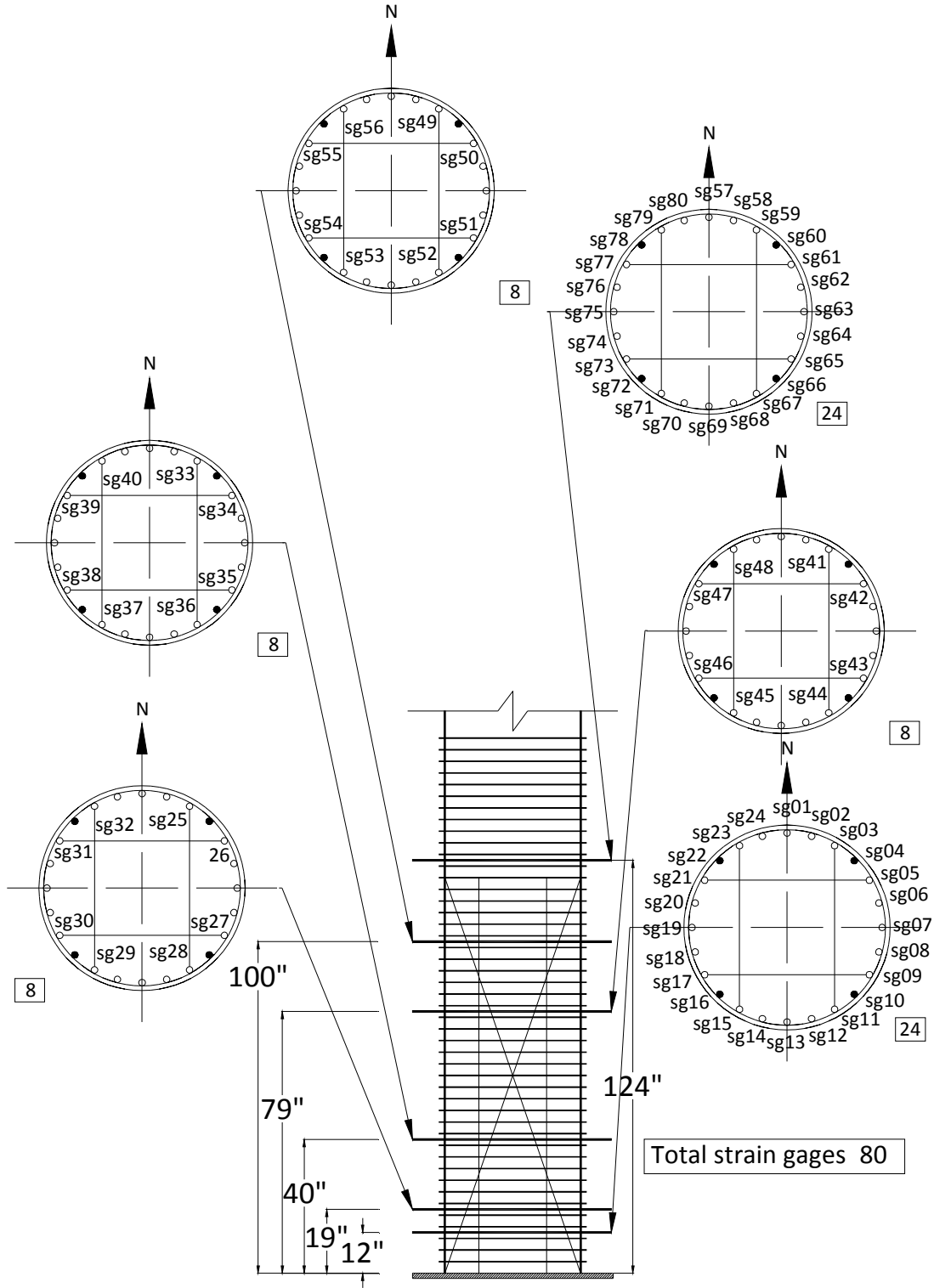
Figure 3.62: Strain Gages Location for Specimen II
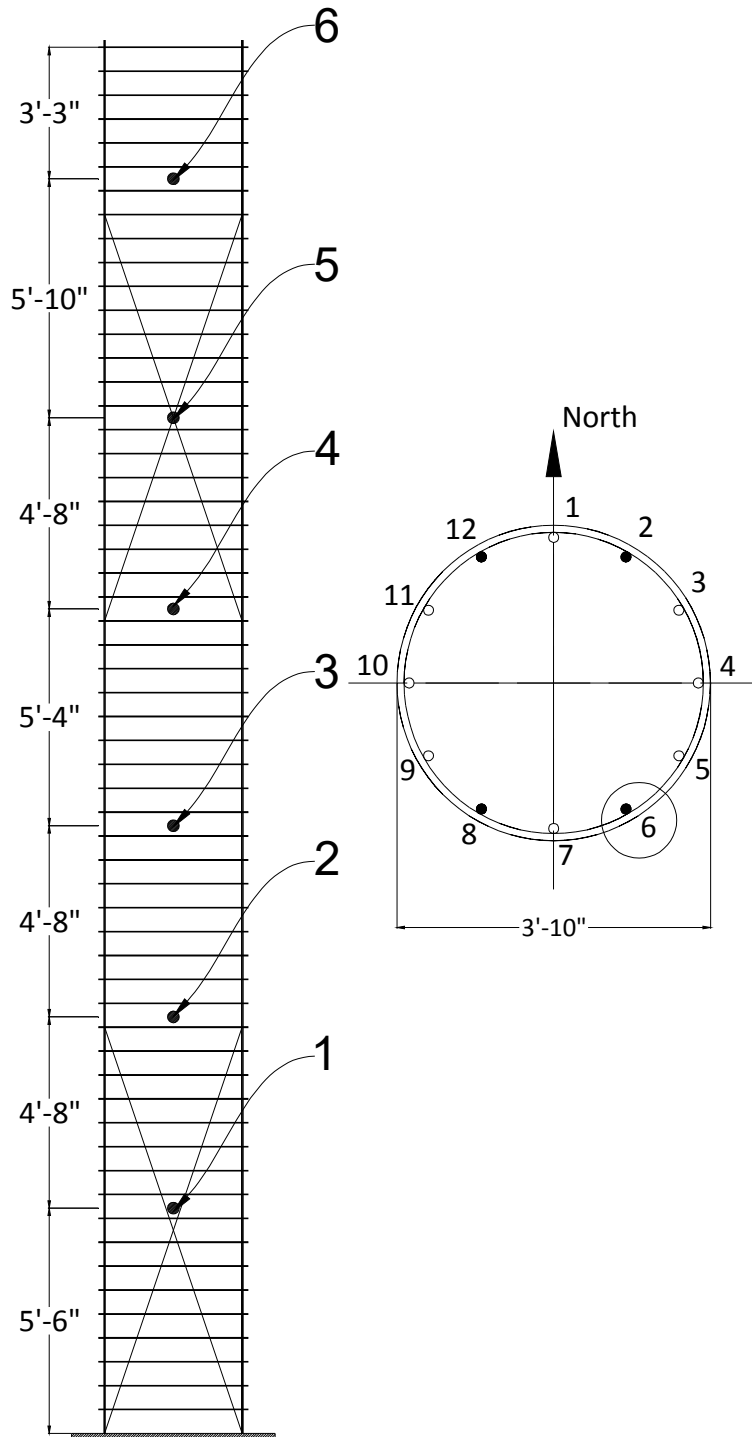
Figure 3.63: Displacement Transducer Location for Specimen I

126
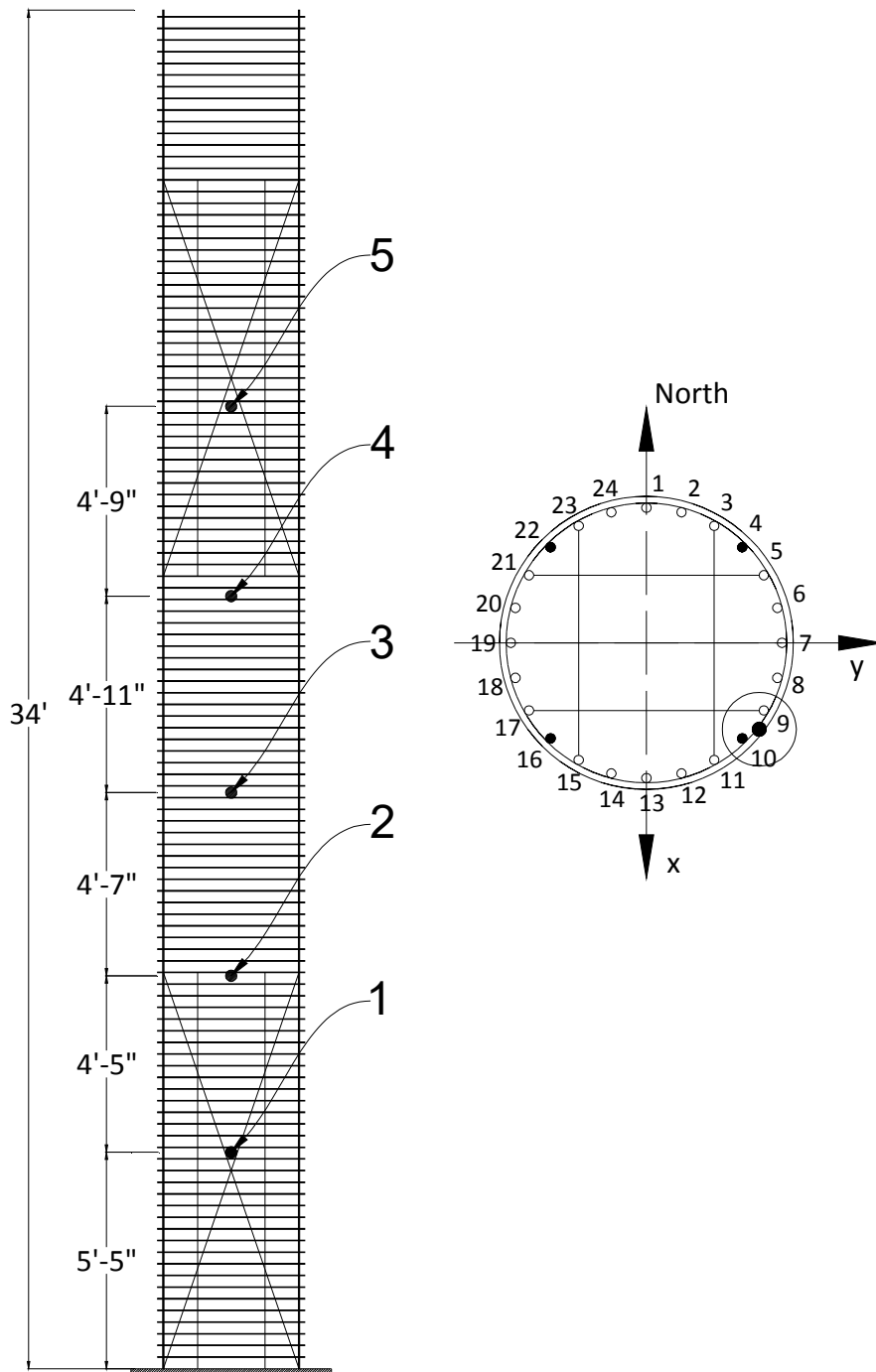
Figure 3.64: Displacement Transducer Location for Specimen II
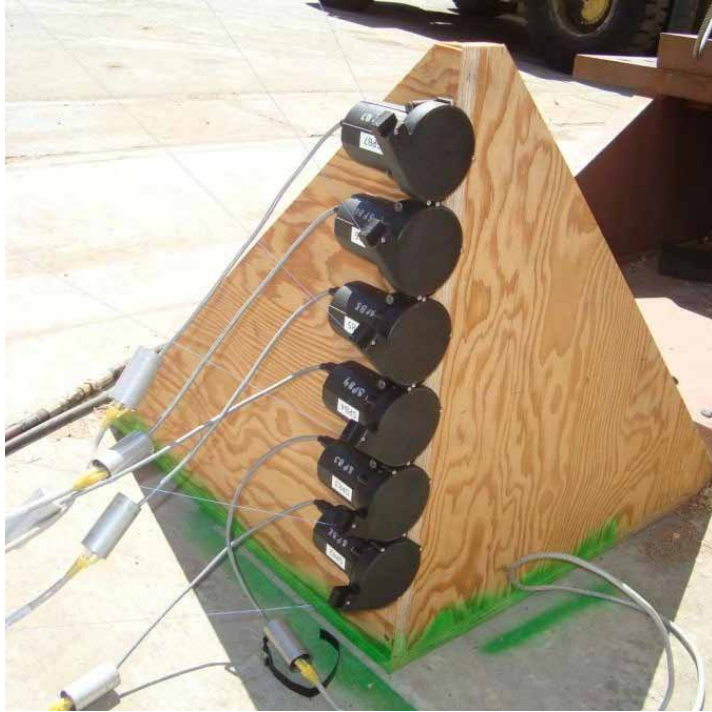
Figure 3.65: South fixed point of the string pots
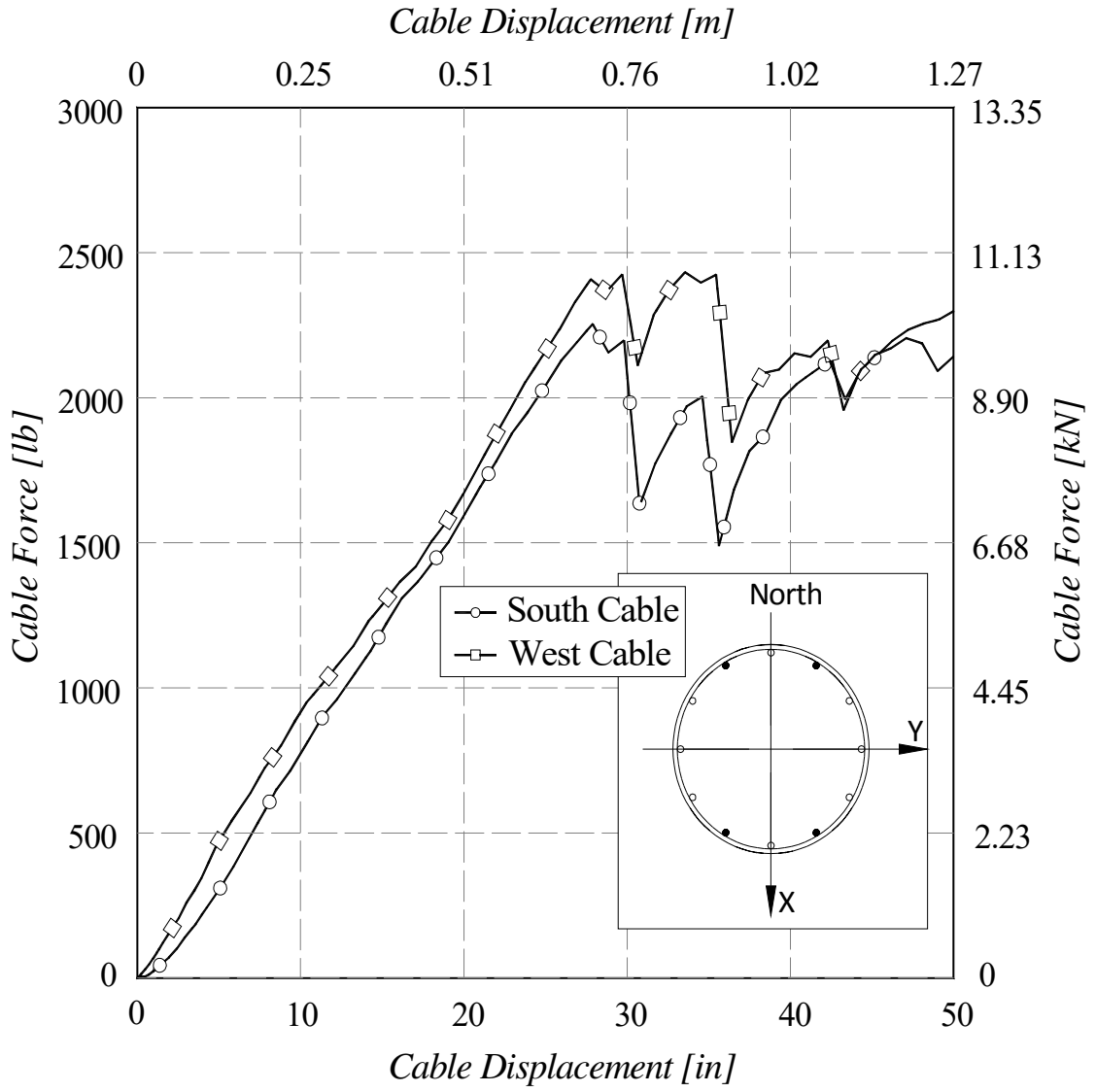
Figure 3.66: Cable Force-Displacement response for Specimen I

Figure 3.67: Collapse of Specimen I
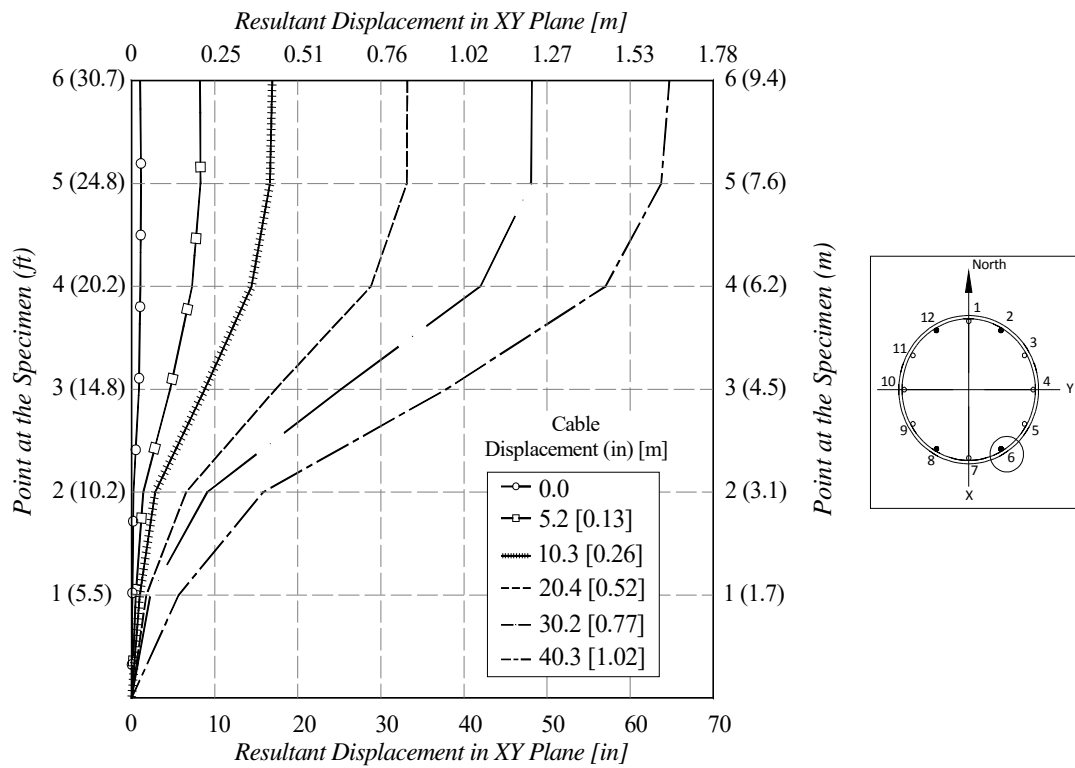
Figure 3.68: Resultant Displacement obtained from Displacement Transducers, Specimen I

Figure 3.69: Specimen I deformed shape, view from South-West

Figure 3.70: Specimen I deformed shape, view from South
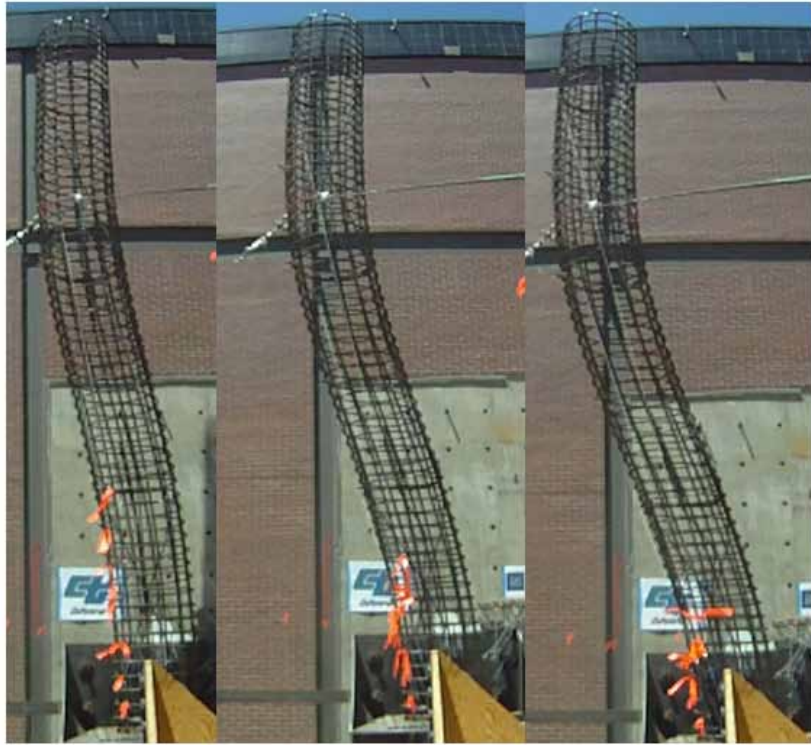
Figure 3.71: Sequence of deformed shapes for Specimen I, view from West
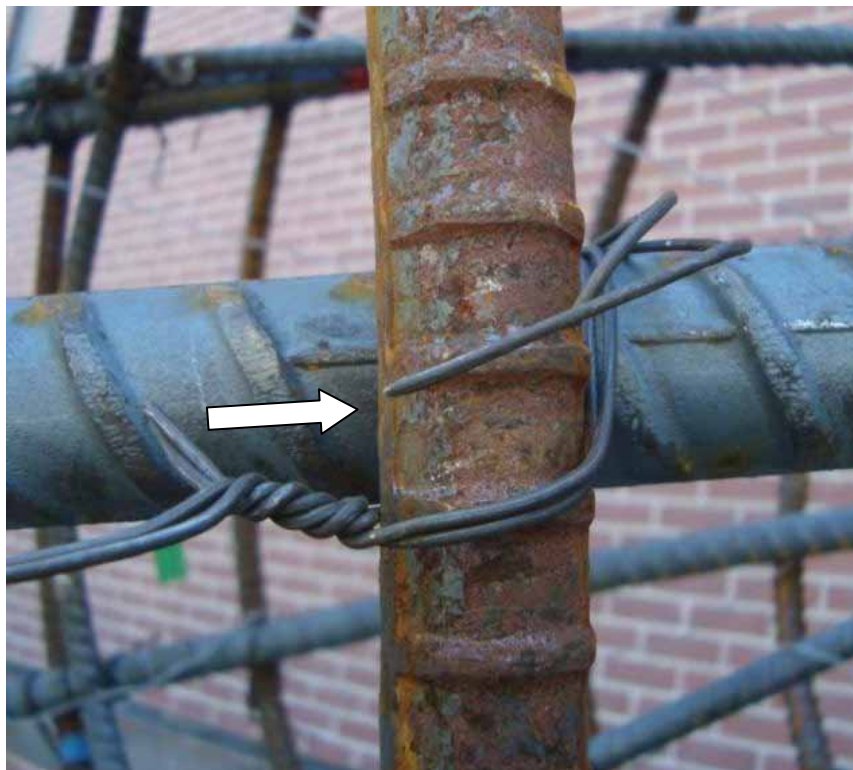
Figure 3.72: Failed Quadruple-snap tie
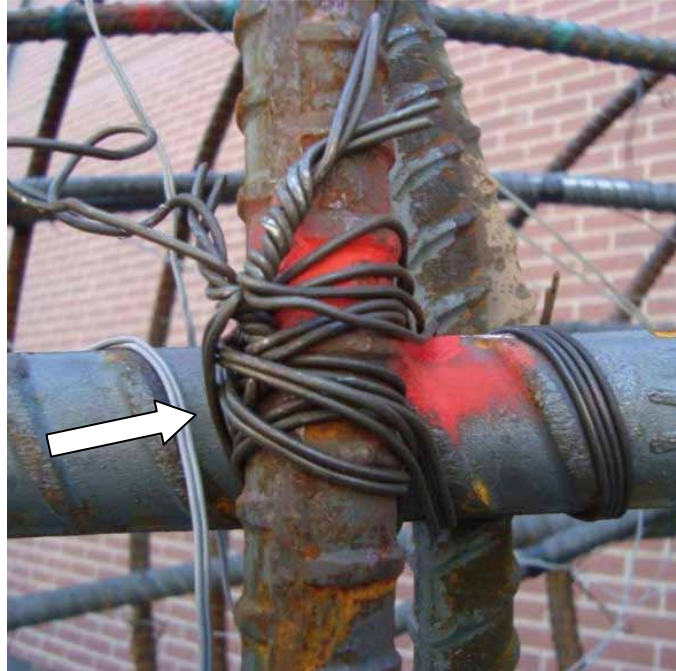
Figure 3.73: Strong-tie intact after rebar cage collapse
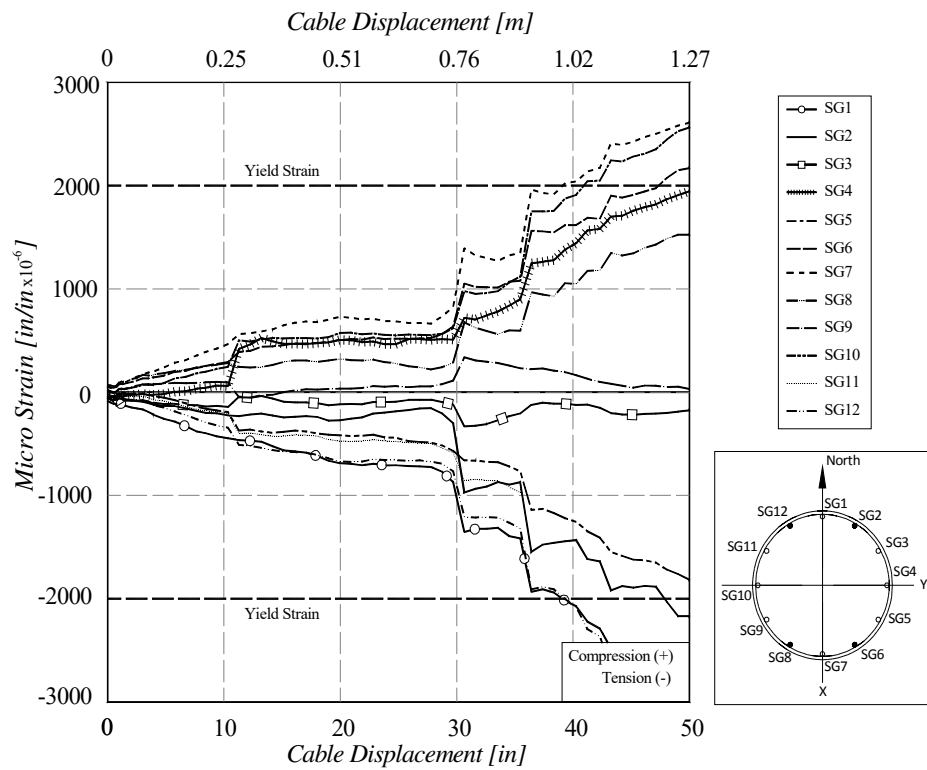
Figure 3.74: Strains at the Bottom of Specimen I
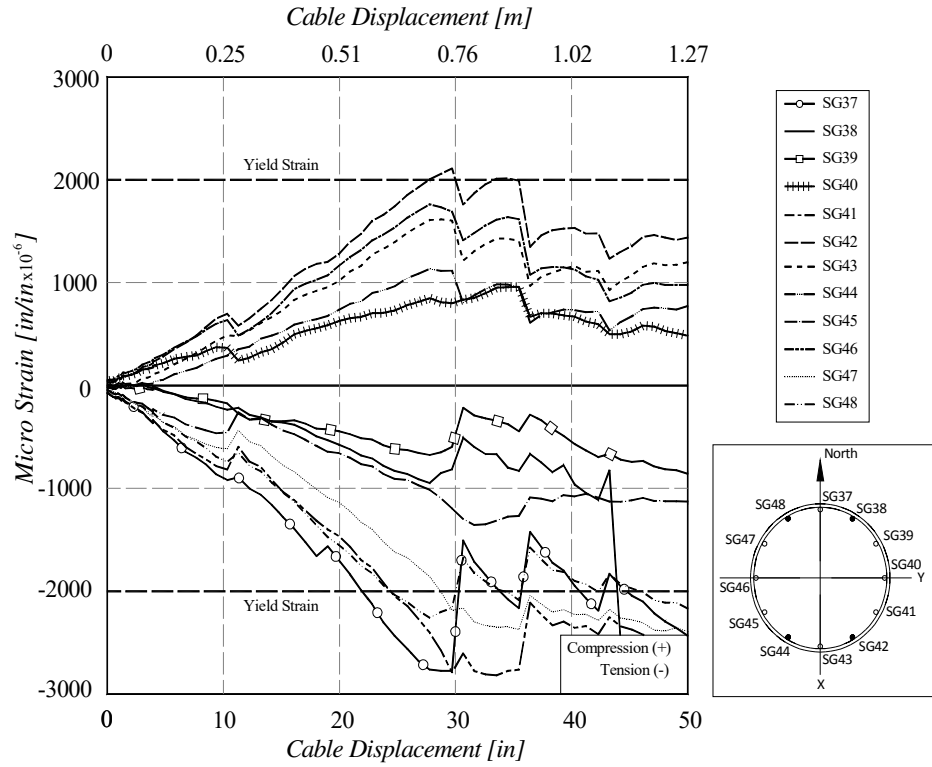
Figure 3.75: Strains at the Top of the Bottom brace
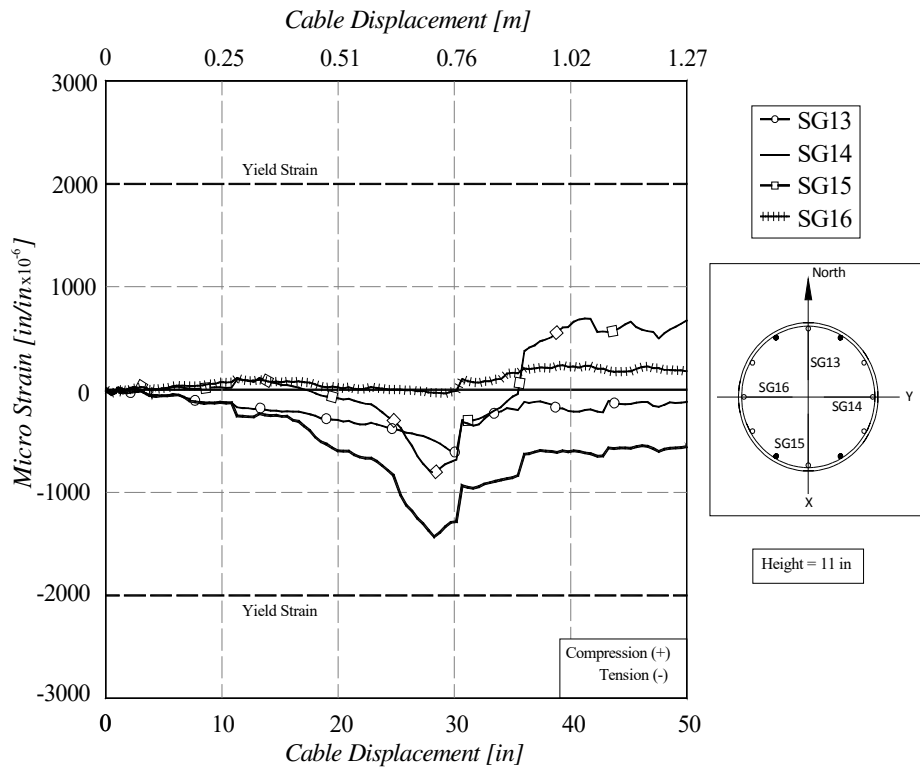
Figure 3.76: Strains at the First level (11-in) of Bottom Brace
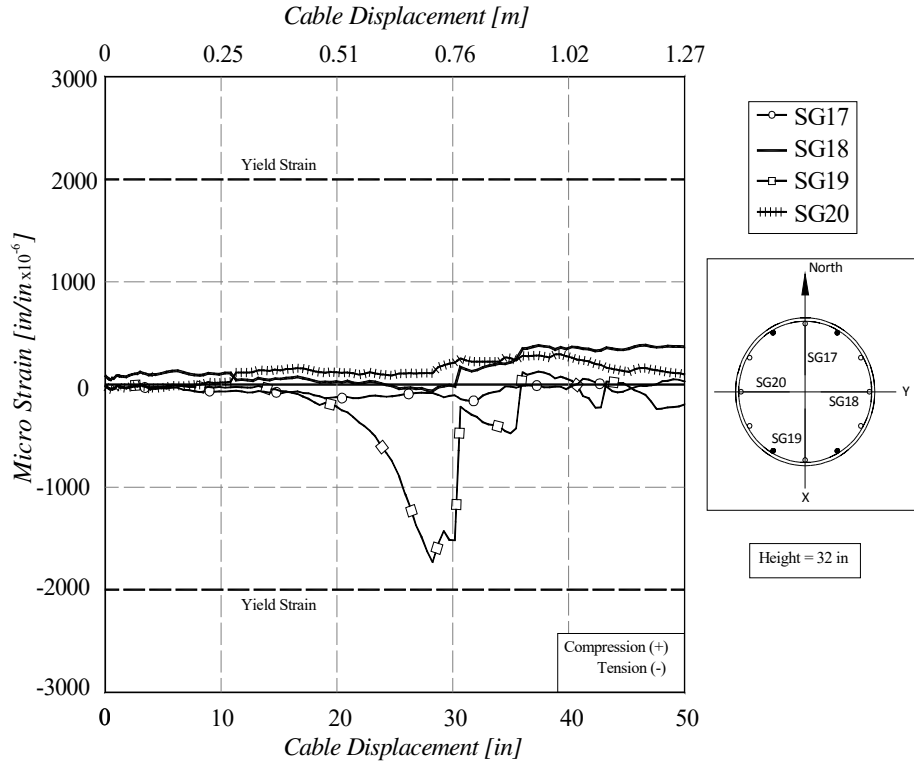
Figure 3.77: Strains at the Second level (32-in) of Bottom Brace
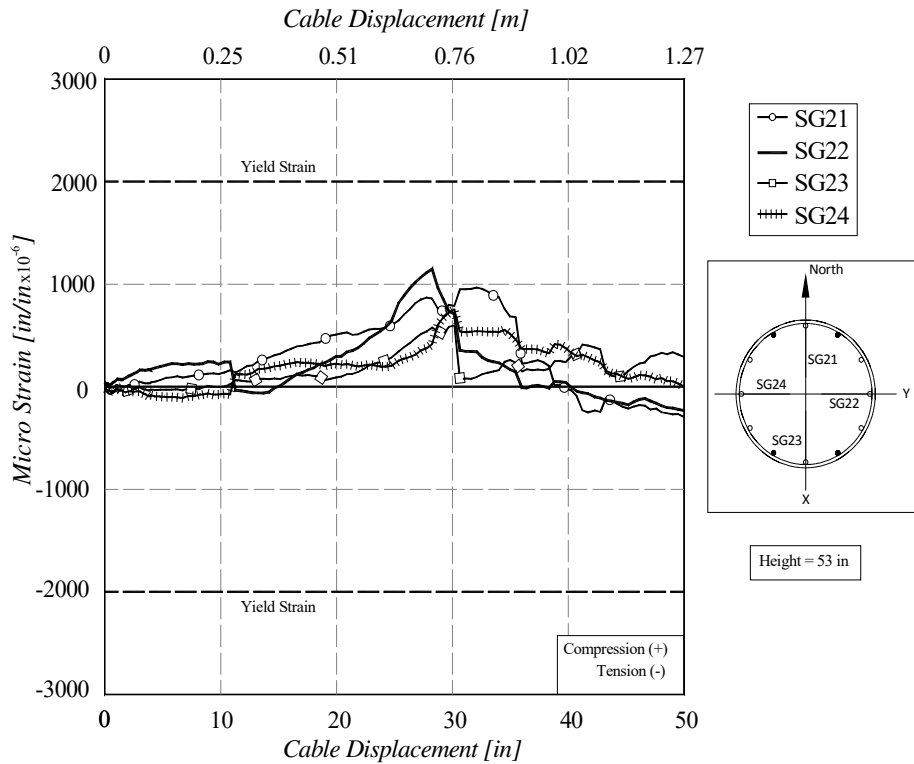
Figure 3.78: Strains at the Third level (53-in) of Bottom Brace

135
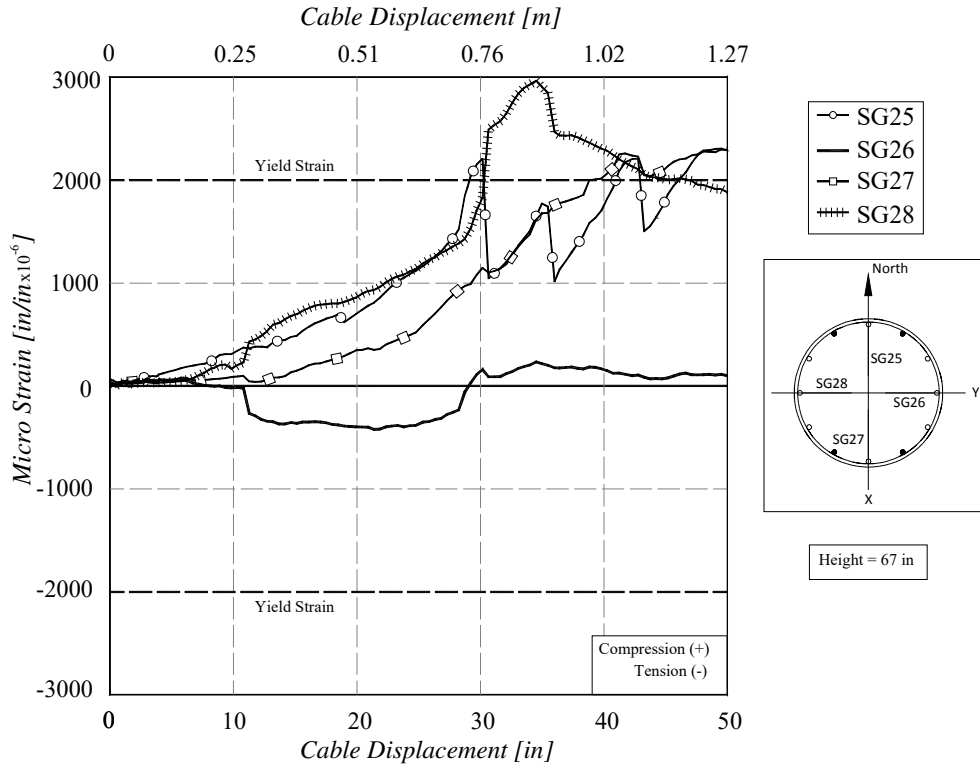
Figure 3.79: Strains at the Fourth level (67-in) of Bottom Brace
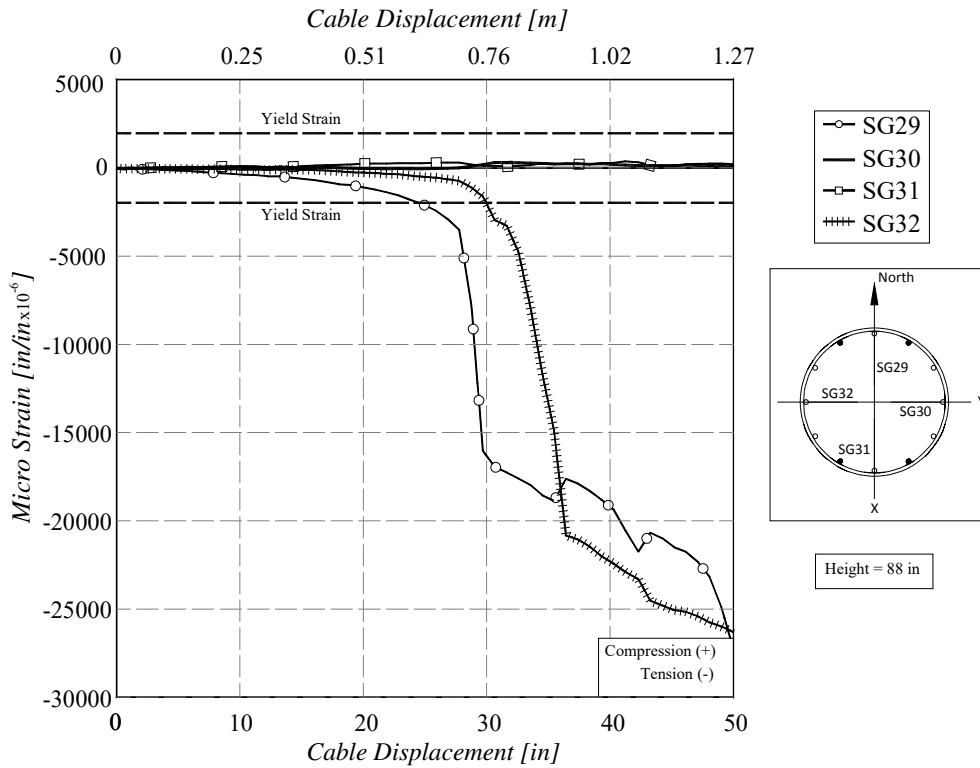
Figure 3.80: Strains at the Fifth level (88-in) of Bottom Brace

136
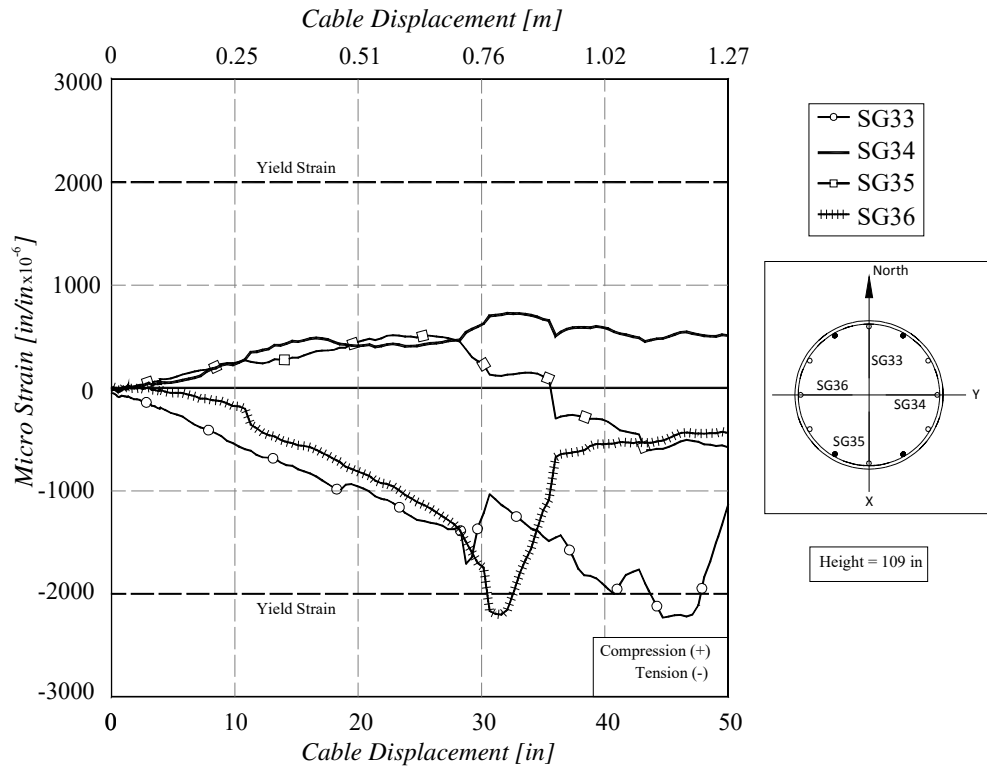
Figure 3.81: Strains at the Sixth level (88-in) of Bottom Brace

Figure 3.82: Close up of buckled brace bar after collapse of Specimen I

137

Figure 3.83: Common Point of Bottom Brace after collapse of Specimen I

Figure 3.84: Top Brace after collapse of Specimen I

Figure 3.85: Close up of bottom of Specimen I after collapse
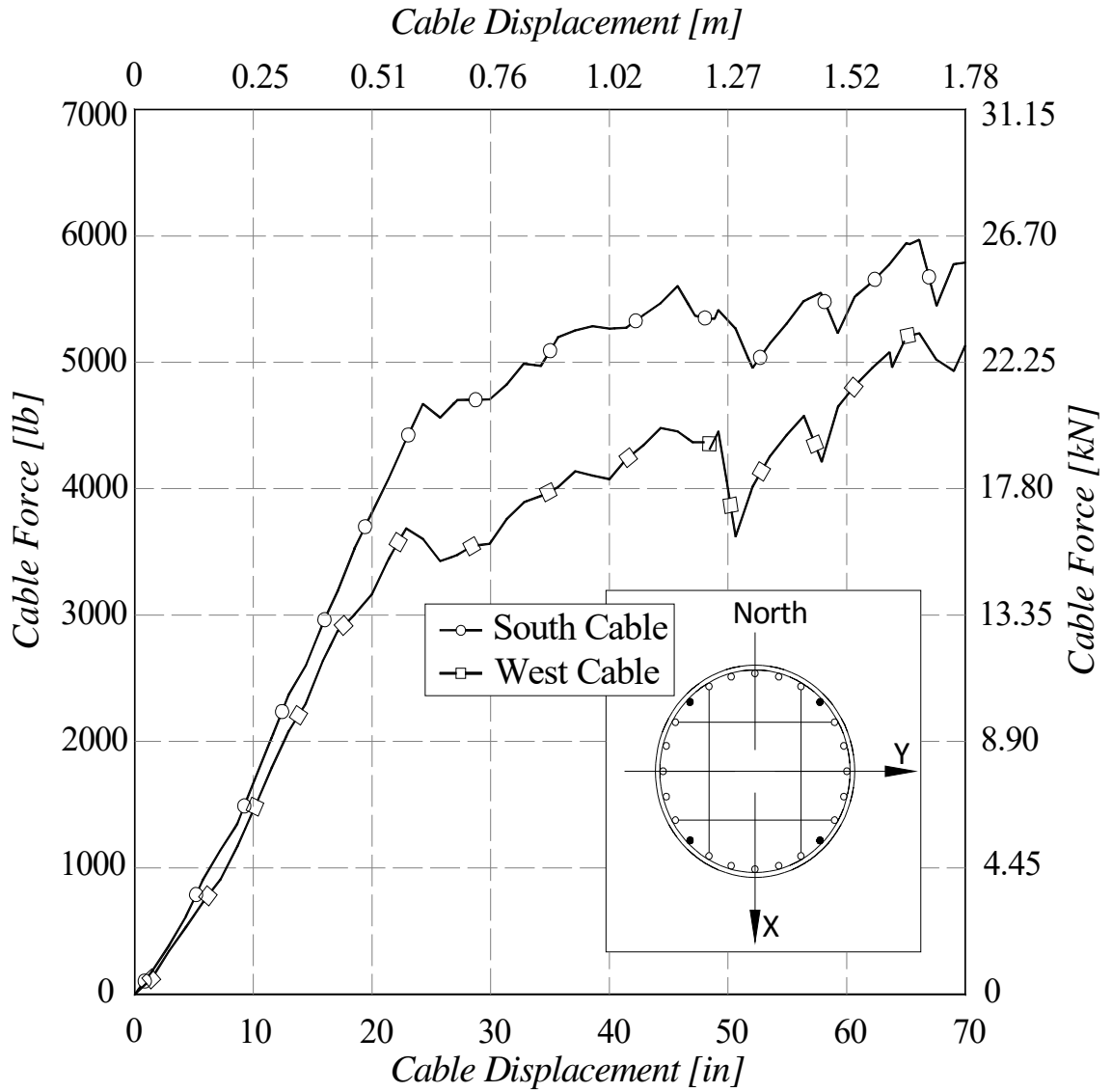
Figure 3.86: Cable Force-Displacement response for Specimen II

Figure 3.87: Collapse of Specimen II
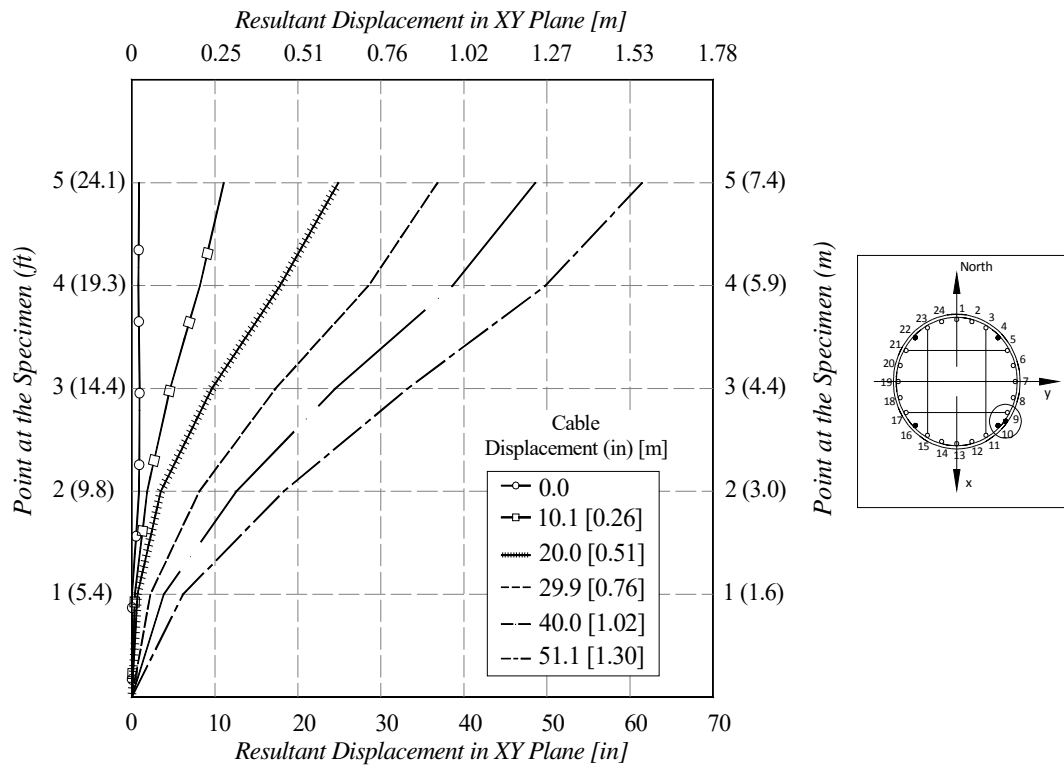
Figure 3.88: Resultant Displacement obtained from Displacement Transducers, Specimen II

Figure 3.89: Sequence of deformed shapes for Specimen II, view from North
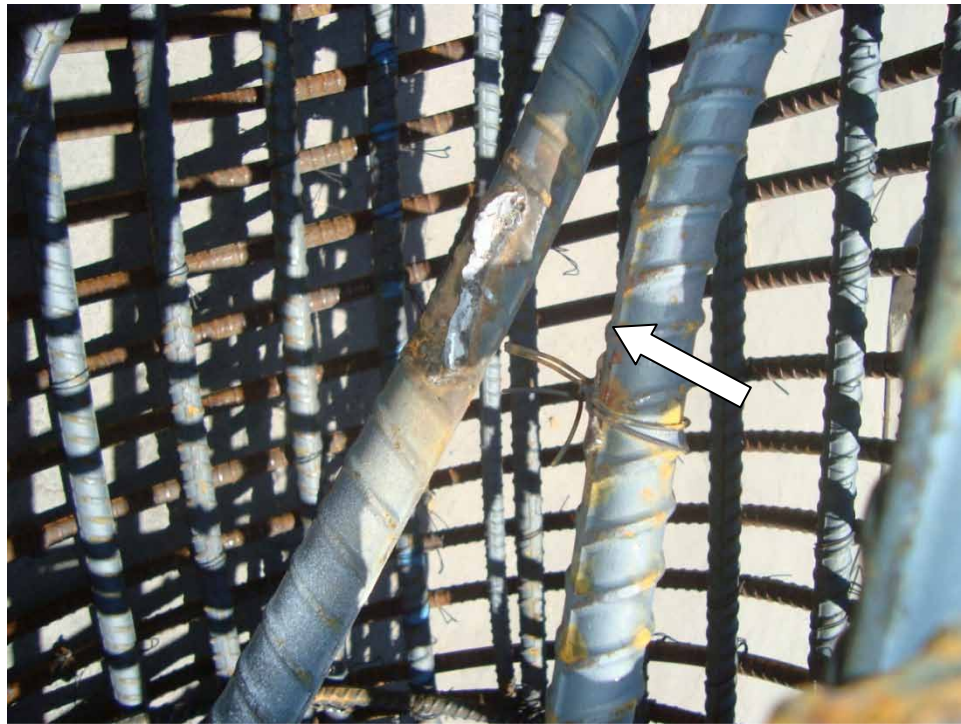
Figure 3.90: Failure of Connection at Common point of Square-braces in Specimen II

Figure 3.91: Top brace after collapse of Specimen II
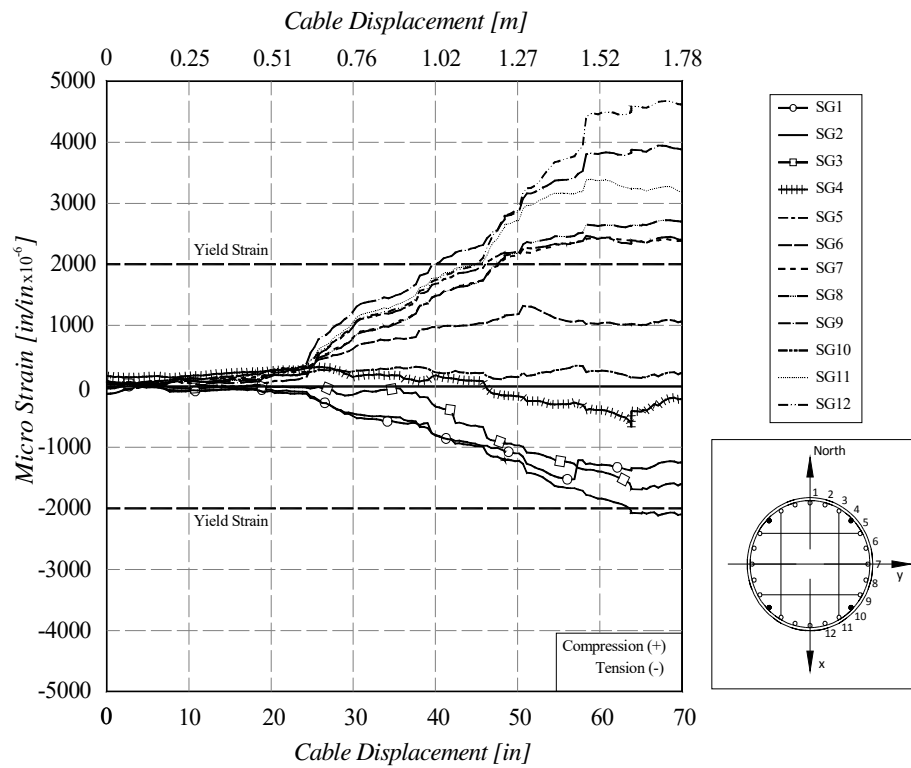
Figure 3.92: Strains at the Bottom of Specimen II (SG1-SG-12)
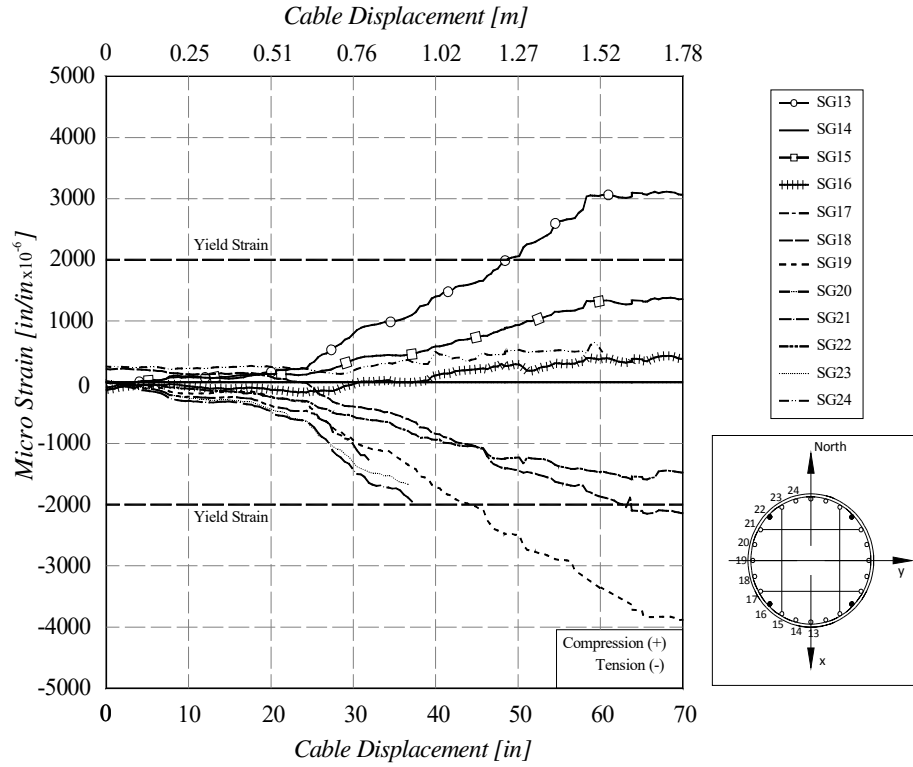
Figure 3.93: Strains at the Bottom of Specimen II (SG13-SG-24)
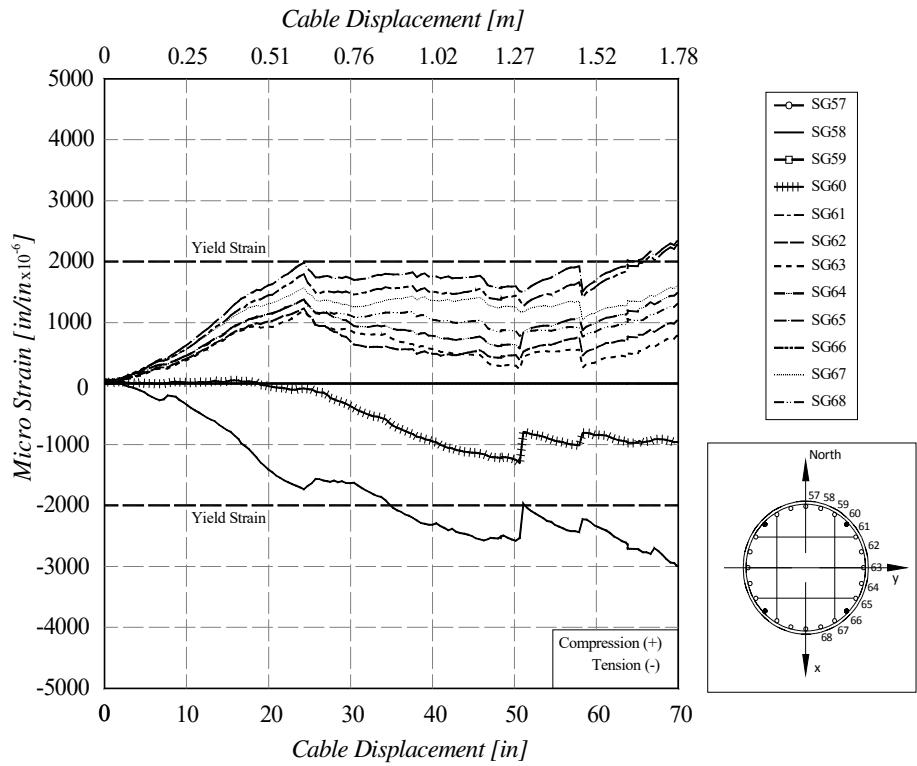
Figure 3.94: Strains at the Top of the Bottom Brace of Specimen II (SG57-SG-68)

144
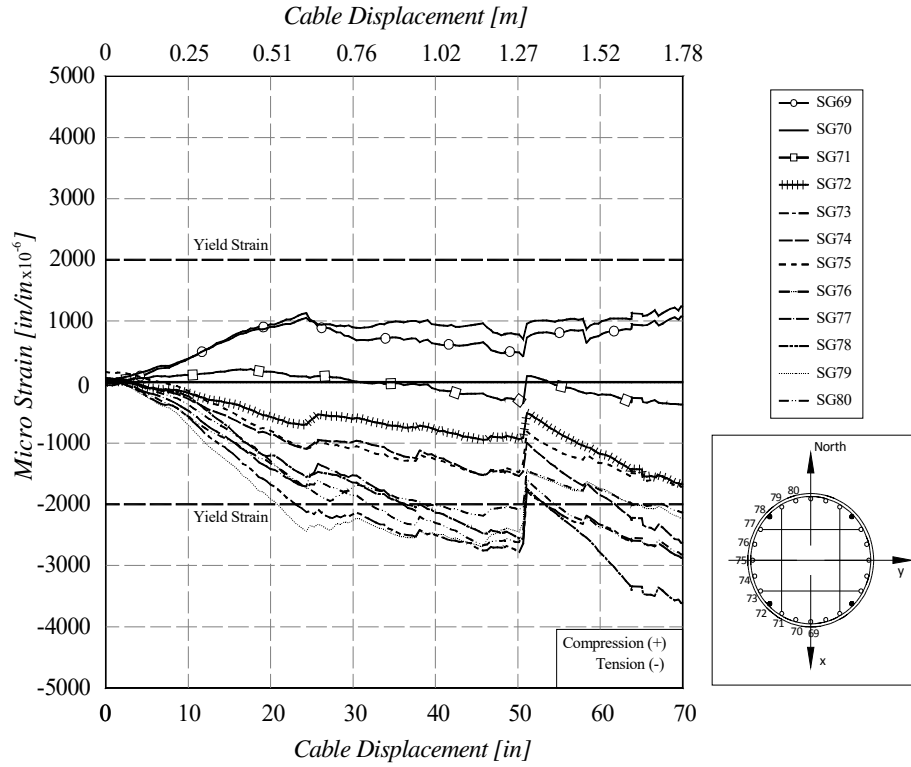
Figure 3.95: Strains at the Top of the Bottom Brace of Specimen II (SG69-SG-80)
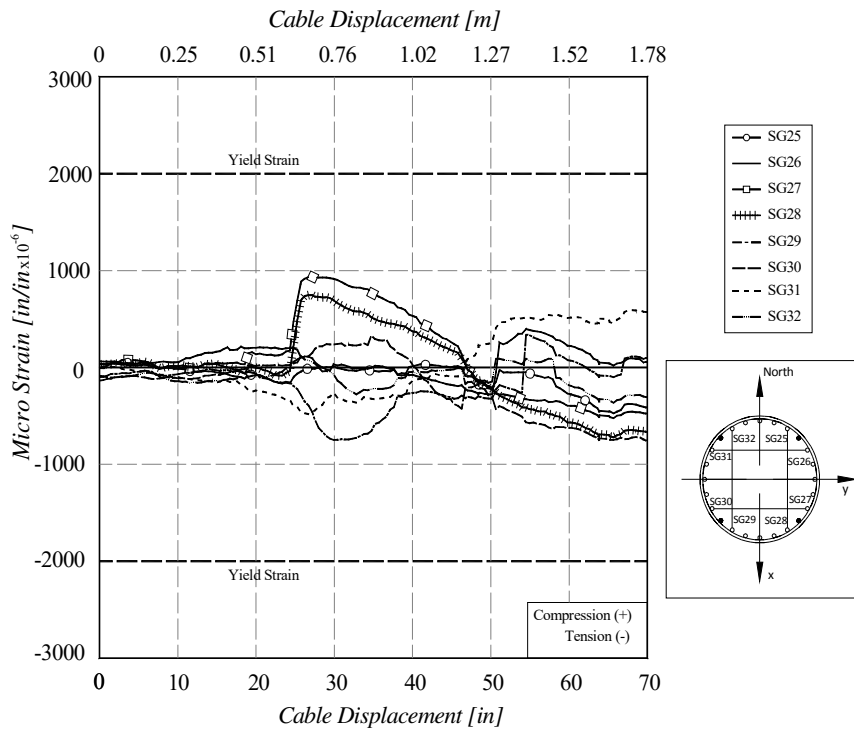
Figure 3.96: Strains at the First level (19-in) of Bottom Brace

145
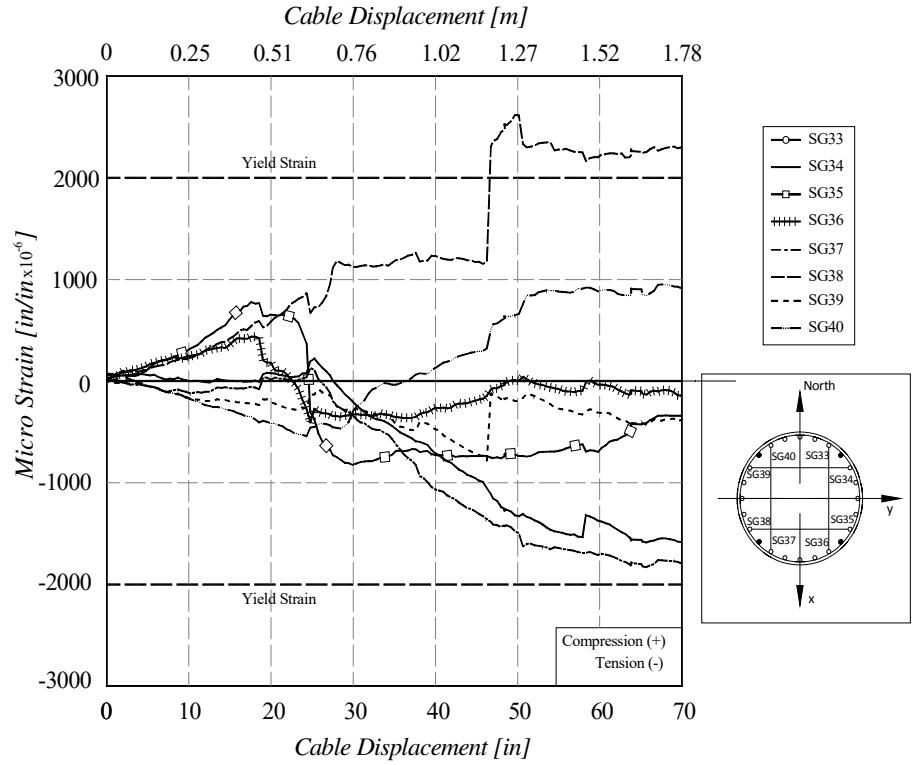
Figure 3.97: Strains at the Second level (40-in) of Bottom Brace
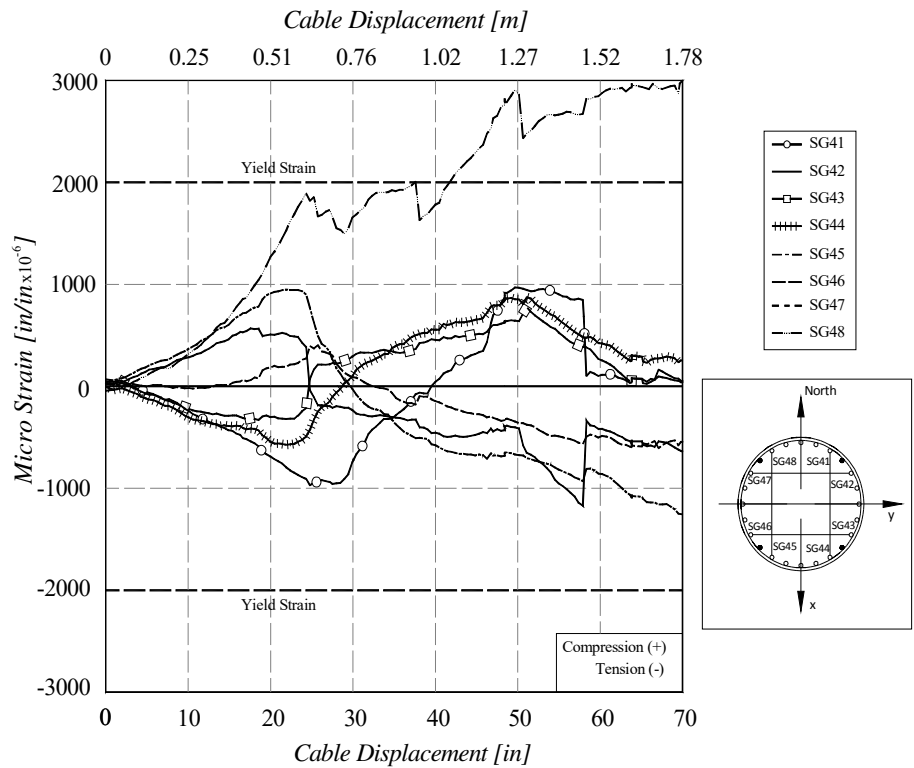
Figure 3.98: Strains at the Third level (79-in) of Bottom Brace

146
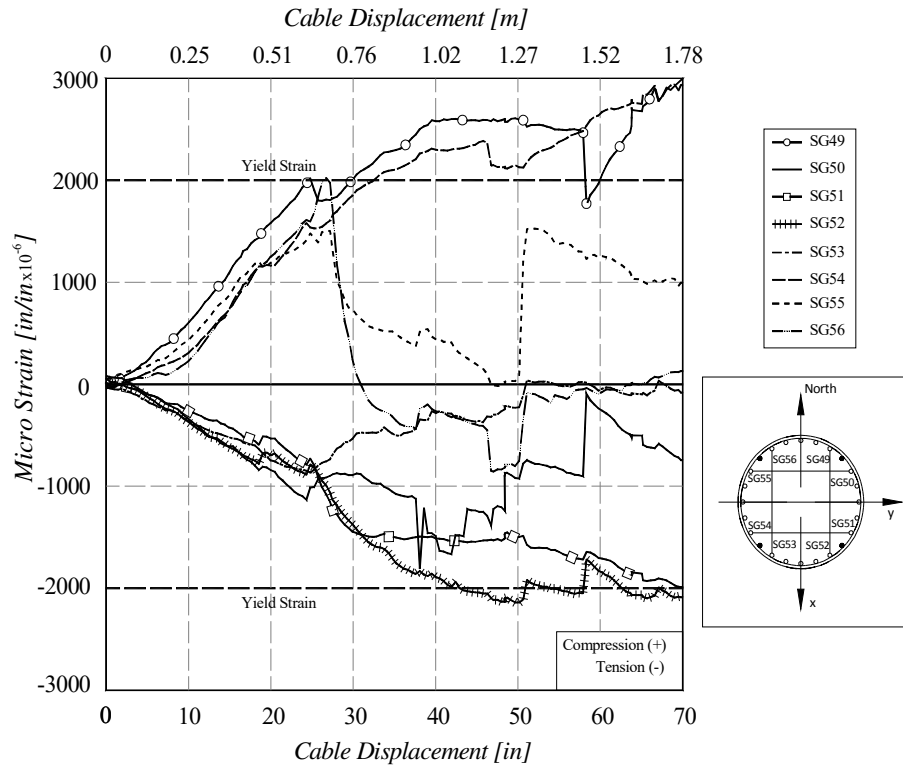
Figure 3.99: Strains at the Fourth level (100-in) of Bottom Brace
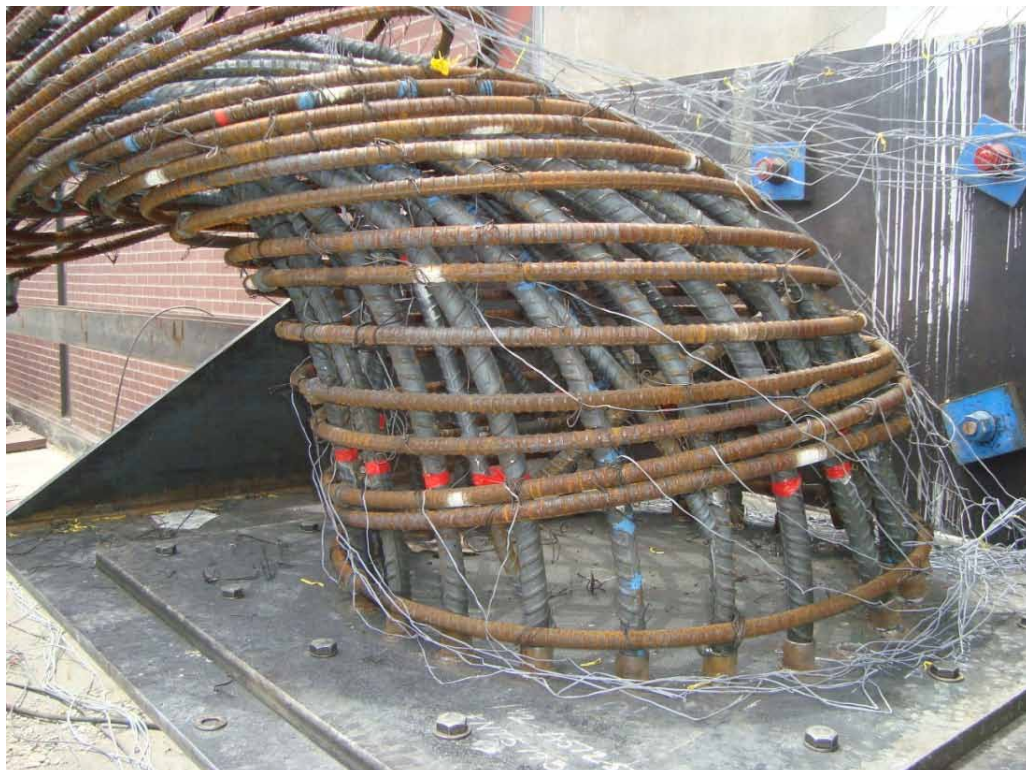
Figure 3.100: Close up of Specimen II bottom after collapse
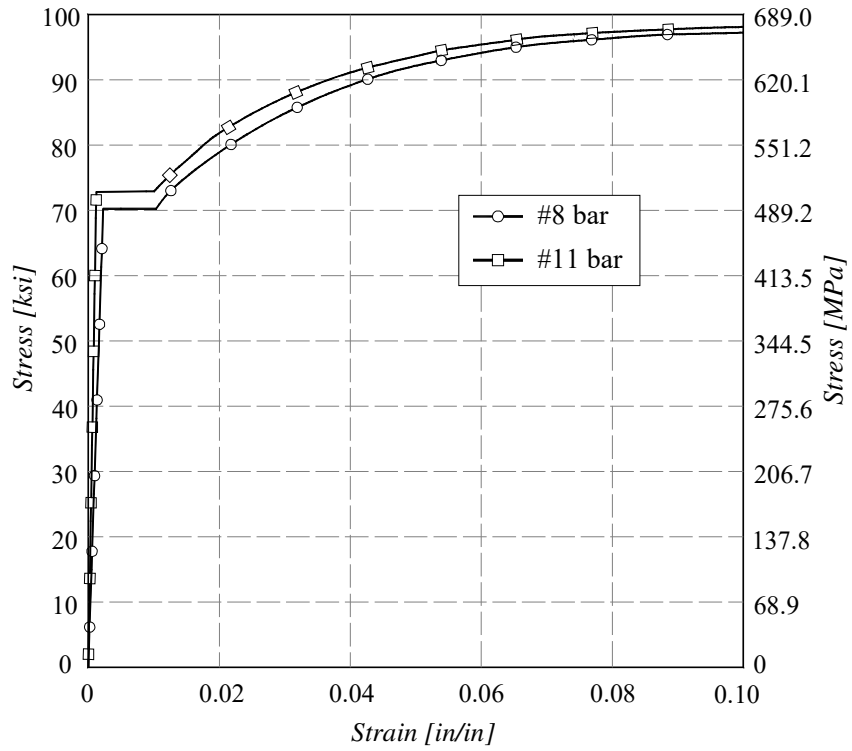
Figure 4.1: Stress-strain curve of #8 and #11 bar in the Computational Model
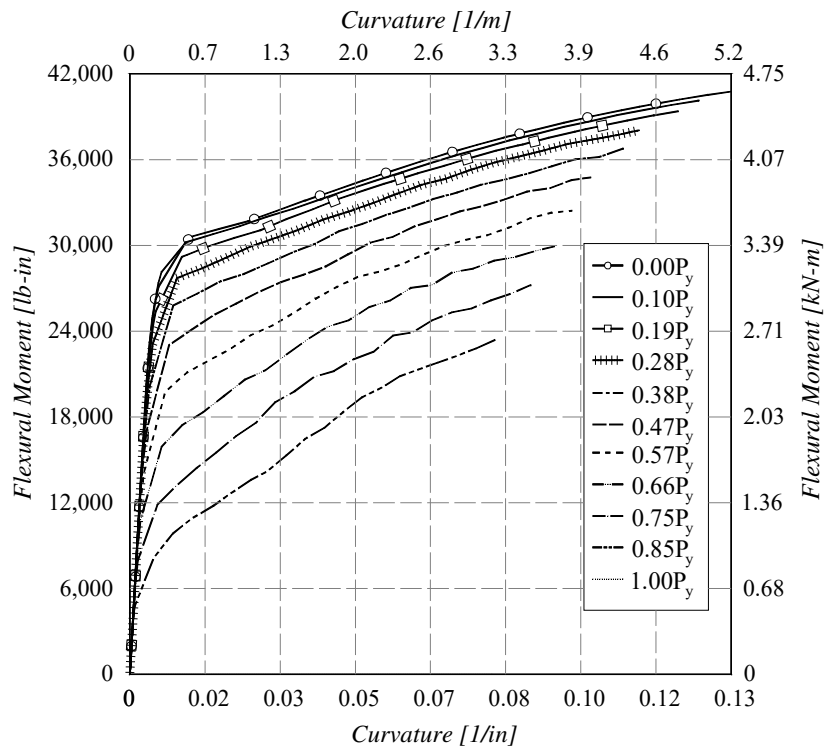
Figure 4.2: Flexural Moment-Curvature for A709 #11 Rebar
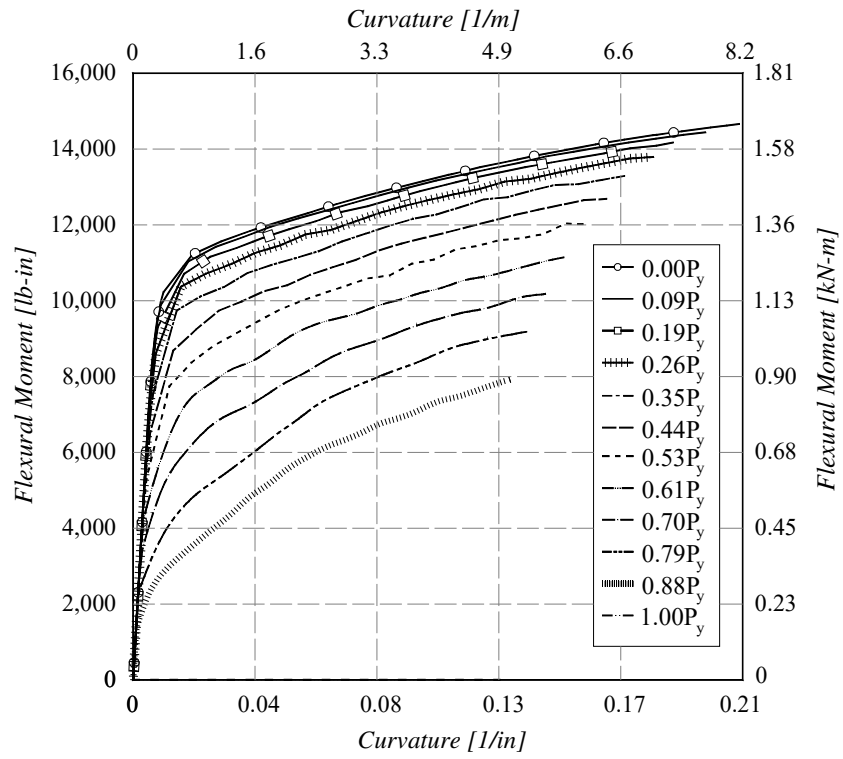
Figure 4.3: Flexural Moment-Curvature for A709 #8 Rebar
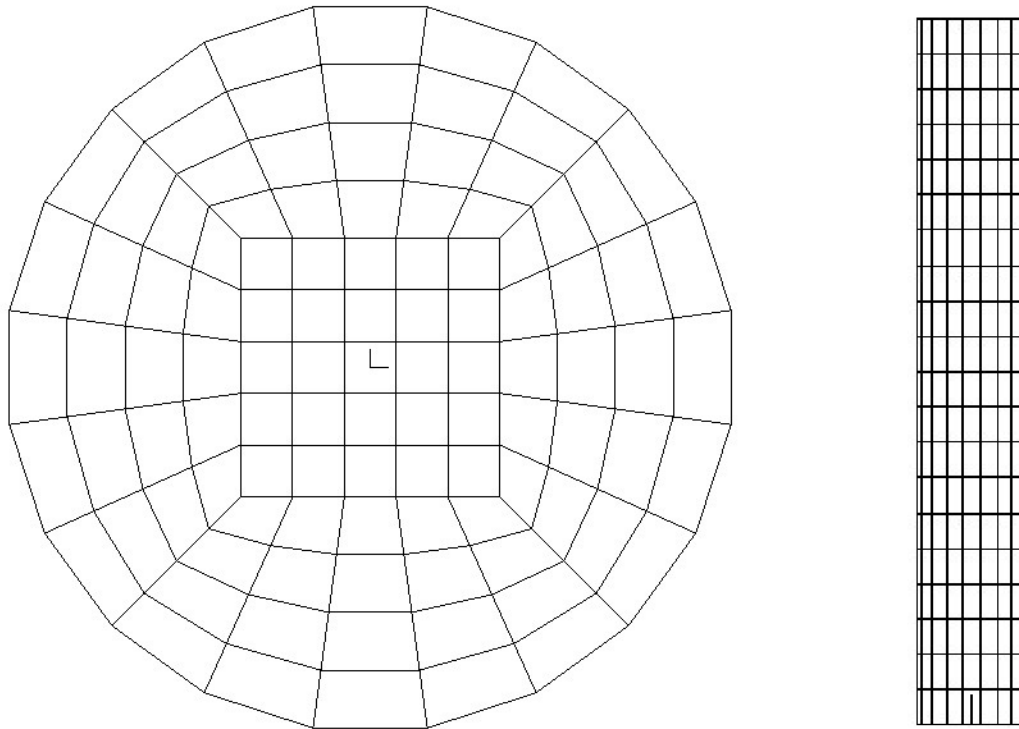
Figure 4.4: Computational model of Bar under Torsion

149
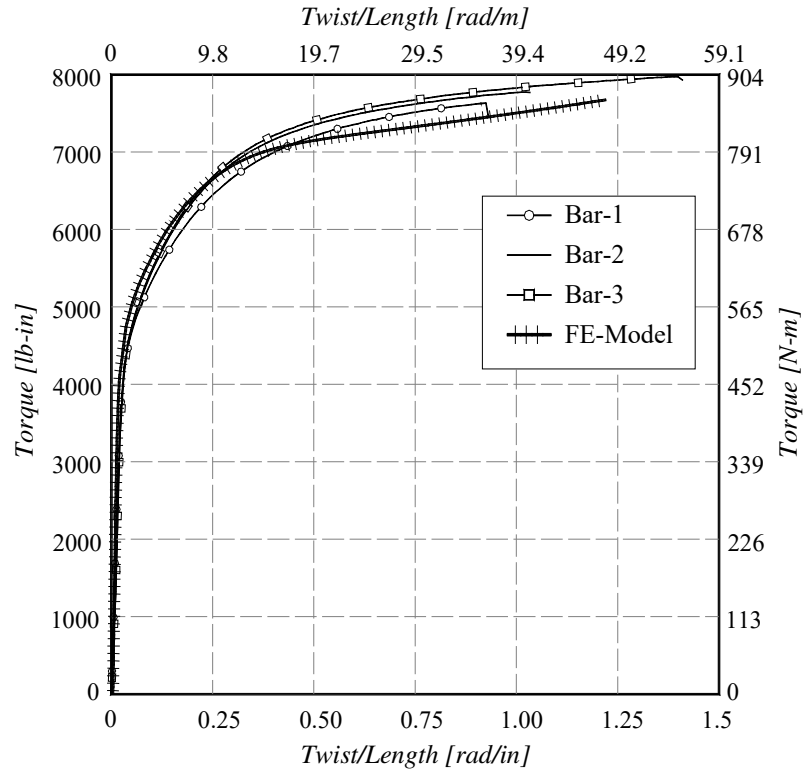
Figure 4.5: Comparison of Experimental and Analytical results of #6 bar under Torsion
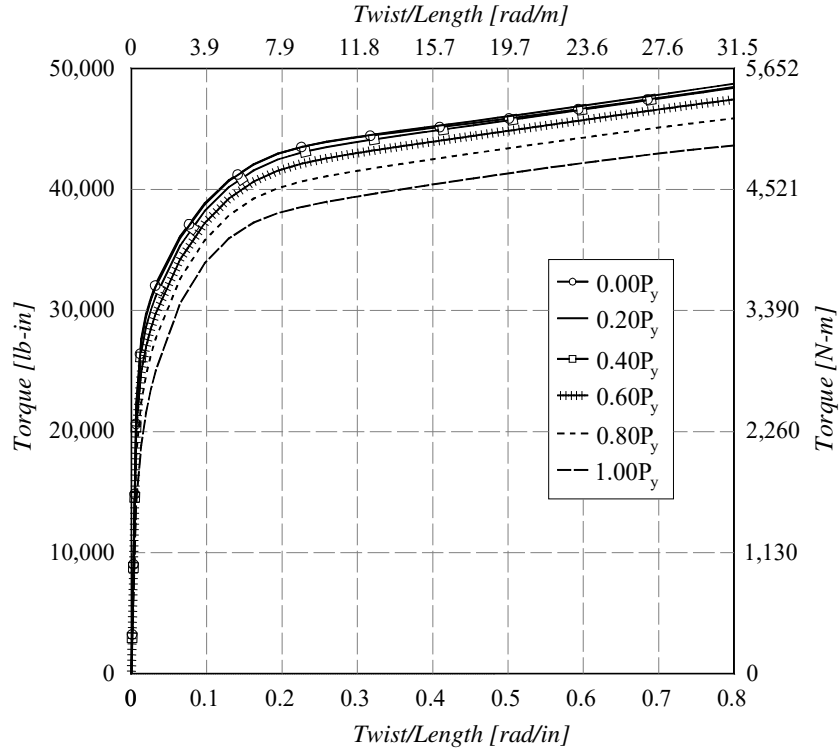
Figure 4.6: Torque-twist curves for #11 bar for Tension Axial forces

150
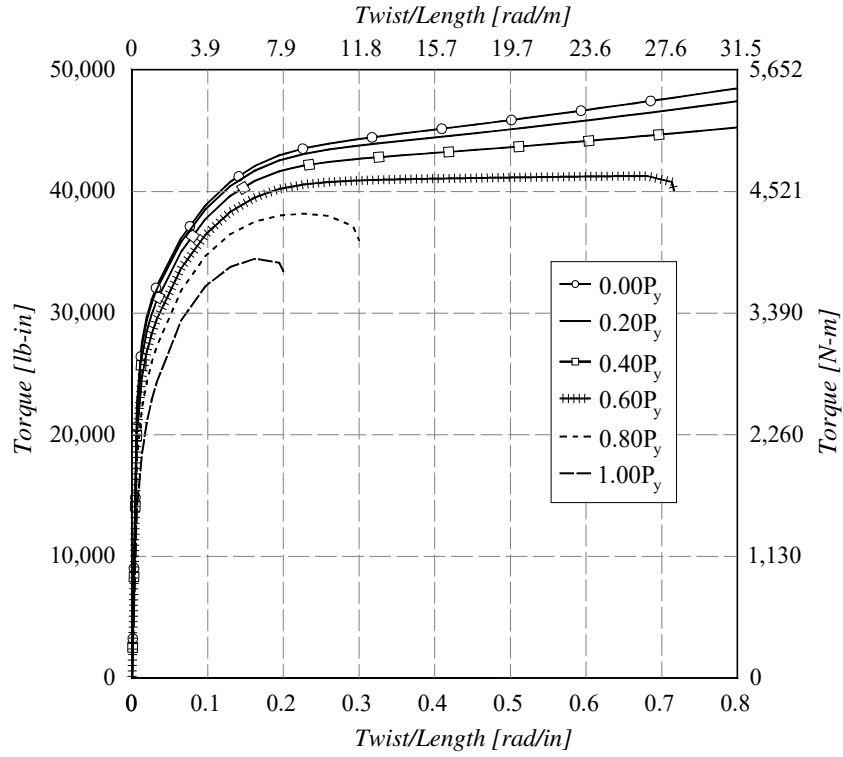
Figure 4.7: Torque-twist curves for #11 bar for Compression Axial forces
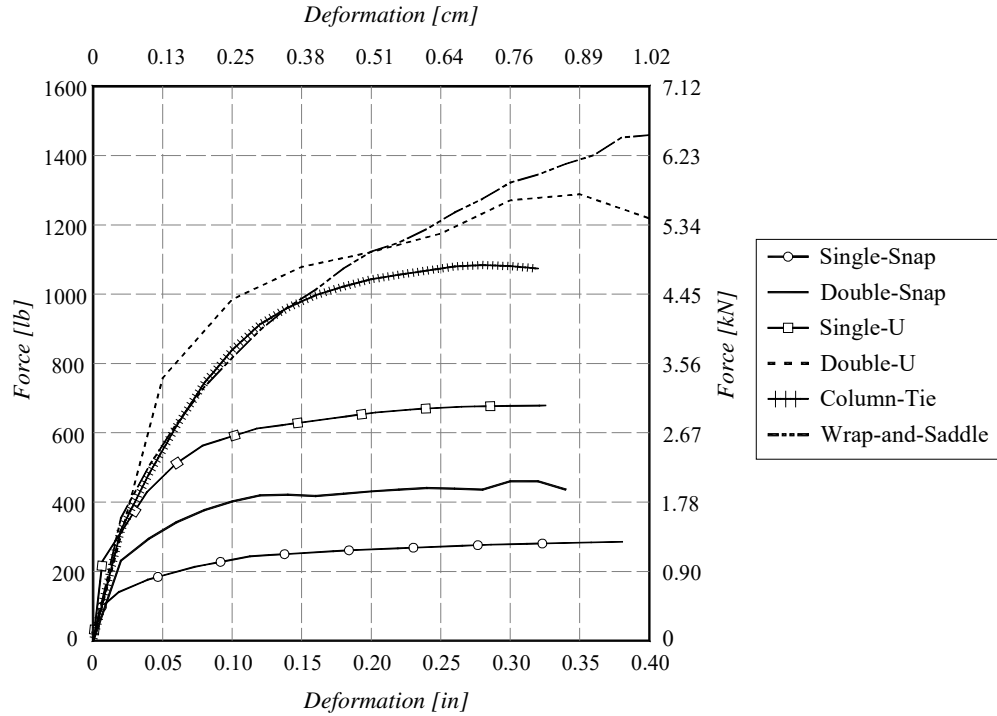
Figure 4.8: Force-deformation Curves for Springs in Δx

151
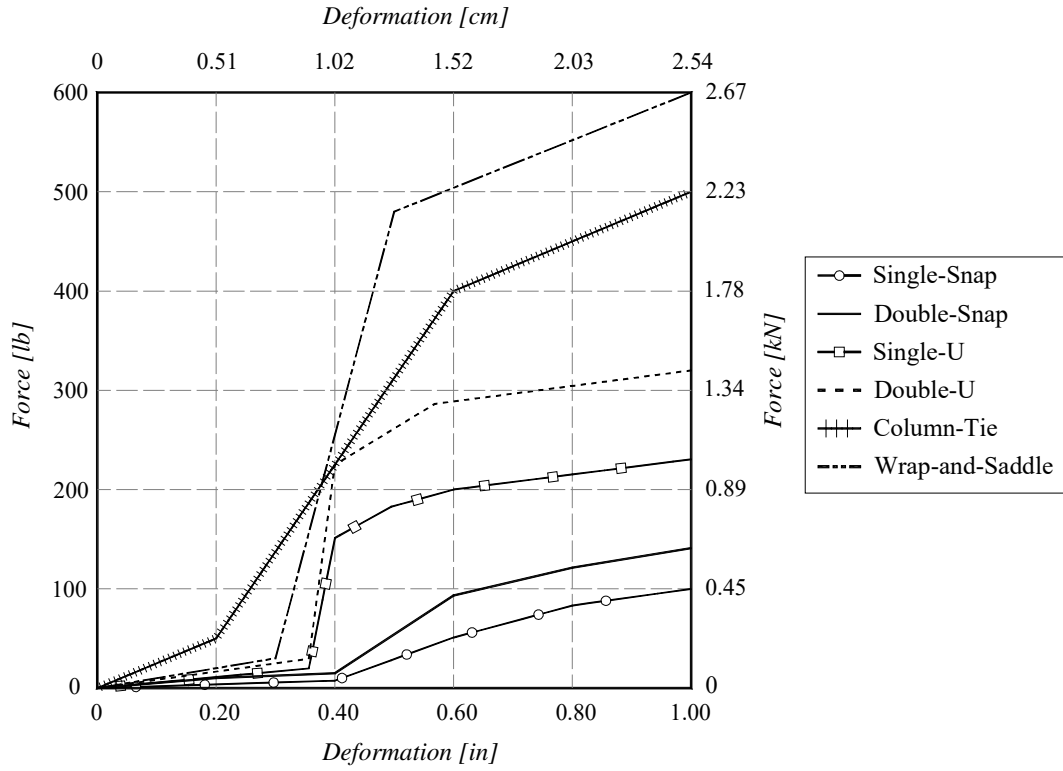
Figure 4.9: Force-deformation Curves for Springs in Δy and Δz
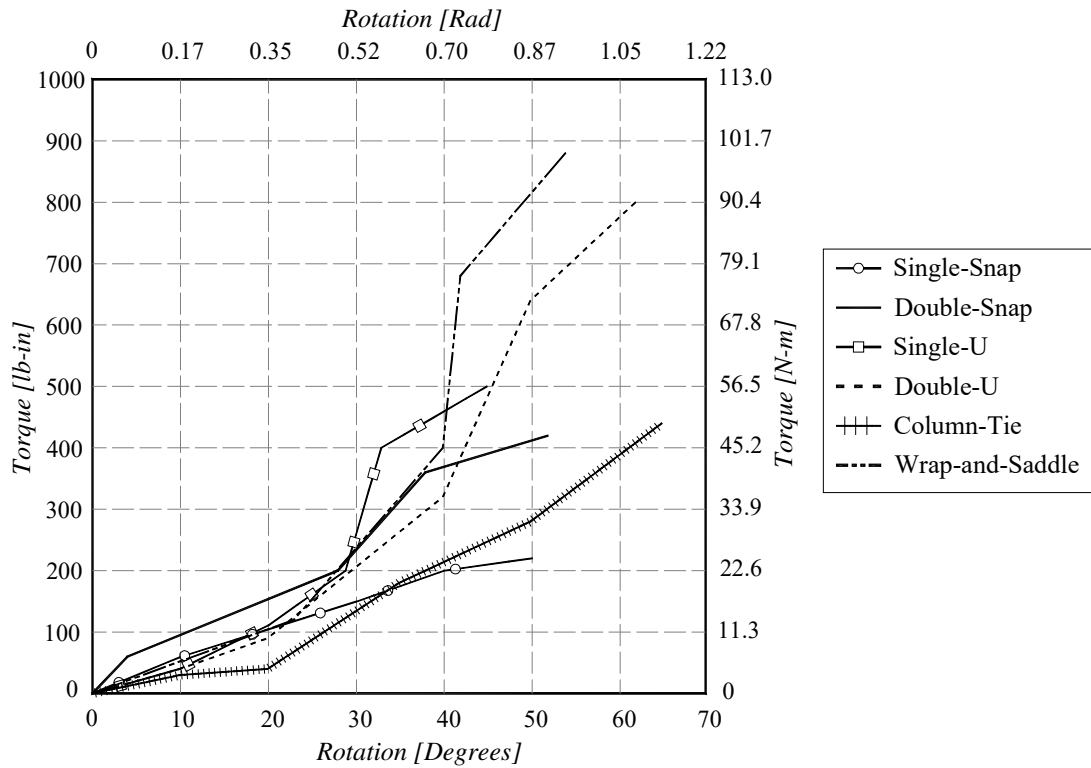
Figure 4.10: Torque-rotation Curves for Springs in θx

152
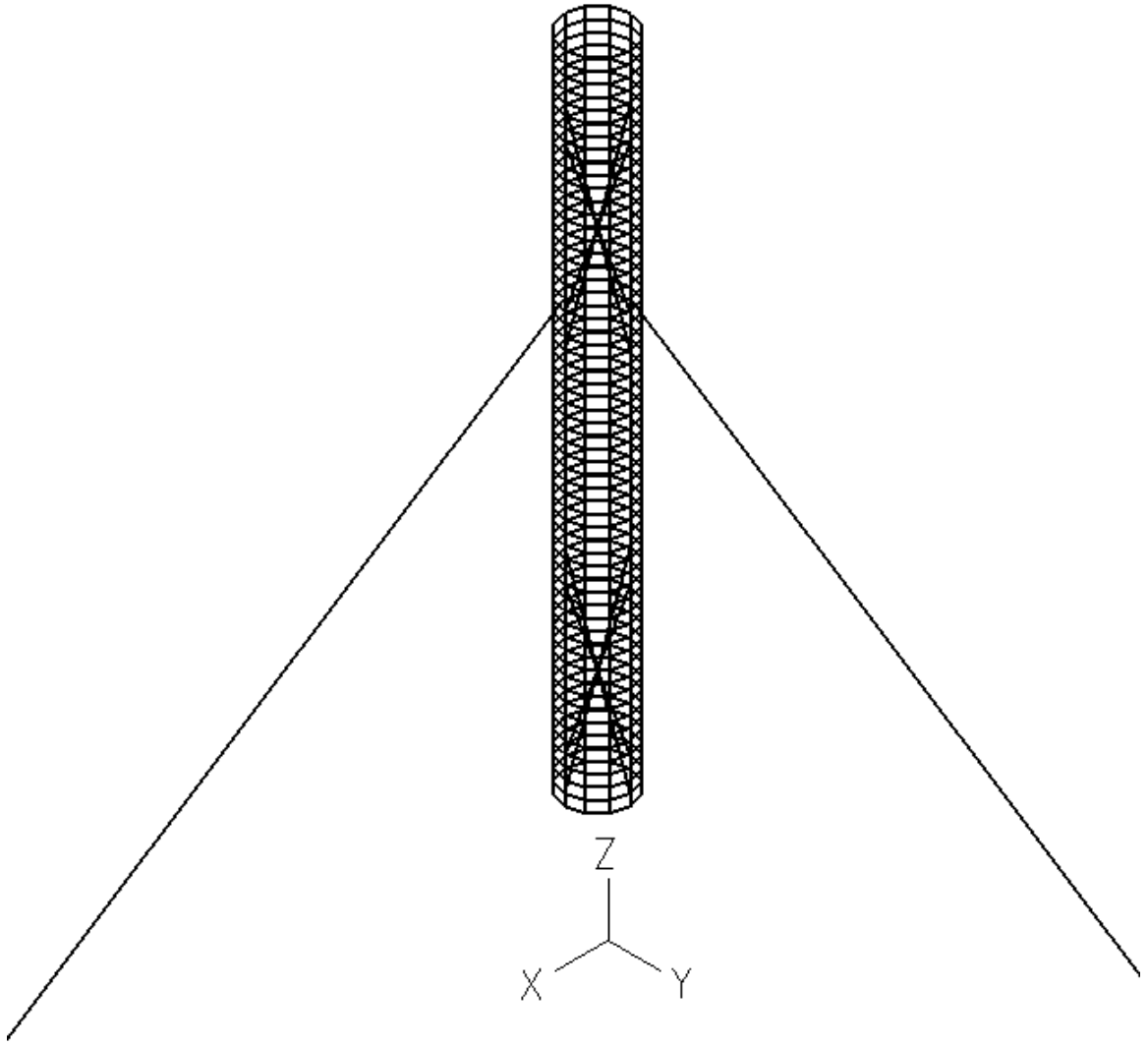
Figure 4.11: Computational Model of Specimen I
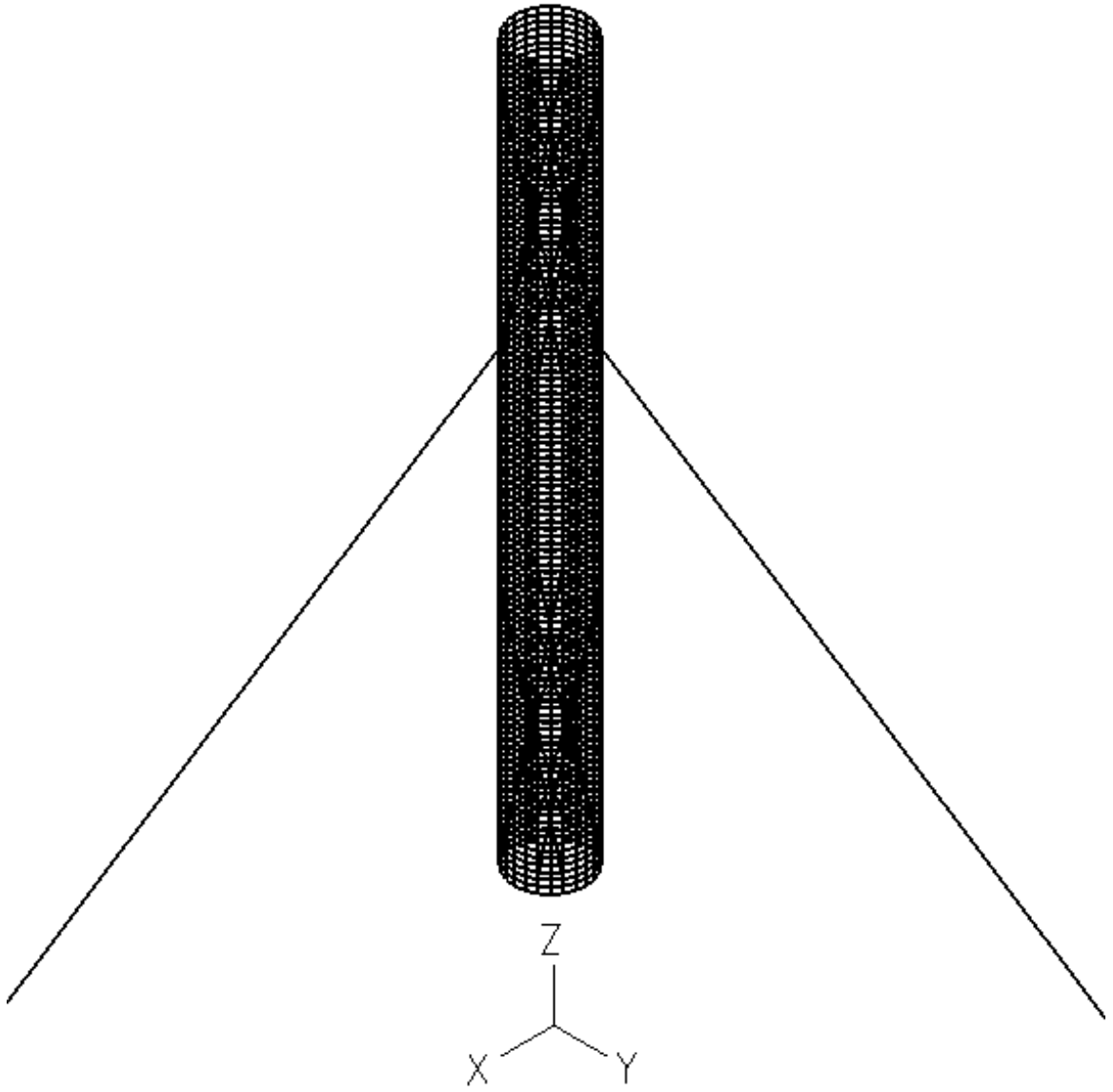
Figure 4.12: Computational Model of Specimen II
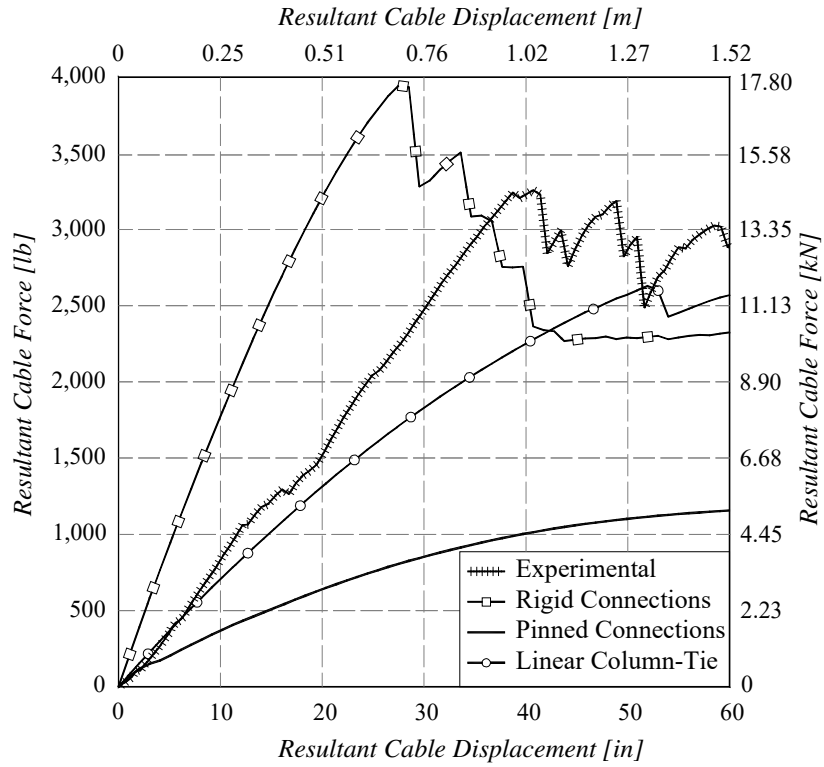
Figure 4.13: Response of Specimen I with different Brace Boundary Conditions
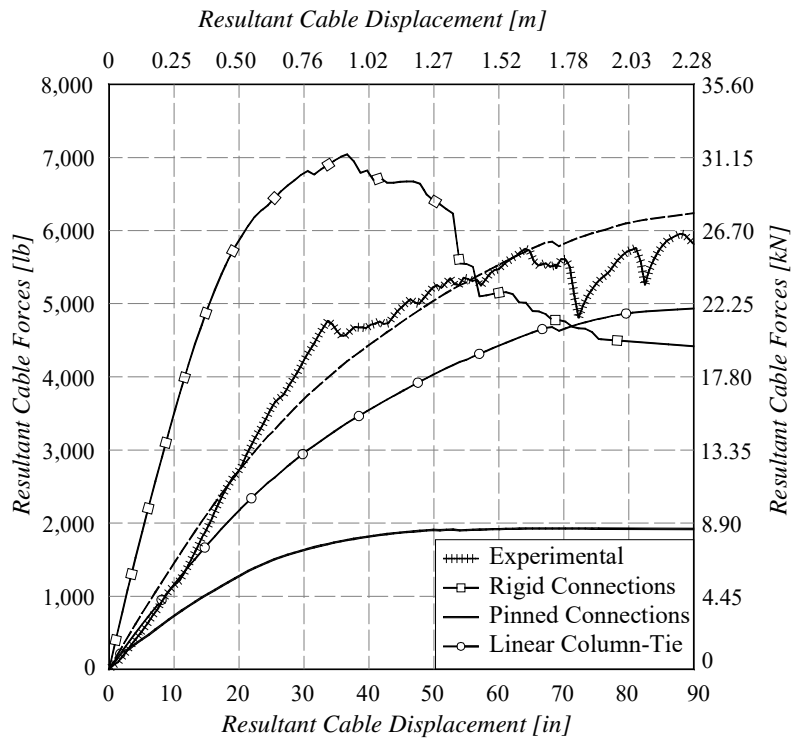
Figure 4.14: Response of Specimen II with different Brace Boundary Conditions

155
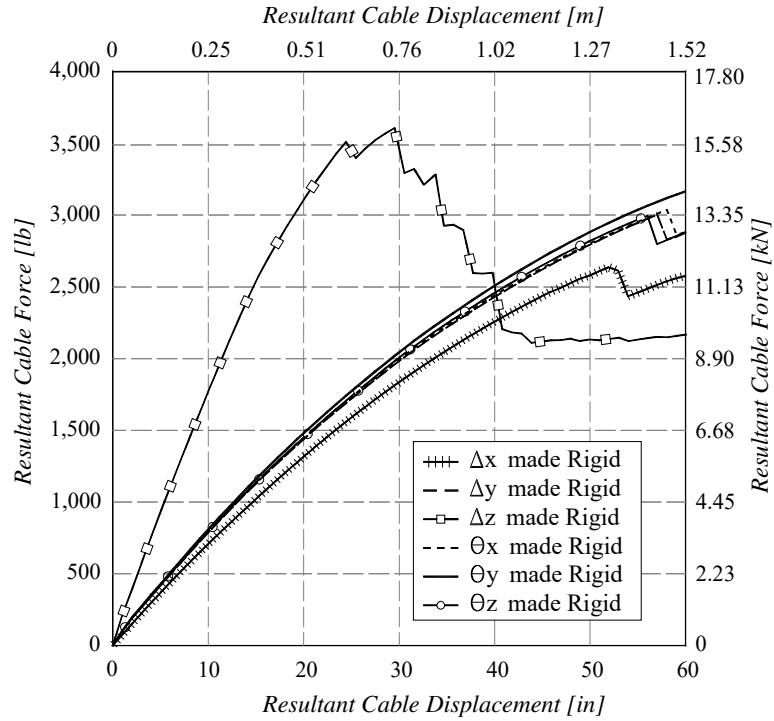
Figure 4.15: Response of Specimen I varying the rigidity of the degrees of freedom of the longitudinal bar to brace bar connection
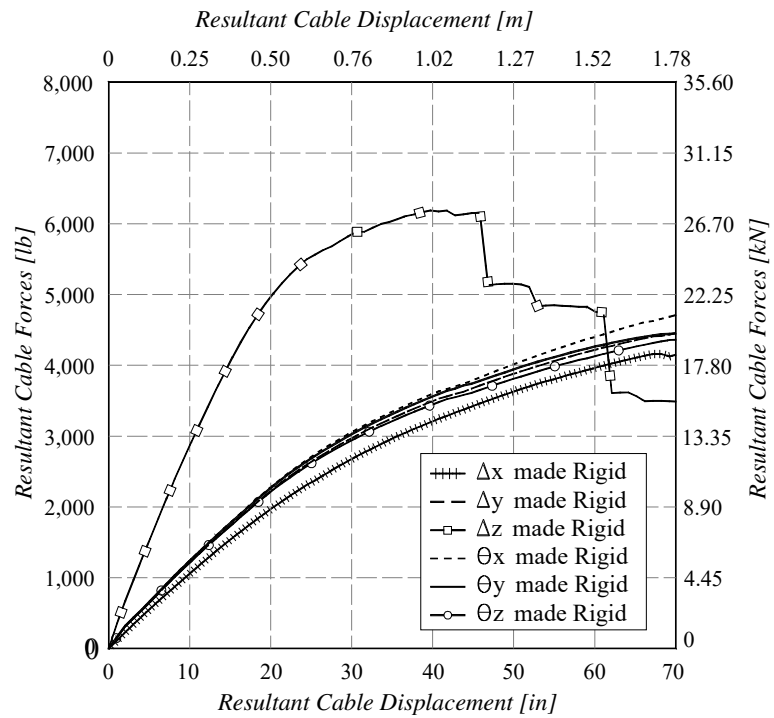
Figure 4.16: Response of Specimen II varying the rigidity of the degrees of freedom of the longitudinal bar to brace bar connection

156
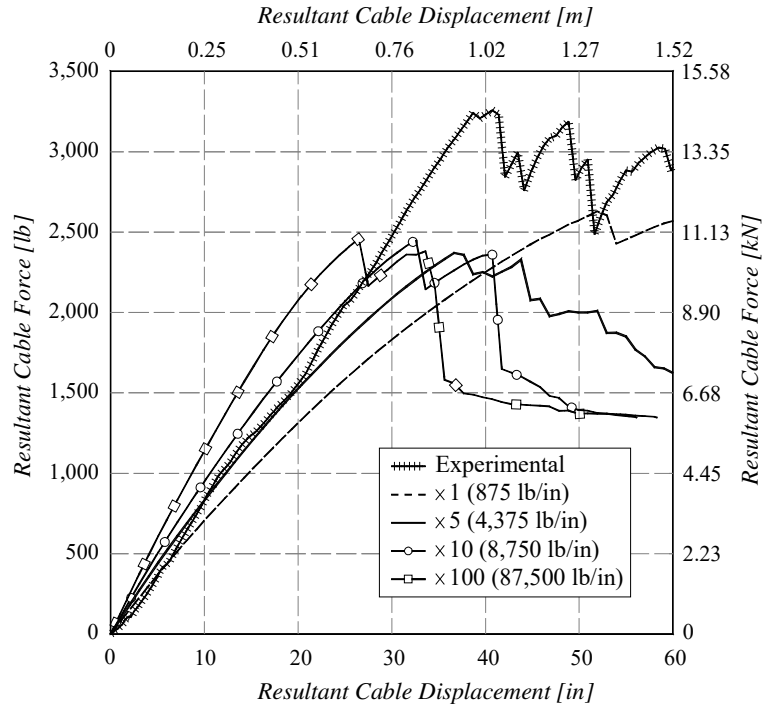
Figure 4.17: Response of Specimen I with Linear Behavior of Vertical Translational Springs (Δz) in the Bracing Elements Boundary Condition
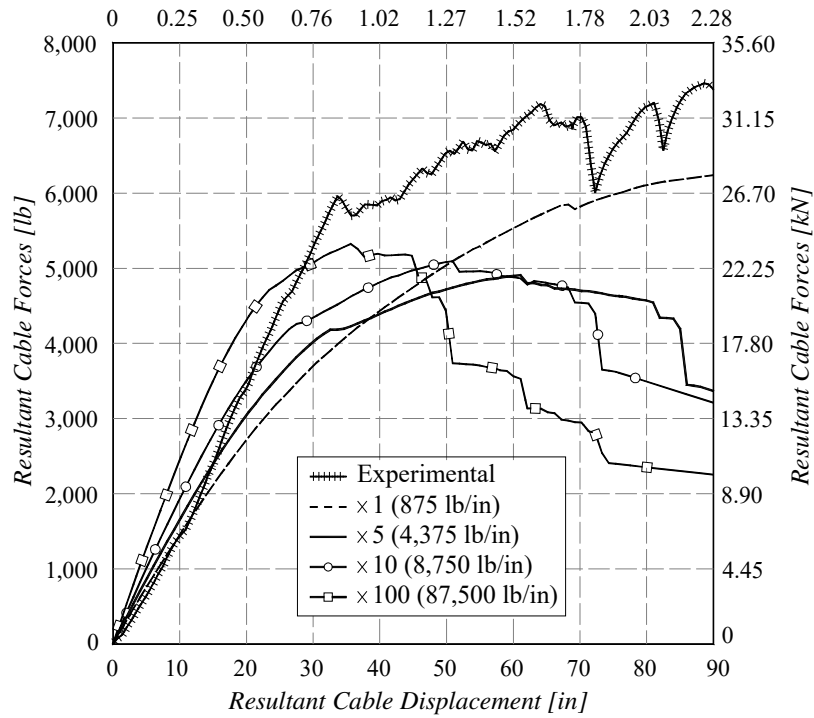
Figure 4.18: Response of Specimen II with Linear Behavior of Vertical Translational Springs (Δz) in the Bracing Elements Boundary Condition

157
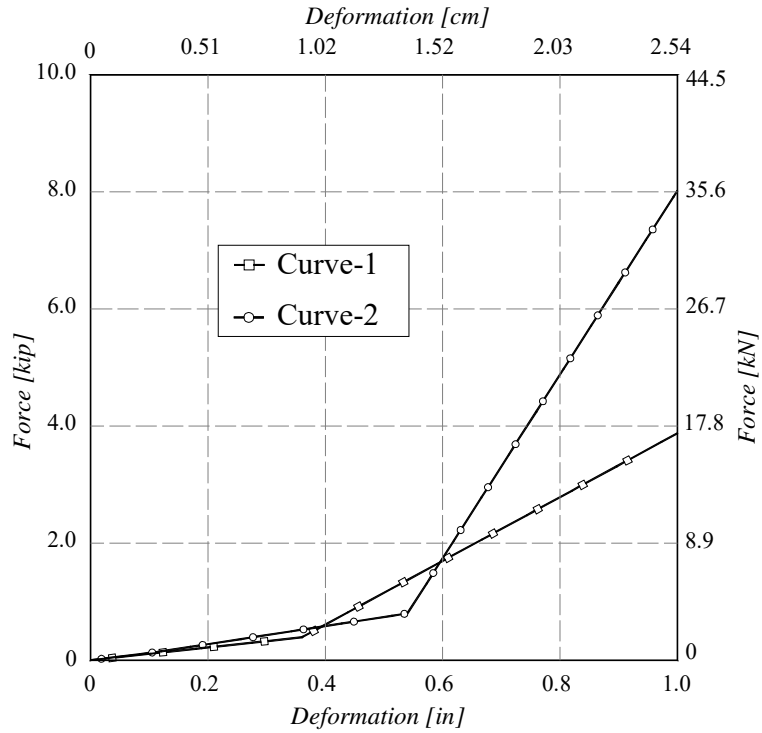
Figure 4.19: Force-deformation Curves for Vertical Springs (Δz) in the Bracing Elements Boundary Condition
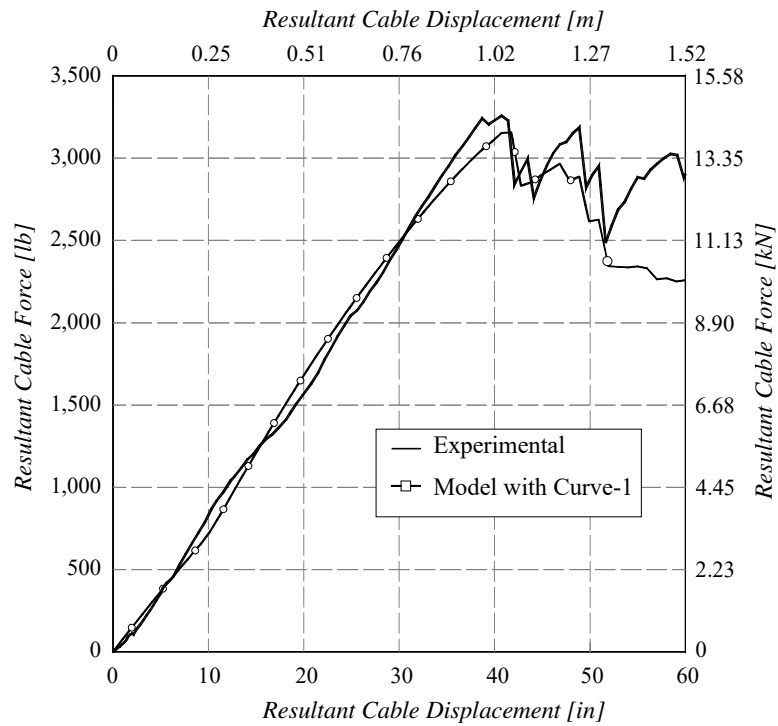
Figure 4.20: Response of Specimen I using Curve-1 for Vertical Springs (Δz) in the Bracing Elements Boundary Condition

Figure 4.15
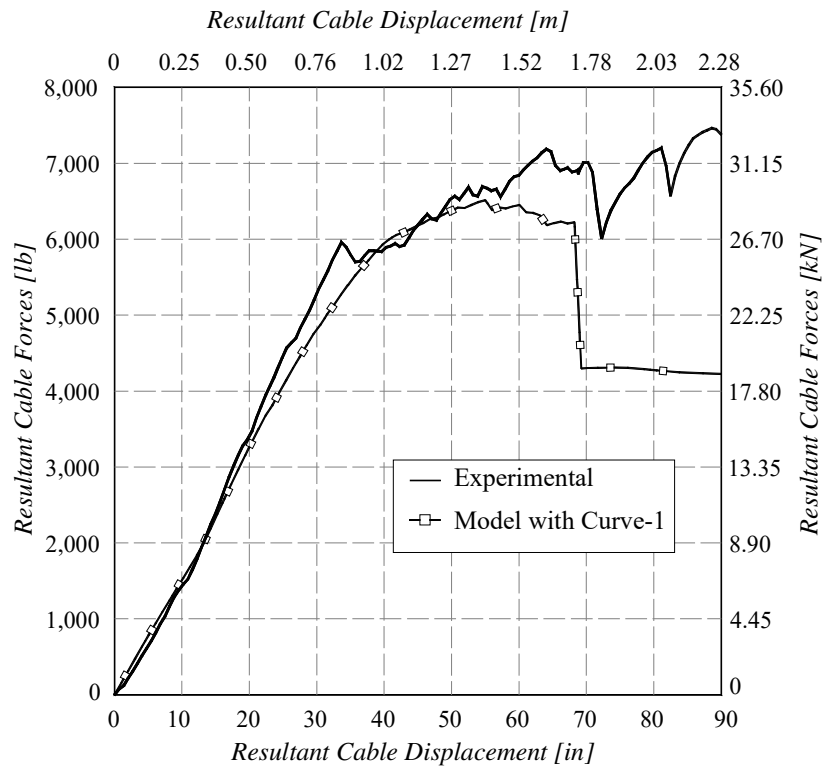
Figure 4.21: Response of Specimen II using Curve-1 for Vertical Springs (Δz) in the Bracing Elements Boundary Condition
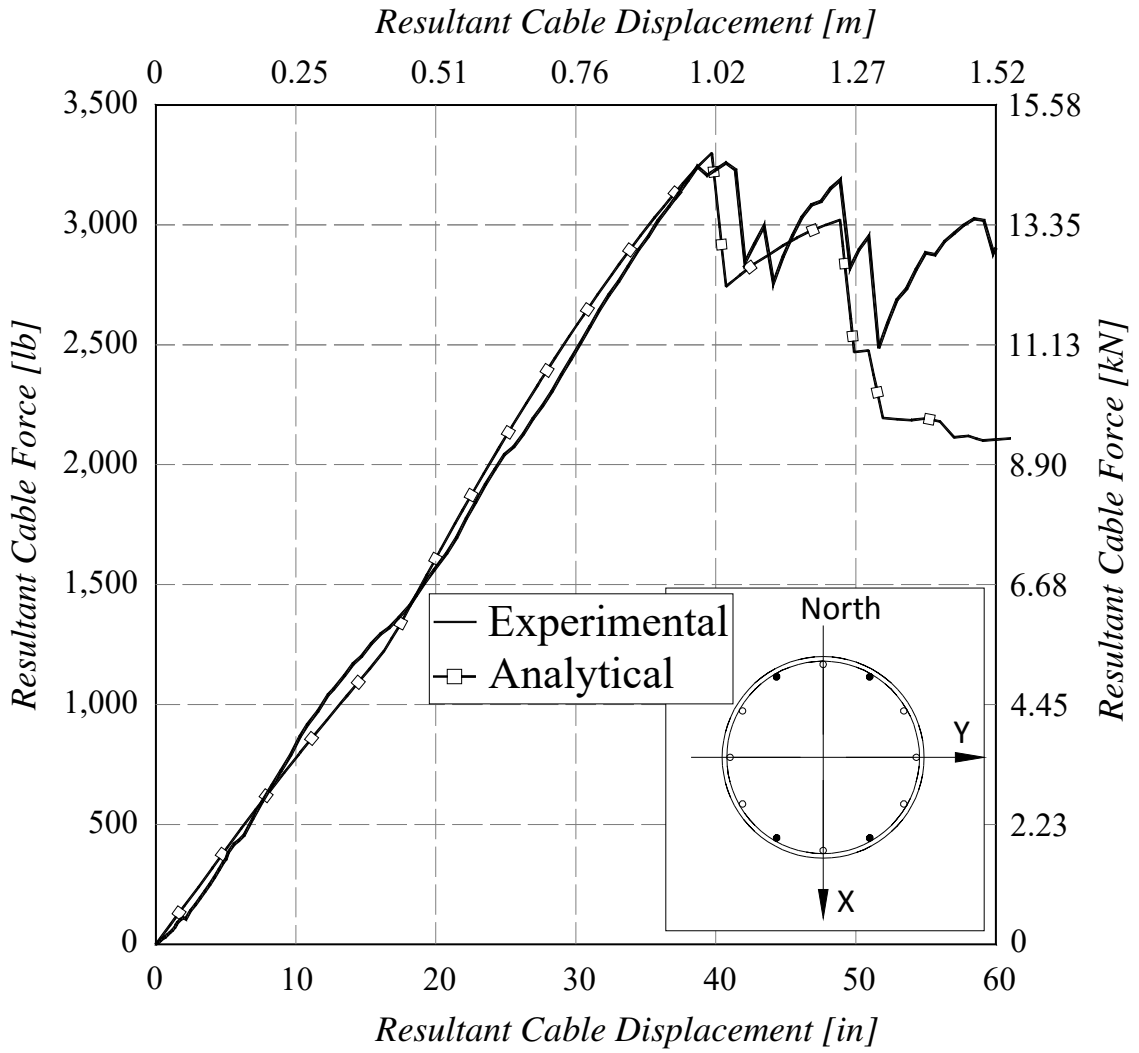
Figure 4.22: Comparison of Experimental and Calibrated Computational Model Results for Specimen I
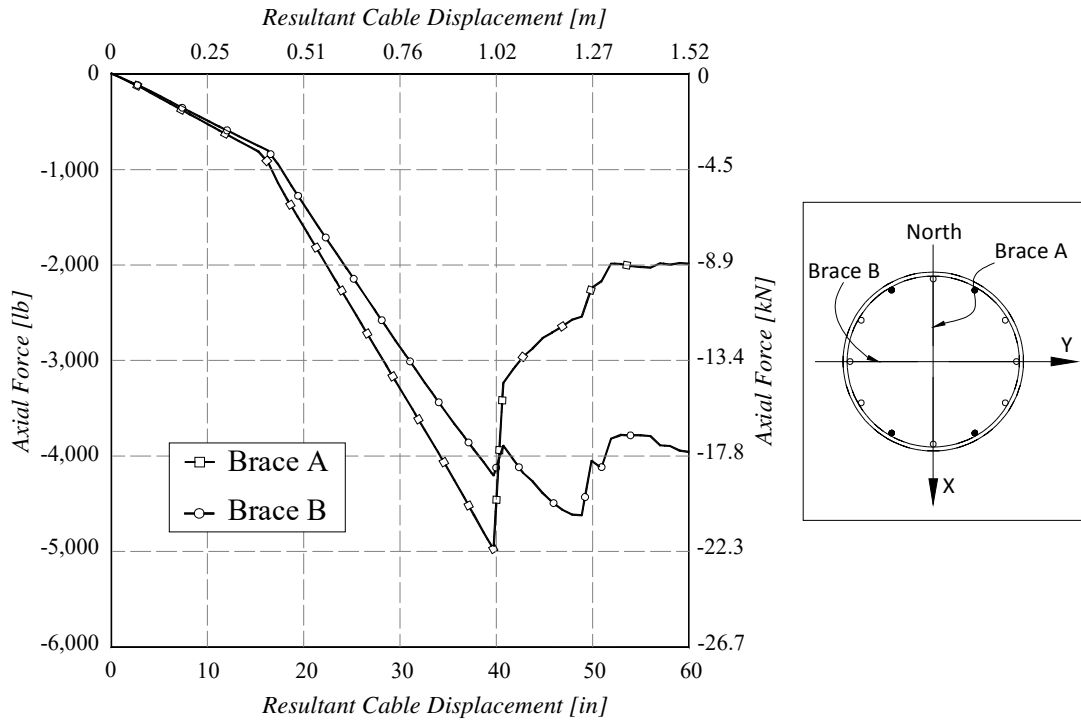
**Figure 4.23: Axial Force for bar A and B of the Bottom Brace of Specimen I**
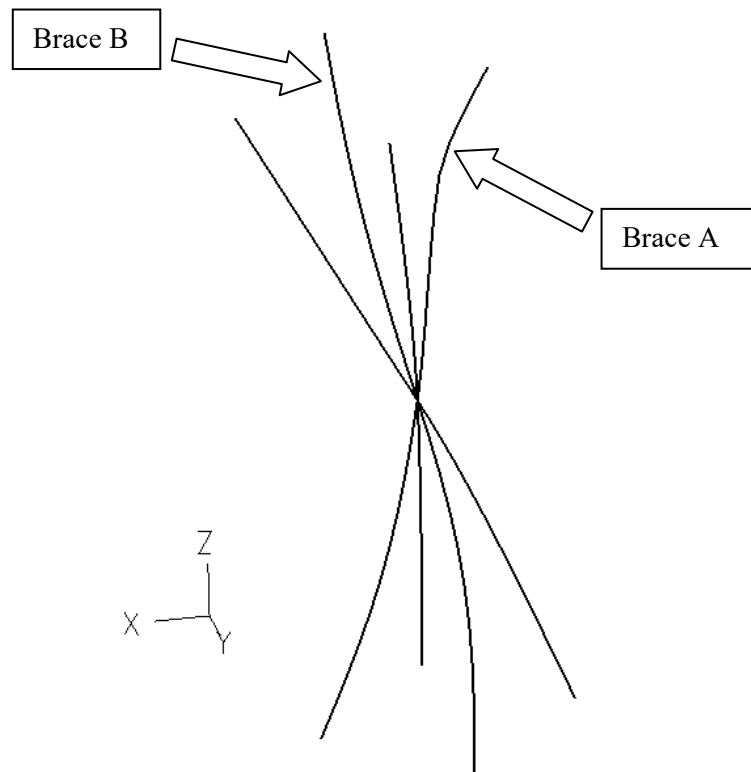
**Figure 4.24: Buckling of Bar A in the Bottom Brace**
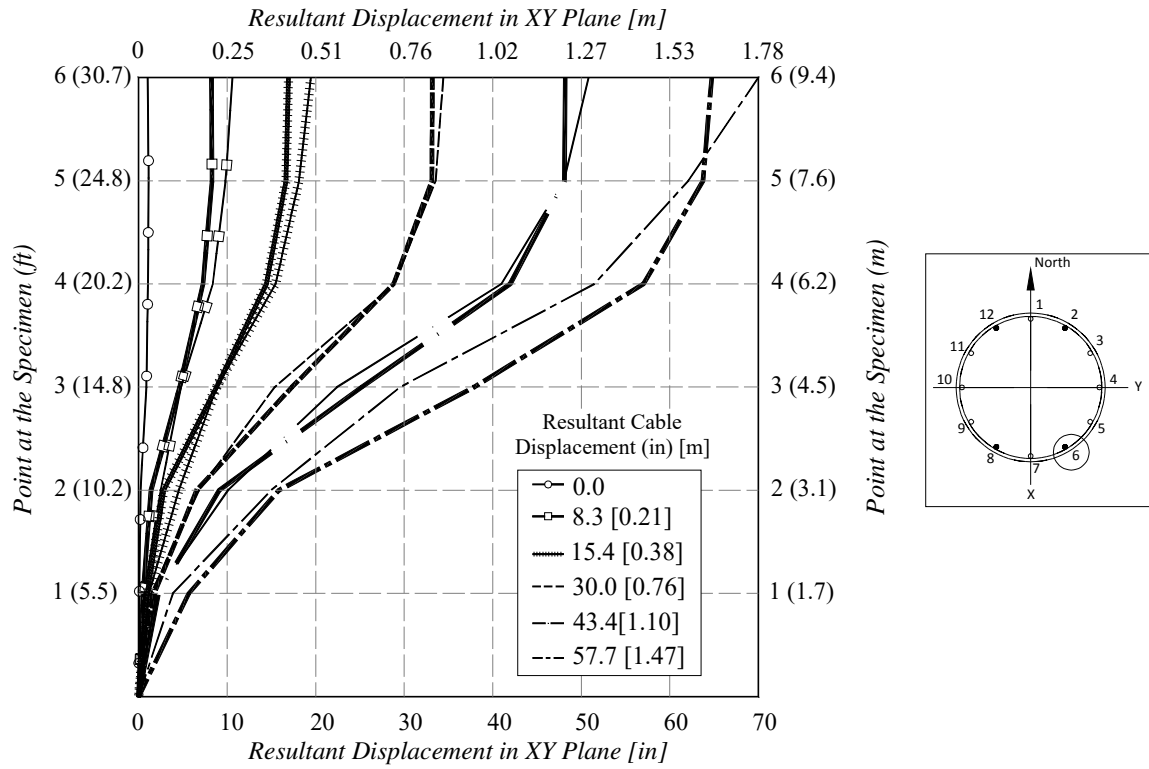
Figure 4.25: Measured (Dark) and Analytical (Light) Resultant Displacement in XY Plane for Specimen I
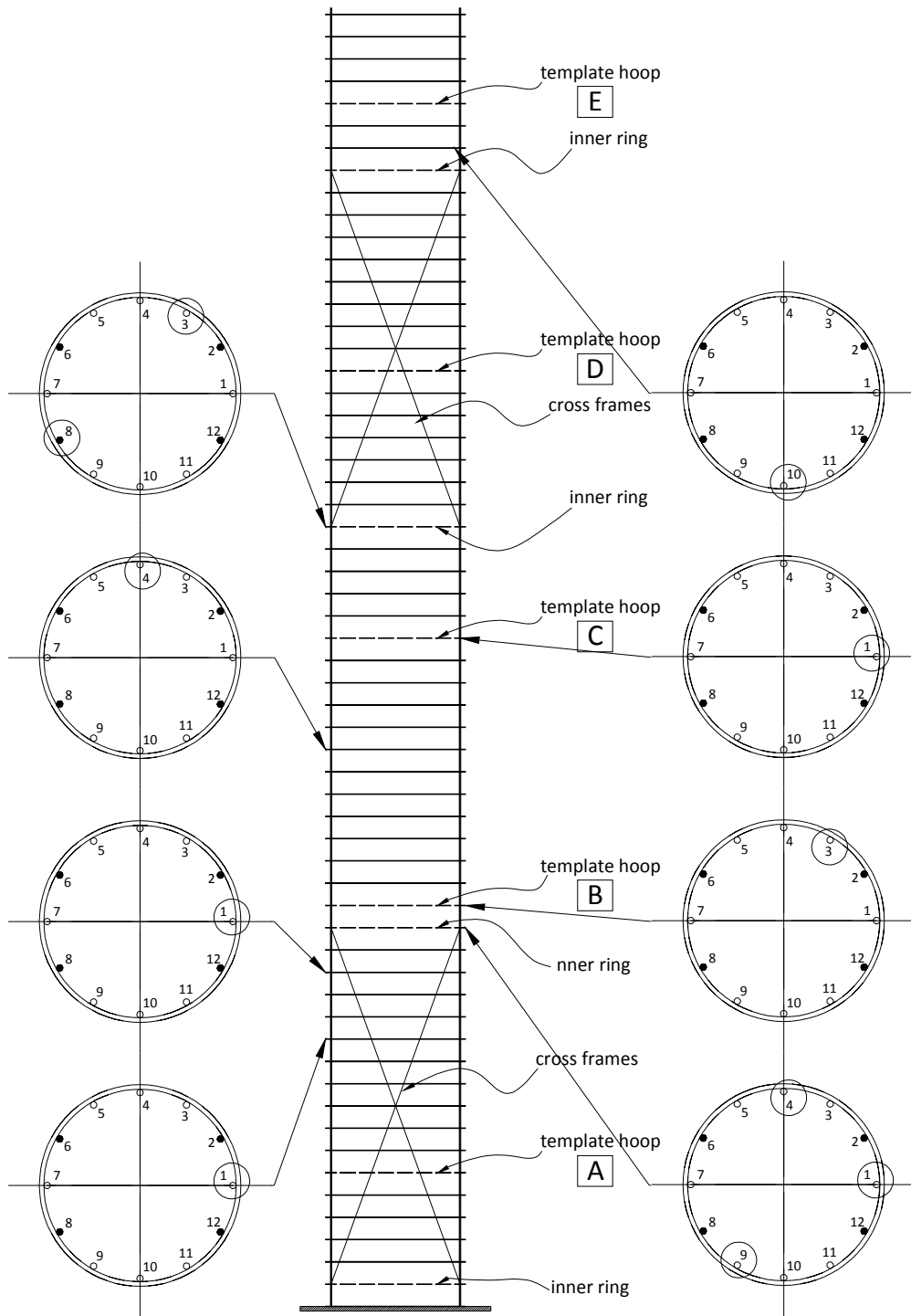
Figure 4.26: Fractured Tie Wire Connections in Specimen I up to 40-in of Resultant Cable Displacement
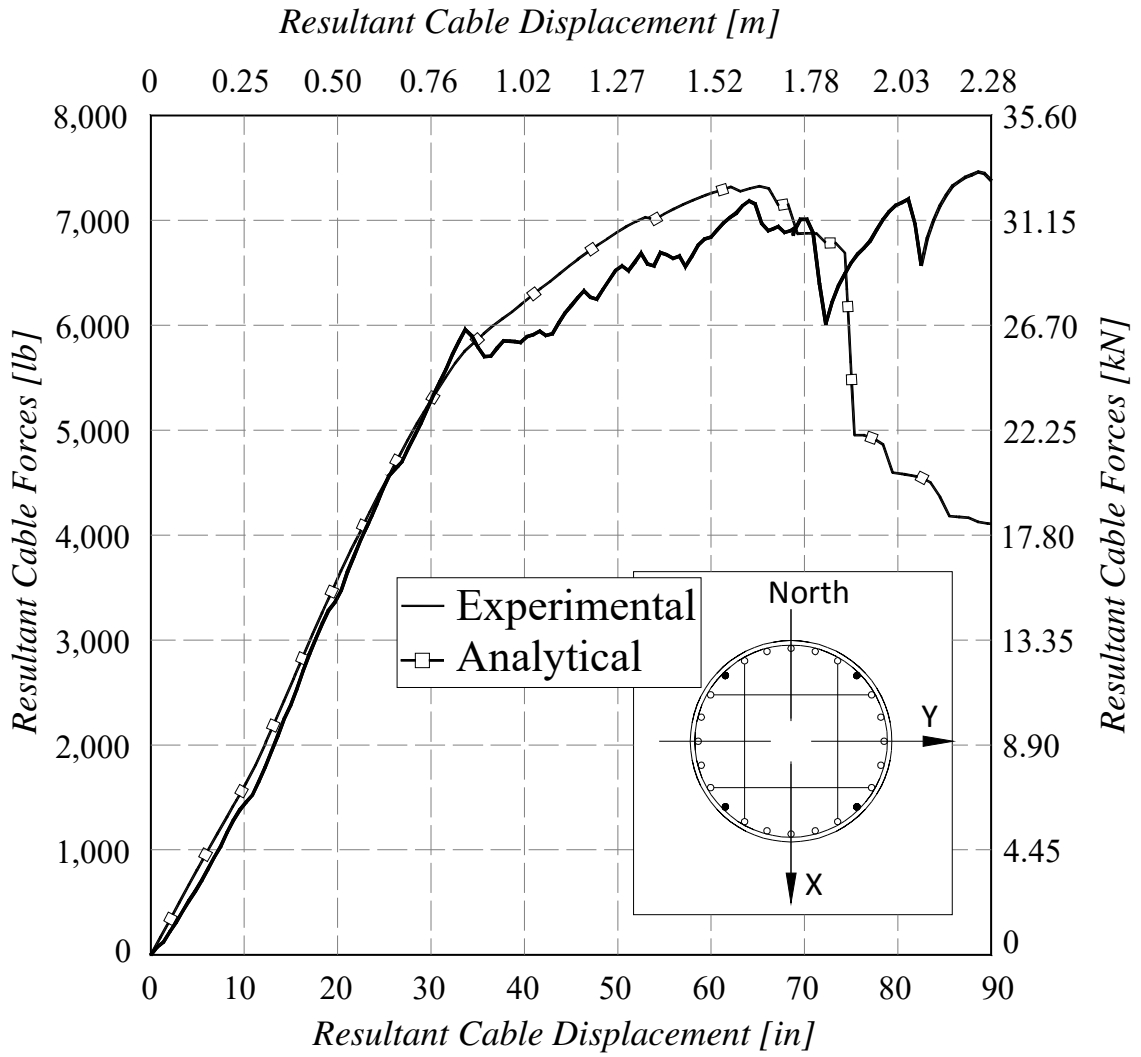
Figure 4.27: Comparison of Experimental and Calibrated Computational Model Results for Specimen II
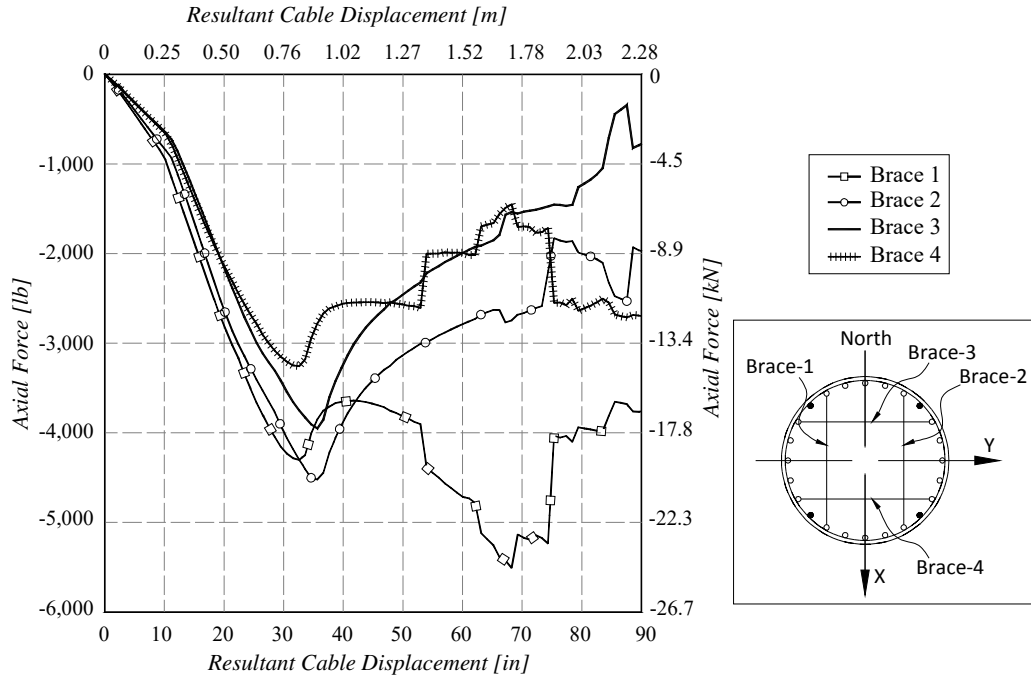
41Figure 4.28: Axial Force for bars of the Bottom Brace of Specimen II
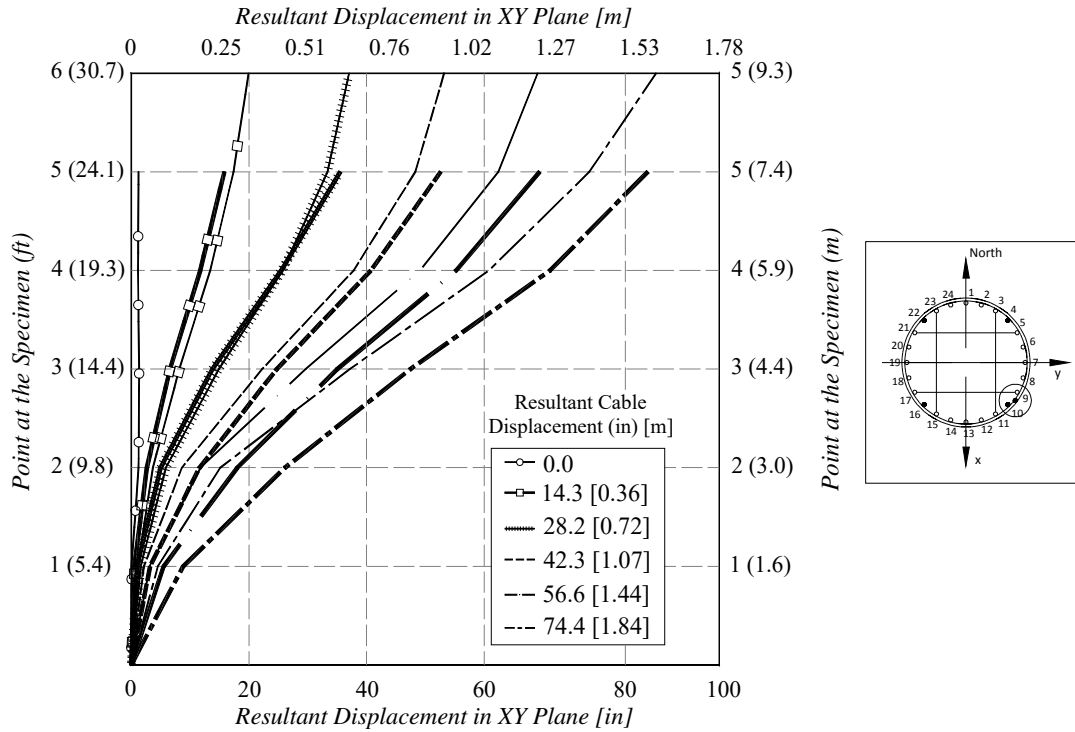

Figure 4.29: Measured (Dark) and Analytical (Light) Resultant Displacement in XY Plane for Specimen II
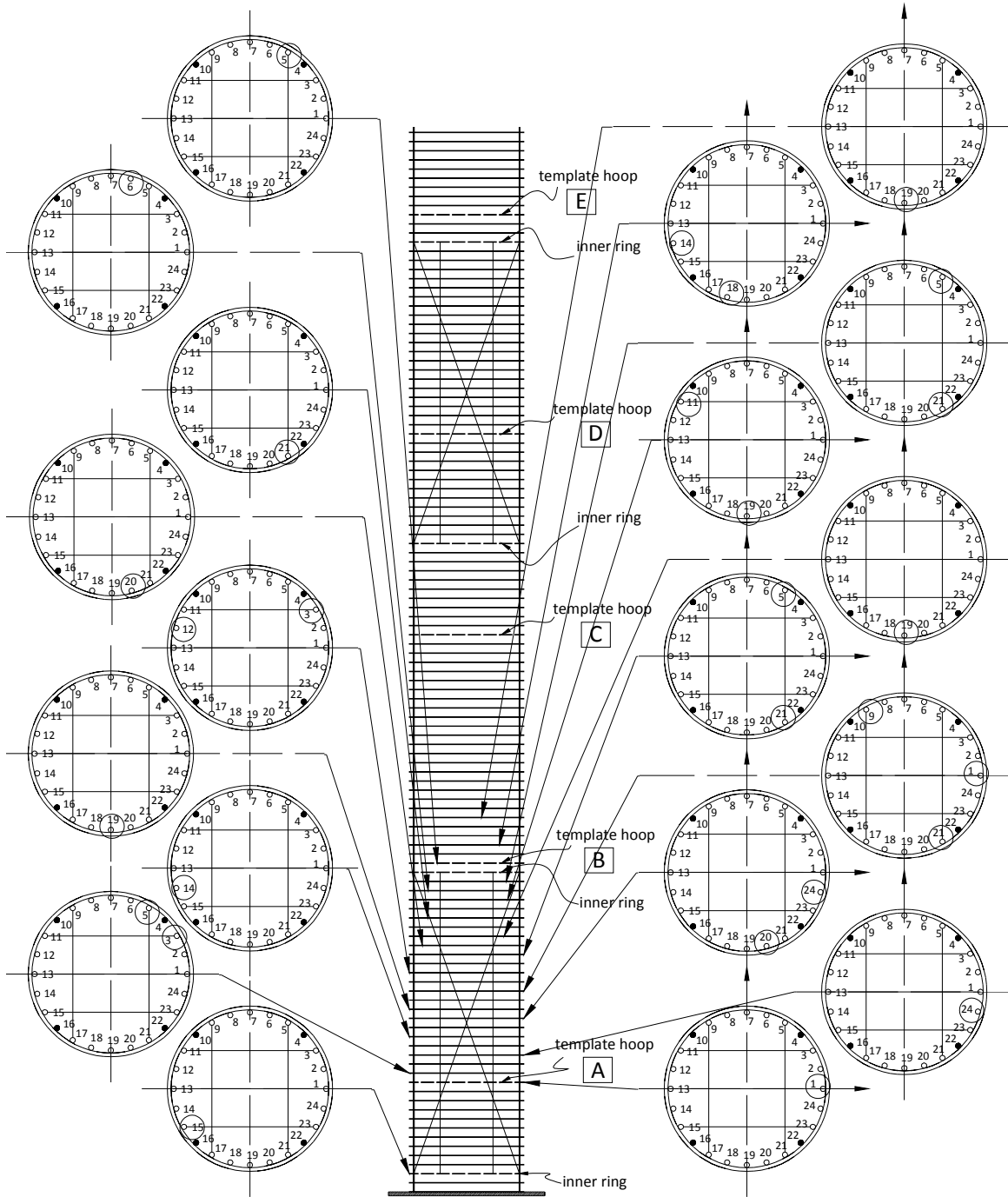
Figure 4.30: Fractured Tie Wire Connections in Specimen II up to 70-in of Resultant Cable Displacement (Part 1)

166
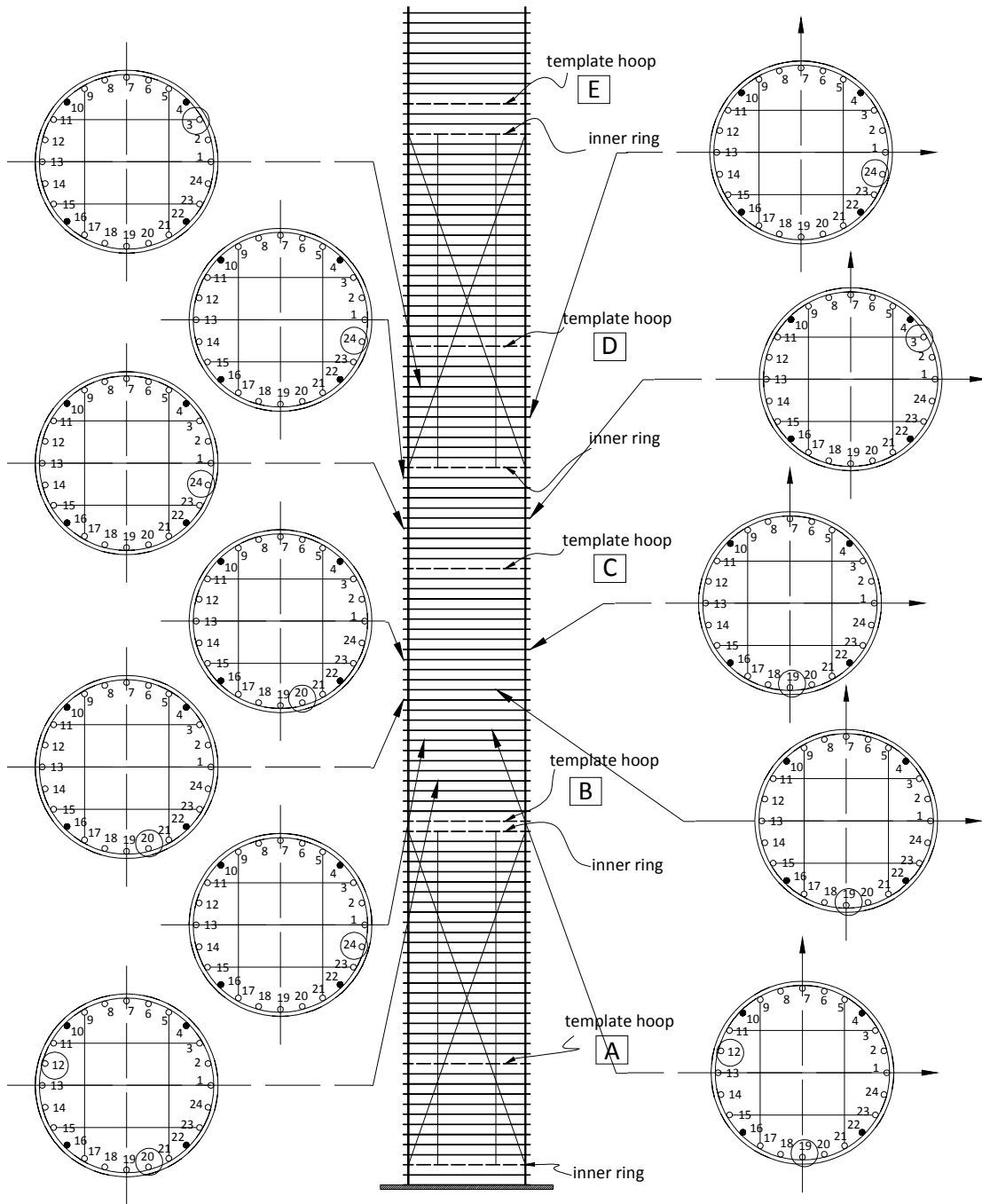
Figure 4.31: Fractured Tie Wire Connections in Specimen II up to 70-in of Resultant Cable Displacement (Part 2)
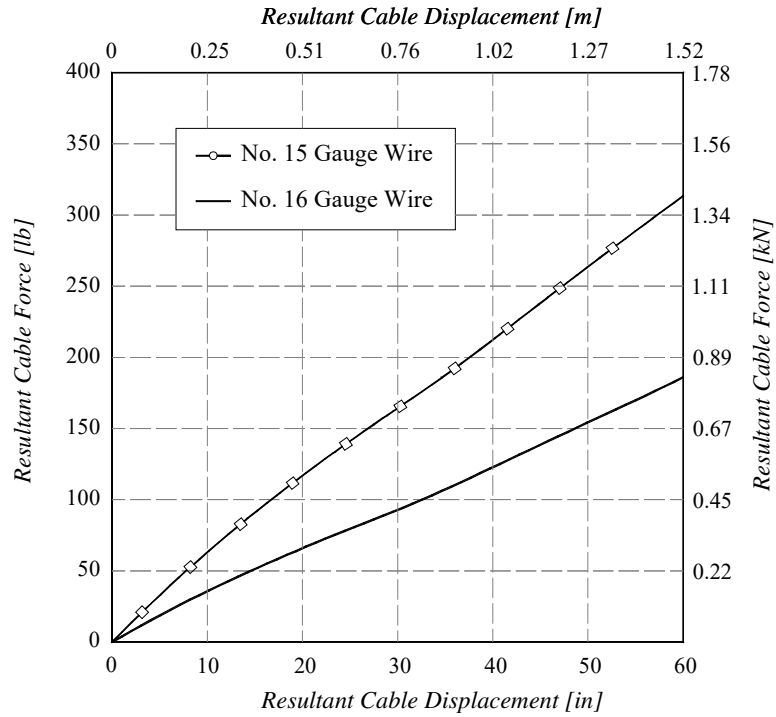
Figure 4.32: Response of Specimen I without braces and minimum tying with No. 15 gauge and No. 16 gauge wrap-and-saddle tie wire connections
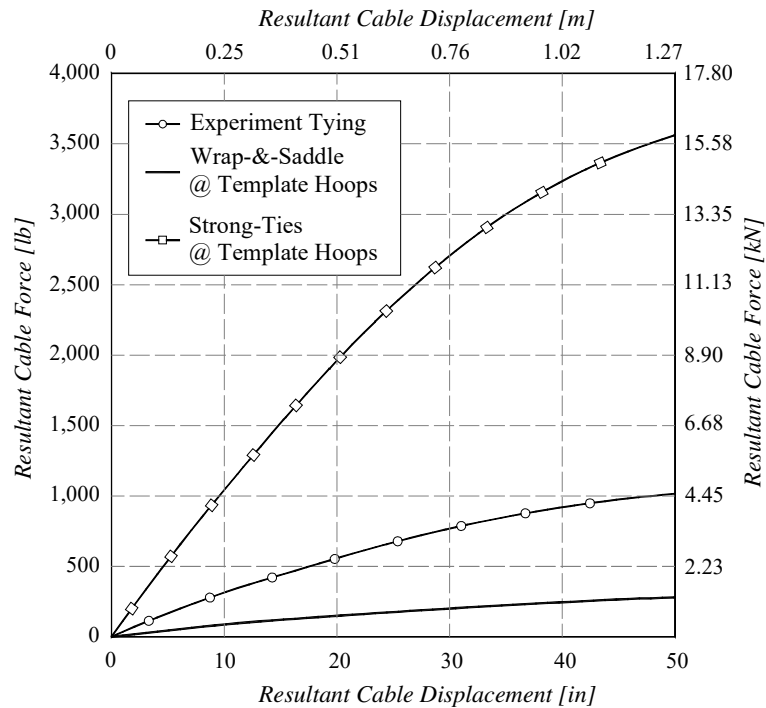
Figure 4.33: Response of Specimen I without Braces with different Tie Wire connections at Template Hoops
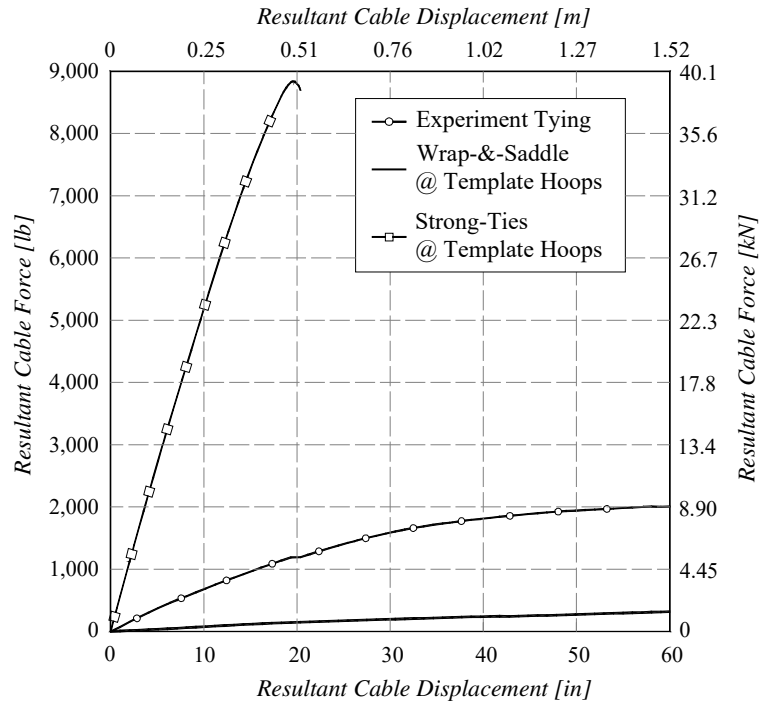
Figure 4.34: Response of Specimen II without Braces with different Tie Wire connections at Template Hoops
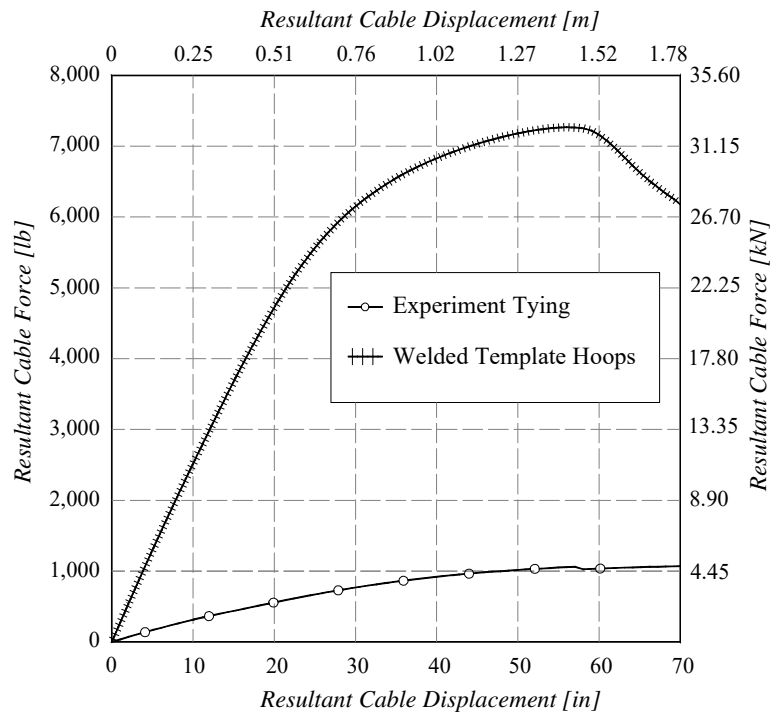
Figure 4.35: Response of Specimen I without Braces with Experimental Tying and Welded Template Hoops
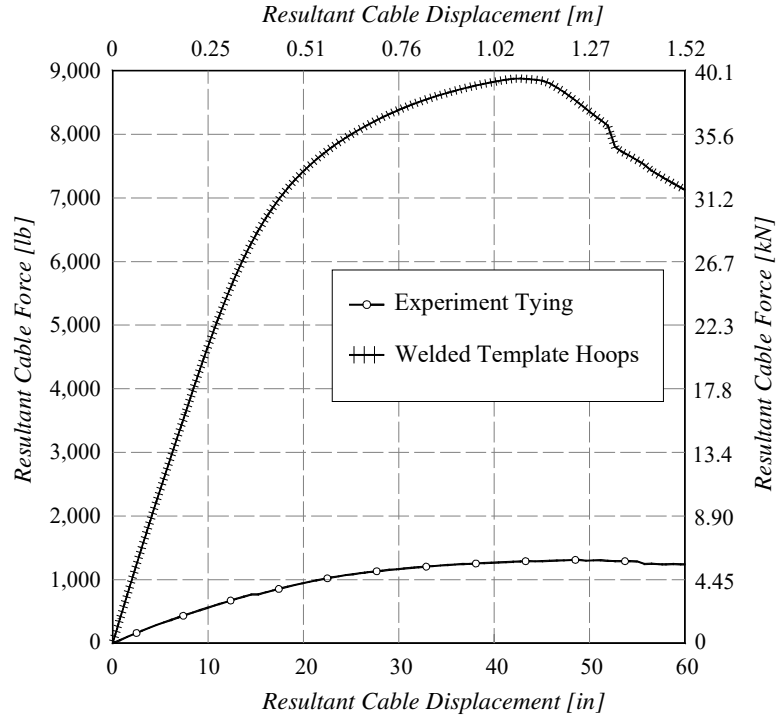
Figure 4.36: Response of Specimen II without Braces with Experimental Tying and Welded Template Hoops
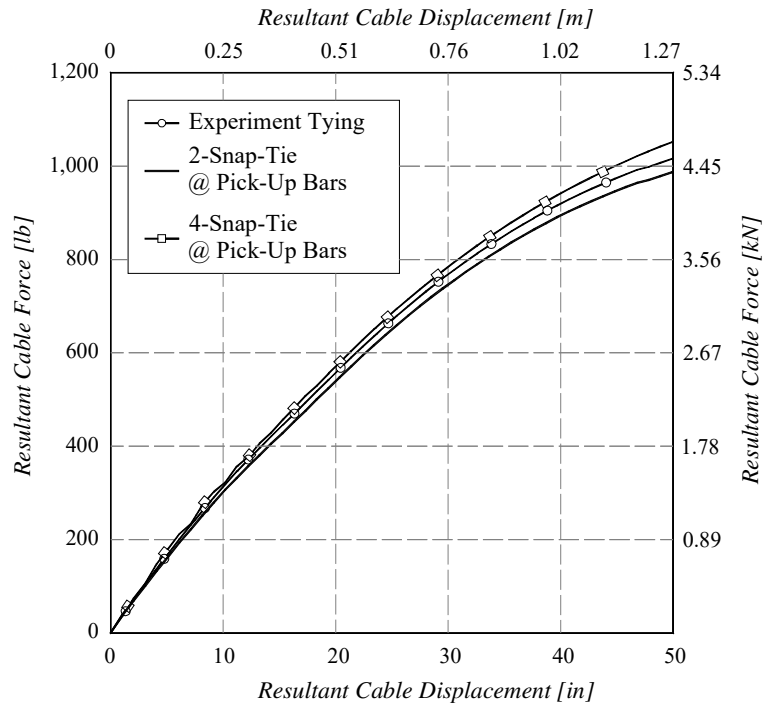
Figure 4.37: Response of Specimen I without Braces with different Tie Wire connections at Pick-up bars
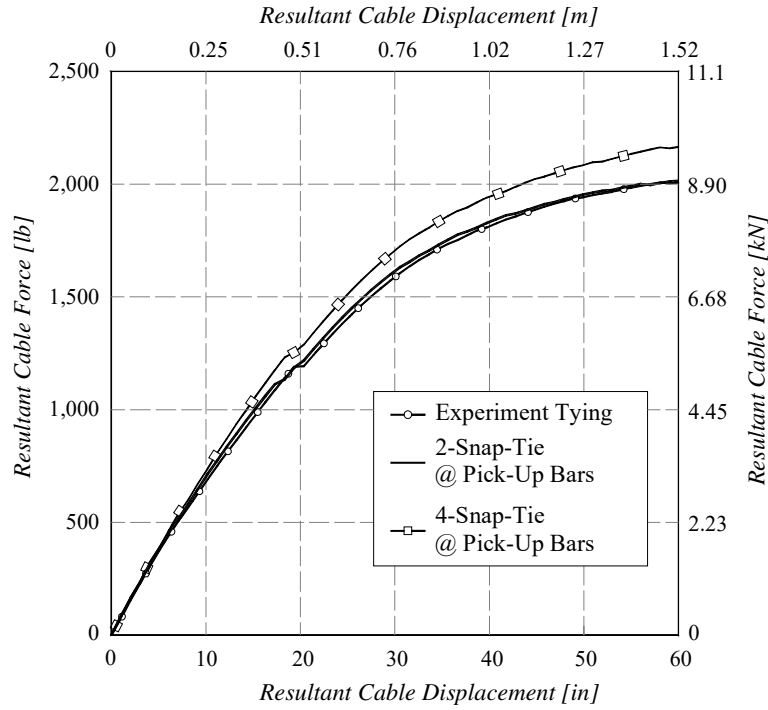
Figure 4.38: Response of Specimen II without Braces with different Tie Wire connections at Pick-up bars
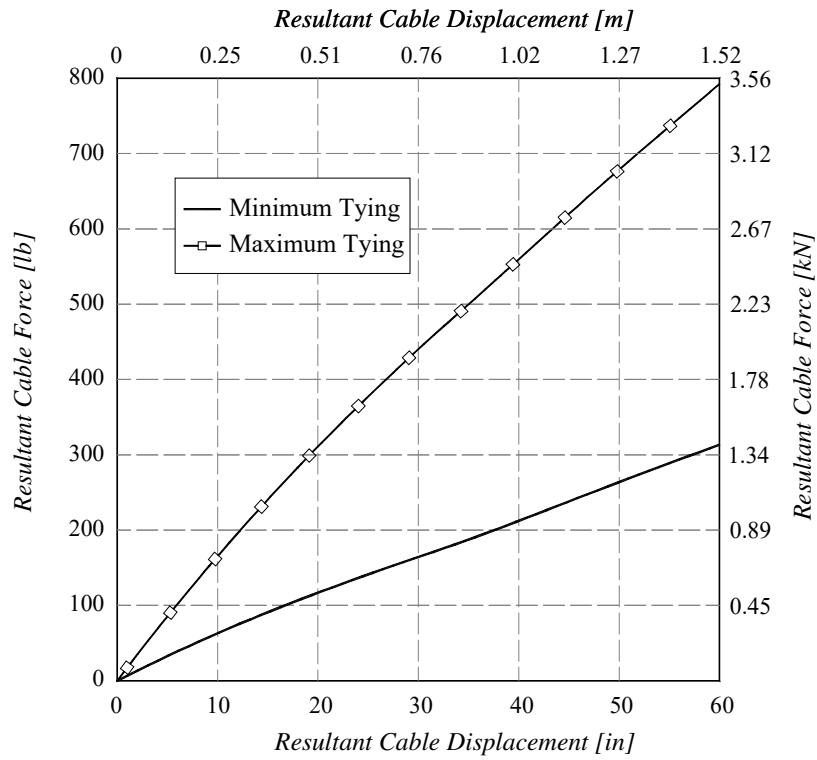
Figure 4.39: Response of Specimen I with Minimum and Maximum Tying using Wrap-and-Saddle
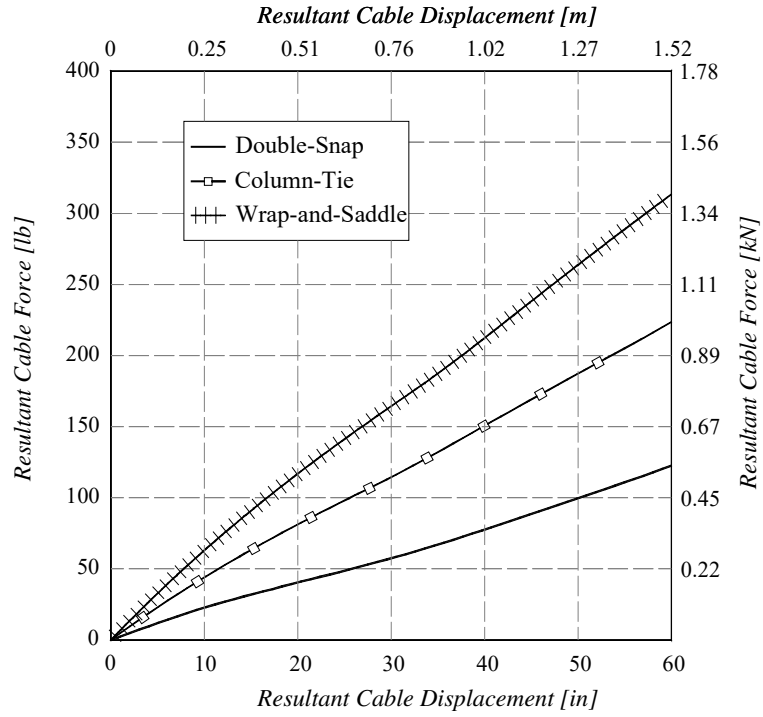
Figure 4.40: Response of Specimen I without braces with Minimum Tying using Double-Snap, Column-Tie and Wrap-and-Saddle Tie Wire connections
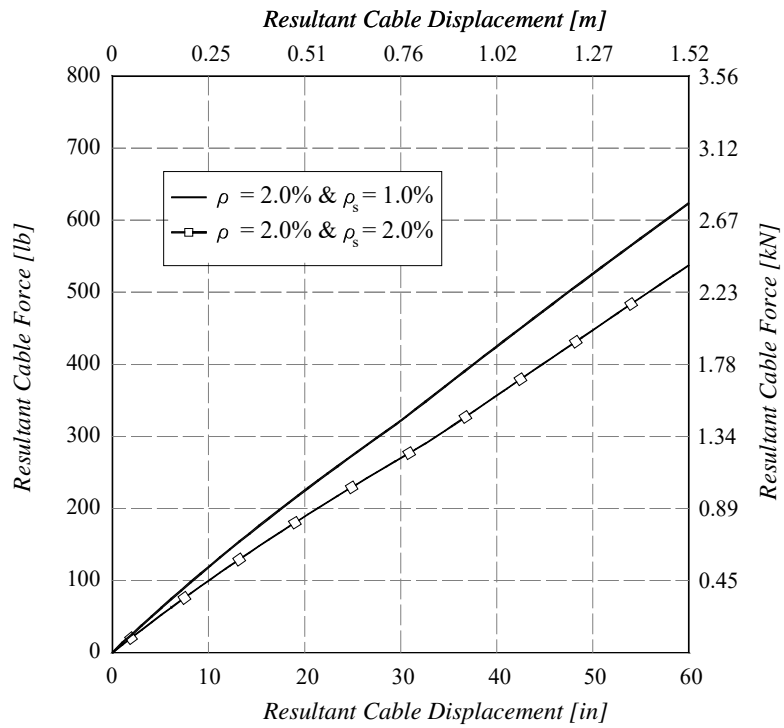
Figure 4.41: Response of Column Rebar Cages without braces and Transverse Reinforcement Ratio equal to 1% and 2%
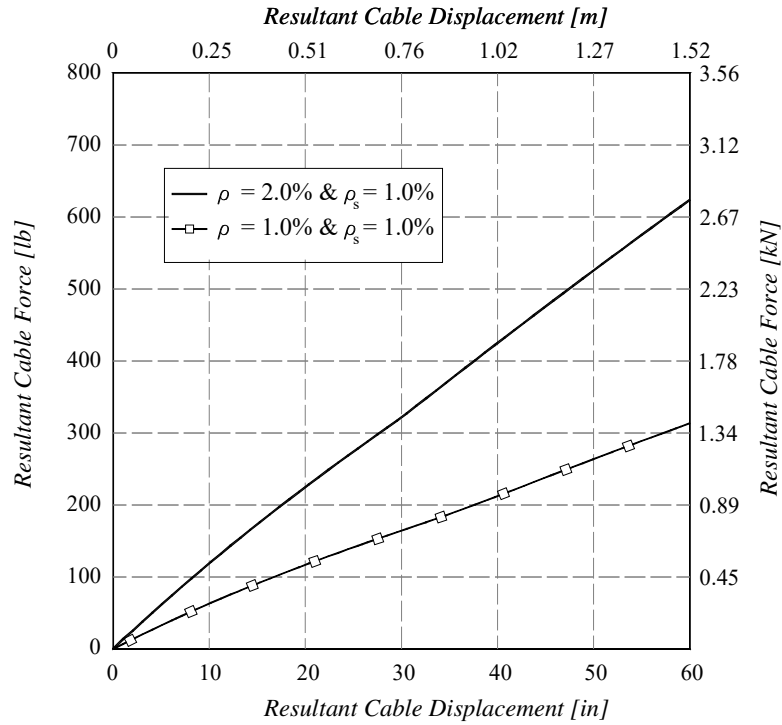
Figure 4.42: Response of Column Rebar Cages without braces and Longitudinal Reinforcement Ratio equal to 1% and 2%
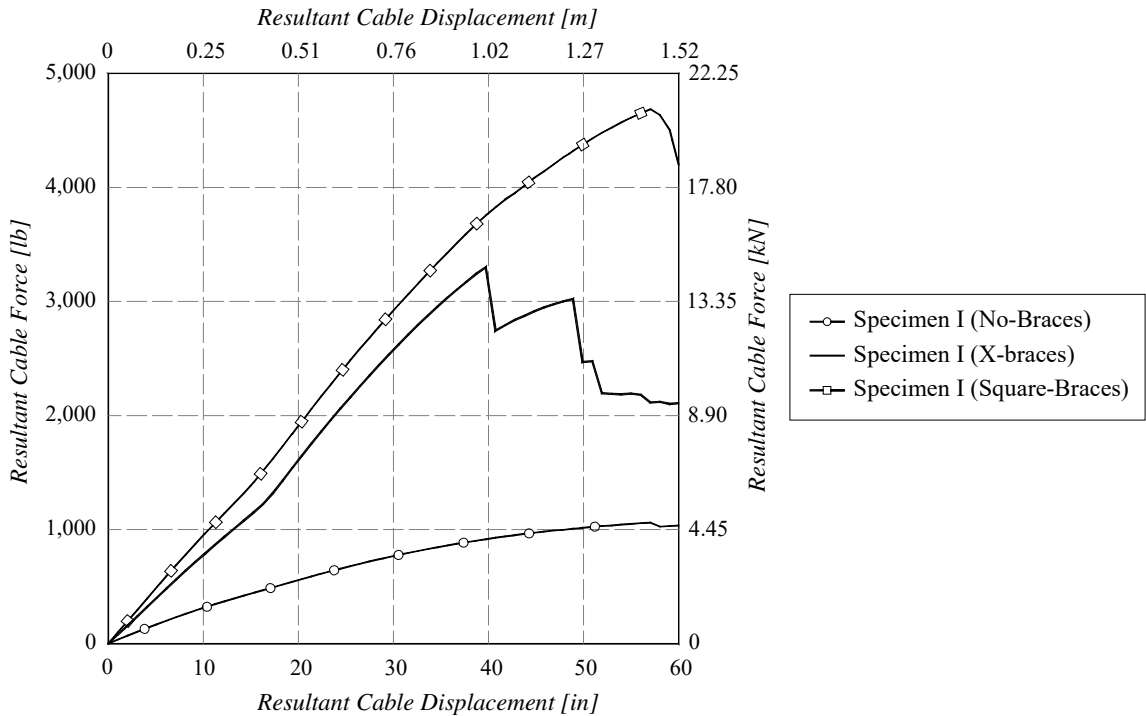
Figure 4.43: Response of Specimen I with X-braces and Square braces and without braces

Figure 4.33
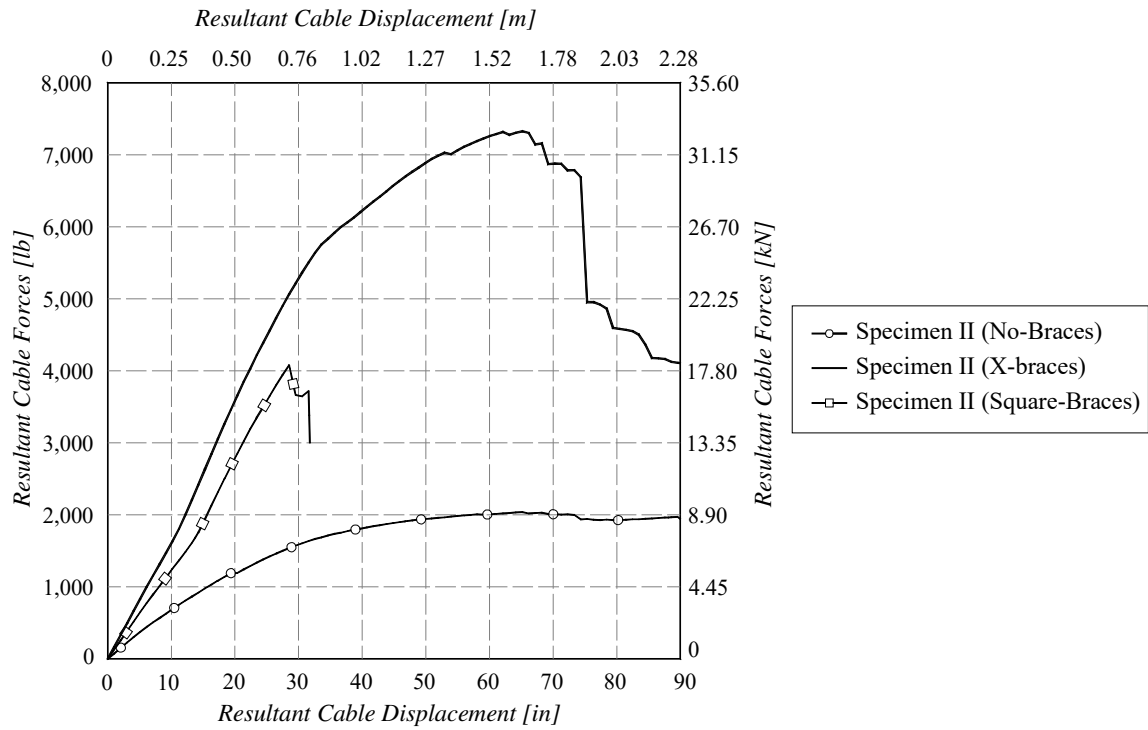
Figure 4.44: Response of Specimen II with X-braces and Square braces and without braces
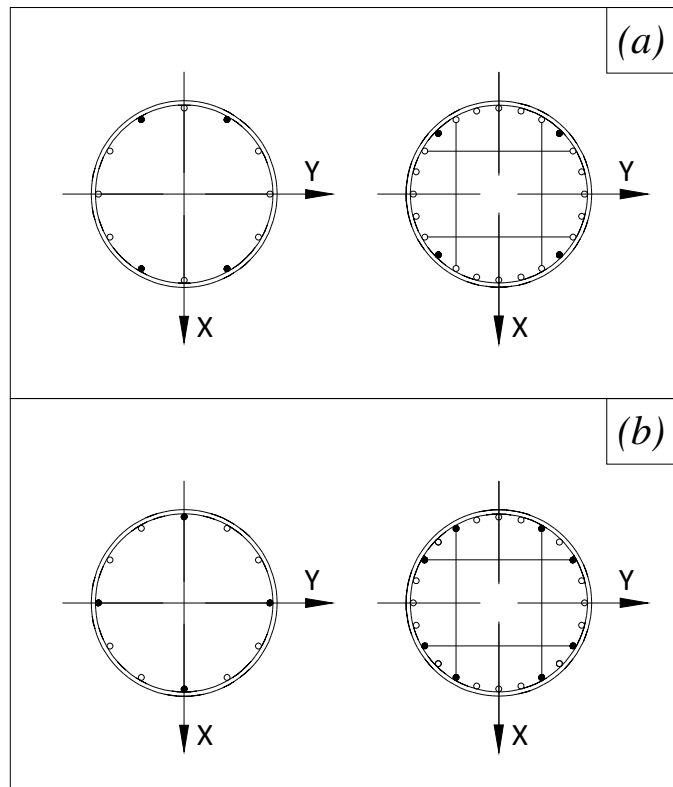
Figure 4.45: Locations of pick-up bars: (a) Location 1, (b) Location 2
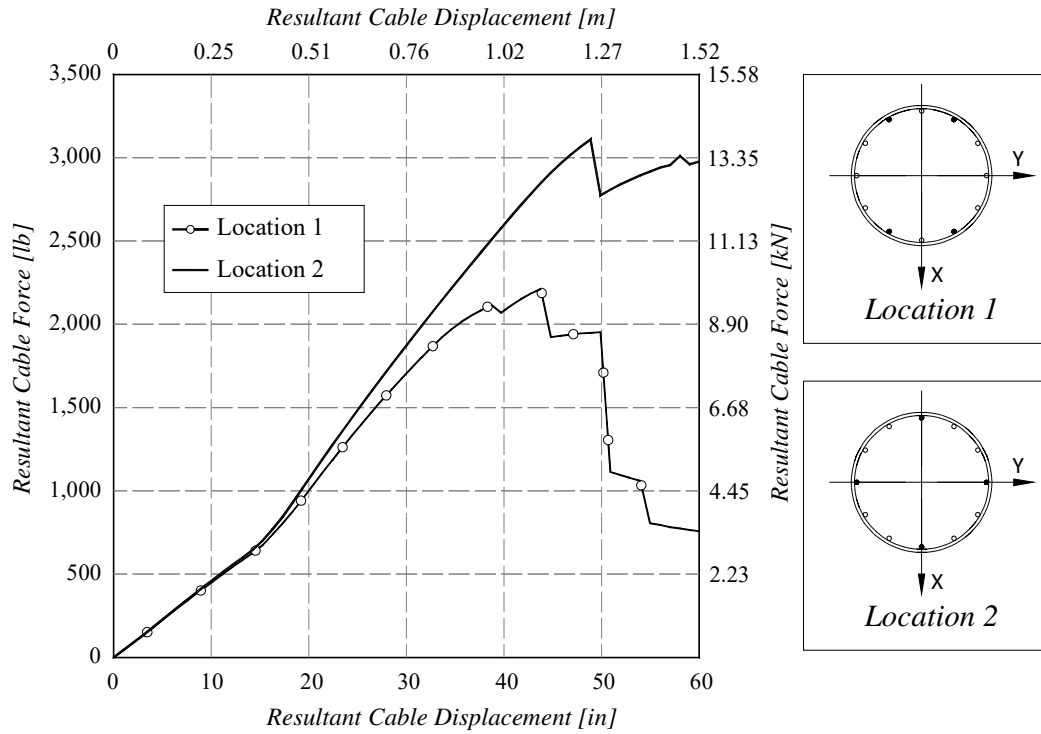
Figure 4.46: Response of Specimen I with different Location of Pick-up bars
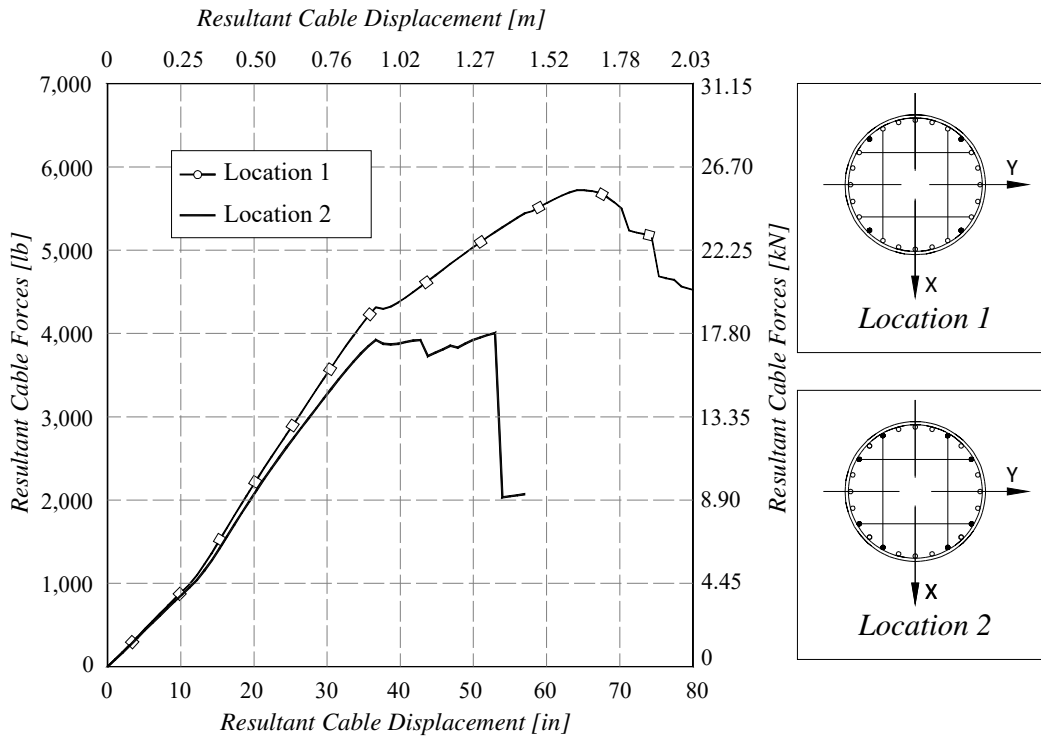
Figure 4.47: Response of Specimen II with different Location of Pick-up bars

175
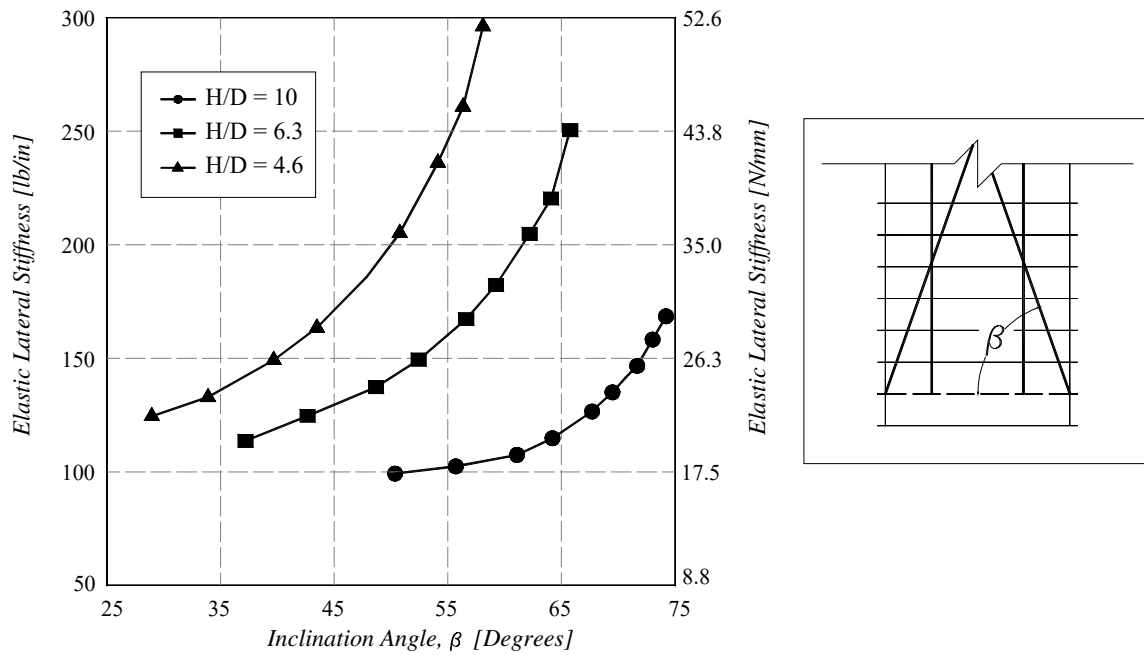
Figure 4.48: Parametric Study on the Elastic Stiffness of Bridge Column Rebar Cages
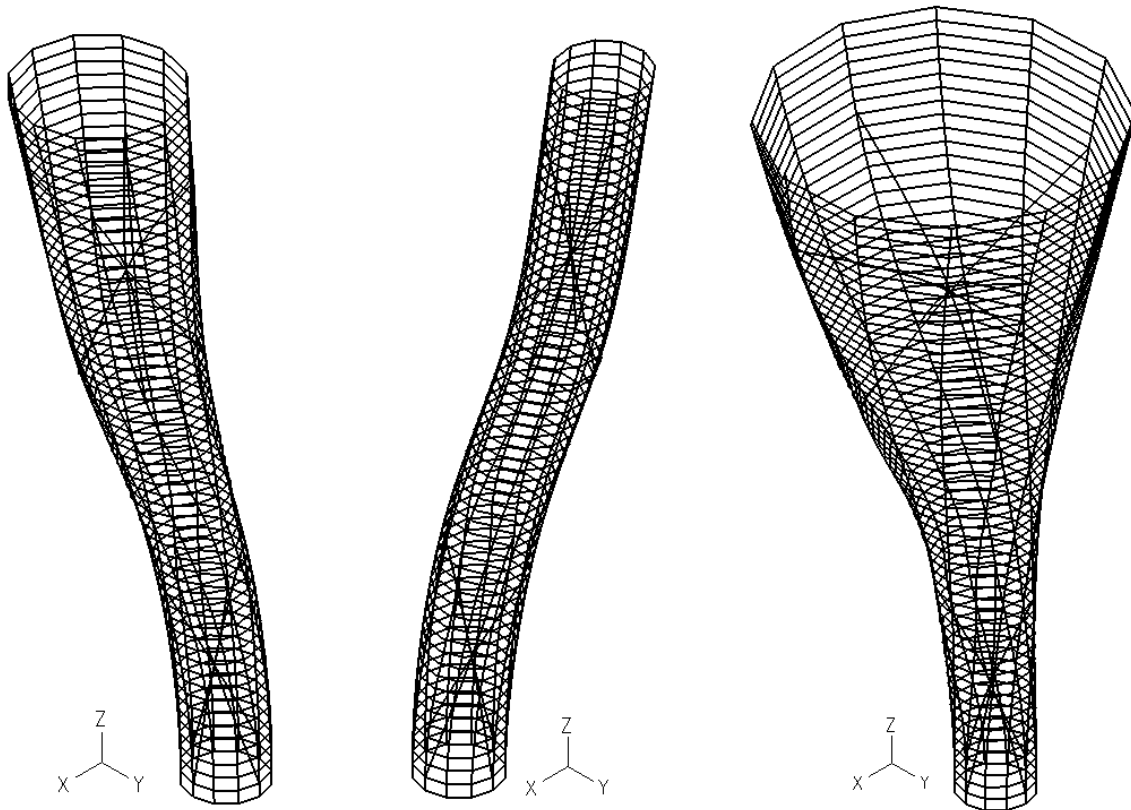
Figure 4.49: Mode Shapes of Specimen I: (Left) First mode, (Middle) Second mode and (Right) Third mode
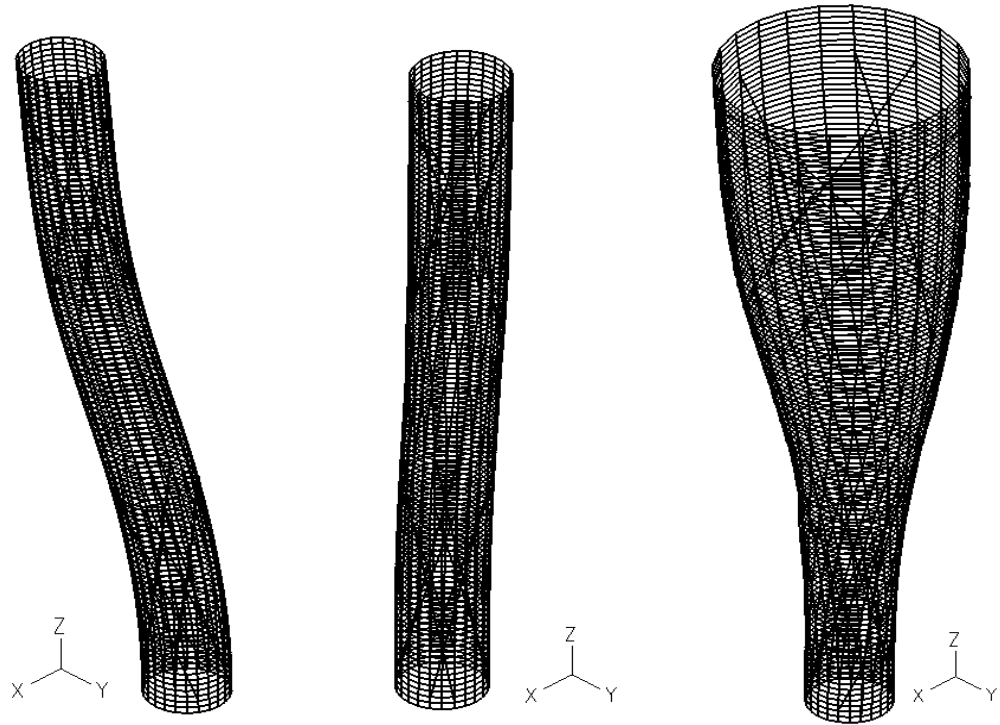
Figure 4.50: Mode Shapes of Specimen II: (Left) First mode, (Middle) Second mode and (Right) Third mode
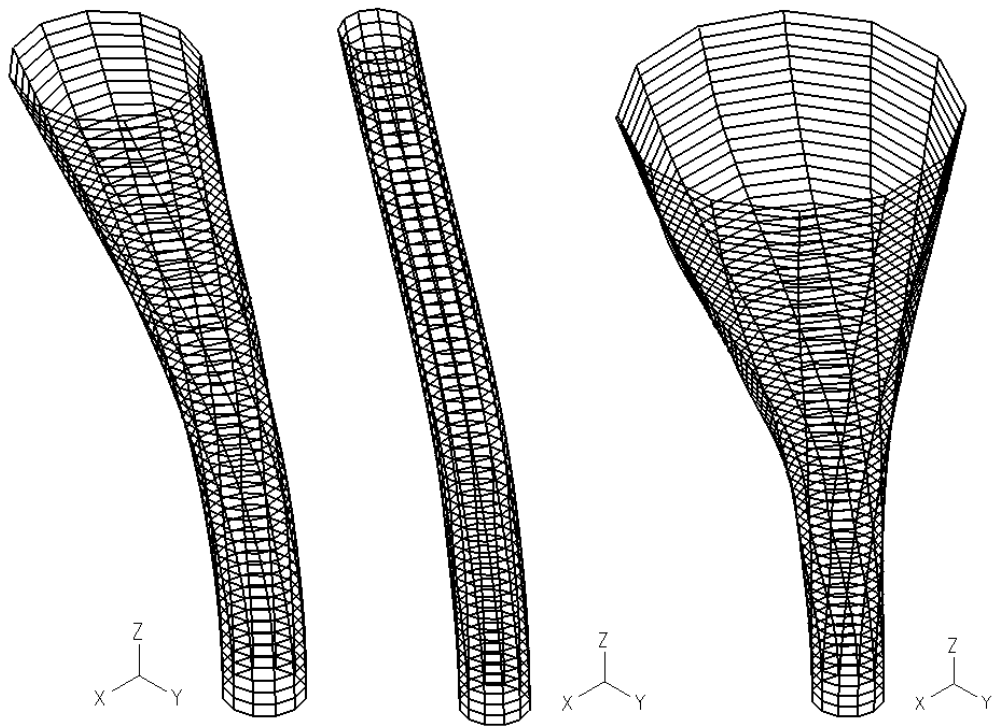
Figure 4.51: Mode Shapes of Specimen I without braces: (Left) First mode, (Middle) Second mode and (Right) Third mode

177
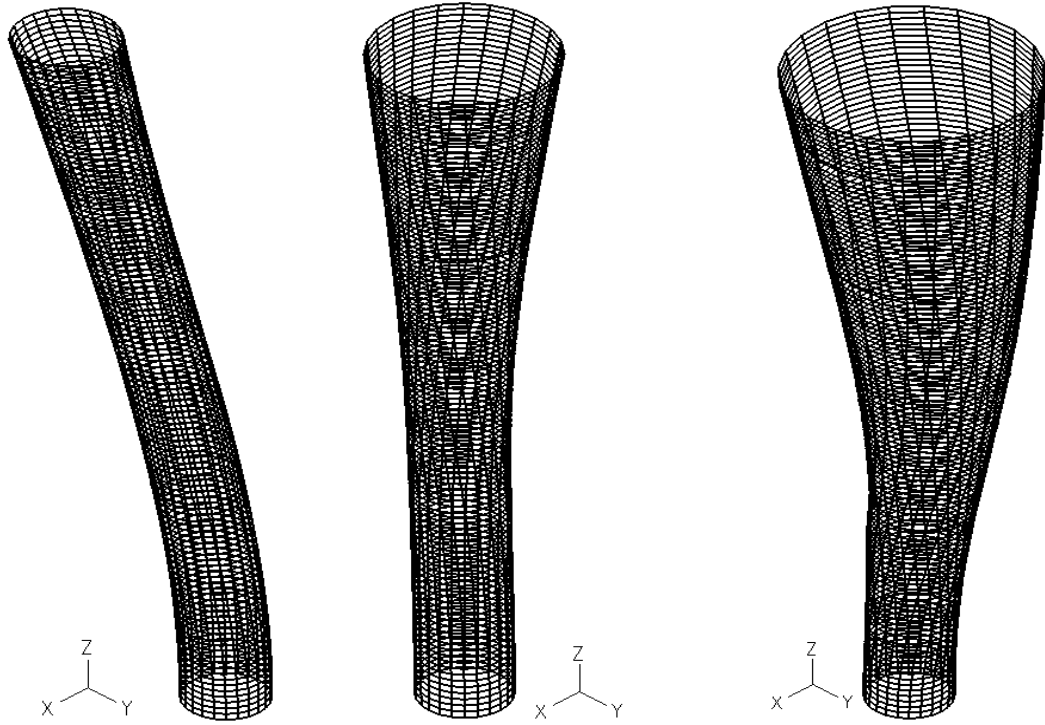
Figure 4.52: Mode Shapes of Specimen II without braces: (Left) First mode, (Middle) Second mode and (Right) Third mode
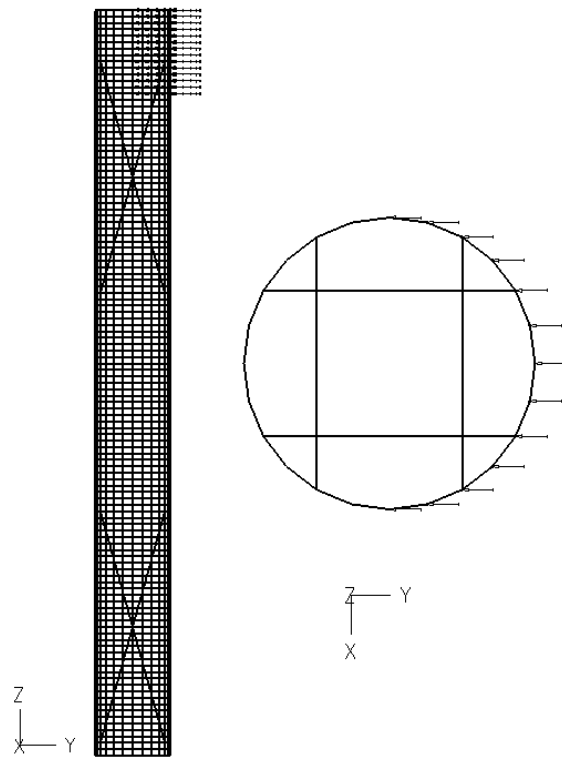
Figure 4.53: Accidental Lateral Loading: (Left) Lateral view and (Right) Top view

178
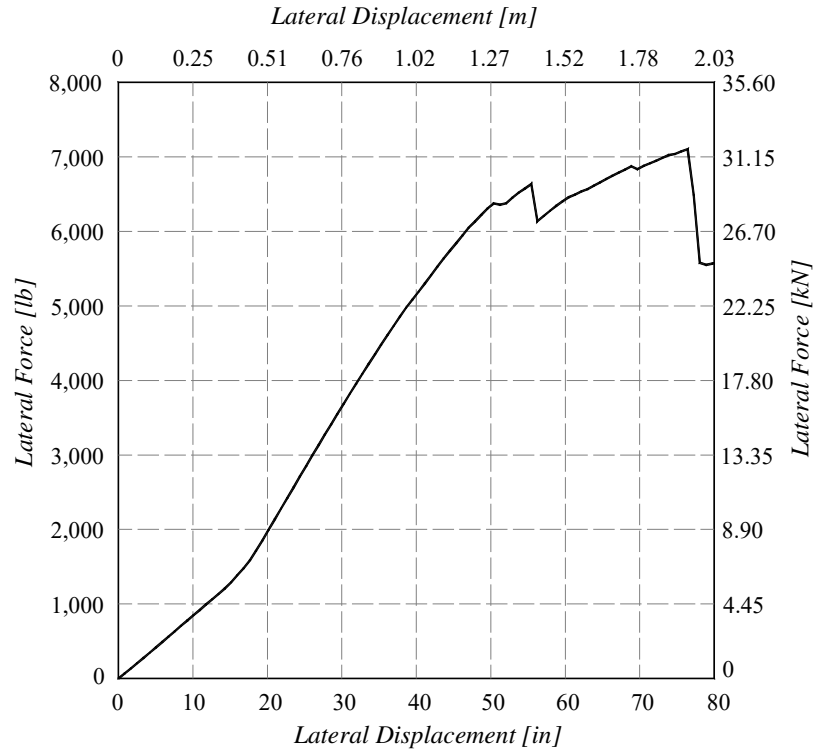
Figure 4.54: Lateral Response of Specimen II under accidental lateral loading
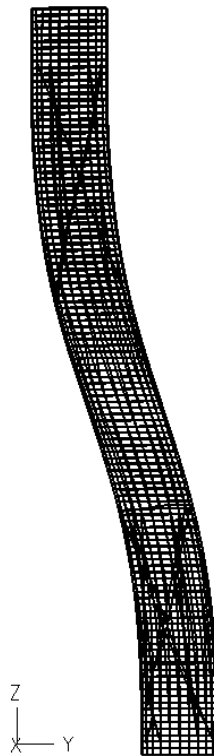
Figure 4.55: Deformed Shape under Accidental Lateral Loading

179
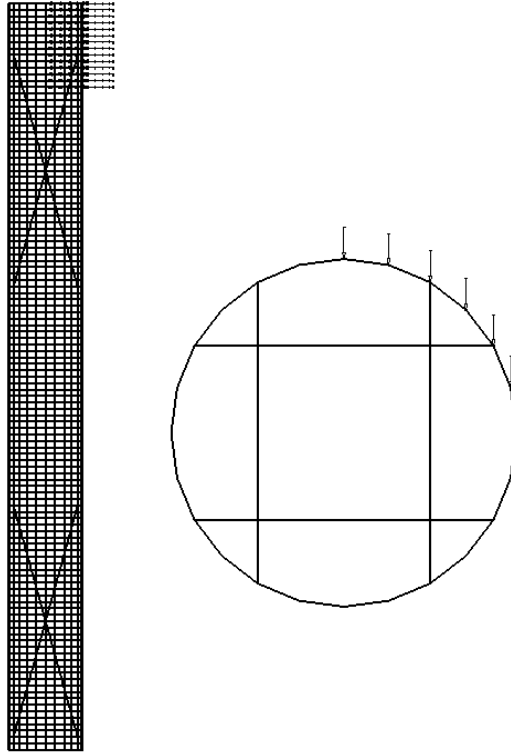
Figure 4.56: Unsymmetrical Accidental Lateral Loading: (Left) Lateral view and (Right) Top view
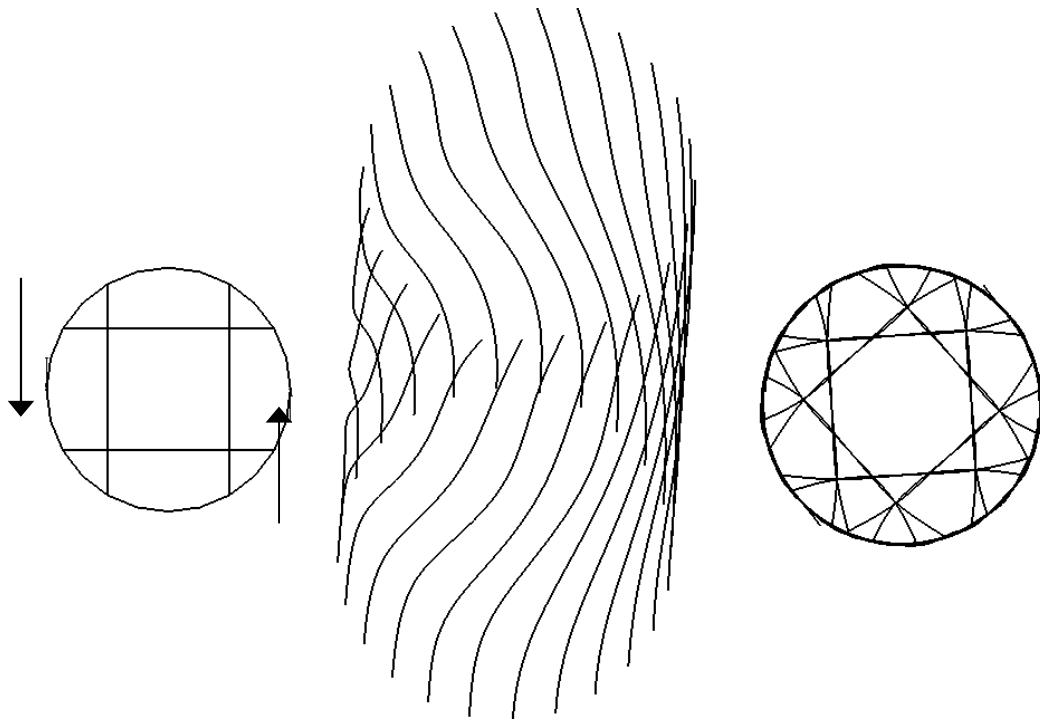
Figure 4.57: Torsional loading (Left), Deformed shape of Longitudinal Bars (Middle) and Top View of Deformed Shape (Left)

180
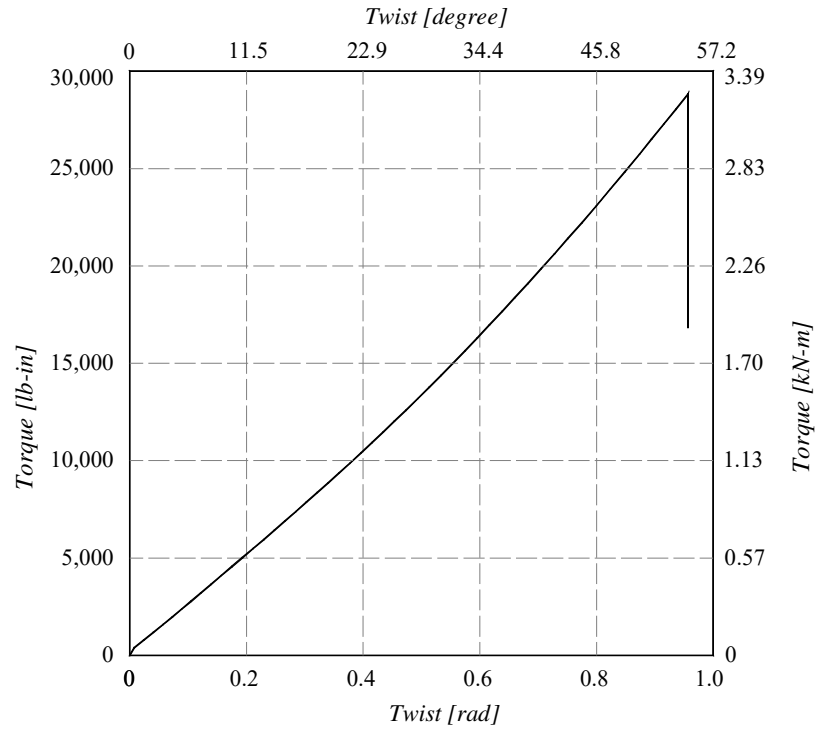
Figure 4.58: Response of Specimen II without Braces under Torsional Loading
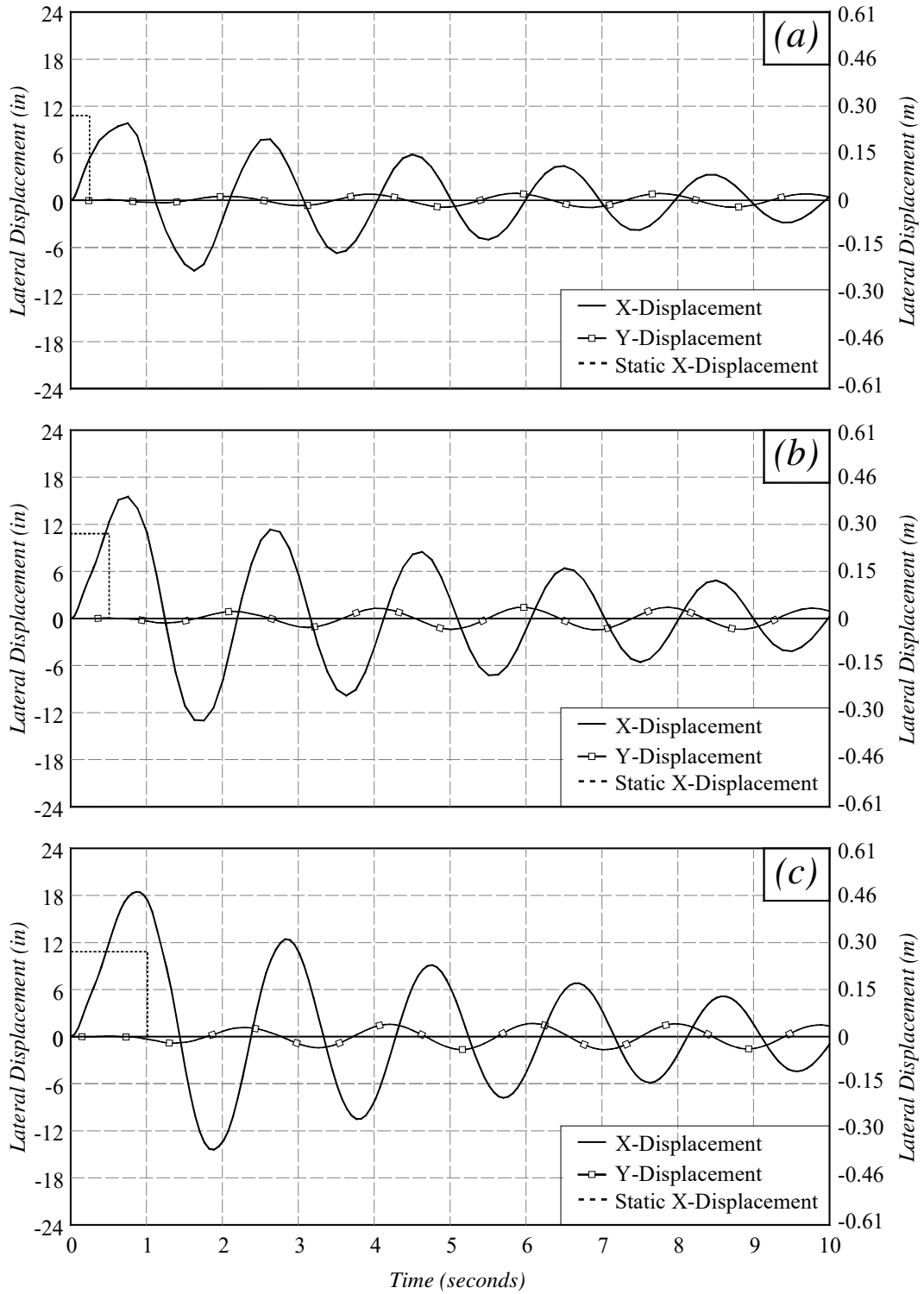
Figure 4.59: Dynamic Response of Bridge Column Rebar Cages: (a) $t_d/T_n = 1/8$, (b) $t_d/T_n = 1/4$, and (c) $t_d/T_n = 1/2$

182
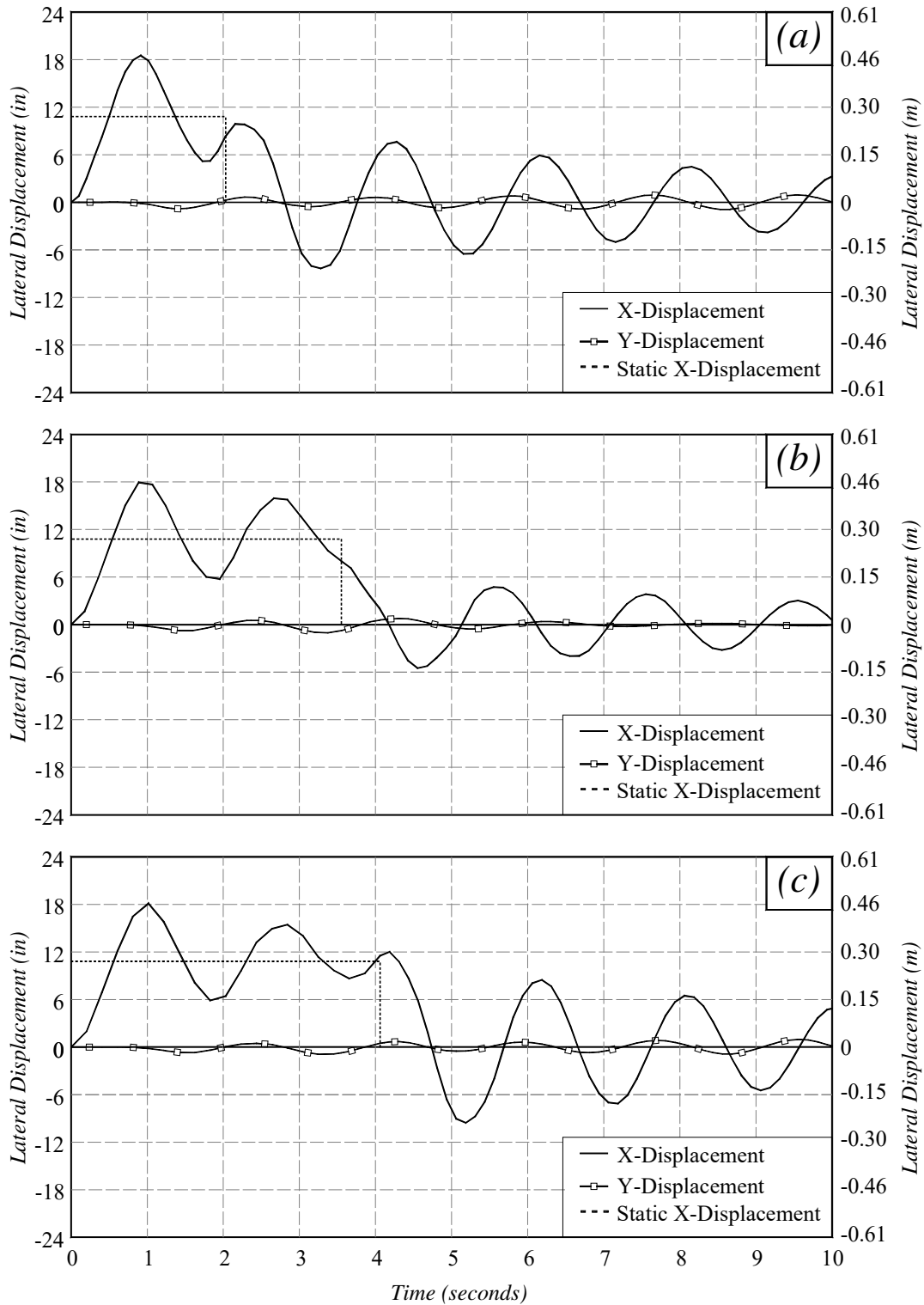
Figure 4.60: Dynamic Response of Bridge Column Rebar Cages: (a) t_d/T_n =1, (b) t_d/T_n =1.75, and (c) t_d/T_n =2
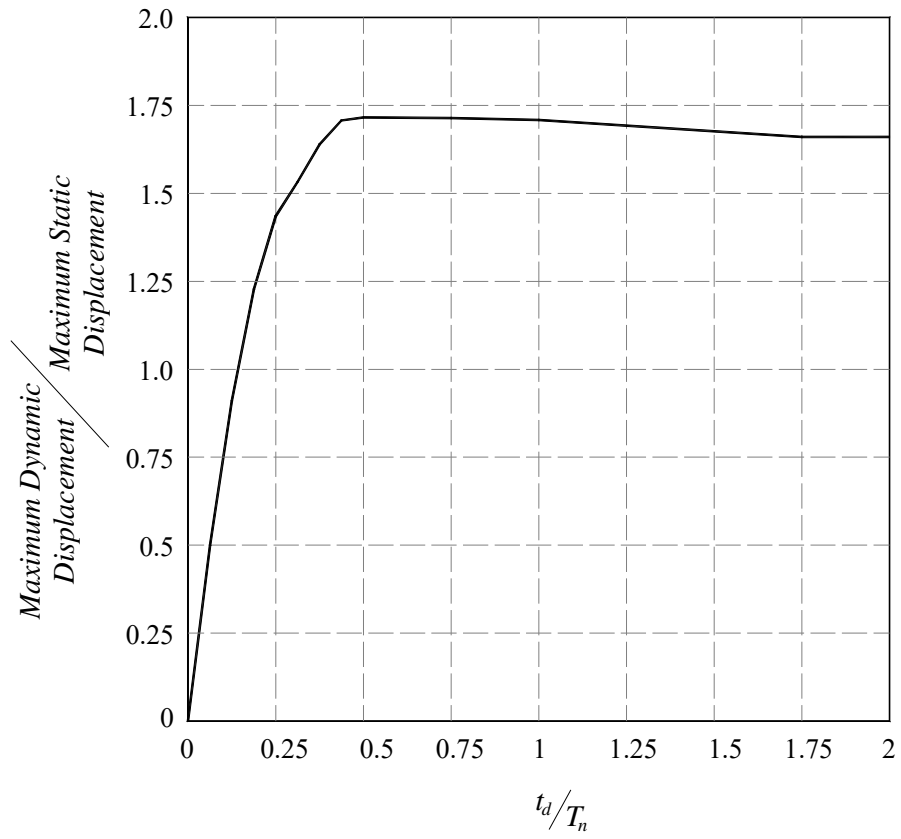
Figure 4.61: Shock Spectrum for Bridge Column Rebar Cages
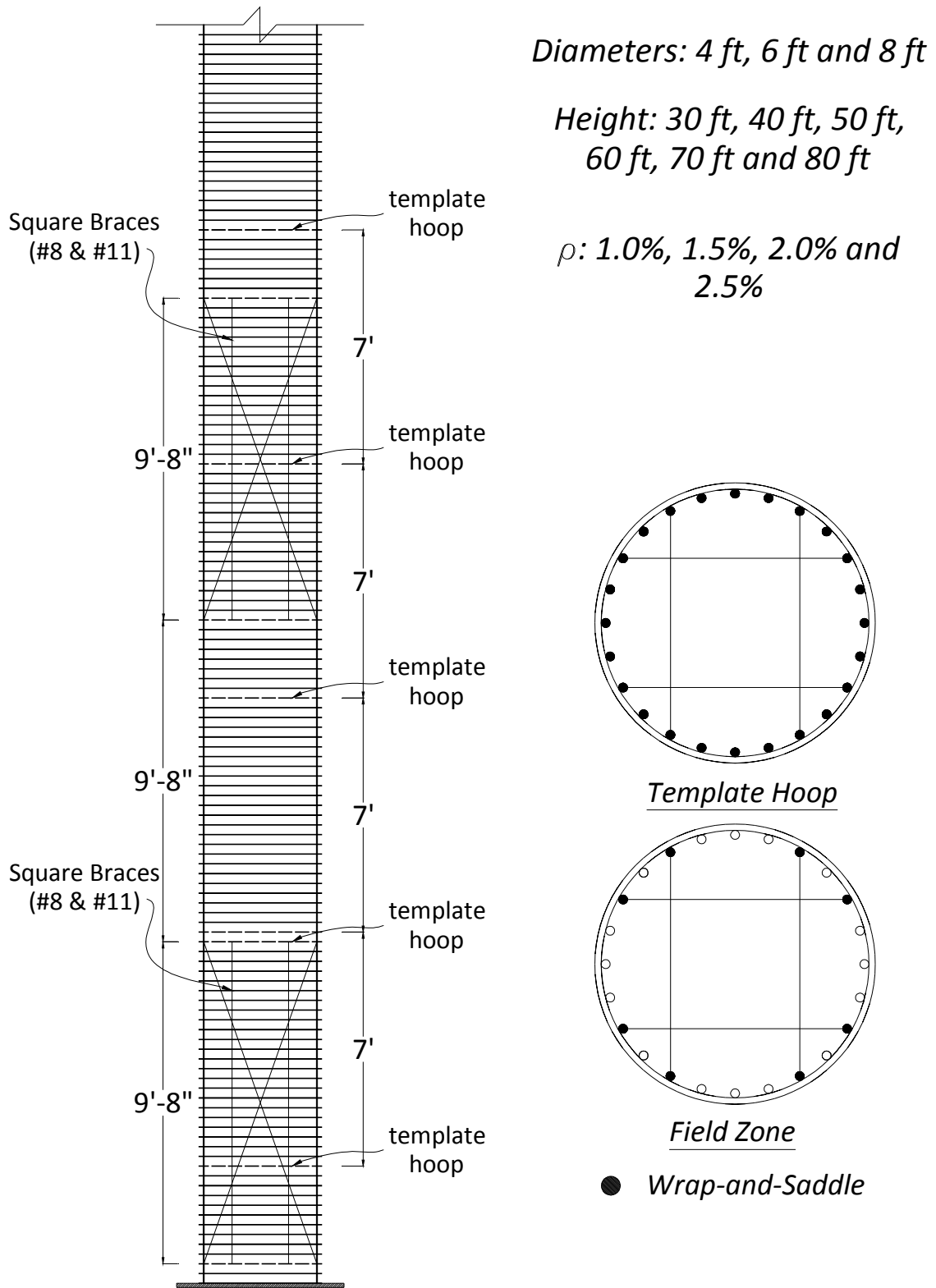
Figure 4.62: Typical Layout of Bridge Column Rebar Cage model in Parametric Analysis
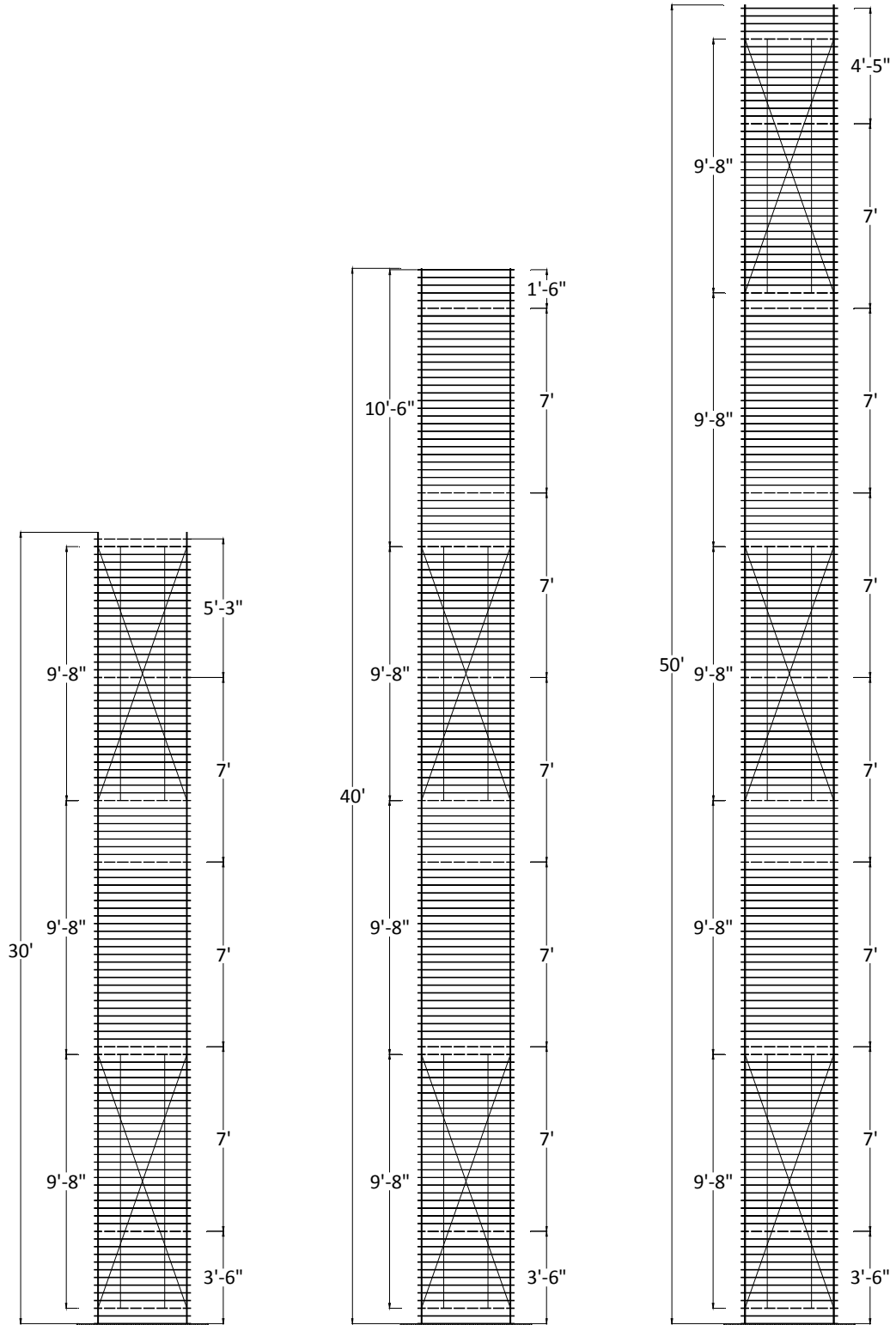
Figure 4.63: Template hoops and braces spacing for Bridge Column Rebar cages with Height equal to: (Left) 30-ft, (Middle) 40-ft and (Left) 50-ft
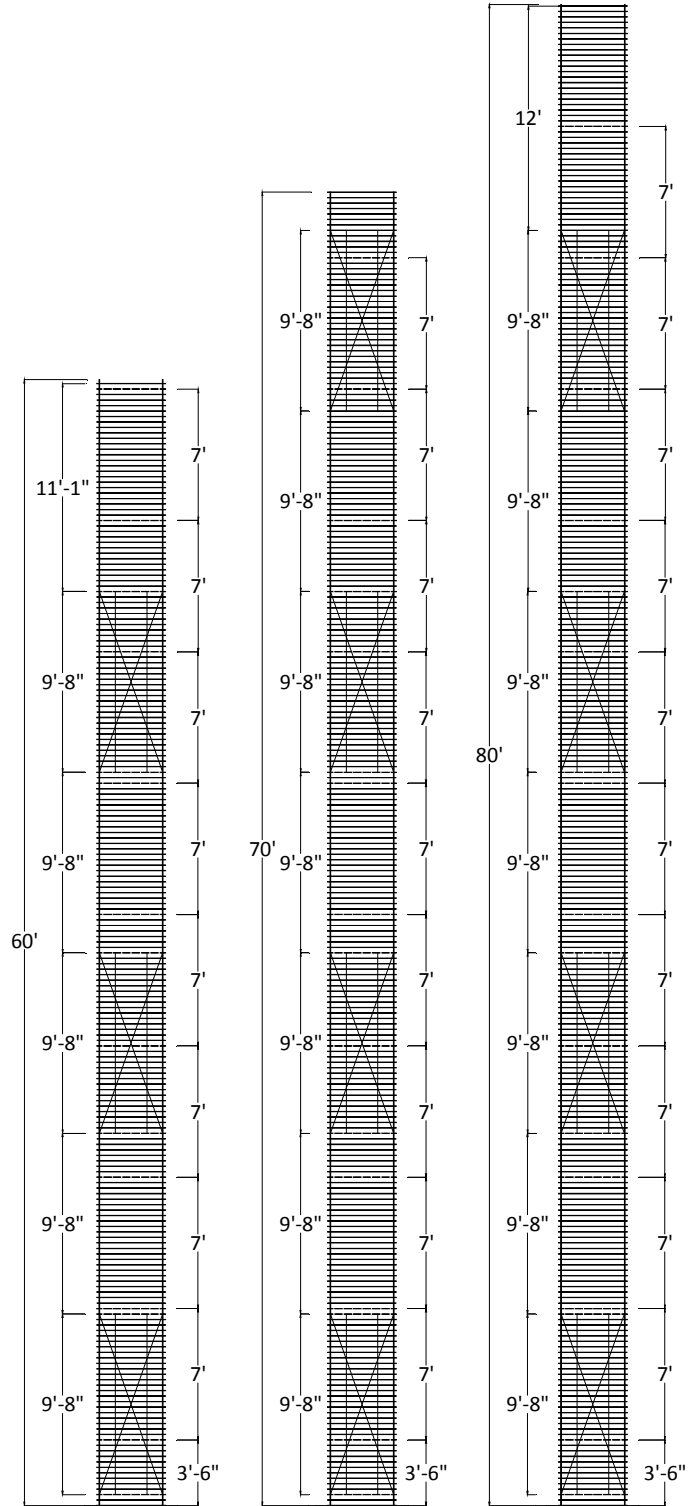
Figure 4.64: Template hoops and braces spacing for Bridge Column Rebar cages with Height equal to: (Left) 60-ft, (Middle) 70-ft and (Left) 80-ft

187
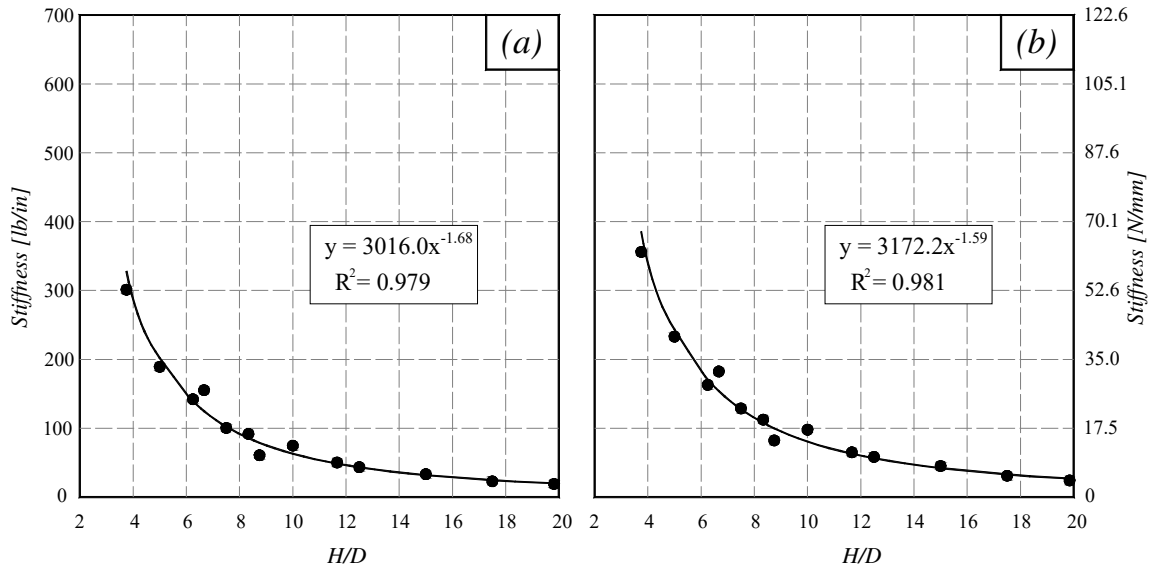
Figure 4.65: Results of Parametric Analysis with #8 brace bars: (a) ρ = 1.0%, and (b) ρ = 1.5%
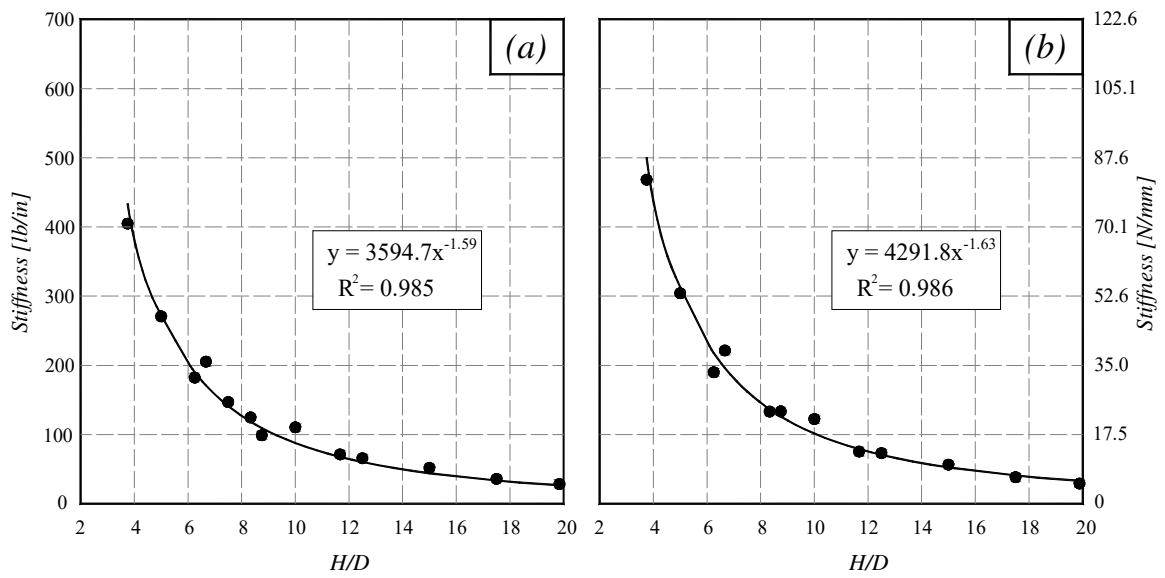
Figure 4.66: Results of Parametric Analysis with #8 brace bars: (a) ρ = 2.0%, and (b) ρ = 2.5%
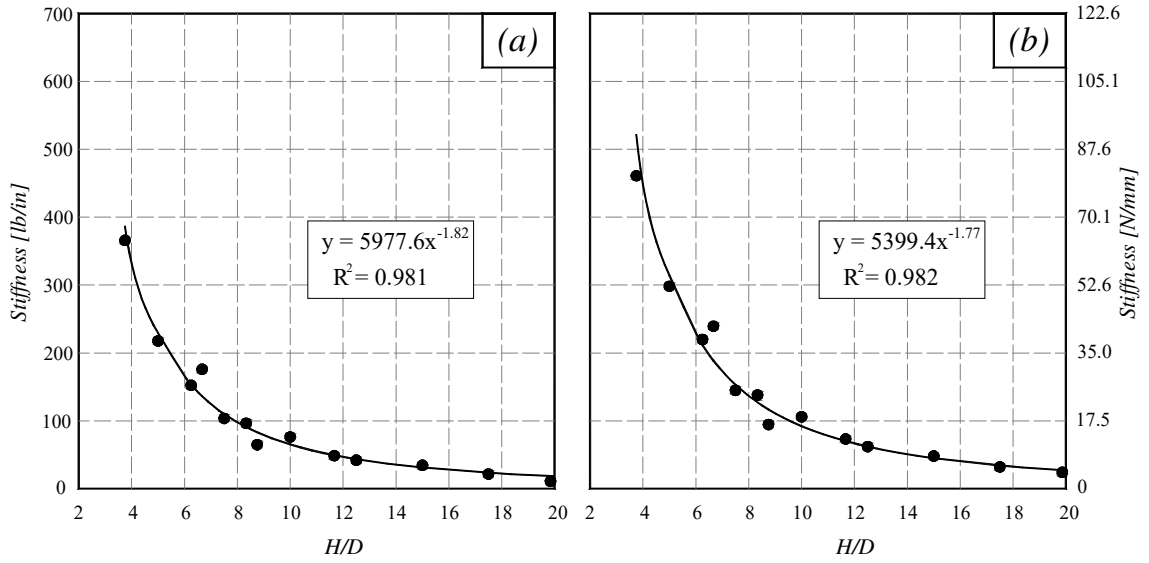
Figure 4.67: Results of Parametric Analysis with #11 brace bars: (a) ρ = 1.0%, and (b) ρ = 1.5%
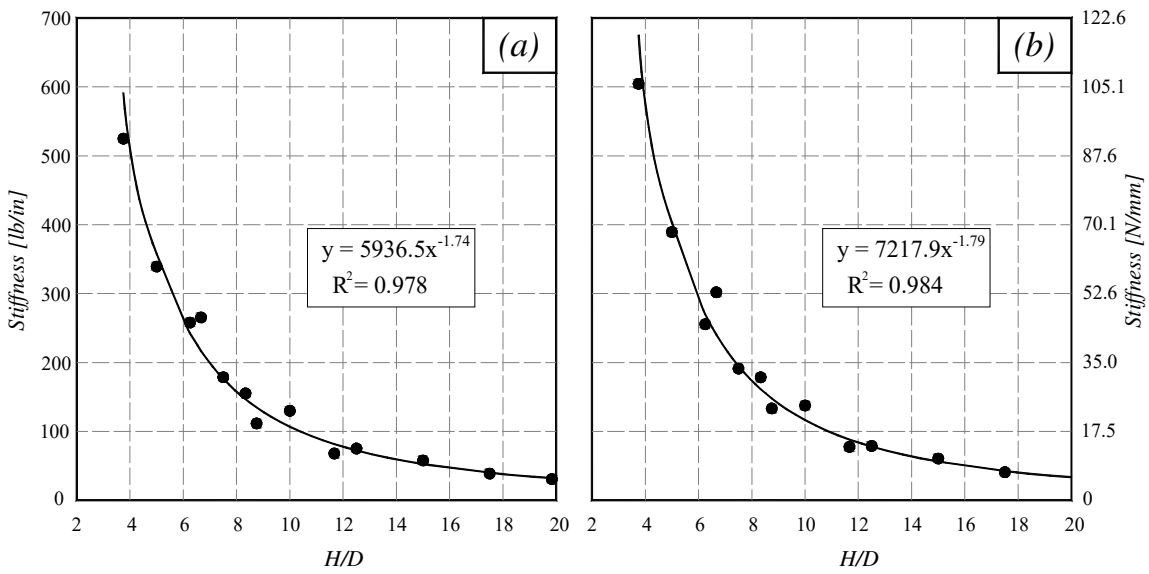
Figure 4.68: Results of Parametric Analysis with #11 brace bars: (a) ρ = 2.0%, and (b) ρ = 2.5%

189
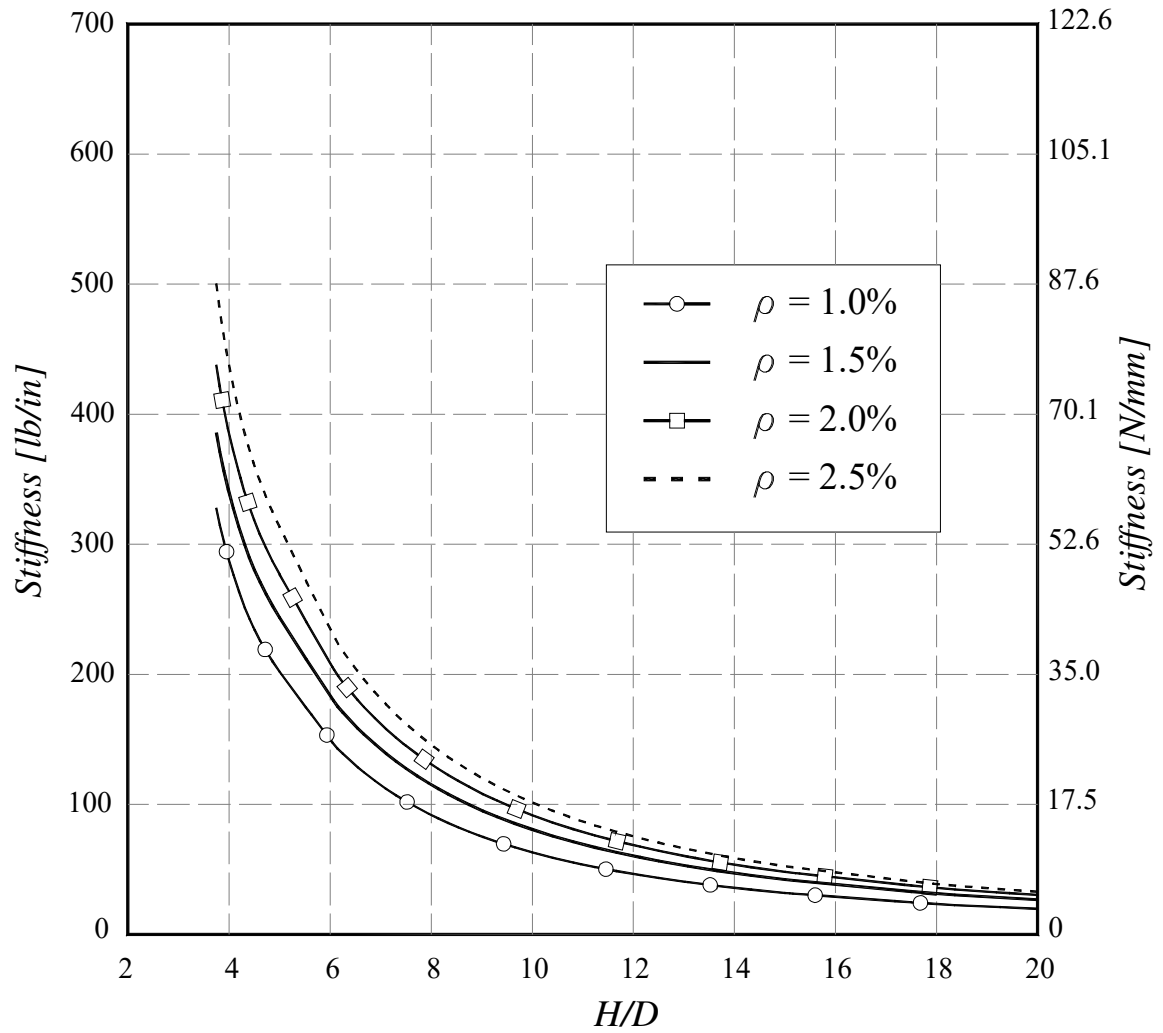
Figure 4.69: Results of Parametric Analysis with #8 brace bars
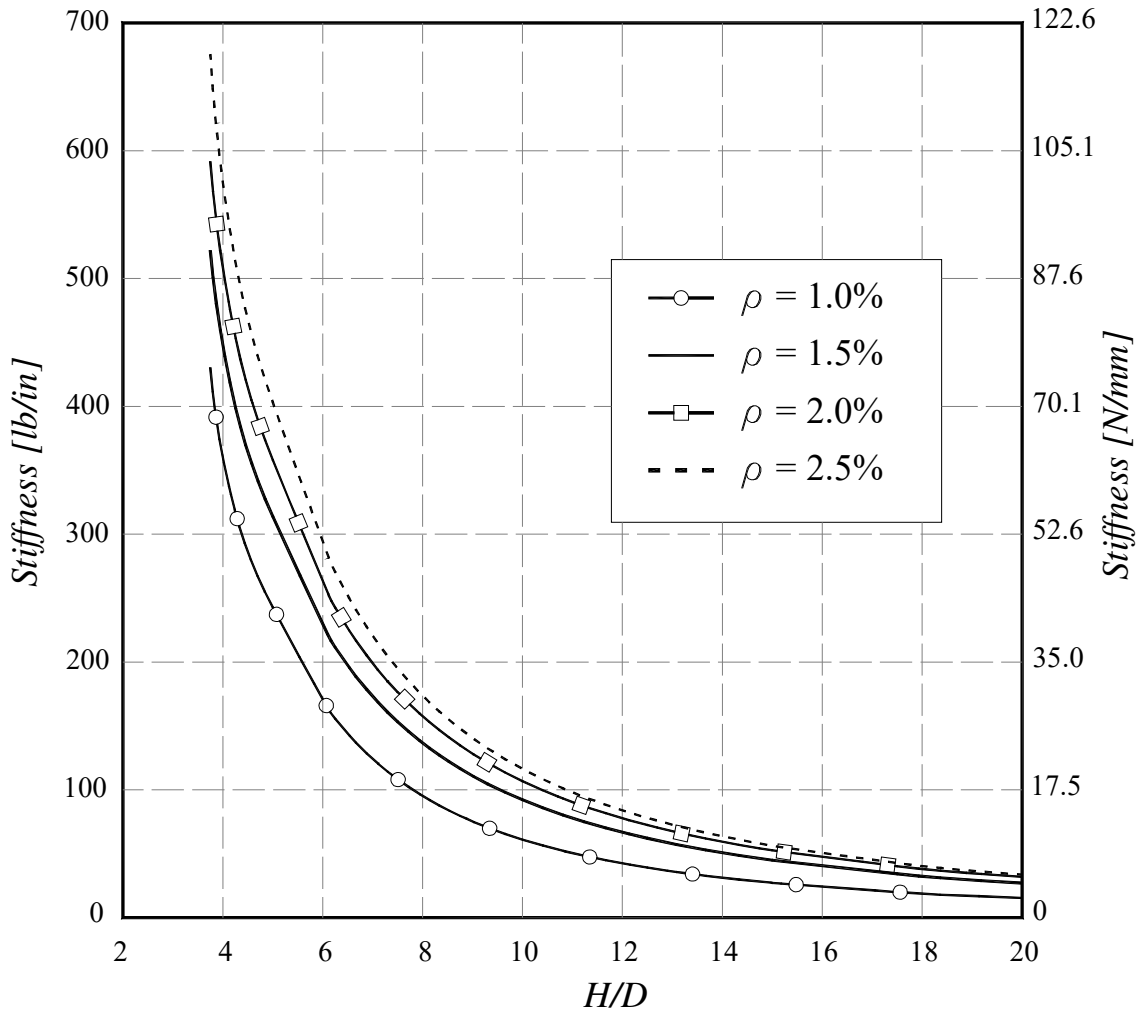
Figure 4.70: Results of Parametric Analysis with #11 brace bars
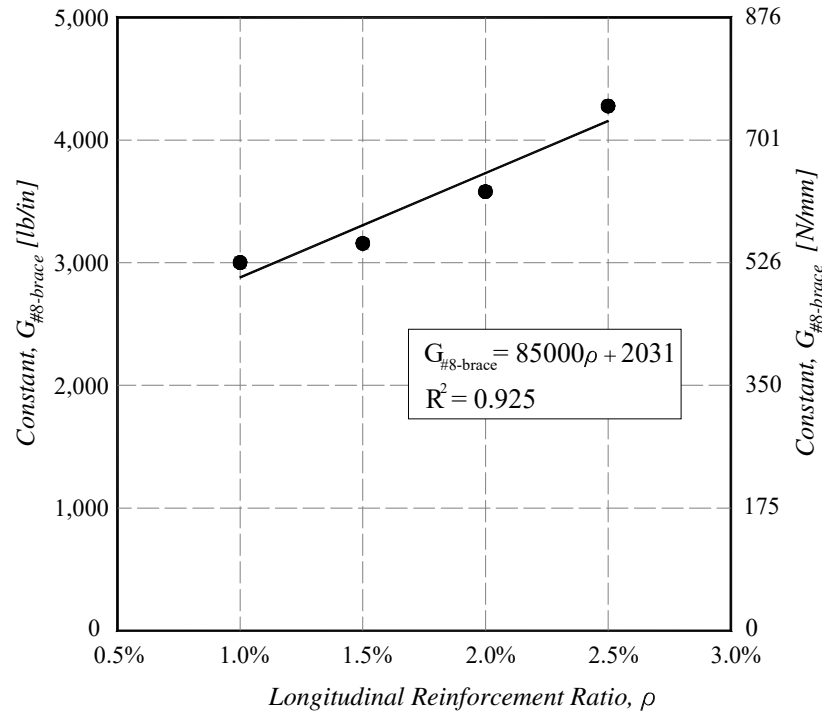
Figure 4.71: Linear Trend line for Constant G_{#8-brace} in the Elastic Stiffness vs. Height-Diameter ratio relationship
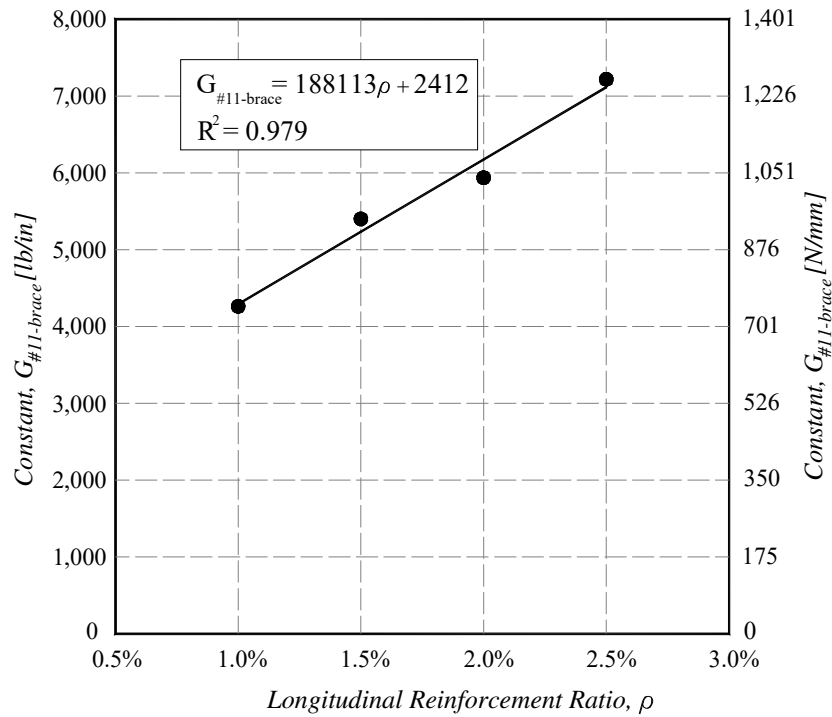
Figure 4.72: Linear Trend line for Constant G_{#11-brace} in the Elastic Stiffness vs. Height-Diameter
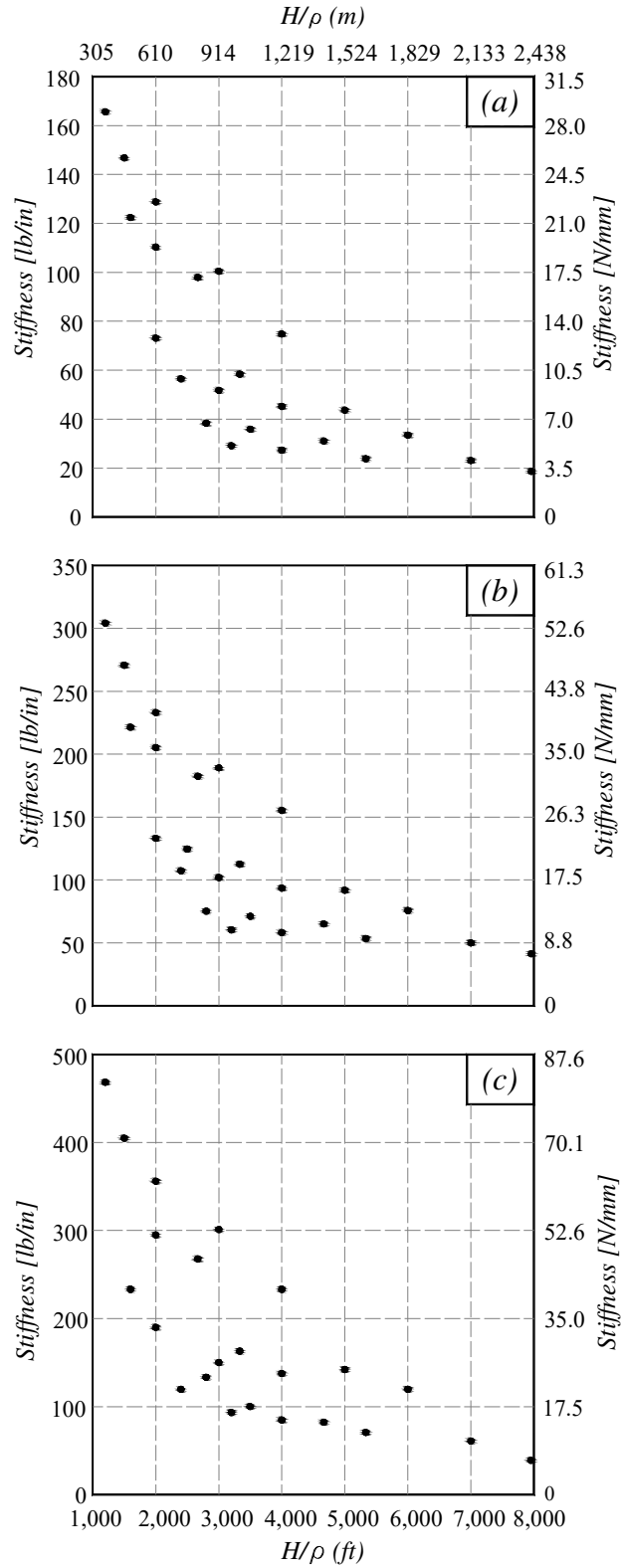
Figure 4.73: Results of Parametric Analysis with #8 brace bars: (a) Diameter = 4-ft, (b) Diameter = 6-ft, and (c) Diameter = 8-ft
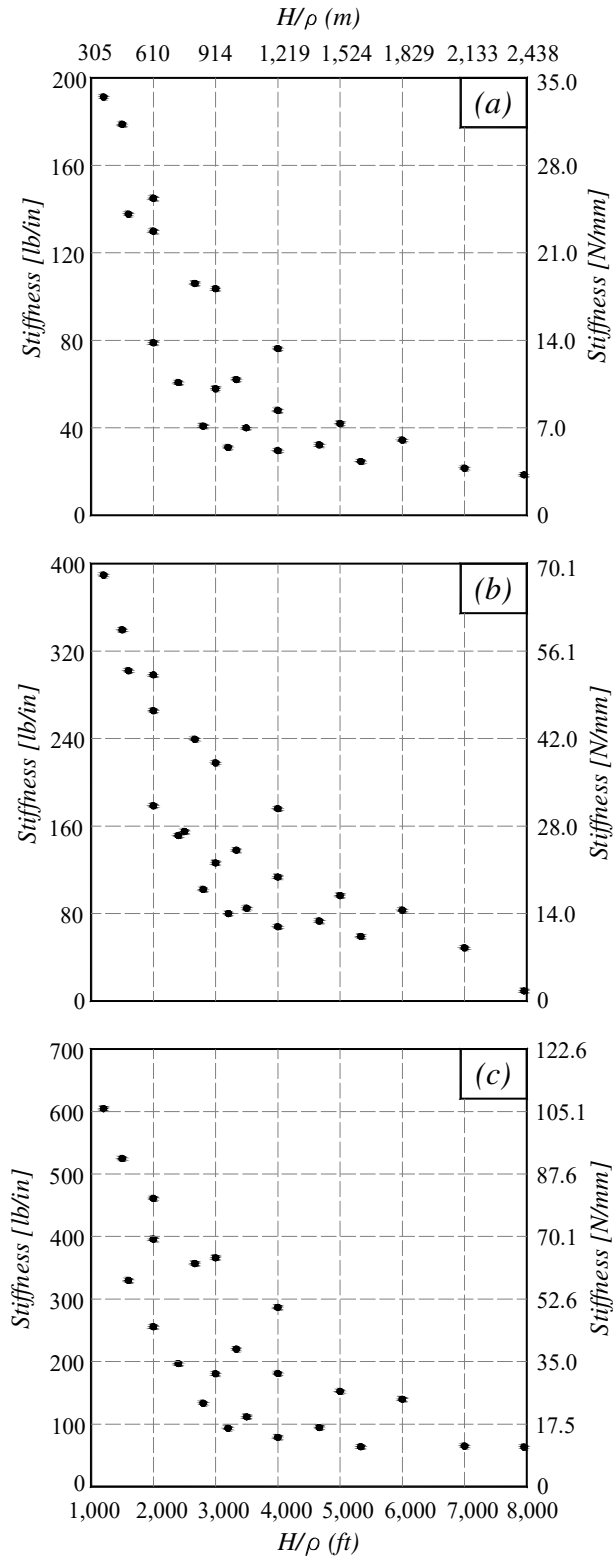
Figure 4.74: Results of Parametric Analysis with #11 brace bars: (a) Diameter = 4-ft, (b) Diameter = 6-ft, and (c) Diameter = 8-ft
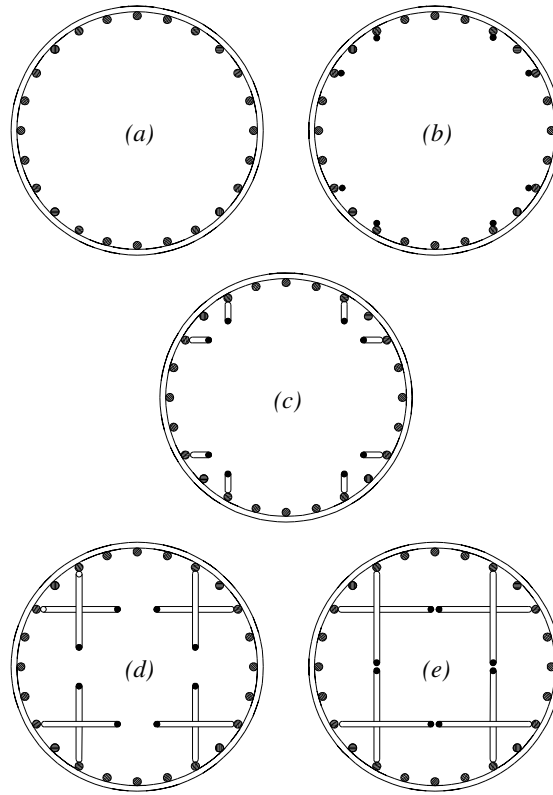
Figure 4.75: Sections along the Height of the R/C Bridge Column
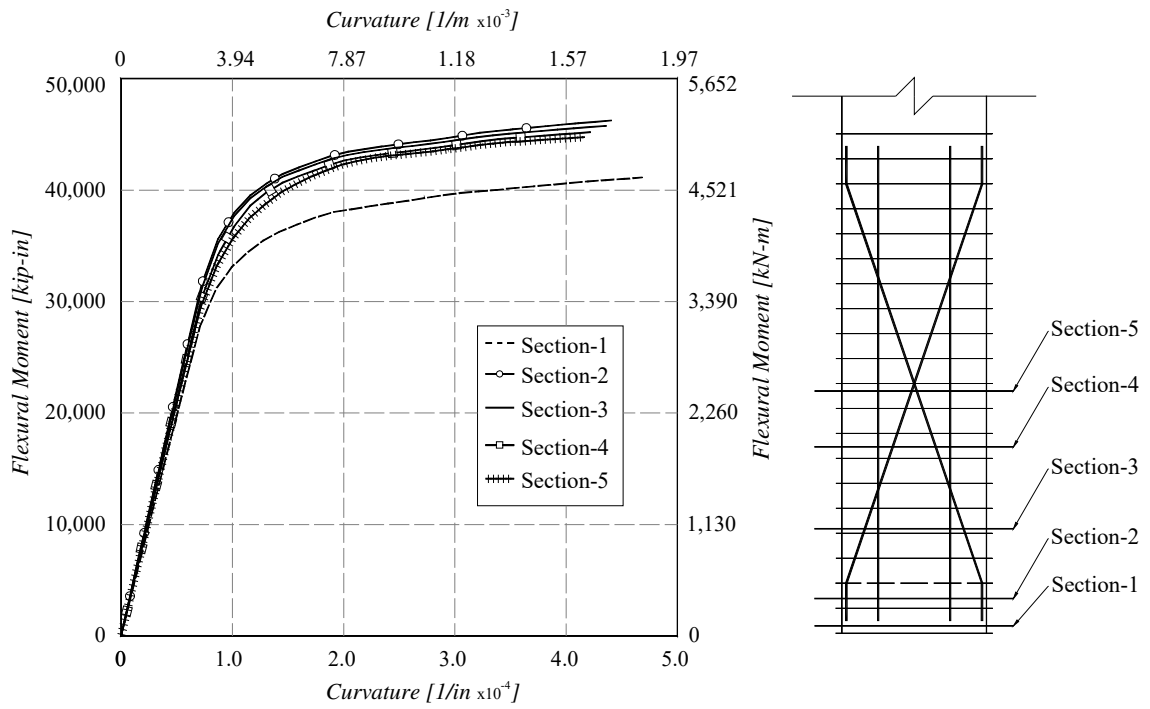
Figure 4.76: Section Analyses at various Locations

195

Appendix I

This Appendix shows the Material Testing Reports for the reinforcing bars used in the full-scale rebar cage experiments.

Figure AI.1: Material Testing Report (MTR) for #8 reinforcing Bars

Figure A1.2: Material Testing Report (MTR) for #11 reinforcing Bars

TAMCO ⊕

Post Office Box 325
Rancho Cucamonga, California 91739
(909) 899-0680

Shipper
No. 213942

#11-60
A706

Sold To: PAC COAST STEEL - NAPA
7155 MISSION GORGE

SAN DIEGO CA   92120 CA

Ship To: PCS - NAPA (BAY AREA)
1060 KAISER ROAD
NAPA

Custr No.	Customer Order No.	F.O.B. Point	Our Order No	Ship Date	Routing	Frieght	Carrier	BL No.
17001	41291	MILL	515904	4/08/10	RC #80	WLC		117355

Commodity Code	Length	Description	Pounds	Units Shipped	Bdls	Tons Shipped
216447	60.00	#11/36 A706/A706M 06a Heat# 91009 Bndl#/Units: 20/ 20, 21/ 20, 22/ 20, 23/ 20, 24/ 20, 25/ 20, 31/ 20, 32/ 20	51008	160	8	25.504

deformations diagonal
5/8" o.c.

PCS-NAPA
RECEIVED
APR 12 2010
BY

Received By: _____

Heat No.	C	Mn	P	S	Si	Cr	Ni	Cu	Mo	V	CE	Yield psi	Yield MSa	Tensile psi	Tensile MSa	EL	BD	
91009	.26	1.02	.018	.032	.36	.25	.16	.42	.04	.029	.47	73,500	507	99,500	686	18	OK	

We hereby certify that all of the manufacturing processes of TAMCO products, including melting of the scrap, occurred in the United States of America. The steel has been sampled, tested and measured in accordance with the applicable ASTM specifications for Chemical Composition, Tensile Requirements, Bending Requirements, Foot Weight and Deformation. These goods were produced in compliance with all applicable requirements of Sections 6, 7, and 12 of the Fair Labor Standards Act.

Appendix II

This Appendix shows the results from the parametric analysis performed in bridge column rebar cages.
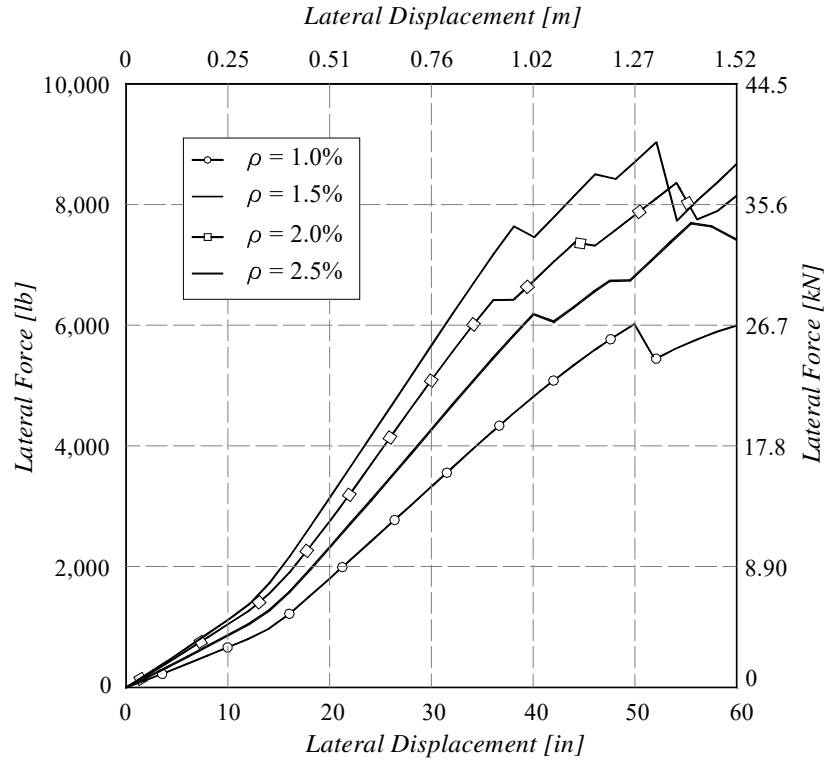
Figure AII.1: Response of Rebar Cage Models with #8 Braces, Height = 30-ft and Diameter = 4-ft
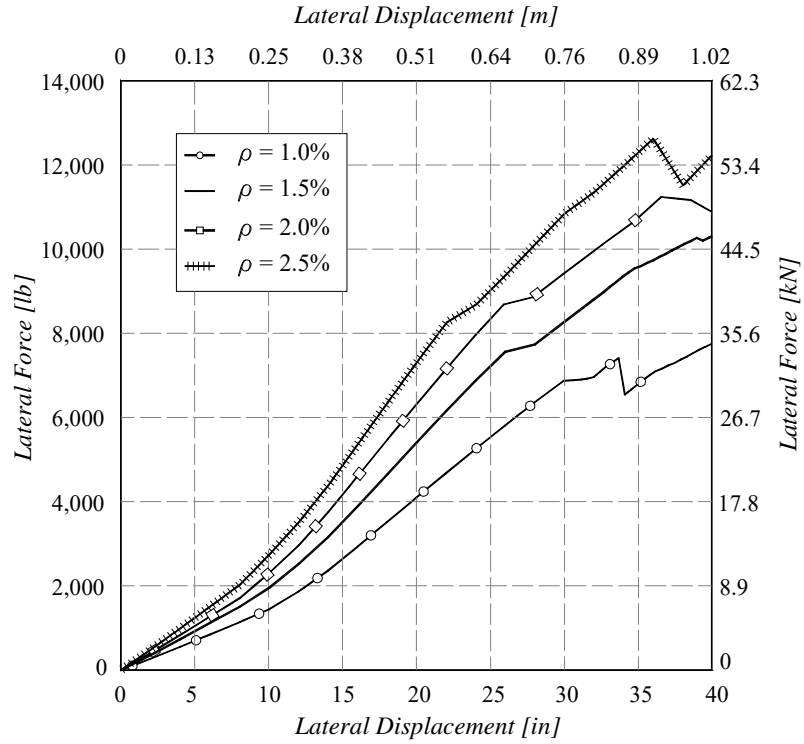
Figure AII.2: Response of Rebar Cage Models with #8 Braces, Height = 30-ft and Diameter = 6-ft
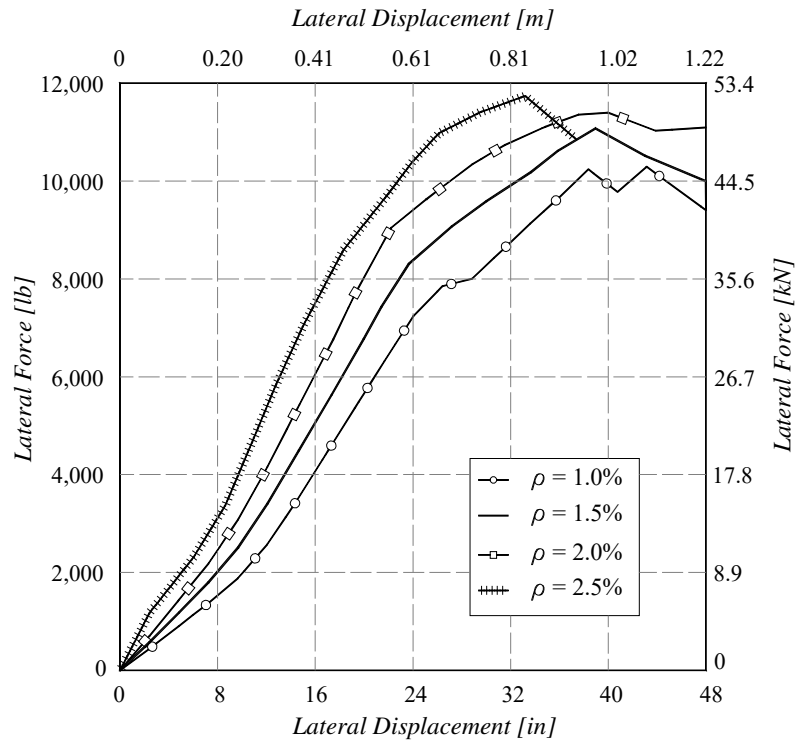
Figure AII.3: Response of Rebar Cage Models with #8 Braces, Height = 30-ft and Diameter = 8-ft
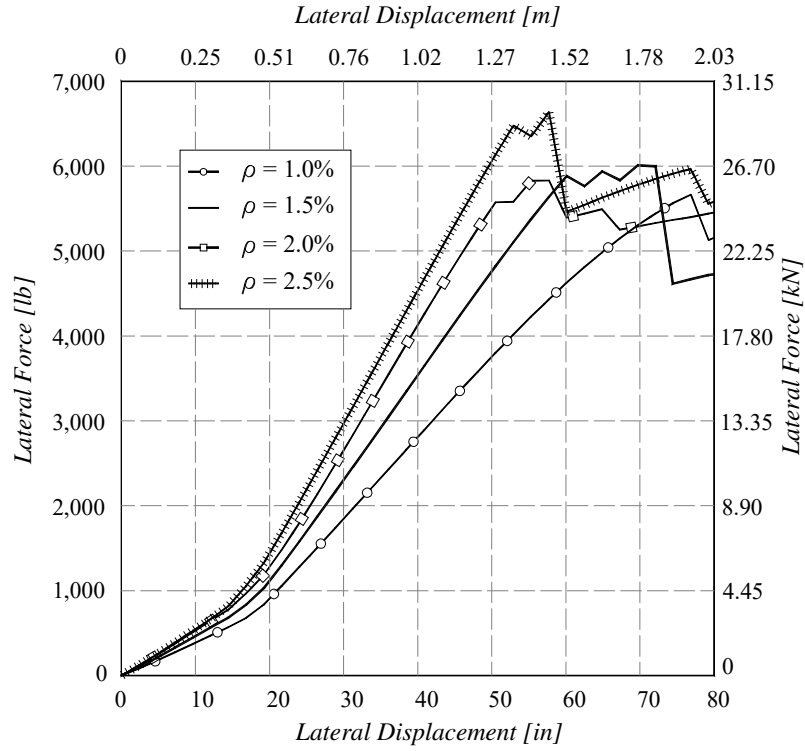
Figure AII.4: Response of Rebar Cage Models with #8 Braces, Height = 40-ft and Diameter = 4-ft
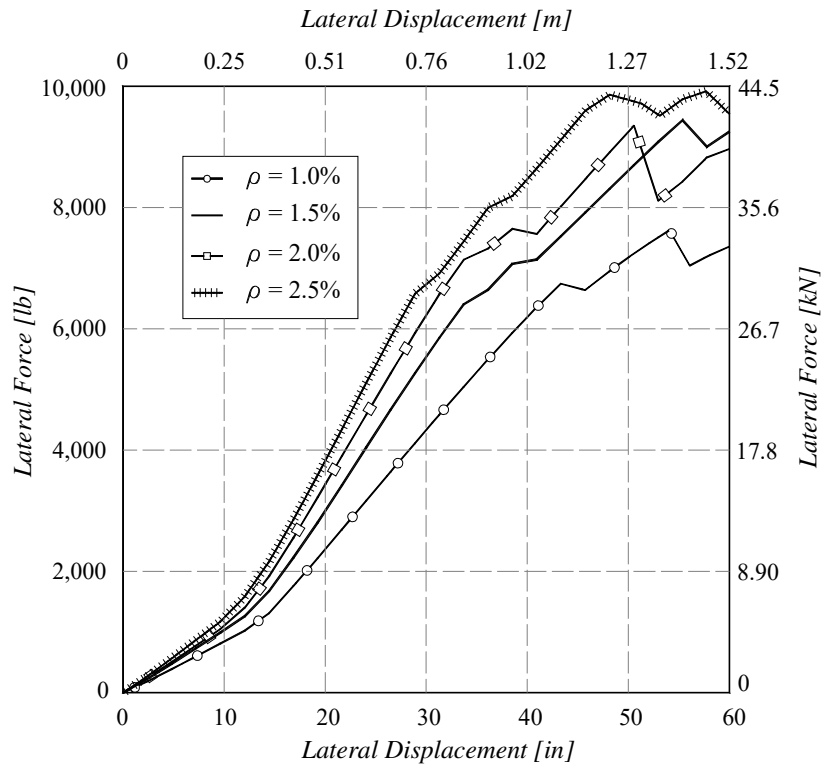
Figure AII.5: Response of Rebar Cage Models with #8 Braces, Height = 40-ft and Diameter = 6-ft

202
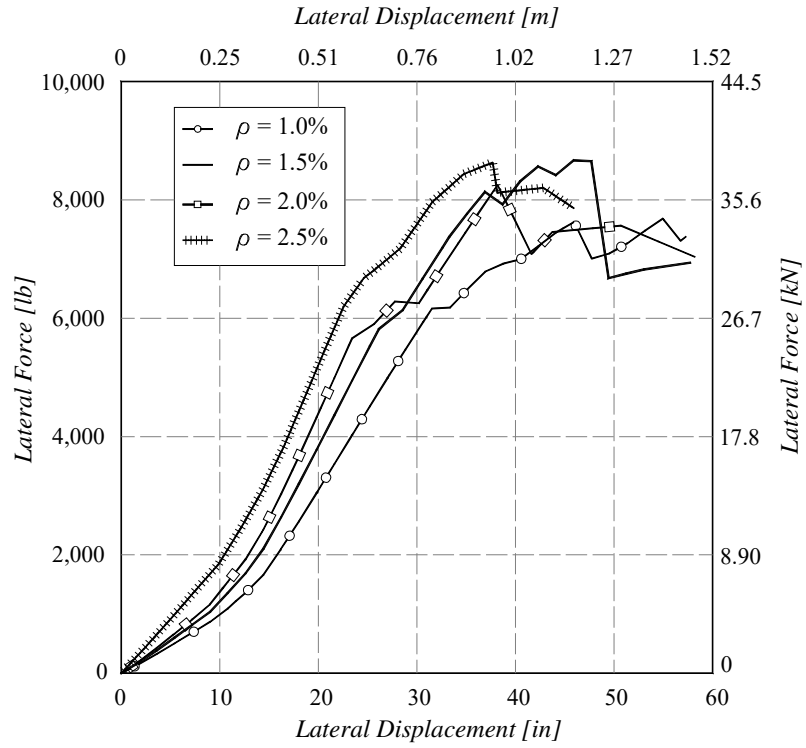
Figure AII.6: Response of Rebar Cage Models with #8 Braces, Height = 40-ft and Diameter = 8-ft
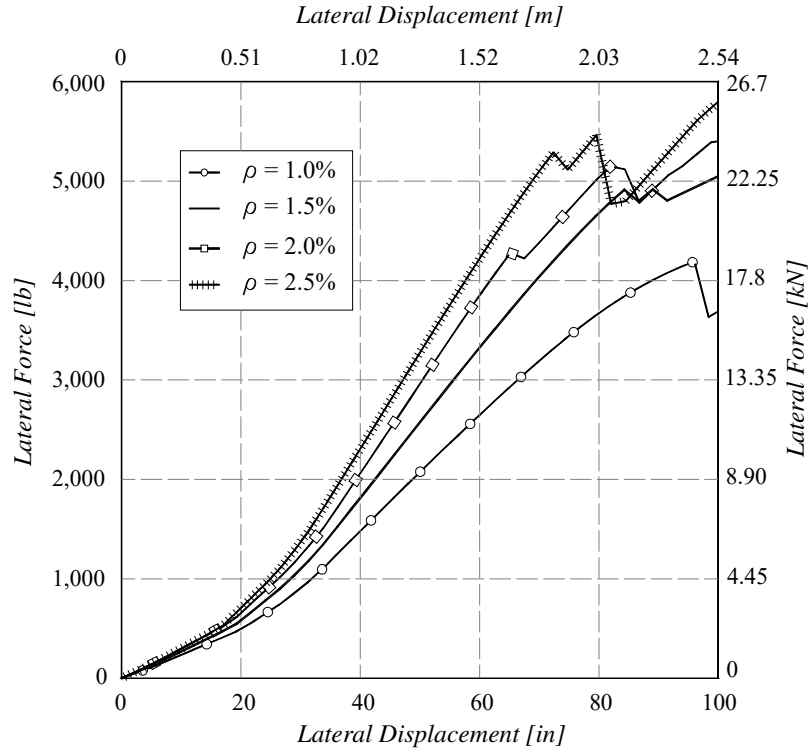
Figure AII.7: Response of Rebar Cage Models with #8 Braces, Height = 50-ft and Diameter = 4-ft
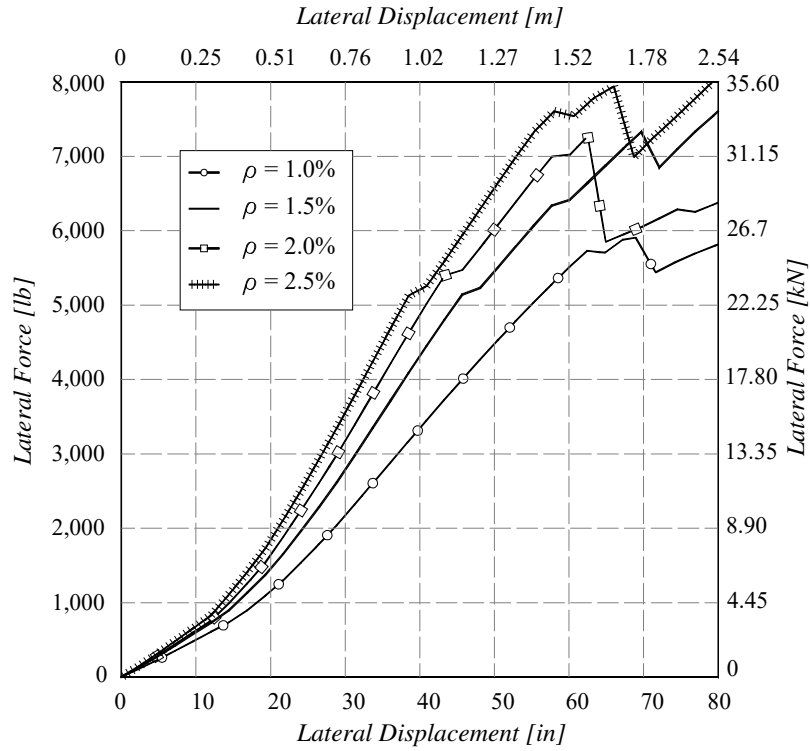
Figure AII.8: Response of Rebar Cage Models with #8 Braces, Height = 50-ft and Diameter = 6-ft
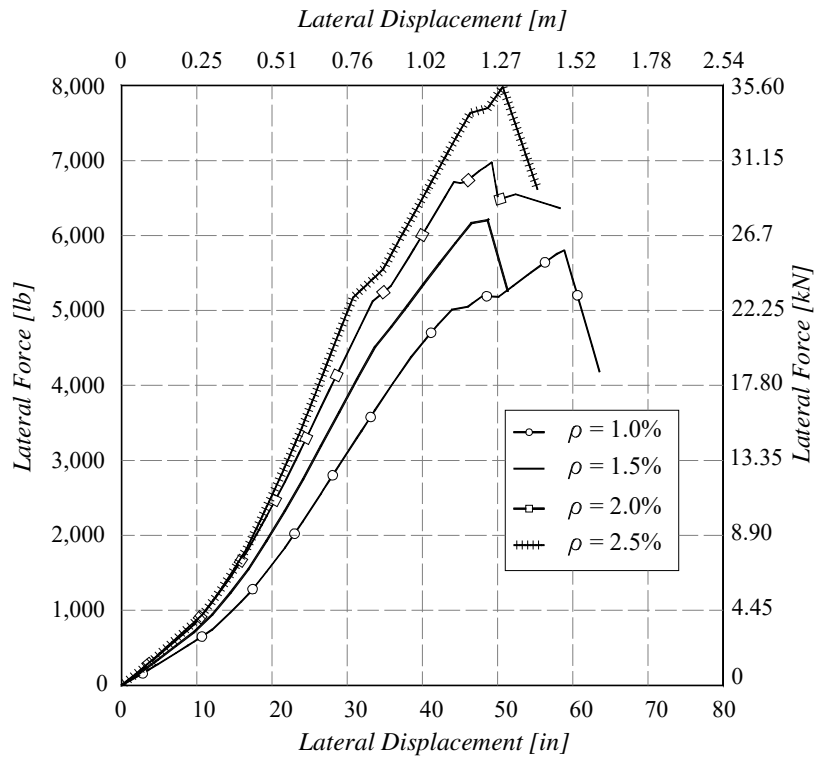
Figure AII.9: Response of Rebar Cage Models with #8 Braces, Height = 50-ft and Diameter = 8-ft

204
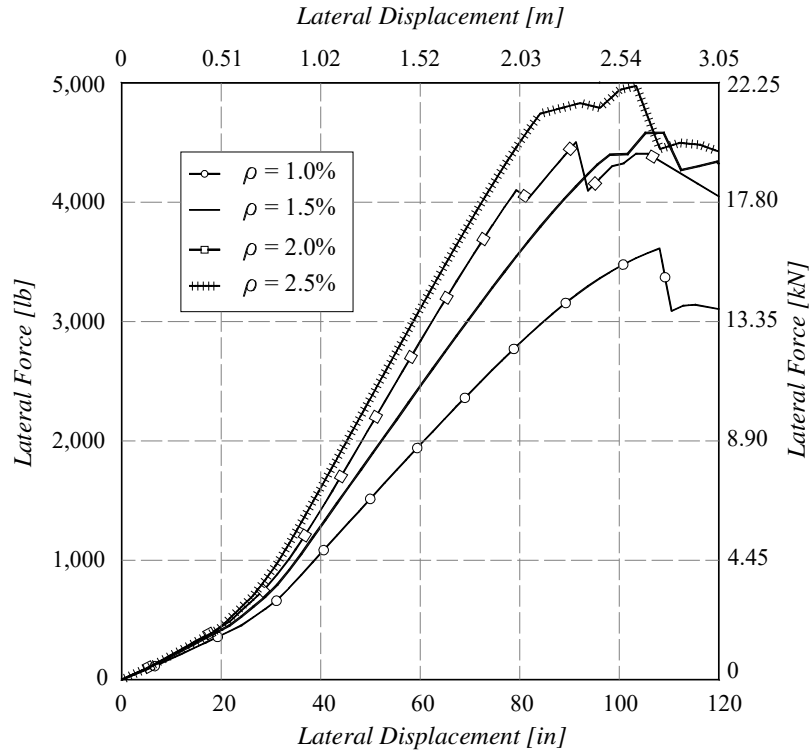
Figure AII.10: Response of Rebar Cage Models with #8 Braces, Height = 60-ft and Diameter = 4-ft
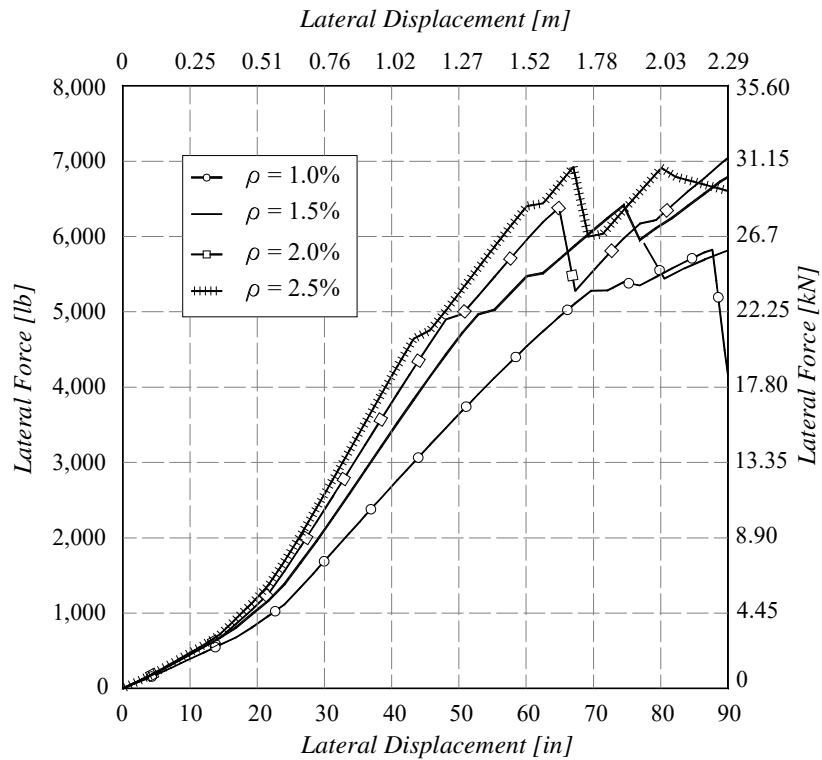
Figure AII.11: Response of Rebar Cage Models with #8 Braces, Height = 60-ft and Diameter = 6-ft
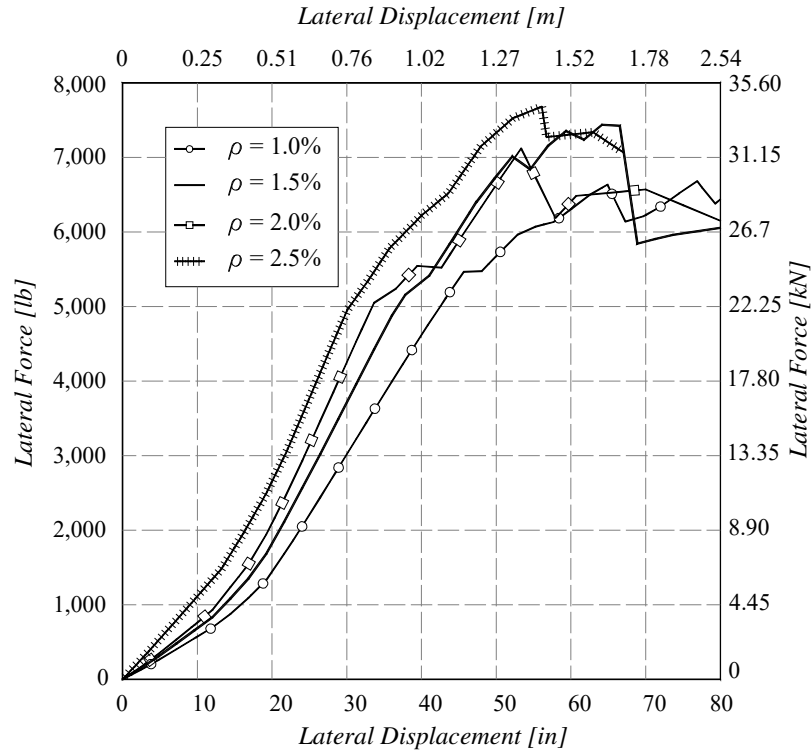
Figure AII.12: Response of Rebar Cage Models with #8 Braces, Height = 60-ft and Diameter = 8-ft
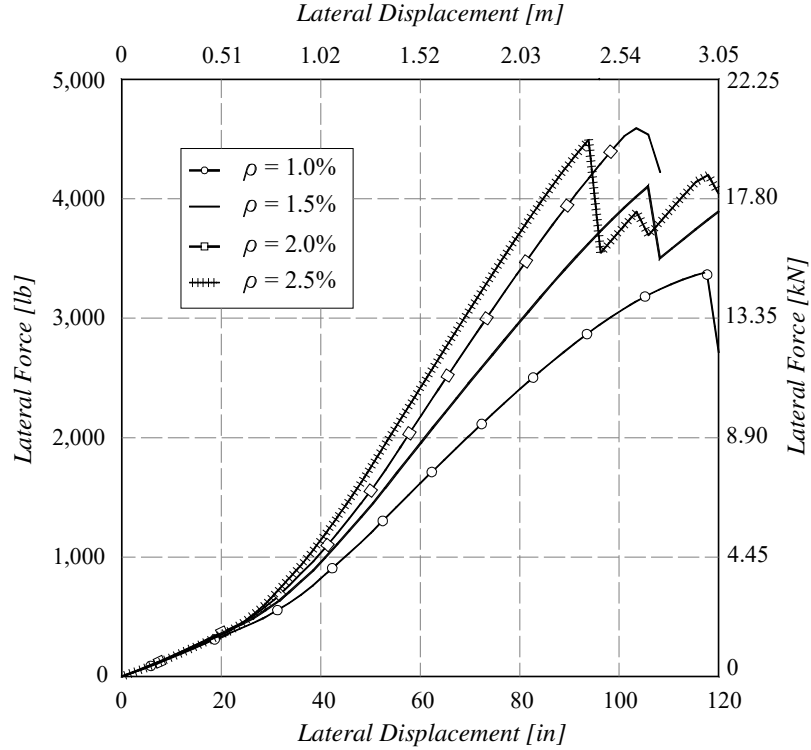
Figure AII.13: Response of Rebar Cage Models with #8 Braces, Height = 70-ft and Diameter = 4-ft
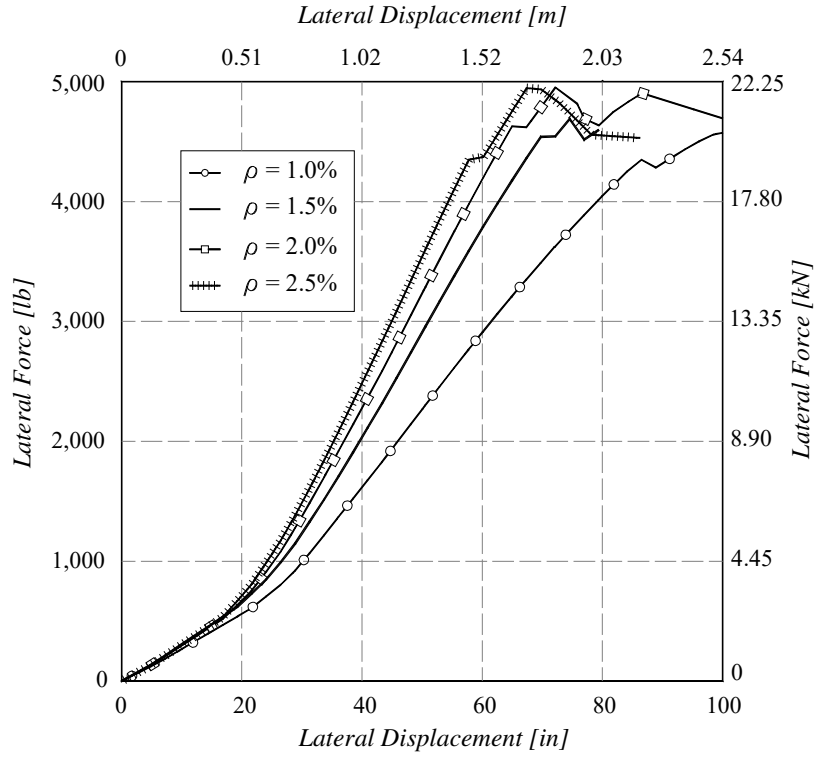
Figure AII.14: Response of Rebar Cage Models with #8 Braces, Height = 70-ft and Diameter = 6-ft
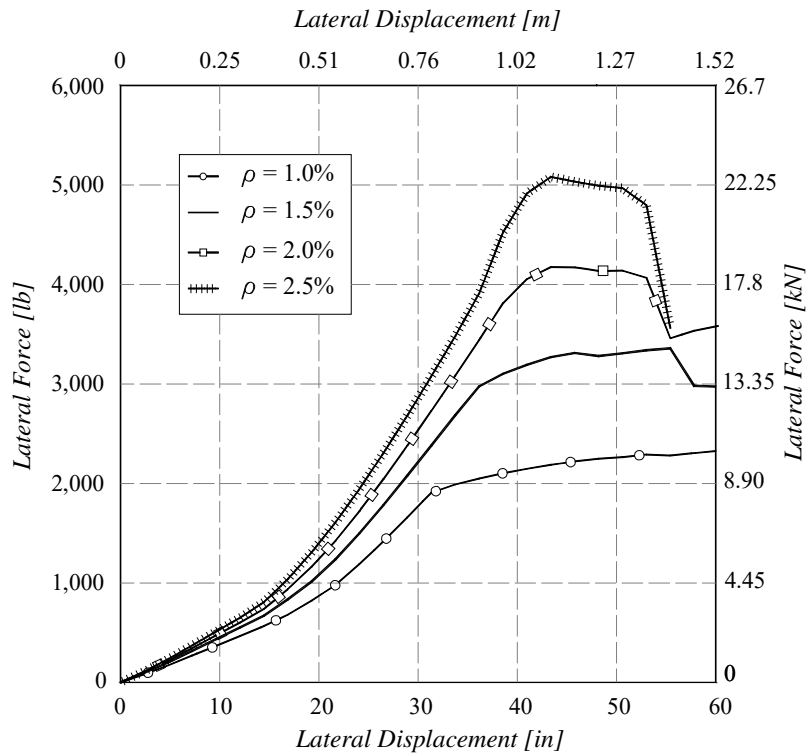
Figure AII.15: Response of Rebar Cage Models with #8 Braces, Height = 70-ft and Diameter = 8-ft
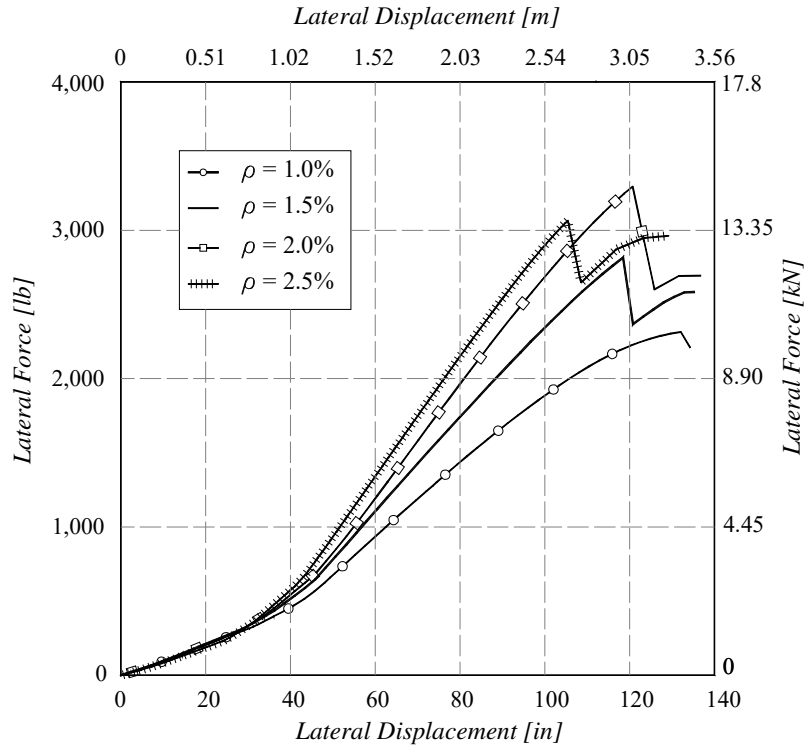
Figure AII.16: Response of Rebar Cage Models with #8 Braces, Height = 80-ft and Diameter = 4-ft
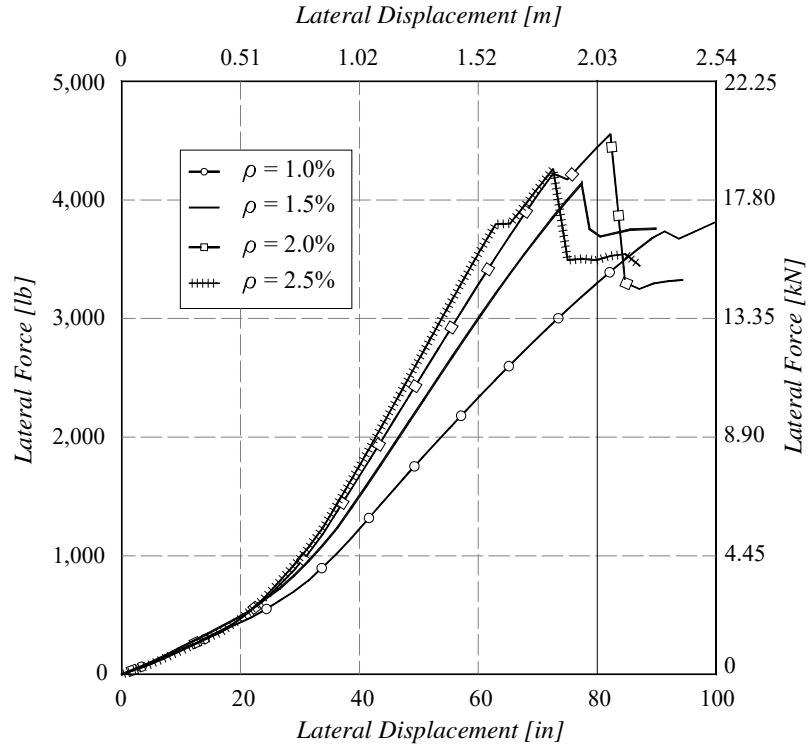
Figure AII.17: Response of Rebar Cage Models with #8 Braces, Height = 80-ft and Diameter = 6-ft
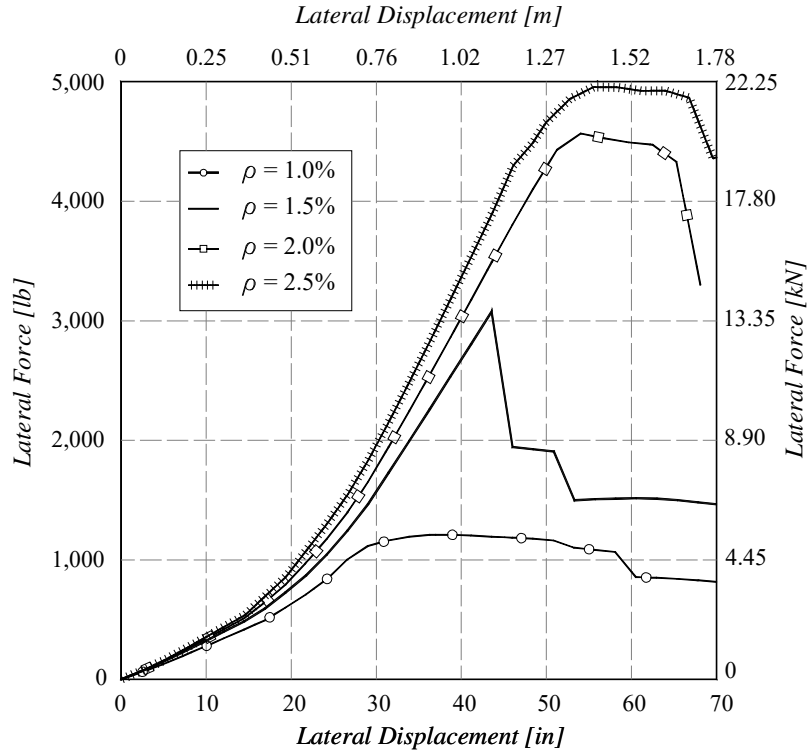
Figure AII.18: Response of Rebar Cage Models with #8 Braces, Height = 80-ft and Diameter = 8-ft
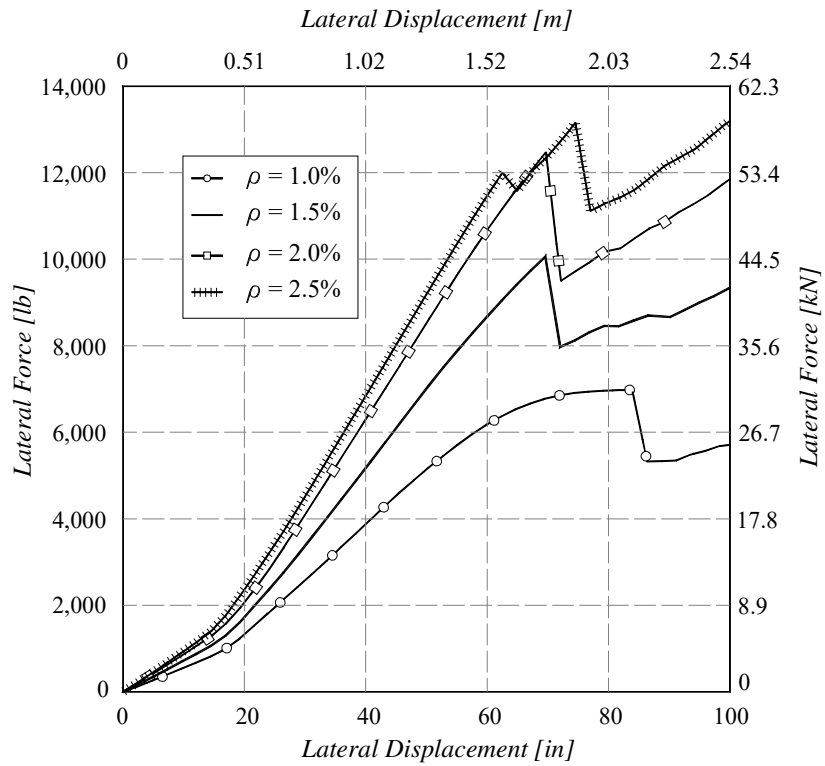
Figure AII.19: Response of Rebar Cage Models with #11 Braces, Height = 30-ft and Diameter = 4-ft

209
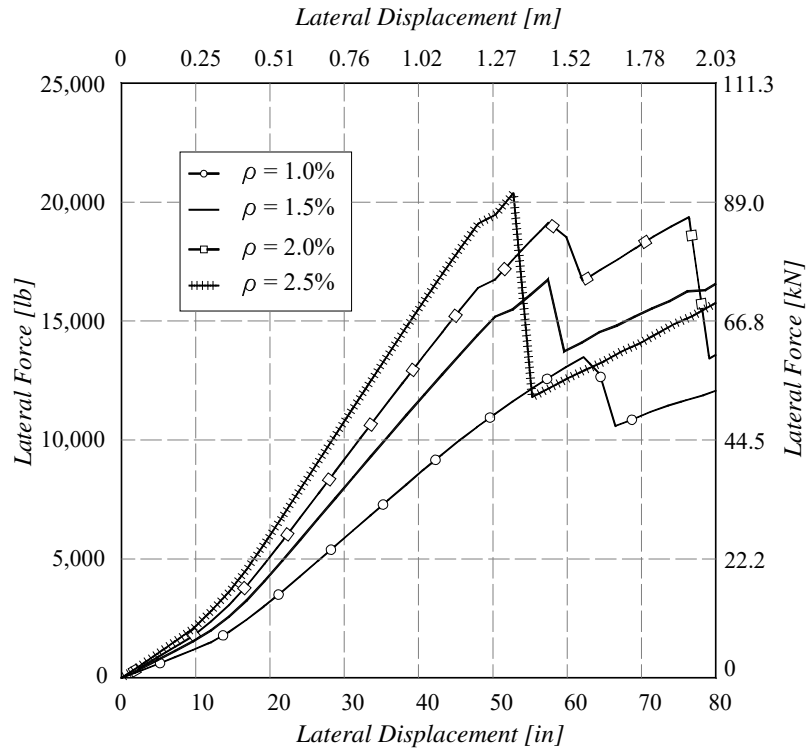
Figure AII.20: Response of Rebar Cage Models with #11 Braces, Height = 30-ft and Diameter = 6-ft
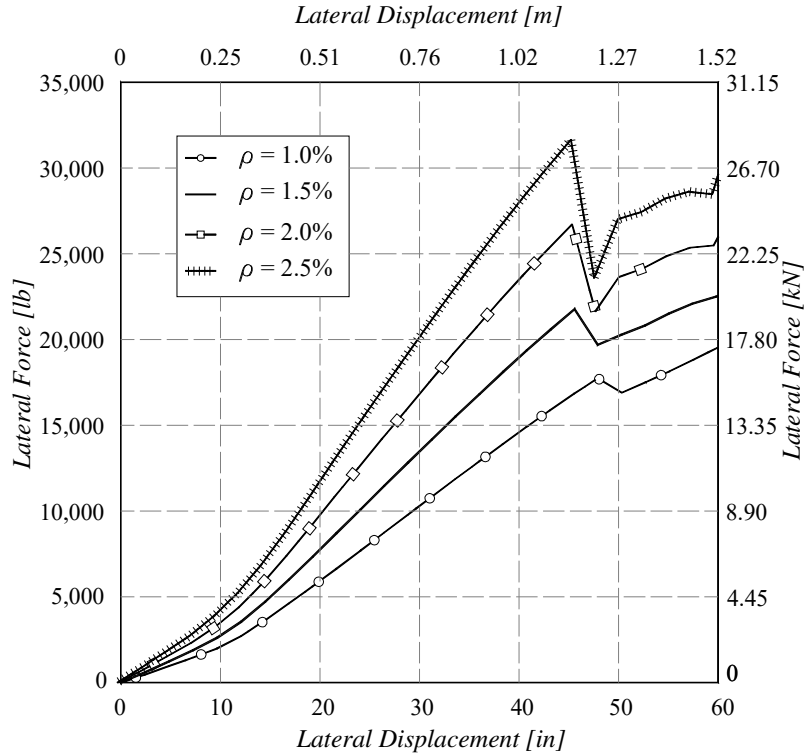
Figure AII.21: Response of Rebar Cage Models with #11 Braces, Height = 30-ft and Diameter = 8-ft

210
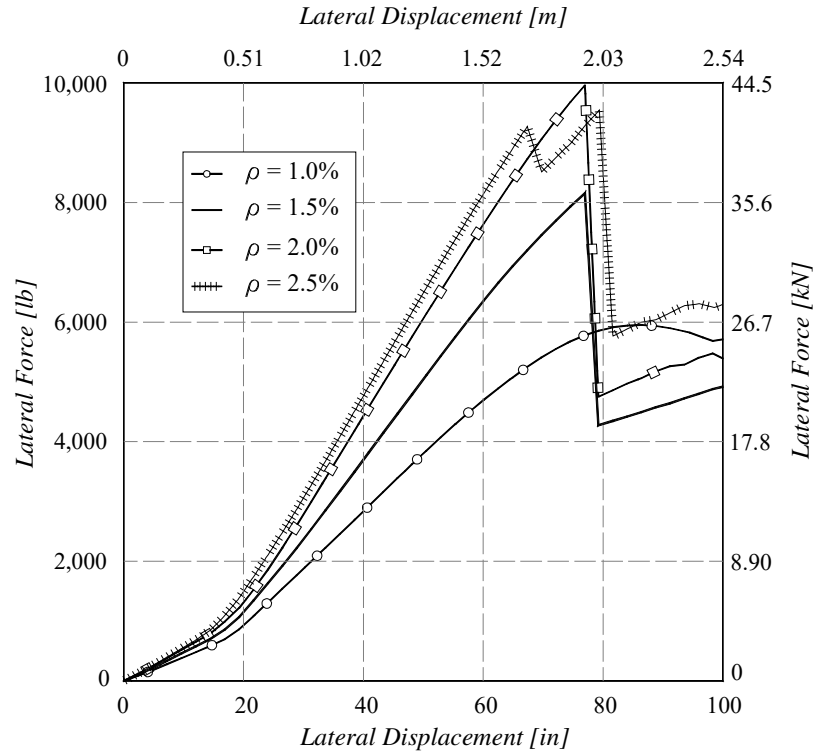
Figure AII.22: Response of Rebar Cage Models with #11 Braces, Height = 40-ft and Diameter = 4-ft
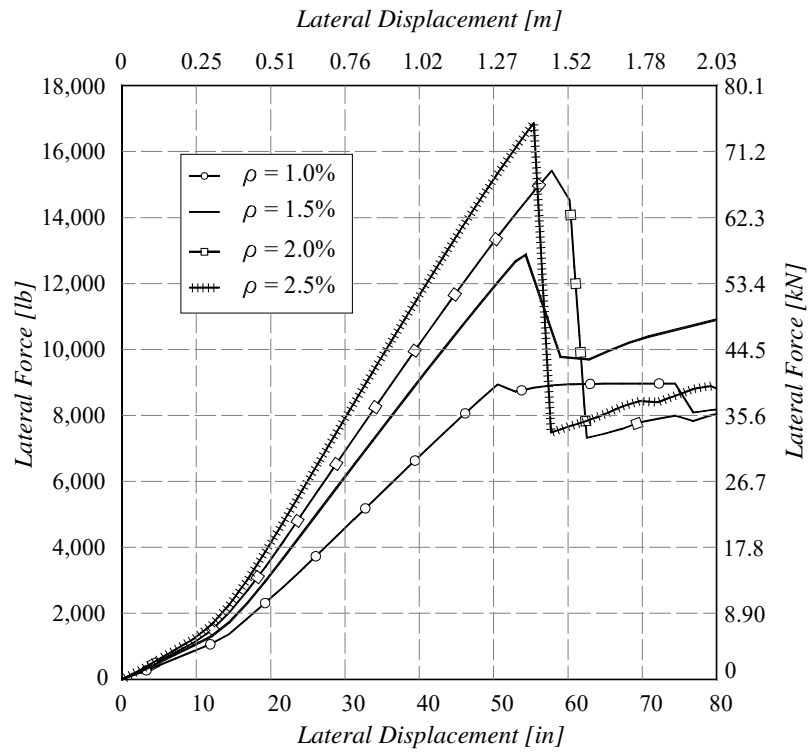
Figure AII.23: Response of Rebar Cage Models with #11 Braces, Height = 40-ft and Diameter = 6-ft

Figure AII.24: Response of Rebar Cage Models with #11 Braces, Height = 40-ft and Diameter = 8-ft
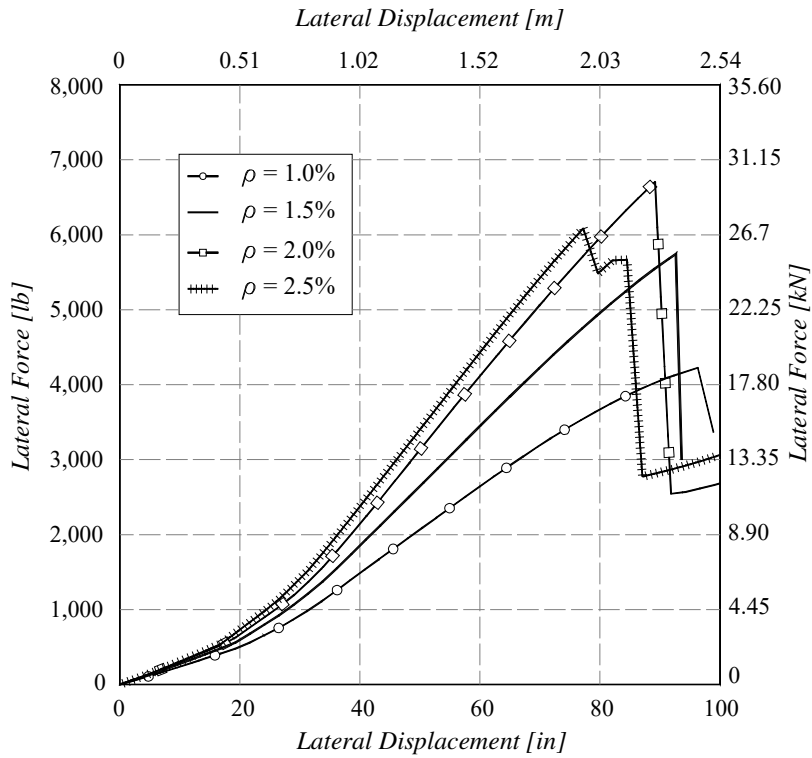
Figure AII.25: Response of Rebar Cage Models with #11 Braces, Height = 50-ft and Diameter = 4-ft
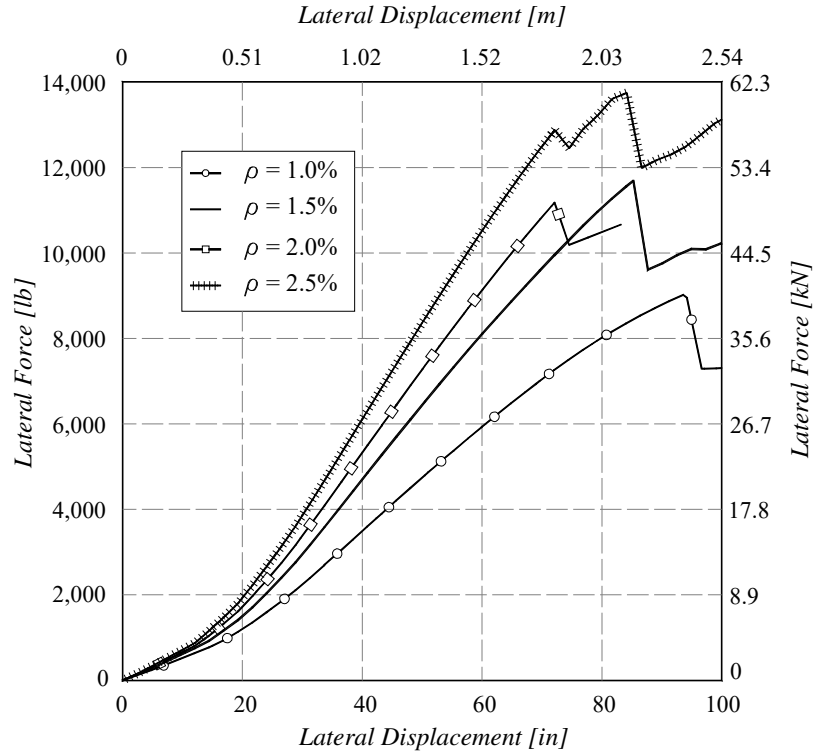
Figure AII.26: Response of Rebar Cage Models with #11 Braces, Height = 50-ft and Diameter = 6-ft
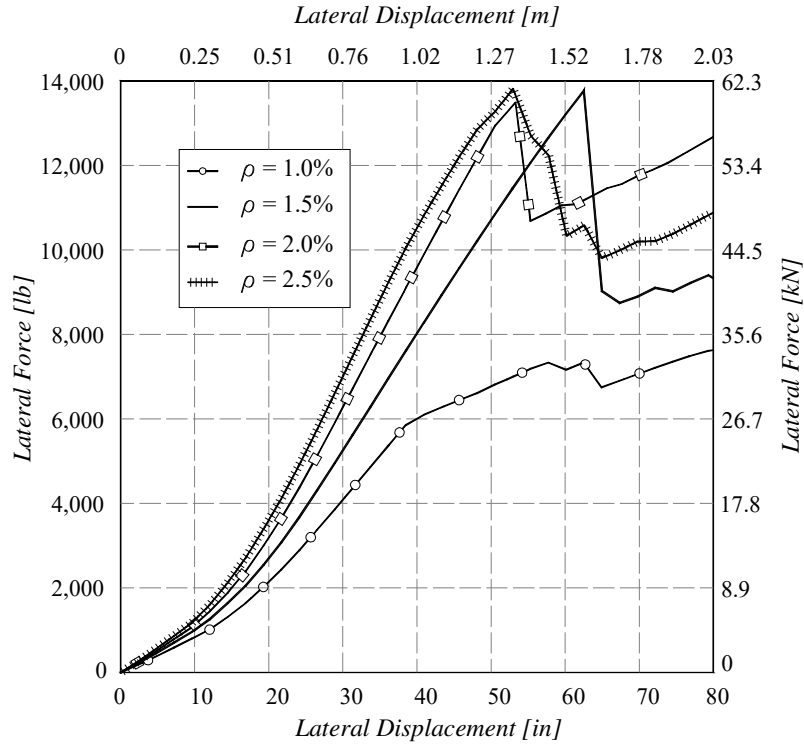
Figure AII.27: Response of Rebar Cage Models with #11 Braces, Height = 50-ft and Diameter = 8-ft

213
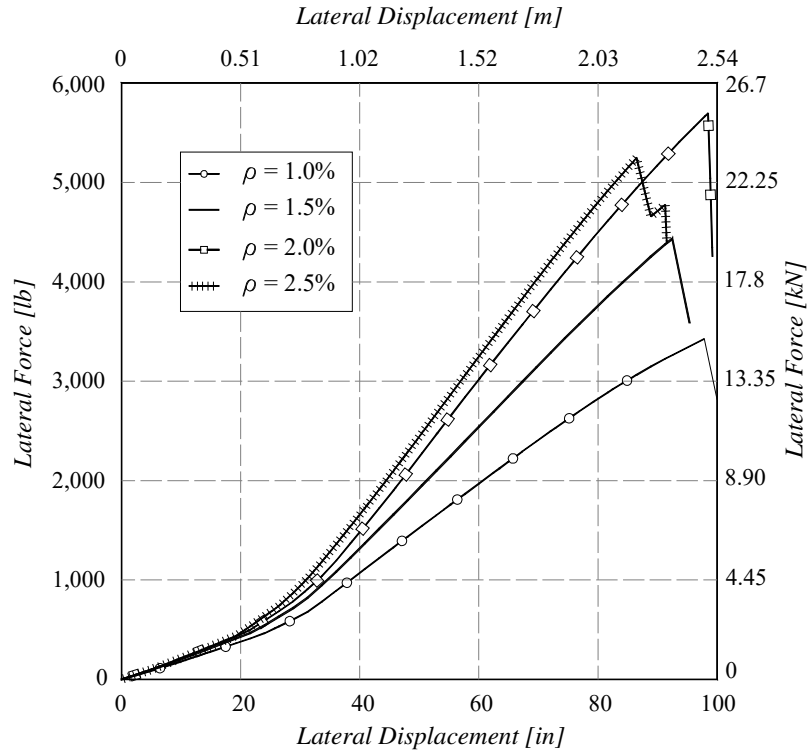
Figure AII.28: Response of Rebar Cage Models with #11 Braces, Height = 60-ft and Diameter = 4-ft
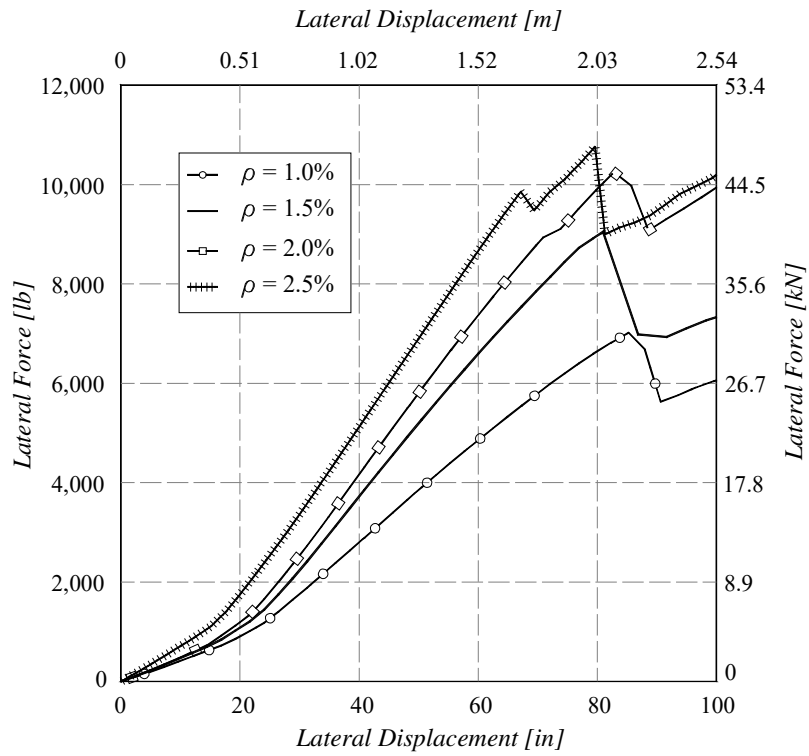
Figure AII.29: Response of Rebar Cage Models with #11 Braces, Height = 60-ft and Diameter = 6-ft

214
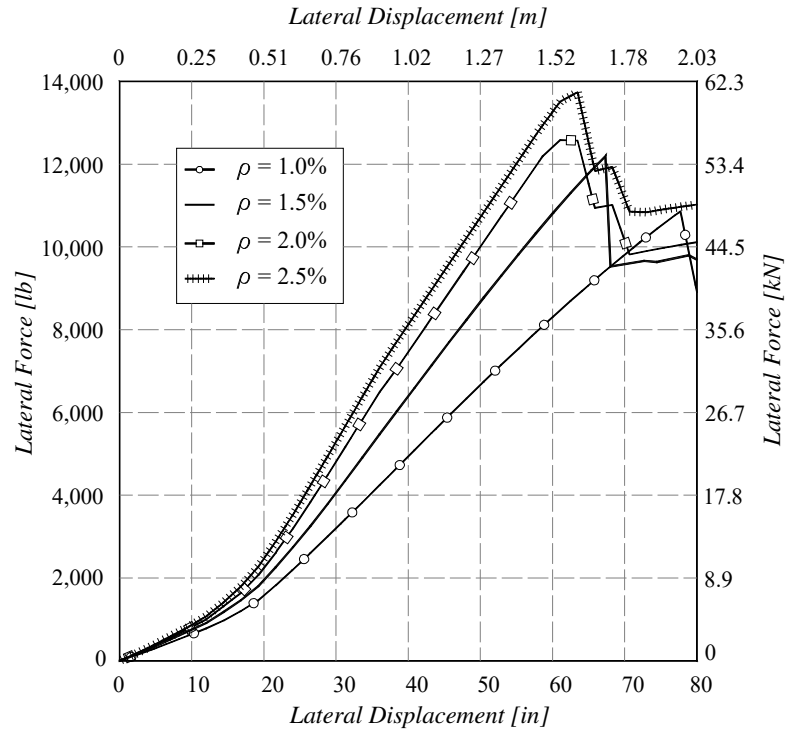
Figure AII.30: Response of Rebar Cage Models with #11 Braces, Height = 60-ft and Diameter = 8-ft
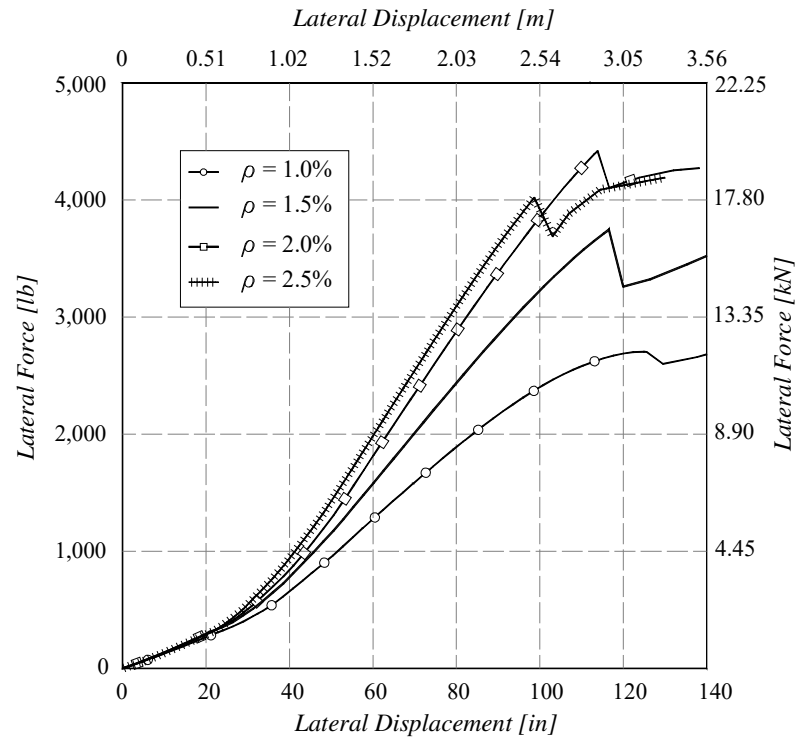
Figure AII.31: Response of Rebar Cage Models with #11 Braces, Height = 70-ft and Diameter = 4-ft

215
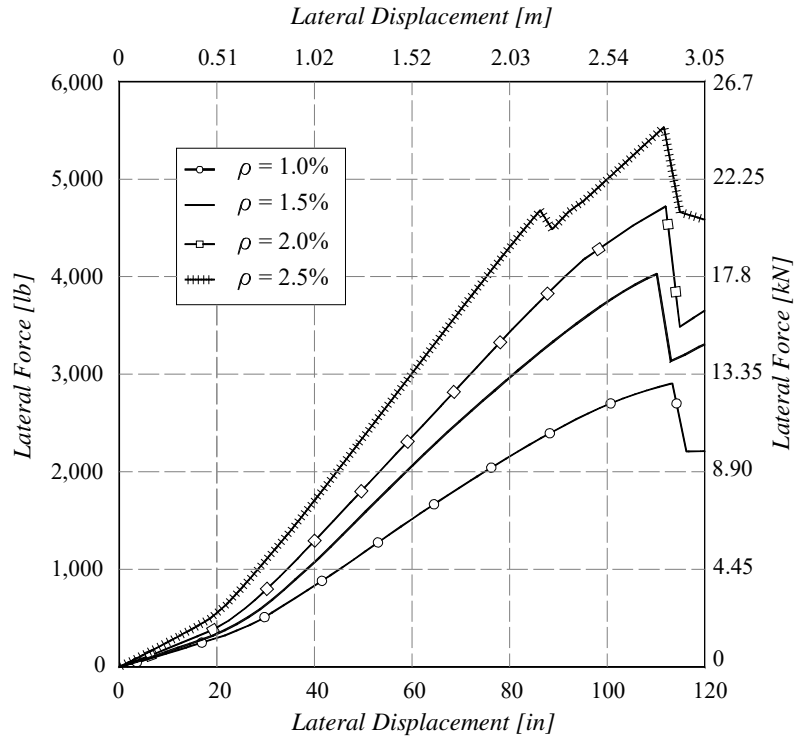
Figure AII.32: Response of Rebar Cage Models with #11 Braces, Height = 70-ft and Diameter = 6-ft
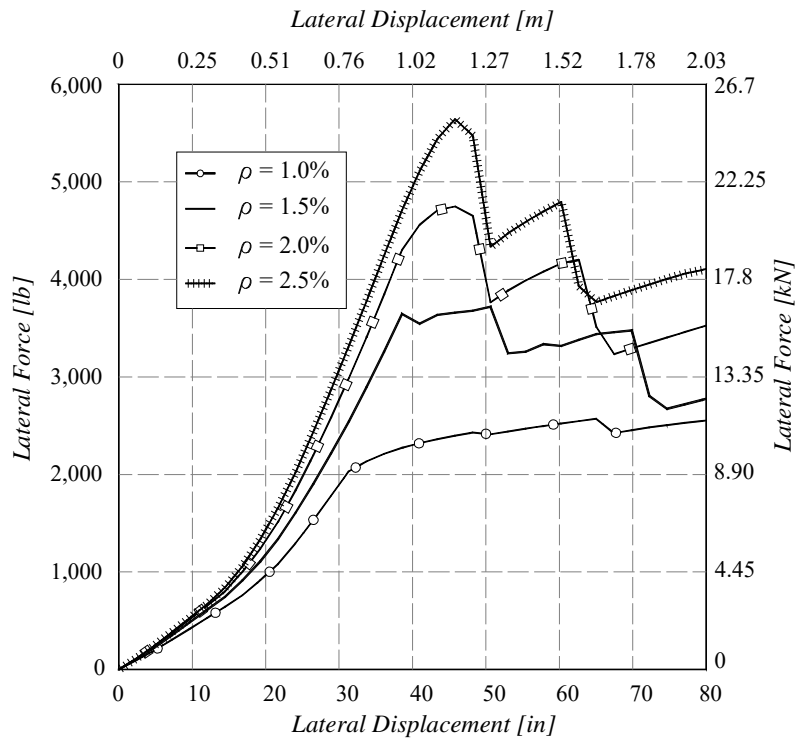
Figure AII.33: Response of Rebar Cage Models with #11 Braces, Height = 70-ft and Diameter = 8-ft

216
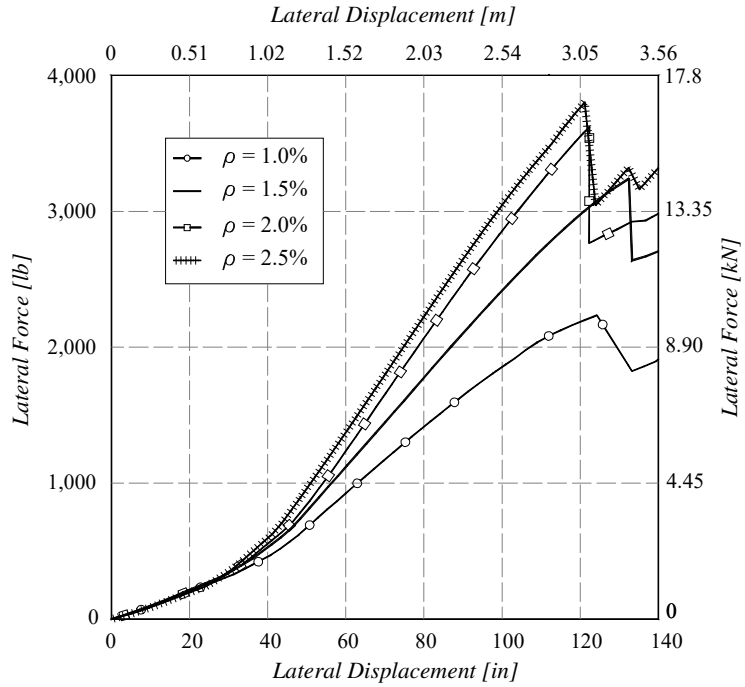
Figure AII.34: Response of Rebar Cage Models with #11 Braces, Height = 80-ft and Diameter = 4-ft
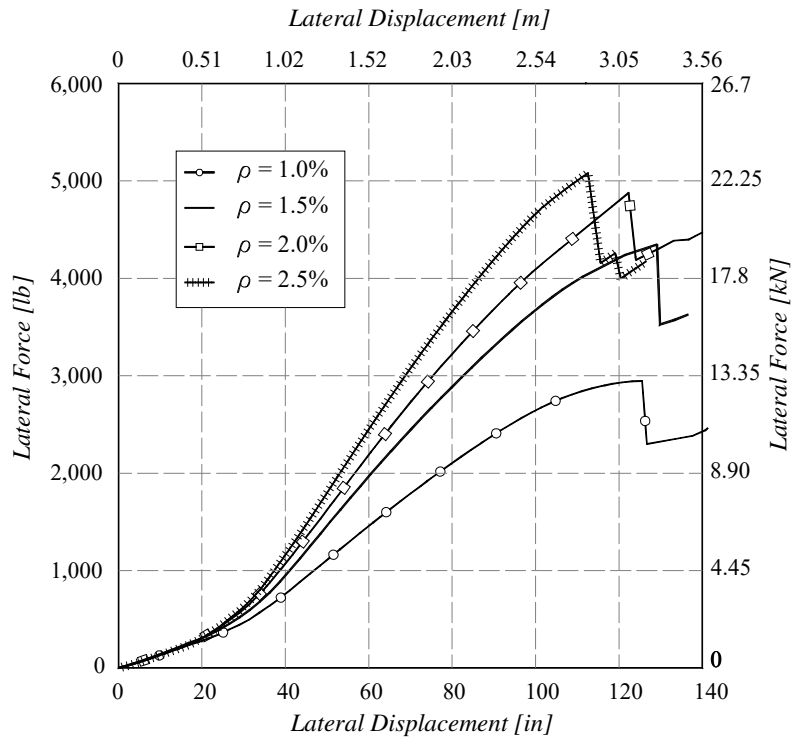

**Figure AII.35: Response of Rebar Cage Models with #11 Braces, Height = 80-ft and Diameter = 6-ft**
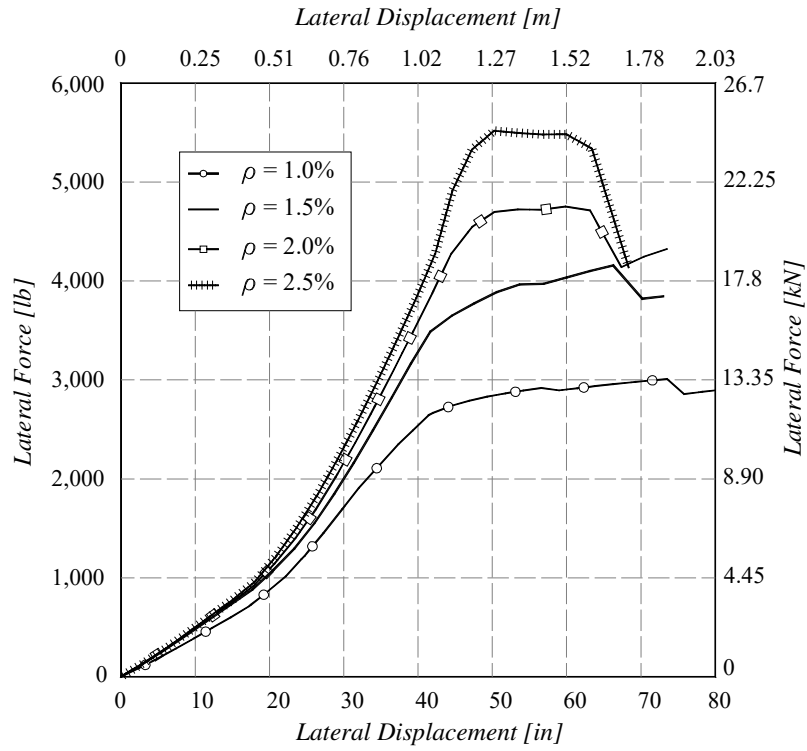
Figure AII.36: Response of Rebar Cage Models with #11 Braces, Height = 80-ft and Diameter = 8-ft

LIST OF CCEER PUBLICATIONS

Report No.   **Publication**

CCEER-84-1   Saiidi, M., and R. Lawver, "User's Manual for LZAK-C64, A Computer Program to Implement the Q-Model on Commodore 64," Civil Engineering Department, Report No. CCEER-84-1, University of Nevada, Reno, January 1984.

CCEER-84-1   Douglas, B., Norris, G., Saiidi, M., Dodd, L., Richardson, J. and Reid, W., "Simple Bridge Models for Earthquakes and Test Data," Civil Engineering Department, Report No. CCEER-84-1 Reprint, University of Nevada, Reno, January 1984.

CCEER-84-2   Douglas, B. and T. Iwasaki, "Proceedings of the First USA-Japan Bridge Engineering Workshop," held at the Public Works Research Institute, Tsukuba, Japan, Civil Engineering Department, Report No. CCEER-84-2, University of Nevada, Reno, April 1984.

CCEER-84-3   Saiidi, M., J. Hart, and B. Douglas, "Inelastic Static and Dynamic Analysis of Short R/C Bridges Subjected to Lateral Loads," Civil Engineering Department, Report No. CCEER-84-3, University of Nevada, Reno, July 1984.

CCEER-84-4   Douglas, B., "A Proposed Plan for a National Bridge Engineering Laboratory," Civil Engineering Department, Report No. CCEER-84-4, University of Nevada, Reno, December 1984.

CCEER-85-1   Norris, G. and P. Abdollaholiaee, "Laterally Loaded Pile Response: Studies with the Strain Wedge Model," Civil Engineering Department, Report No. CCEER-85-1, University of Nevada, Reno, April 1985.

CCEER-86-1   Ghusn, G. and M. Saiidi, "A Simple Hysteretic Element for Biaxial Bending of R/C in NEABS-86," Civil Engineering Department, Report No. CCEER-86-1, University of Nevada, Reno, July 1986.

CCEER-86-2   Saiidi, M., R. Lawver, and J. Hart, "User's Manual of ISADAB and SIBA, Computer Programs for Nonlinear Transverse Analysis of Highway Bridges Subjected to Static and Dynamic Lateral Loads," Civil Engineering Department, Report No. CCEER-86-2, University of Nevada, Reno, September 1986.

CCEER-87-1   Siddharthan, R., "Dynamic Effective Stress Response of Surface and Embedded Footings in Sand," Civil Engineering Department, Report No. CCEER-86-2, University of Nevada, Reno, June 1987.

CCEER-87-2   Norris, G. and R. Sack, "Lateral and Rotational Stiffness of Pile Groups for Seismic Analysis of Highway Bridges," Civil Engineering Department, Report No. CCEER-87-2, University of Nevada, Reno, June 1987.

CCEER-88-1   Orie, J. and M. Saiidi, "A Preliminary Study of One-Way Reinforced Concrete Pier Hinges Subjected to Shear and Flexure," Civil Engineering Department, Report No. CCEER-88-1, University of Nevada, Reno, January 1988.

CCEER-88-2   Orie, D., M. Saiidi, and B. Douglas, "A Micro-CAD System for Seismic Design of Regular Highway Bridges," Civil Engineering Department, Report No. CCEER-88-2, University of Nevada, Reno, June 1988.

CCEER-88-3   Orie, D. and M. Saiidi, "User's Manual for Micro-SARB, a Microcomputer Program for Seismic Analysis of Regular Highway Bridges," Civil Engineering Department, Report No. CCEER-88-3, University of Nevada, Reno, October 1988.

CCEER-89-1   Douglas, B., M. Saiidi, R. Hayes, and G. Holcomb, "A Comprehensive Study of the Loads and Pressures Exerted on Wall Forms by the Placement of Concrete," Civil Engineering Department, Report No. CCEER-89-1, University of Nevada, Reno, February 1989.

CCEER-89-2   Richardson, J. and B. Douglas, "Dynamic Response Analysis of the Dominion Road Bridge Test Data," Civil Engineering Department, Report No. CCEER-89-2, University of Nevada, Reno, March 1989.

CCEER-89-2   Vrontinos, S., M. Saiidi, and B. Douglas, "A Simple Model to Predict the Ultimate Response of R/C Beams with Concrete Overlays," Civil Engineering Department, Report NO. CCEER-89-2, University of Nevada, Reno, June 1989.

CCEER-89-3   Ebrahimpour, A. and P. Jagadish, "Statistical Modeling of Bridge Traffic Loads - A Case Study," Civil Engineering Department, Report No. CCEER-89-3, University of Nevada, Reno, December 1989.

CCEER-89-4   Shields, J. and M. Saiidi, "Direct Field Measurement of Prestress Losses in Box Girder Bridges," Civil Engineering Department, Report No. CCEER-89-4, University of Nevada, Reno, December 1989.

CCEER-90-1   Saiidi, M., E. Maragakis, G. Ghusn, Y. Jiang, and D. Schwartz, "Survey and Evaluation of Nevada's Transportation Infrastructure, Task 7.2 - Highway Bridges, Final Report," Civil Engineering Department, Report No. CCEER 90-1, University of Nevada, Reno, October 1990.

CCEER-90-2   Abdel-Ghaffar, S., E. Maragakis, and M. Saiidi, "Analysis of the Response of Reinforced Concrete Structures During the Whittier Earthquake 1987," Civil

Engineering Department, Report No. CCEER 90-2, University of Nevada, Reno, October 1990.

CCEER-91-1   Saiidi, M., E. Hwang, E. Maragakis, and B. Douglas, "Dynamic Testing and the Analysis of the Flamingo Road Interchange," Civil Engineering Department, Report No. CCEER-91-1, University of Nevada, Reno, February 1991.

CCEER-91-2   Norris, G., R. Siddharthan, Z. Zafir, S. Abdel-Ghaffar, and P. Gowda, "Soil-Foundation-Structure Behavior at the Oakland Outer Harbor Wharf," Civil Engineering Department, Report No. CCEER-91-2, University of Nevada, Reno, July 1991.

CCEER-91-3   Norris, G., "Seismic Lateral and Rotational Pile Foundation Stiffnesses at Cypress," Civil Engineering Department, Report No. CCEER-91-3, University of Nevada, Reno, August 1991.

CCEER-91-4   O'Connor, D. and M. Saiidi, "A Study of Protective Overlays for Highway Bridge Decks in Nevada, with Emphasis on Polyester-Styrene Polymer Concrete," Civil Engineering Department, Report No. CCEER-91-4, University of Nevada, Reno, October 1991.

CCEER-91-5   O'Connor, D.N. and M. Saiidi, "Laboratory Studies of Polyester-Styrene Polymer Concrete Engineering Properties," Civil Engineering Department, Report No. CCEER-91-5, University of Nevada, Reno, November 1991.

CCEER-92-1   Straw, D.L. and M. Saiidi, "Scale Model Testing of One-Way Reinforced Concrete Pier Hinges Subject to Combined Axial Force, Shear and Flexure," edited by D.N. O'Connor, Civil Engineering Department, Report No. CCEER-92-1, University of Nevada, Reno, March 1992.

CCEER-92-2   Wehbe, N., M. Saiidi, and F. Gordaninejad, "Basic Behavior of Composite Sections Made of Concrete Slabs and Graphite Epoxy Beams," Civil Engineering Department, Report No. CCEER-92-2, University of Nevada, Reno, August 1992.

CCEER-92-3   Saiidi, M. and E. Hutchens, "A Study of Prestress Changes in A Post-Tensioned Bridge During the First 30 Months," Civil Engineering Department, Report No. CCEER-92-3, University of Nevada, Reno, April 1992.

CCEER-92-4   Saiidi, M., B. Douglas, S. Feng, E. Hwang, and E. Maragakis, "Effects of Axial Force on Frequency of Prestressed Concrete Bridges," Civil Engineering Department, Report No. CCEER-92-4, University of Nevada, Reno, August 1992.

CCEER-92-5   Siddharthan, R., and Z. Zafir, "Response of Layered Deposits to Traveling

Surface Pressure Waves," Civil Engineering Department, Report No. CCEER-92-5, University of Nevada, Reno, September 1992.

CCEER-92-6   Norris, G., and Z. Zafir, "Liquefaction and Residual Strength of Loose Sands from Drained Triaxial Tests," Civil Engineering Department, Report No. CCEER-92-6, University of Nevada, Reno, September 1992.

CCEER-92-6-A Norris, G., Siddharthan, R., Zafir, Z. and Madhu, R. "Liquefaction and Residual Strength of Sands from Drained Triaxial Tests," Civil Engineering Department, Report No. CCEER-92-6-A, University of Nevada, Reno, September 1992.

CCEER-92-7   Douglas, B., "Some Thoughts Regarding the Improvement of the University of Nevada, Reno's National Academic Standing," Civil Engineering Department, Report No. CCEER-92-7, University of Nevada, Reno, September 1992.

CCEER-92-8   Saiidi, M., E. Maragakis, and S. Feng, "An Evaluation of the Current Caltrans Seismic Restrainer Design Method," Civil Engineering Department, Report No. CCEER-92-8, University of Nevada, Reno, October 1992.

CCEER-92-9   O'Connor, D., M. Saiidi, and E. Maragakis, "Effect of Hinge Restrainers on the Response of the Madrone Drive Undercrossing During the Loma Prieta Earthquake," Civil Engineering Department, Report No. CCEER-92-9, University of Nevada, Reno, February 1993.

CCEER-92-10   O'Connor, D., and M. Saiidi, "Laboratory Studies of Polyester Concrete: Compressive Strength at Elevated Temperatures and Following Temperature Cycling, Bond Strength to Portland Cement Concrete, and Modulus of Elasticity," Civil Engineering Department, Report No. CCEER-92-10, University of Nevada, Reno, February 1993.

CCEER-92-11   Wehbe, N., M. Saiidi, and D. O'Connor, "Economic Impact of Passage of Spent Fuel Traffic on Two Bridges in Northeast Nevada," Civil Engineering Department, Report No. CCEER-92-11, University of Nevada, Reno, December 1992.

CCEER-93-1   Jiang, Y., and M. Saiidi, "Behavior, Design, and Retrofit of Reinforced Concrete One-way Bridge Column Hinges," edited by D. O'Connor, Civil Engineering Department, Report No. CCEER-93-1, University of Nevada, Reno, March 1993.

CCEER-93-2   Abdel-Ghaffar, S., E. Maragakis, and M. Saiidi, "Evaluation of the Response of the Aptos Creek Bridge During the 1989 Loma Prieta Earthquake," Civil Engineering Department, Report No. CCEER-93-2, University of Nevada, Reno, June 1993.

CCEER-93-3   Sanders, D.H., B.M. Douglas, and T.L. Martin, "Seismic Retrofit Prioritization of

222

Nevada Bridges," Civil Engineering Department, Report No. CCEER-93-3, University of Nevada, Reno, July 1993.

CCEER-93-4   Abdel-Ghaffar, S., E. Maragakis, and M. Saiidi, "Performance of Hinge Restrainers in the Huntington Avenue Overhead During the 1989 Loma Prieta Earthquake," Civil Engineering Department, Report No. CCEER-93-4, University of Nevada, Reno, June 1993 (in final preparation).

CCEER-93-5   Maragakis, E., M. Saiidi, S. Feng, and L. Flournoy, "Effects of Hinge Restrainers on the Response of the San Gregorio Bridge during the Loma Prieta Earthquake," (in final preparation) Civil Engineering Department, Report No. CCEER-93-5, University of Nevada, Reno.

CCEER-93-6   Saiidi, M., E. Maragakis, S. Abdel-Ghaffar, S. Feng, and D. O'Connor, "Response of Bridge Hinge Restrainers during Earthquakes -Field Performance, Analysis, and Design," Civil Engineering Department, Report No. CCEER-93-6, University of Nevada, Reno, May 1993.

CCEER-93-7   Wehbe, N., Saiidi, M., Maragakis, E., and Sanders, D., "Adequacy of Three Highway Structures in Southern Nevada for Spent Fuel Transportation," Civil Engineering Department, Report No. CCEER-93-7, University of Nevada, Reno, August 1993.

CCEER-93-8   Roybal, J., Sanders, D.H., and Maragakis, E., "Vulnerability Assessment of Masonry in the Reno-Carson City Urban Corridor," Civil Engineering Department, Report No. CCEER-93-8, University of Nevada, Reno, May 1993.

CCEER-93-9   Zafir, Z. and Siddharthan, R., "MOVLOAD: A Program to Determine the Behavior of Nonlinear Horizontally Layered Medium Under Moving Load," Civil Engineering Department, Report No. CCEER-93-9, University of Nevada, Reno, August 1993.

CCEER-93-10   O'Connor, D.N., Saiidi, M., and Maragakis, E.A., "A Study of Bridge Column Seismic Damage Susceptibility at the Interstate 80/U.S. 395 Interchange in Reno, Nevada," Civil Engineering Department, Report No. CCEER-93-10, University f Nevada, Reno, October 1993.

CCEER-94-1   Maragakis, E., B. Douglas, and E. Abdelwahed, "Preliminary Dynamic Analysis of a Railroad Bridge," Report CCEER-94-1, January 1994.

CCEER-94-2   Douglas, B.M., Maragakis, E.A., and Feng, S., "Stiffness Evaluation of Pile Foundation of Cazenovia Creek Overpass," Civil Engineering Department, Report No. CCEER-94-2, University of Nevada, Reno, March 1994.

CCEER-94-3   Douglas, B.M., Maragakis, E.A., and Feng, S., "Summary of Pretest Analysis of

Cazenovia Creek Bridge," Civil Engineering Department, Report No. CCEER-94-3, University of Nevada, Reno, April 1994.

CCEER-94-4   Norris, G.M., Madhu, R., Valceschini, R., and Ashour, M., "Liquefaction and Residual Strength of Loose Sands from Drained Triaxial Tests," Report 2, Vol. 1&2, Civil Engineering Department, Report No. CCEER-94-4, University of Nevada, Reno, August 1994.

CCEER-94-5   Saiidi, M., Hutchens, E., and Gardella, D., "Prestress Losses in a Post-Tensioned R/C Box Girder Bridge in Southern Nevada," Civil Engineering Department, CCEER-94-5, University of Nevada, Reno, August 1994.

CCEER-95-1   Siddharthan, R., El-Gamal, M., and Maragakis, E.A., "Nonlinear Bridge Abutment , Verification, and Design Curves," Civil Engineering Department, CCEER-95-1, University of Nevada, Reno, January 1995.

CCEER-95-2   Ashour, M. and Norris, G., "Liquefaction and Undrained Response Evaluation of Sands from Drained Formulation," Civil Engineering Department, Report No. CCEER-95-2, University of Nevada, Reno, February 1995.

CCEER-95-3   Wehbe, N., Saiidi, M., Sanders, D. and Douglas, B., "Ductility of Rectangular Reinforced Concrete Bridge Columns with Moderate Confinement," Civil Engineering Department, Report No. CCEER-95-3, University of Nevada, Reno, July 1995.

CCEER-95-4   Martin, T.., Saiidi, M. and Sanders, D., "Seismic Retrofit of Column-Pier Cap Connections in Bridges in Northern Nevada," Civil Engineering Department, Report No. CCEER-95-4, University of Nevada, Reno, August 1995.

CCEER-95-5   Darwish, I., Saiidi, M. and Sanders, D., "Experimental Study of Seismic Susceptibility Column-Footing Connections in Bridges in Northern Nevada," Civil Engineering Department, Report No. CCEER-95-5, University of Nevada, Reno, September 1995.

CCEER-95-6   Griffin, G., Saiidi, M. and Maragakis, E., "Nonlinear Seismic Response of Isolated Bridges and Effects of Pier Ductility Demand," Civil Engineering Department, Report No. CCEER-95-6, University of Nevada, Reno, November 1995.

CCEER-95-7   Acharya, S.., Saiidi, M. and Sanders, D., "Seismic Retrofit of Bridge Footings and Column-Footing Connections," Civil Engineering Department, Report No. CCEER-95-7, University of Nevada, Reno, November 1995.

CCEER-95-8   Maragakis, E., Douglas, B., and Sandirasegaram, U., "Full-Scale Field Resonance Tests of a Railway Bridge," A Report to the Association of American

Railroads, Civil Engineering Department, Report No. CCEER-95-8, University of Nevada, Reno, December 1995.

CCEER-95-9   Douglas, B., Maragakis, E. and Feng, S., "System Identification Studies on Cazenovia Creek Overpass," Report for the National Center for Earthquake Engineering Research, Civil Engineering Department, Report No. CCEER-95-9, University of Nevada, Reno, October 1995.

CCEER-96-1   El-Gamal, M.E. and Siddharthan, R.V., "Programs to Computer Translational Stiffness of Seat-Type Bridge Abutment," Civil Engineering Department, Report No. CCEER-96-1, University of Nevada, Reno, March 1996.

CCEER-96-2   Labia, Y., Saiidi, M. and Douglas, B., "Evaluation and Repair of Full-Scale Prestressed Concrete Box Girders," A Report to the National Science Foundation, Research Grant CMS-9201908, Civil Engineering Department, Report No. CCEER-96-2, University of Nevada, Reno, May 1996.

CCEER-96-3   Darwish, I., Saiidi, M. and Sanders, D., "Seismic Retrofit of R/C Oblong Tapered Bridge Columns with Inadequate Bar Anchorage in Columns and Footings," A Report to the Nevada Department of Transportation, Civil Engineering Department, Report No. CCEER-96-3, University of Nevada, Reno, May 1996.

CCEER-96-4   Ashour, M., Pilling, R., Norris, G. and Perez, H., "The Prediction of Lateral Load Behavior of Single Piles and Pile Groups Using the Strain Wedge Model," A Report to the California Department of Transportation, Civil Engineering Department, Report No. CCEER-96-4, University of Nevada, Reno, June 1996.

CCEER-97-1-A Rimal, P. and Itani, A.   "Sensitivity Analysis of Fatigue Evaluations of Steel Bridges," Center for Earthquake Research, Department of Civil Engineering, University of Nevada, Reno, Nevada Report No. CCEER-97-1-A, September, 1997.

CCEER-97-1-B Maragakis, E., Douglas, B., and Sandirasegaram, U. "Full-Scale Field Resonance Tests of a Railway Bridge," A Report to the Association of American Railroads, Civil Engineering Department, University of Nevada, Reno, May, 1996.

CCEER-97-2   Wehbe, N., Saiidi, M., and D. Sanders, "Effect of Confinement and Flares on the Seismic Performance of Reinforced Concrete Bridge Columns," Civil Engineering Department, Report No. CCEER-97-2, University of Nevada, Reno, September 1997.

CCEER-97-3   Darwish, I., M. Saiidi, G. Norris, and E. Maragakis, "Determination of In-Situ Footing Stiffness Using Full-Scale Dynamic Field Testing," A Report to the Nevada Department of Transportation, Structural Design Division, Carson City, Nevada, Report No. CCEER-97-3, University of Nevada, Reno, October 1997.

CCEER-97-4-A Itani, A. "Cyclic Behavior of Richmond-San Rafael Tower Links," Center for Civil Engineering Earthquake Research, Department of Civil Engineering, University of Nevada, Reno, Nevada, Report No. CCEER-97-4, August 1997.

CCEER-97-4-B Wehbe, N., and M. Saiidi, "User's Manual for RCMC v. 1.2 : A Computer Program for Moment-Curvature Analysis of Confined and Unconfined Reinforced Concrete Sections," Center for Civil Engineering Earthquake Research, Department of Civil Engineering, University of Nevada, Reno, Nevada, Report No. CCEER-97-4, November, 1997.

CCEER-97-5 Isakovic, T., M. Saiidi, and A. Itani, "Influence of new Bridge Configurations on Seismic Performance," Department of Civil Engineering, University of Nevada, Reno, Report No. CCEER-97-5, September, 1997.

CCEER-98-1 Itani, A., Vesco, T. and Dietrich, A., "Cyclic Behavior of "as Built" Laced Members With End Gusset Plates on the San Francisco Bay Bridge," Center for Civil Engineering Earthquake Research, Department of Civil Engineering, University of Nevada, Reno, Nevada Report No. CCEER-98-1, March, 1998.

CCEER-98-2 G. Norris and M. Ashour, "Liquefaction and Undrained Response Evaluation of Sands from Drained Formulation," Center for Civil Engineering Earthquake Research, Department of Civil Engineering, University of Nevada, Reno, Nevada, Report No. CCEER-98-2, May, 1998.

CCEER-98-3 Qingbin, Chen, B. M. Douglas, E. Maragakis, and I. G. Buckle, "Extraction of Nonlinear Hysteretic Properties of Seismically Isolated Bridges from Quick-Release Field Tests," Center for Civil Engineering Earthquake Research, Department of Civil Engineering, University of Nevada, Reno, Nevada, Report No. CCEER-98-3, June, 1998.

CCEER-98-4 Maragakis, E., B. M. Douglas, and C. Qingbin, "Full-Scale Field Capacity Tests of a Railway Bridge," Center for Civil Engineering Earthquake Research, Department of Civil Engineering, University of Nevada, Reno, Nevada, Report No. CCEER-98-4, June, 1998.

CCEER-98-5 Itani, A., Douglas, B., and Woodgate, J., "Cyclic Behavior of Richmond-San Rafael Retrofitted Tower Leg," Center for Civil Engineering Earthquake Research, Department of Civil Engineering, University of Nevada, Reno. Report No. CCEER-98-5, June 1998

CCEER-98-6 Moore, R., Saiidi, M., and Itani, A., "Seismic Behavior of New Bridges with Skew and Curvature," Center for Civil Engineering Earthquake Research, Department of Civil Engineering, University of Nevada, Reno. Report No. CCEER-98-6, October, 1998.

CCEER-98-7   Itani, A and Dietrich, A, "Cyclic Behavior of Double Gusset Plate Connections," Center for Civil Engineering Earthquake Research, Department of Civil Engineering, University of Nevada, Reno, Nevada, Report No. CCEER-98-5, December, 1998.

CCEER-99-1   Caywood, C., M. Saiidi, and D. Sanders, "Seismic Retrofit of Flared Bridge Columns with Steel Jackets," Civil Engineering Department, University of Nevada, Reno, Report No. CCEER-99-1, February 1999.

CCEER-99-2   Mangoba, N., M. Mayberry, and M. Saiidi, "Prestress Loss in Four Box Girder Bridges in Northern Nevada," Civil Engineering Department, University of Nevada, Reno, Report No. CCEER-99-2, March 1999.

CCEER-99-3   Abo-Shadi, N., M. Saiidi, and D. Sanders, "Seismic Response of Bridge Pier Walls in the Weak Direction," Civil Engineering Department, University of Nevada, Reno, Report No. CCEER-99-3, April 1999.

CCEER-99-4   Buzick, A., and M. Saiidi, "Shear Strength and Shear Fatigue Behavior of Full-Scale Prestressed Concrete Box Girders," Civil Engineering Department, University of Nevada, Reno, Report No. CCEER-99-4, April 1999.

CCEER-99-5   Randall, M., M. Saiidi, E. Maragakis and T. Isakovic, "Restrainer Design Procedures For Multi-Span Simply-Supported Bridges," Civil Engineering Department, University of Nevada, Reno, Report No. CCEER-99-5, April 1999.

CCEER-99-6   Wehbe, N. and M. Saiidi, "User's Manual for RCMC v. 1.2, A Computer Program for Moment-Curvature Analysis of Confined and Unconfined Reinforced Concrete Sections," Civil Engineering Department, University of Nevada, Reno, Report No. CCEER-99-6, May 1999.

CCEER-99-7   Burda, J. and A. Itani, "Studies of Seismic Behavior of Steel Base Plates," Civil Engineering Department, University of Nevada, Reno, Report No. CCEER-99-7, May 1999.

CCEER-99-8   Ashour, M. and G. Norris, "Refinement of the Strain Wedge Model Program," Civil Engineering Department, University of Nevada, Reno, Report No. CCEER-99-8, March 1999.

CCEER-99-9   Dietrich, A., and A. Itani, "Cyclic Behavior of Laced and Perforated Steel Members on the San Francisco-Oakland Bay Bridge," Civil Engineering Department, University, Reno, Report No. CCEER-99-9, December 1999.

CCEER 99-10   Itani, A., A. Dietrich, "Cyclic Behavior of Built Up Steel Members and their Connections," Civil Engineering Department, University of Nevada, Reno, Report No. CCEER-99-10, December 1999.

CCEER 99-10-A   Itani, A., E. Maragakis and P. He, "Fatigue Behavior of Riveted Open Deck Railroad Bridge Girders," Civil Engineering Department, University of Nevada, Reno, Report No. CCEER-99-10-A, August 1999.

CCEER 99-11   Itani, A., J. Woodgate, "Axial and Rotational Ductility of Built Up Structural Steel Members," Civil Engineering Department, University of Nevada, Reno, Report No. CCEER-99-11, December 1999.

CCEER-99-12   Sgambelluri, M., Sanders, D.H., and Saiidi, M.S., "Behavior of One-Way Reinforced Concrete Bridge Column Hinges in the Weak Direction," Department of Civil Engineering, University of Nevada, Reno, Report No. CCEER-99-12, December 1999.

CCEER-99-13   Laplace, P., Sanders, D.H., Douglas, B, and Saiidi, M, "Shake Table Testing of Flexure Dominated Reinforced Concrete Bridge Columns", Department of Civil Engineering, University of Nevada, Reno, Report No. CCEER-99-13, December 1999.

CCEER-99-14   Ahmad M. Itani, Jose A. Zepeda, and Elizabeth A. Ware "Cyclic Behavior of Steel Moment Frame Connections for the Moscone Center Expansion," Department of Civil Engineering, University of Nevada, Reno, Report No. CCEER-99-14, December 1999.

CCEER 00-1   Ashour, M., and Norris, G. "Undrained Lateral Pile and Pile Group Response in Saturated Sand," Civil Engineering Department, University of Nevada, Reno, Report No. CCEER-00-1, May 1999. January 2000.

CCEER 00-2   Saiidi, M. and Wehbe, N., "A Comparison of Confinement Requirements in Different Codes for Rectangular, Circular, and Double-Spiral RC Bridge Columns," Civil Engineering Department, University of Nevada, Reno, Report No. CCEER-00-2, January 2000.

CCEER 00-3   McElhaney, B., M. Saiidi, and D. Sanders, "Shake Table Testing of Flared Bridge Columns With Steel Jacket Retrofit," Civil Engineering Department, University of Nevada, Reno, Report No. CCEER-00-3, January 2000.

CCEER 00-4   Martinovic, F., M. Saiidi, D. Sanders, and F. Gordaninejad, "Dynamic Testing of Non-Prismatic Reinforced Concrete Bridge Columns Retrofitted with FRP Jackets," Civil Engineering Department, University of Nevada, Reno, Report No. CCEER-00-4, January 2000.

CCEER 00-5   Itani, A., and M. Saiidi, "Seismic Evaluation of Steel Joints for UCLA Center for Health Science Westwood Replacement Hospital," Civil Engineering Department, University of Nevada, Reno, Report No. CCEER-00-5, February 2000.

CCEER 00-6   Will, J. and D. Sanders, "High Performance Concrete Using Nevada Aggregates," Civil Engineering Department, University of Nevada, Reno, Report No. CCEER-00-6, May 2000.

CCEER 00-7   French, C., and M. Saiidi, "A Comparison of Static and Dynamic Performance of Models of Flared Bridge Columns," Civil Engineering Department, University of Nevada, Reno, Report No. CCEER-00-7, October 2000.

CCEER 00-8   Itani, A., H. Sedarat, "Seismic Analysis of the AISI LRFD Design Example of Steel Highway Bridges," Civil Engineering Department, University of Nevada, Reno, Report No. CCEER 00-08, November 2000.

CCEER 00-9   Moore, J., D. Sanders, and M. Saiidi, "Shake Table Testing of 1960's Two Column Bent with Hinges Bases," Civil Engineering Department, University of Nevada, Reno, Report No. CCEER 00-09, December 2000.

CCEER 00-10   Asthana, M., D. Sanders, and M. Saiidi, "One-Way Reinforced Concrete Bridge Column Hinges in the Weak Direction," Civil Engineering Department, University of Nevada, Reno, Report No. CCEER 00-10, April 2001.

CCEER 01-1   Ah Sha, H., D. Sanders, M. Saiidi, "Early Age Shrinkage and Cracking of Nevada Concrete Bridge Decks," Civil Engineering Department, University of Nevada, Reno, Report No. CCEER 01-01, May 2001.

CCEER 01-2   Ashour, M. and G. Norris, "Pile Group program for Full Material Modeling a Progressive Failure," Civil Engineering Department, University of Nevada, Reno, Report No. CCEER 01-02, July 2001.

CCEER 01-3   Itani, A., C. Lanaud, and P. Dusicka, "Non-Linear Finite Element Analysis of Built-Up Shear Links," Civil Engineering Department, University of Nevada, Reno, Report No. CCEER 01-03, July 2001.

CCEER 01-4   Saiidi, M., J. Mortensen, and F. Martinovic, "Analysis and Retrofit of Fixed Flared Columns with Glass Fiber-Reinforced Plastic Jacketing," Civil Engineering Department, University of Nevada, Reno, Report No. CCEER 01-4, August 2001

CCEER 01-5   Saiidi, M., A. Itani, I. Buckle, and Z. Cheng, "Performance of A Full-Scale Two-Story Wood Frame Structure Supported on Ever-Level Isolators," Civil Engineering Department, University of Nevada, Reno, Report No. CCEER 01-5, October 2001

CCEER 01-6   Laplace, P., D. Sanders, and M. Saiidi, "Experimental Study and Analysis of Retrofitted Flexure and Shear Dominated Circular Reinforced Concrete Bridge

Columns Subjected to Shake Table Excitation," Civil Engineering Department, University of Nevada, Reno, Report No. CCEER 01-6, June 2001.

CCEER 01-7   Reppi, F., and D. Sanders, "Removal and Replacement of Cast-in-Place, Post-tensioned, Box Girder Bridge," Civil Engineering Department, University of Nevada, Reno, Report No. CCEER 01-7, December 2001.

CCEER 02-1   Pulido, C., M. Saiidi, D. Sanders, and A. Itani, "Seismic Performance and Retrofitting of Reinforced Concrete Bridge Bents," Civil Engineering Department, University of Nevada, Reno, Report No. CCEER 02-1, January 2002.

CCEER 02-2   Yang, Q., M. Saiidi, H. Wang, and A. Itani, "Influence of Ground Motion Incoherency on Earthquake Response of Multi-Support Structures," Civil Engineering Department, University of Nevada, Reno, Report No. CCEER 02-2, May 2002.

CCEER 02-3   M. Saiidi, B. Gopalakrishnan, E. Reinhardt, and R. Siddharthan, "A Preliminary Study of Shake Table Response of A Two-Column Bridge Bent on Flexible Footings," Civil Engineering Department, University of Nevada, Reno, Report No. CCEER 02-03, June 2002.

CCEER 02-4   Not Published

CCEER 02-5   Banghart, A., Sanders, D., Saiidi, M., "Evaluation of Concrete Mixes for Filling the Steel Arches in the Galena Creek Bridge," Civil Engineering Department, University of Nevada, Reno, Report No. CCEER 02-05, June 2002.

CCEER 02-6   Dusicka, P., Itani, A., Buckle, I. G., "Cyclic Behavior of Shear Links and Tower Shaft Assembly of San Francisco – Oakland Bay Bridge Tower," Civil Engineering Department, University of Nevada, Reno, Report No. CCEER 02-06, July 2002.

CCEER 02-7   Mortensen, J., and M. Saiidi, "A Performance-Based Design Method for Confinement in Circular Columns," Civil Engineering Department, University of Nevada, Reno, Report No. CCEER 02-07, November 2002.

CCEER 03-1   Wehbe, N., and M. Saiidi, "User's manual for SPMC v. 1.0 : A Computer Program for Moment-Curvature Analysis of Reinforced Concrete Sections with Interlocking Spirals," Center for Civil Engineering Earthquake Research, Department of Civil Engineering, University of Nevada, Reno, Nevada, Report No. CCEER-03-1, May, 2003.

CCEER 03-2   Wehbe, N., and M. Saiidi, "User's manual for RCMC v. 2.0 : A Computer Program for Moment-Curvature Analysis of Confined and Unconfined Reinforced Concrete Sections," Center for Civil Engineering Earthquake

Research, Department of Civil Engineering, University of Nevada, Reno, Nevada, Report No. CCEER-03-2, June, 2003.

CCEER 03-3   Nada, H., D. Sanders, and M. Saiidi, "Seismic Performance of RC Bridge Frames with Architectural-Flared Columns," Civil Engineering Department, University of Nevada, Reno, Report No. CCEER 03-3, January 2003.

CCEER 03-4   Reinhardt, E., M. Saiidi, and R. Siddharthan, "Seismic Performance of a CFRP/ Concrete Bridge Bent on Flexible Footings," Civil Engineering Department, University of Nevada, Reno, Report No. CCEER 03-4, August 2003.

CCEER 03-5   Johnson, N., M. Saiidi, A. Itani, and S. Ladkany, "Seismic Retrofit of Octagonal Columns with Pedestal and One-Way Hinge at the Base," Center for Civil Engineering Earthquake Research, Department of Civil Engineering, University of Nevada, Reno, Nevada, and Report No. CCEER-03-5, August 2003.

CCEER 03-6   Mortensen, C., M. Saiidi, and S. Ladkany, "Creep and Shrinkage Losses in Highly Variable Climates," Center for Civil Engineering Earthquake Research, Department of Civil Engineering, University of Nevada, Reno, Report No. CCEER-03-6, September 2003.

CCEER 03- 7   Ayoub, C., M. Saiidi, and A. Itani, "A Study of Shape-Memory-Alloy-Reinforced Beams and Cubes," Center for Civil Engineering Earthquake Research, Department of Civil Engineering, University of Nevada, Reno, Nevada, Report No. CCEER-03-7, October 2003.

CCEER 03-8   Chandane, S., D. Sanders, and M. Saiidi, "Static and Dynamic Performance of RC Bridge Bents with Architectural-Flared Columns," Center for Civil Engineering Earthquake Research, Department of Civil Engineering, University of Nevada, Reno, Nevada, Report No. CCEER-03-8, November 2003.

CCEER 04-1   Olaegbe, C., and Saiidi, M., "Effect of Loading History on Shake Table Performance of A Two-Column Bent with Infill Wall," Center for Civil Engineering Earthquake Research, Department of Civil Engineering, University of Nevada, Reno, Nevada, Report No. CCEER-04-1, January 2004.

CCEER 04-2   Johnson, R., Maragakis, E., Saiidi, M., and DesRoches, R., "Experimental Evaluation of Seismic Performance of SMA Bridge Restrainers," Center for Civil Engineering Earthquake Research, Department of Civil Engineering, University of Nevada, Reno, Nevada, Report No. CCEER-04-2, February 2004.

CCEER 04-3   Moustafa, K., Sanders, D., and Saiidi, M., "Impact of Aspect Ratio on Two-Column Bent Seismic Performance," Center for Civil Engineering Earthquake Research, Department of Civil Engineering, University of Nevada, Reno, Nevada, Report No. CCEER-04-3, February 2004.

CCEER 04-4   Maragakis, E., Saiidi, M., Sanchez-Camargo, F., and Elfass, S., "Seismic Performance of Bridge Restrainers At In-Span Hinges," Center for Civil Engineering Earthquake Research, Department of Civil Engineering, University of Nevada, Reno, Nevada, Report No. CCEER-04-4, March 2004.

CCEER 04-5   Ashour, M., Norris, G. and Elfass, S., "Analysis of Laterally Loaded Long or Intermediate Drilled Shafts of Small or Large Diameter in Layered Soil," Center for Civil Engineering Earthquake Research, Department of Civil Engineering, University of Nevada, Reno, Nevada, Report No. CCEER-04-5, June 2004.

CCEER 04-6   Correal, J., Saiidi, M. and Sanders, D., "Seismic Performance of RC Bridge Columns Reinforced with Two Interlocking Spirals," Center for Civil Engineering Earthquake Research, Department of Civil Engineering, University of Nevada, Reno, Nevada, Report No. CCEER-04-6, August 2004.

CCEER 04-7   Dusicka, P., Itani, A. and Buckle, I., "Cyclic Response and Low Cycle Fatigue Characteristics of Plate Steels," Center for Civil Engineering Earthquake Research, Department of Civil Engineering, University of Nevada, Reno, Nevada, Report No. CCEER-04-7, November 2004.

CCEER 04-8   Dusicka, P., Itani, A. and Buckle, I., "Built-up Shear Links as Energy Dissipaters for Seismic Protection of Bridges," Center for Civil Engineering Earthquake Research, Department of Civil Engineering, University of Nevada, Reno, Nevada, Report No. CCEER-04-8, November 2004.

CCEER 04-9   Sureshkumar, K., Saiidi, S., Itani, A. and Ladkany, S., "Seismic Retrofit of Two-Column Bents with Diamond Shape Columns," Center for Civil Engineering Earthquake Research, Department of Civil Engineering, University of Nevada, Reno, Nevada, Report No. CCEER-04-9, November 2004.

CCEER 05-1   Wang, H. and Saiidi, S., "A Study of RC Columns with Shape Memory Alloy and Engineered Cementitious Composites," Center for Civil Engineering Earthquake Research, Department of Civil Engineering, University of Nevada, Reno, Nevada, Report No. CCEER-05-1, January 2005.

CCEER 05-2   Johnson, R., Saiidi, S. and Maragakis, E., "A Study of Fiber Reinforced Plastics for Seismic Bridge Restrainers," Center for Civil Engineering Earthquake Research, Department of Civil Engineering, University of Nevada, Reno, Nevada, Report No. CCEER-05-2, January 2005.

CCEER 05-3   Carden, L.P., Itani, A.M., Buckle, I.G, "Seismic Load Path in Steel Girder Bridge Superstructures," Center for Civil Engineering Earthquake Research, Department of Civil Engineering, University of Nevada, Reno, Nevada, Report No. CCEER-05-3, January 2005.

CCEER 05-4   Carden, L.P., Itani, A.M., Buckle, I.G, "Seismic Performance of Steel Girder Bridge Superstructures with Ductile End Cross Frames and Seismic Isolation," Center for Civil Engineering Earthquake Research, Department of Civil Engineering, University of Nevada, Reno, Nevada, Report No. CCEER-05-4, January 2005.

CCEER 05-5   Goodwin, E., Maragakis, M., Itani, A. and Luo, S., "Experimental Evaluation of the Seismic Performance of Hospital Piping Subassemblies," Center for Civil Engineering Earthquake Research, Department of Civil Engineering, University of Nevada, Reno, Nevada, Report No. CCEER-05-5, February 2005.

CCEER 05-6   Zadeh M. S., Saiidi, S, Itani, A. and Ladkany, S., "Seismic Vulnerability Evaluation and Retrofit Design of Las Vegas Downtown Viaduct," Center for Civil Engineering Earthquake Research, Department of Civil Engineering, University of Nevada, Reno, Nevada, Report No. CCEER-05-6, February 2005.

CCEER 05-7   Phan, V., Saiidi, S. and Anderson, J., "Near Fault (Near Field) Ground Motion Effects on Reinforced Concrete Bridge Columns," Center for Civil Engineering Earthquake Research, Department of Civil Engineering, University of Nevada, Reno, Nevada, Report No. CCEER-05-7, August 2005.

CCEER 05-8   Carden, L., Itani, A. and Laplace, P., "Performance of Steel Props at the UNR Fire Science Academy subjected to Repeated Fire," Center for Civil Engineering Earthquake Research, Department of Civil Engineering, University of Nevada, Reno, Nevada, Report No. CCEER-05-8, August 2005.

CCEER 05-9   Yamashita, R. and Sanders, D., "Shake Table Testing and an Analytical Study of Unbonded Prestressed Hollow Concrete Column Constructed with Precast Segments," Center for Civil Engineering Earthquake Research, Department of Civil Engineering, University of Nevada, Reno, Nevada, Report No. CCEER-05-9, August 2005.

CCEER 05-10   Not Published

CCEER 05-11   Carden, L., Itani., A., and Peckan, G., "Recommendations for the Design of Beams and Posts in Bridge Falsework," Center for Civil Engineering Earthquake Research, Department of Civil Engineering, University of Nevada, Reno, Nevada, Report No. CCEER-05-11, October 2005.

CCEER 06-01   Cheng, Z., Saiidi, M., and Sanders, D., "Development of a Seismic Design Method for Reinforced Concrete Two-Way Bridge Column Hinges," Center for Civil Engineering Earthquake Research, Department of Civil Engineering, University of Nevada, Reno, Nevada, Report No. CCEER-06-01, February 2006.

CCEER 06-02   Johnson, N., Saiidi, M., and Sanders, D., "Large-Scale Experimental and Analytical Studies of a Two-Span Reinforced Concrete Bridge System," Center

for Civil Engineering Earthquake Research, Department of Civil Engineering, University of Nevada, Reno, Nevada, Report No. CCEER-06-02, March 2006.

CCEER 06-03   Saiidi, M., Ghasemi, H. and Tiras, A., "Seismic Design and Retrofit of Highway Bridges," Proceedings, Second US-Turkey Workshop, Center for Civil Engineering Earthquake Research, Department of Civil Engineering, University of Nevada, Reno, Nevada, Report No. CCEER-06-03, May 2006.

CCEER 07-01   O'Brien, M., Saiidi, M. and Sadrossadat-Zadeh, M., "A Study of Concrete Bridge Columns Using Innovative Materials Subjected to Cyclic Loading," Center for Civil Engineering Earthquake Research, Department of Civil Engineering, University of Nevada, Reno, Nevada, Report No. CCEER-07-01, January 2007.

CCEER 07-02   Sadrossadat-Zadeh, M. and Saiidi, M., "Effect of Strain rate on Stress-Strain Properties and Yield Propagation in Steel Reinforcing Bars," Center for Civil Engineering Earthquake Research, Department of Civil Engineering, University of Nevada, Reno, Nevada, Report No. CCEER-07-02, January 2007.

CCEER 07-03   Sadrossadat-Zadeh, M. and Saiidi, M., "Analytical Study of NEESR-SG 4-Span Bridge Model Using OpenSees," Center for Civil Engineering Earthquake Research, Department of Civil Engineering, University of Nevada, Reno, Nevada, Report No. CCEER-07-03, January 2007.

CCEER 07-04   Nelson, R., Saiidi, M. and Zadeh, S., "Experimental Evaluation of Performance of Conventional Bridge Systems," Center for Civil Engineering Earthquake Research, Department of Civil Engineering, University of Nevada, Reno, Nevada, Report No. CCEER-07-04, October 2007.

CCEER 07-05   Bahen, N. and Sanders, D., "Strut-and-Tie Modeling for Disturbed Regions in Structural Concrete Members with Emphasis on Deep Beams," Center for Civil Engineering Earthquake Research, Department of Civil Engineering, University of Nevada, Reno, Nevada, Report No. CCEER-07-05, December 2007.

CCEER 07-06   Choi, H., Saiidi, M. and Somerville, P., "Effects of Near-Fault Ground Motion and Fault-Rupture on the Seismic Response of Reinforced Concrete Bridges," Center for Civil Engineering Earthquake Research, Department of Civil Engineering, University of Nevada, Reno, Nevada, Report No. CCEER-07-06, December 2007.

CCEER 07-07   Ashour M. and Norris, G., "Report and User Manual on Strain Wedge Model Computer Program for Files and Large Diameter Shafts with LRFD Procedure," Center for Civil Engineering Earthquake Research, Department of Civil Engineering, University of Nevada, Reno, Nevada, Report No. CCEER-07-07, October 2007.

CCEER 08-01   Doyle, K. and Saiidi, M., "Seismic Response of Telescopic Pipe Pin Connections," Center for Civil Engineering Earthquake Research, Department of Civil Engineering, University of Nevada, Reno, Nevada, Report No. CCEER-08-01, February 2008.

CCEER 08-02   Taylor, M. and Sanders, D., "Seismic Time History Analysis and Instrumentation of the Galena Creek Bridge," Center for Civil Engineering Earthquake Research, Department of Civil Engineering, University of Nevada, Reno, Nevada, Report No. CCEER-08-02, April 2008.

CCEER 08-03   Abdel-Mohti, A. and Pekcan, G., "Seismic Response Assessment and Recommendations for the Design of Skewed Post-Tensioned Concrete Box-Girder Highway Bridges," Center for Civil Engineering Earthquake Research, Department of Civil and Environmental Engineering, University of Nevada, Reno, Nevada, Report No. CCEER-08-03, September 2008.

CCEER 08-04   Saiidi, M., Ghasemi, H. and Hook, J., "Long Term Bridge Performance Monitoring, Assessment & Management," Proceedings, FHWA/NSF Workshop on Future Directions," Center for Civil Engineering Earthquake Research, Department of Civil and Environmental Engineering, University of Nevada, Reno, Nevada, Report No. CCEER 08-04, September 2008.

CCEER 09-01   Brown, A., and Saiidi, M., "Investigation of Near-Fault Ground Motion Effects on Substandard Bridge Columns and Bents," Center for Civil Engineering Earthquake Research, Department of Civil and Environmental Engineering, University of Nevada, Reno, Nevada, Report No. CCEER-09-01, July 2009.

CCEER 09-02   Linke, C., Pekcan, G., and Itani, A., "Detailing of Seismically Resilient Special Truss Moment Frames," Center for Civil Engineering Earthquake Research, Department of Civil and Environmental Engineering, University of Nevada, Reno, Nevada, Report No. CCEER-09-02, August 2009.

CCEER 09-03   Hillis, D., and Saiidi, M., "Design, Construction, and Nonlinear Dynamic Analysis of Three Bridge Bents Used in a Bridge System Test," Center for Civil Engineering Earthquake Research, Department of Civil and Environmental Engineering, University of Nevada, Reno, Nevada, Report No. CCEER-09-03, August 2009.

CCEER 09-04   Bahrami, H., Itani, A., and Buckle, I., "Guidelines for the Seismic Design of Ductile End Cross Frames in Steel Girder Bridge Superstructures," Center for Civil Engineering Earthquake Research, Department of Civil and Environmental Engineering, University of Nevada, Reno, Nevada, Report No. CCEER-09-04, September 2009.

CCEER 10-01   Zaghi, A. E., and Saiidi, M., "Seismic Design of Pipe-Pin Connections in Concrete Bridges," Center for Civil Engineering Earthquake Research,

Department of Civil and Environmental Engineering, University of Nevada, Reno, Nevada, Report No. CCEER-10-01, January 2010.

CCEER 10-02   Pooranampillai, S., Elfass, S., and Norris, G., "Laboratory Study to Assess Load Capacity Increase of Drilled Shafts through Post Grouting," Center for Civil Engineering Earthquake Research, Department of Civil and Environmental Engineering, University of Nevada, Reno, Nevada, Report No. CCEER-10-02, January 2010.

CCEER 10-03   Itani, A., Grubb, M., and Monzon, E, "Proposed Seismic Provisions and Commentary for Steel Plate Girder Superstructures," Center for Civil Engineering Earthquake Research, Department of Civil and Environmental Engineering, University of Nevada, Reno, Nevada, Report No. CCEER-10-03, June 2010.

CCEER 10-04   Cruz-Noguez, C., Saiidi, M., "Experimental and Analytical Seismic Studies of a Four-Span Bridge System with Innovative Materials," Center for Civil Engineering Earthquake Research, Department of Civil and Environmental Engineering, University of Nevada, Reno, Nevada, Report No. CCEER-10-04, September 2010.

CCEER 10-05   Vosooghi, A., Saiidi, M., "Post-Earthquake Evaluation and Emergency Repair of Damaged RC Bridge Columns Using CFRP Materials," Center for Civil Engineering Earthquake Research, Department of Civil and Environmental Engineering, University of Nevada, Reno, Nevada, Report No. CCEER-10-05, September 2010.

CCEER 10-06   Ayoub, M., Sanders, D., "Testing of Pile Extension Connections to Slab Bridges," Center for Civil Engineering Earthquake Research, Department of Civil and Environmental Engineering, University of Nevada, Reno, Nevada, Report No. CCEER-10-06, October 2010.

CCEER 10-07   Builes-Mejia, J. C., Itani, A. and Sedarat, H., "Stability of Bridge Column Rebar Cages during Construction," Center for Civil Engineering Earthquake Research, Department of Civil and Environmental Engineering, University of Nevada, Reno, Nevada, Report No. CCEER-10-07, November 2010.